

Development of a New High Performance Cold Mix Asphalt

Manar Hamzah Herez

A thesis submitted in partial fulfilment of the
requirements of Liverpool John Moores University
for the degree of Doctor of Philosophy

February 2019

DECLARATION

The research reported in this thesis was conducted at Liverpool John Moores University, Civil Engineering Department. I declare that the work is my own and has not been submitted for a degree at another University.

Manar Hamzah Herez

Liverpool John Moores University

February 2019

ABSTRACT

In recent years, global climate change and energy shortages have become serious issues of common concern internationally. The majority of roads and highways are paved using hot mix asphalt (HMA) technology. The manufacture of hot mix asphalt is a key source of energy consumption, greenhouse gas emissions and air pollution. As such, efforts have been made to develop sustainable techniques to reduce energy consumption by lowering manufacturing temperatures, which in turn, will reduce CO₂ emissions and subsequent negative impacts on the environment. Cold bitumen emulsion mixtures (CBEMs) are an excellent alternative to traditional HMA, from both an economic and environmental point of views. However, there are certain issues related to the mechanical properties of CBEMs that make them inferior to HMA, limiting their use to low traffic roads, reinstatement works and footways. Accordingly, the development of a CBEM with high early strength and minimal curing time is of increasing interest to researchers in the asphalt industry.

The aim of this research work was to develop a new, high performance and environmentally friendly, surface course, cold bitumen emulsion mixture for heavily trafficked roads. This aim has been achieved by i) addressing the longstanding problems associated with conventional bitumen emulsions, namely large and non-uniform distribution of bitumen droplets within the emulsion, and ii) reducing the long curing time of CBEMs by replacing conventional limestone filler (LF) with a new secondary cementitious filler made primarily from waste materials. Ultrasound technology was used to reduce the size of the bitumen droplets through the cavitation phenomenon. A cationic bitumen emulsion (C50B4) was treated using ultrasound apparatus, over different periods of time. The results revealed an 85% reduction in mean droplet size (D_{50}), under 7 minutes sonication treatment compared to the untreated sample. Reductions in D_{90} and D_{10} were 90% and 86%, respectively, in comparison to the untreated

sample. The particle size distribution (PSD) curve shows more uniformly distributed droplets closer to the mean values, in comparison to the untreated emulsion. The viscosity of the 7-minute sonicated bitumen emulsion decreased by 28%, compared to the untreated emulsion. CBEM-LF, made with 7-minute sonicated bitumen emulsion, showed an enhancement in indirect tensile stiffness modulus (ITSM) at 3 days curing by approximately 70%, compared with the same mixture containing conventional bitumen emulsion.

To eliminate the long curing time required by CBEMs, a new cementitious filler was developed from waste materials and used as a substitute to conventional LF. The new alkali ternary blended filler, ATBF2, comprises ordinary Portland cement (OPC), a high volume of waste sewage sludge fly ash (SSFA) and calcium carbide residue (CCR). A waste calcium hydroxide solution was used as a replacement for the aggregate pre-wetting water in the CBEM. CCR played a vital role activating the SSFA by breaking the glassy phases of the non-amorphous silica in the SSFA, while the waste calcium hydroxide solution increased the hydraulic reactivity of the cementitious components. Scanning electron microscopy (SEM) and x-ray diffraction (XRD) were used to investigate the development of hydration products in the new CBEM. Concentrations of heavy metals in the samples incorporating ATBF2, were observed to be less than the regulatory levels determined for hazardous materials.

The mechanical properties of the novel CBEM incorporating both the sonicated bitumen emulsion and ATBF2 filler, were investigated in terms of ITSM at different curing times, rutting resistance, fatigue resistance, water damage resistance and age hardening. The said mixture offers a substantial improvement in stiffness modulus, compared to HMA and CBEM containing conventional emulsion and LF. The ITSM for the newly developed CBEM at 3 days of age, increased by approximately 19 times that of the conventional cold mixture, and almost 2.5 times that of traditional 100/150 HMA. The new mixture also displayed considerably higher

resistance to permanent deformation in comparison to the reference cold and hot asphalt mixtures, demonstrating its potential for use in heavily trafficked roads. Resistance to fatigue was significantly enhanced by the use of both ATBF2 and the modified emulsion in the CBEM, compared to conventional cold and hot mixtures. This mixture is more durable because of improvements in resistance to water damage and enhanced long term ageing performance. This improvement has been achieved by the presence of smaller bitumen droplets that provide more bitumen surface area and even coating of aggregate particles. This helps form a cohesive mixture working in parallel with the hydration products which resulted from the hydration process of the cementitious filler in the presence of water within the bitumen-water solution.

DEDICATION

I would like to dedicate this work to:

God almighty, the most Gracious and the most Merciful ...

Prophet Mohammed (May Allah bless him) and his household ...

My parents, the most precious persons in my life, for their unlimited love, inspiration, sacrifices and prayers ...

My husband who encouraged me every step of the way and supported me to achieve my goal ...

My dear brothers and sister for their love, support and encouragement ...

My beloved children, Noran, Ali and Lian who supplied the motivation to get through the long days ...

ACKNOWLEDGEMENTS

First and foremost, I would like to express my deepest gratitude to my main supervisor Professor Hassan Al Nageim, Head of the Liverpool Centre for Materials and Technology (LCMT) for the great help, excellent guidance, generous support and close supervision throughout the entire work.

I would like to express my sincere thanks to my second supervisor, Dr Clare Harris for her advice and support. Also, I would like to convey my deepest gratitude to my third supervisor, Dr Linda Seton, for her encouragement and assistance when using different equipment in the pharmacy and bio-molecular science laboratory.

I am deeply indebted to Dr Anmar Dulaimi for his helpful advice during the period of this study. I would also like to express my warmest thanks to all my friends and colleagues who supported me during my study.

In addition, I would like to acknowledge the financial support provided by the Ministry of Higher Education & Scientific Research, Iraq and Al Kufa University, Iraq.

I would like to extend my thanks and appreciation to all the technicians and administrative staff in the Department of Civil Engineering, Faculty of Engineering and Technology, Liverpool John Moores University, especially those involved with this research. Special thanks go to Miss Alexia Montaubin, Dr Nicola Dempster, Mr Mal Feegan, Mr Paul Gibbons, and Mr David William, for their assistance.

I am also very thankful to Jobling Purser and Colas for the supply of materials, free of charge, during the course of the research. Their support is kindly acknowledged.

Last but not least, I would like to thank my parents, husband, siblings and friends for their prayers and sacrifices to help me reach my goal. I am so lucky to have them in this world and may Allah bless them.

Thank you very much for all of you and for all the others who I did not mention.....

TABLE OF CONTENTS

DECLARATION	I
ABSTRACT.....	II
DEDICATION.....	V
ACKNOWLEDGEMENTS.....	VI
TABLE OF CONTENTS.....	VII
LIST OF TABLES	XII
LIST OF FIGURES	XIV
ACRONYMS AND ABBREVIATIONS	XXI
Chapter 1: Introduction	1
1.1 Overview.....	1
1.2 Benefits of CBEM.....	2
1.3 Drawbacks of CBEM and Problem Statement.....	3
1.4 Aim and Objectives of Research.....	5
1.5 Research Significance	8
1.6 Thesis Structure	8
Chapter 2: Literature Review	11
2.1 Introduction.....	11
2.2 Cold Mix Asphalt (CMA) Overview	11
2.2.1 Classification of Asphalt Mixtures	11
2.2.2 Practices Associated with the Manufacture of Cold Mix Asphalt (CMA)	14
2.2.3 CBEM Developments	17
2.2.4 Curing of CBEMs	26
2.3 Bitumen Emulsion Technology	29
2.3.1 The Benefits of using Bitumen Emulsion.....	30
2.3.2 Composition of Bitumen Emulsions.....	31

2.3.3 Categories of Bitumen Emulsion	36
2.3.4 Manufacturing Process of Bitumen Emulsions	37
2.3.5 Properties of Bitumen Emulsions	40
2.3.6 Applications of Bitumen Emulsions	49
2.4 Ultrasonic Emulsification	51
2.4.1 Mechanisms of Ultrasound	51
2.4.2 Ultrasonic Process Parameters	53
2.5 Summary	55
Chapter 3: Research Methodology, Materials and Mix Design	56
3.1 Introduction.....	56
3.2 Methodology	56
3.3 Programme of Laboratory Experiments and Testing Equipment	59
3.3.1 Characterisation of the Bitumen Emulsion.....	59
3.3.2 Characterisation of the Candidate Mineral Fillers.....	63
3.3.3 Characterisation of the Developed CBEMs.....	70
3.4 Materials	84
3.4.1 Mineral Aggregate	84
3.4.2 Bitumen & Bitumen Emulsion	85
3.4.3 Mineral Fillers.....	86
3.5 Mix Design.....	87
3.5.1 Selection of Aggregate Gradation.....	88
3.5.2 Determination of Initial Bitumen Emulsion Content (IBEC).....	89
3.5.3 Determination of Optimum Pre-Wetting Water Content (OPWC).....	90
3.5.4 Determination of the Optimum Total Liquid Content at Compaction (OTLC).....	91
3.5.5 Determination of the Optimum Bitumen Emulsion Content (OBEC).....	93
3.5.6 Preparation of Samples	93

3.5.7 The Curing Regime for the CBEMs Samples.....	95
3.6 Summary	96
Chapter 4: Application of a New Technology - Ultrasound Technology - in Bitumen Emulsion	97
4.1 Introduction.....	97
4.2 Sonication Treatment of the Bitumen Emulsion.....	98
4.3 Viscosity Measurements	101
4.4 Droplet Size Measurements	103
4.5 Application of Modified Bitumen Emulsion in CBEMs	107
4.5.1 CBEM incorporating Limestone Filler (LF).....	107
4.5.2 CBEM incorporating Ordinary Portland Cement (OPC).....	112
4.6 Summary	116
Chapter 5: Development of a New Secondary Cementitious Filler.....	117
5.1 Introduction.....	117
5.2 Characterisation of the Selected Mineral Fillers.....	118
5.2.1 Limestone Filler (LF).....	118
5.2.2 Ordinary Portland Cement (OPC).....	120
5.2.3 Sewage Sludge Fly Ash (SSFA)	122
5.2.4 Flue Gas Desulphurisation (FGD) Gypsum.....	125
5.2.5 Calcium Carbide Residue (CCR).....	128
5.3 Comparative Physical and Chemical Characteristics of the Selected Materials.....	131
5.4 Mechanical Activation of SSFA	135
5.5 Physico-chemical Activation by Blending.....	141
5.6 CBEMs incorporating Binary Blended Filler (BBF)	150
5.7 Summary	153
Chapter 6: Further Development of the New Secondary Cementitious Filler.....	154

6.1 Introduction.....	154
6.2 CBEMs incorporating a Ternary Blended Filler (TBF1).....	154
6.3 CBEMs incorporating a Second Ternary Blended Filler (TBF2).....	157
6.4 CBEM incorporating Alkali-activated TBF2 (ATBF2).....	159
6.5 Water Loss in CBEMs	162
6.6 Temperature Susceptibility of CBEMs.....	163
6.7 Summary.....	165
Chapter 7: The Microstructural Characterisation of the New Secondary Cementitious Filler	166
7.1 Introduction.....	166
7.2 X-ray Diffraction (XRD) Analysis	166
7.3 Scanning Electron Microscopy (SEM) Analysis.....	172
7.4 Summary.....	184
Chapter 8: Development of a Novel High Performance CBEM.....	185
8.1 Introduction.....	185
8.2 CBEM incorporated BBF and MBE	185
8.3 CBEM incorporating TBF2 and MBE.....	187
8.4 CBEM incorporating ATBF2 and MBE.....	189
8.5 Water sensitivity	191
8.5.1 Results and Discussion	192
8.6 Long Term Age Hardening.....	194
8.6.1 Results and Discussion	195
8.7 Summary.....	198
Chapter 9: Deformation and Fatigue Resistance of the New CBEMs.....	199
9.1 Introduction.....	199
9.2 Resistance to Permanent Deformation (Wheel Track Test)	199

9.2.1 Test Configuration and Sample Preparation	200
9.2.2 Results and Discussion	202
9.3 Resistance to Fatigue (Four-point Bending Test)	207
9.3.1 Test Configuration and Sample Preparation	207
9.3.2 Results and Discussion	209
9.4 Summary	213
Chapter 10: Environmental Investigation: Leaching of Heavy Metals into Water.....	214
10.1 Introduction.....	214
10.2 Toxicity Characteristics Leaching Procedure (TCLP) test	215
10.3 TCLP Results and Discussion.....	217
10.4 Summary	218
Chapter 11: Conclusions and Recommendations	219
11.1 Introduction.....	219
11.2 Conclusions.....	219
11.2.1 CBEMs containing Limestone Filler and Ordinary Portland Cement	219
11.2.2 Modification of the Bitumen Emulsion	220
11.2.3 Development of the new CBEM containing the new Secondary Cementitious Filler	222
11.2.4 Development of Novel High Performance CBEM including the New Secondary Cementitious Filler and the Modified Bitumen Emulsion using Ultrasound Technology	224
11.3 Recommendations for Future Works	226
References.....	228
Research Contributions	243

LIST OF TABLES

Table 2.1: Bitumen emulsions applications with different breaking rates (James, 2006)	50
Table 3.1: Tests used to specify the properties of CBEMs.....	71
Table 3.2: ITSM test conditions.....	74
Table 3.3: Four-point fatigue test conditions	76
Table 3.4: Wheel tracking test conditions.....	79
Table 3.5: Physical characteristics of the granite aggregate	84
Table 3.6: Properties of bitumen & bitumen emulsion.....	85
Table 3.7: Aggregate gradation for AC10 surface course	88
Table 4.1: Effect of sonication time on PS	106
Table 4.2: Air void contents of CBEMs with treated and untreated bitumen emulsions	111
Table 5.1: The chemical composition of LF and OPC	118
Table 5.2: The chemical compositions of raw SSFA	123
Table 5.3: The chemical compositions of the FGD gypsum	126
Table 5.4: The chemical compositions of the CCR	130
Table 5.5: Comparative chemical properties of the selected materials	133
Table 5.6: Comparative chemical properties of the selected materials in accordance with BS EN 197-1	134
Table 5.7: Comparison of the physical characteristics of the fillers.....	135
Table 5.8: Changes in physical properties after grinding activation	138
Table 5.9: Constituent matrix of the raw SSFA paste specimens.....	143

Table 5.10: Constituent matrix of paste specimens of ground SSFA	145
Table 9.1: Wheel track test results at 45°C.....	204
Table 9.2: Wheel track test results at 60°C.....	206
Table 9.3: Fatigue equations for the developed and controlled mixtures	212
Table 10.1: Results of the TCLP test	218

LIST OF FIGURES

Figure 2.1: The effect of compaction degree on stiffness modulus (Serfass et al, 2004).....	18
Figure 2.2: Effect of incorporating cement on resilient modulus of the CBEMs (Oruc et al, 2007)	21
Figure 2.3: Schematic diagram representing the hardening process of an asphalt-emulsion composite (García et al, 2013)	23
Figure 2.4: ITSM evolution as a function of curing time and temperature (Bocci et al, 2011)	27
Figure 2.5: Typical particle size diagram of bitumen emulsion droplets (Miljković, 2014) ...	30
Figure 2.6: Schematic diagram of charges on a bitumen droplet and the structure of a cationic emulsifier (James, 2006).....	34
Figure 2.7: Schematic diagram illustrating continuous and batch process plants for manufacturing bitumen emulsions (Read and Whiteoak, 2003).....	39
Figure 2.8: Schematic diagram illustrating the destabilising process of a bitumen emulsion (Akzo Nobel, 2008)	42
Figure 2.9: A schematic diagram illustrating emulsifier ions forming a micelle in a stable emulsion (Read and Whiteoak, 2003).....	46
Figure 2.10: A schematic diagram illustrating the breaking process (Read and Whiteoak, 2003)	46
Figure 2.11: Schematic diagram of growth and collapse of a bubble in acoustic cavitation process (Hielscher, 2005).....	52
Figure 3.1: Research methodology flow chart.....	58

Figure 3.2: Ultrasonic set-up and the sequence of energy transformation at different levels of operation	60
Figure 3.3: Viscometer used to measure the viscosity of the emulsion.....	62
Figure 3.4: Laser diffraction particle size distribution analyser	63
Figure 3.5: Energy dispersive X-ray fluorescence (EDXRF) spectrometer	64
Figure 3.6: Rigaku Miniflex X-ray Diffractometer	65
Figure 3.7: Quanta 200 scanning electron microscope.....	66
Figure 3.8: pH meter	67
Figure 3.9: Multi-pycnometer used for measuring the density of fillers	68
Figure 3.10: Vicat apparatus	69
Figure 3.11: Atomic adsorption spectrophotometer	70
Figure 3.12: ITSM test using Cooper Research Technology HYD 25 apparatus.....	73
Figure 3.13: Configuration of the four-point load fatigue test (4PB).....	76
Figure 3.14: Roller compactor equipment	77
Figure 3.15: Wheel tracking apparatus	79
Figure 3.16: Water sensitivity instruments	82
Figure 3.17: Selected mineral fillers	87
Figure 3.18: The gradation of AC 10 close-graded surface course	89
Figure 3.19: Percentages of pre-wetting water content	91
Figure 3.20: The percentage of optimum liquid content.....	92
Figure 3.21: The percentage of optimum residual bitumen content	93

Figure 3.22: Steps of preparing samples of CBEMs.....	94
Figure 4.1: Ultrasound apparatus.....	99
Figure 4.2: Effect of sonication treatment time on temperature	101
Figure 4.3: Effect of sonication time on the viscosity of treated bitumen emulsions.....	103
Figure 4.4: Effect of sonication time on PSD	105
Figure 4.5: Effect of sonication time on cumulative distribution	105
Figure 4.6: Development ITSM values of the control CBEM containing LF	108
Figure 4.7: Effect of sonication time on the ITSM of CBEMs at 3 days	109
Figure 4.8: ITSM values of 7 minutes treated CBEM with curing times	110
Figure 4.9: Air void contents and ITSM of CBEMs at 3 days with different treated emulsions	112
Figure 4.10: Influence of OPC replacement on ITSM values in CBEMs at 3 days	113
Figure 4.11: ITSM values of OPC mixtures at different curing times.....	114
Figure 4.12: Influence of MBE on the ITSM value for CBEM-OPC at 3 days	115
Figure 4.13: ITSM values for CBEM-OPC with MBE at different curing ages	115
Figure 5.1: The XRD pattern for the LF powder (C= calcite, Q= quartz).....	119
Figure 5.2: Particle size distribution of the LF and OPC.....	119
Figure 5.3: SEM image for dry powder LF	120
Figure 5.4: The XRD pattern diagram for the OPC (C= calcite, A= alite, B= belite, P= periclase, F= ferrite).....	121
Figure 5.5: SEM image for dry powder OPC	122

Figure 5.6: Mineralogy of the SSFA (Q= quartz, H= hematite, M= magnetite, W= whitlockite)	124
Figure 5.7: Particle size distribution of the SSFA powder	124
Figure 5.8: SEM image for dry powder SSFA	125
Figure 5.9: XRD patterns of the FGD gypsum (CAS= calcium sulphate hemihydrate, CAD= calcium sulphate dehydrates, Q= quartz).....	127
Figure 5.10: Particle size distribution of the FGD powder	127
Figure 5.11: SEM image for dry powder FGD	128
Figure 5.12: Particle size distribution of the CCR powder	129
Figure 5.13: The XRD pattern of the CCR (CHO= calcium hydroxide, G= graphite, C= calcite)	130
Figure 5.14: SEM image for dry powder CCR	131
Figure 5.15: Comparison of the PSD's of the selected materials	135
Figure 5.16: Mortar grinder	136
Figure 5.17: Comparative change in differential PSD when grinding SSFA using FGD gypsum	138
Figure 5.18: Comparative change in cumulative PSD when grinding SSFA using FGD gypsum	139
Figure 5.19: Comparative powder XRD for FGD and non-FGD assisted ground SSFA (Q= quartz, H= hematite, M= magnetite, W= whitlockite).....	140
Figure 5.20: Microstructural change of SSFA dry particles (a) before grinding (b) after grinding with FGD gypsum.....	141

Figure 5.21: Influence of raw SSFA replacement on compressive strength at 3 days	143
Figure 5.22: Effect of curing time of different raw SSFA replacements on compressive strength	144
Figure 5.23: Influence of different percentages on compressive strength of ground SSFA with 5% FGD gypsum at 3 days	146
Figure 5.24: Effect of curing time on compressive strength for different percentages of ground SSFA with 5% FGD gypsum.....	146
Figure 5.25: SEM images of the OPC paste at 3 days of age	148
Figure 5.26: SEM images of the OPC paste at 28 days	148
Figure 5.27: SEM images of the BBF paste at 3 days of age	149
Figure 5.28: SEM images of the BBF paste at 28 days of age	150
Figure 5.29: Effect of SSFA replacement on the ITSM of CBEMs at 3 days.....	151
Figure 5.30: Effect of curing time on the ITSM of CBEMs	152
Figure 6.1: Effect of partial replacement of BBF with CCR on the ITSM of CBEMs at 3 days	156
Figure 6.2: Influence of curing time on the ITSM of CBEM-TBF1	156
Figure 6.3: Effect of adding CCR to 6% BBF on the ITSM of CEBMs at 3 days	158
Figure 6.4: Effect of curing time on the ITSM of CBEM-TBF2.....	158
Figure 6.5: Stiffness development of CBEM-ATBF2 at 3 days of age	161
Figure 6.6: ITSM values of CBEM-ATBF2 at different curing ages	161
Figure 6.7: Water loss of CBEMs over different curing periods.....	163
Figure 6.8: ITSM results at different testing temperatures	164

Figure 7.1: A schematic explanation of Bragg's equation.....	167
Figure 7.2: XRD spectra for the LF powder and paste at different ages (C= calcite, Q= quartz)	170
Figure 7.3: XRD spectra for the TBF2 powder and AATBF2 pastes at different ages (CHO= calcium hydroxide, Q= quartz, H= hematite, C= calcite, CH= portlandite, AFt= ettringite, CSH= calcium silicate hydrate)	171
Figure 7.4: Secondary electrons (SE), backscattered electrons (BSE), Auger electrons (AE), and X-ray (X) in the diffusion cloud of electron range R for normal incidence of the primary electrons (PE) (El-Desawy, 2007)	173
Figure 7.5: SEM samples preparation.....	175
Figure 7.6: SEM images of the LF powder with 7500x and 4000x.....	176
Figure 7.7: SEM images of the LF paste at 3 days of age	177
Figure 7.8: SEM images of the LF paste at 7 days of age	177
Figure 7.9: SEM images of the LF paste at 14 days of age	178
Figure 7.10: SEM images of the LF paste at 28 days	178
Figure 7.11: SEM images of the TBF2 powder.....	180
Figure 7.12: SEM images of ATBF2 paste at 3 days of age.....	181
Figure 7.13: SEM images of ATBF2 paste at 7 days of age.....	181
Figure 7.14: SEM images of ATBF2 paste at 14 days of age.....	182
Figure 7.15: SEM images of ATBF2 paste at 28 days of age.....	182
Figure 7.16: SEM images of the CBEM-ATBF2 at 28 days of age	183
Figure 8.1: ITSM value of CBEM-BBF with MBE at 3 days of age	186

Figure 8.2: ITSM values of CBEM-BBF with MBE at different curing times	187
Figure 8.3: ITSM values of CBEM-TBF2 with MBE at 3 days curing.....	188
Figure 8.4: ITSMs of CBEM-TBF2 containing MBE at different curing times	188
Figure 8.5: ITSM values of CBEM-ATBF2 with MBE at age 3 days	190
Figure 8.6: ITSM values of CBEM-ATBF2 containing MBE at different curing times.....	190
Figure 8.7: Water sensitivity results for the control and developed mixtures which included NBE.....	193
Figure 8.8: Water sensitivity results for the control and developed mixtures which included MBE.....	194
Figure 8.9: Effect of ageing on ITSM values for all CBEMs with NBE.....	196
Figure 8.10: Effect of ageing on ITSM values for all CBEMs with MBE	197
Figure 9.1: Loose CBEM prior to compaction	201
Figure 9.2: The rut depth of all CBEM and control HMA mixtures at 45°C	203
Figure 9.3: The rut depth of all developed and control mixtures at 60°C	206
Figure 9.4: Fatigue performance for all cold and hot mixtures based on 150 micro-strain...210	
Figure 9.5: Fatigue line for all developed and control mixtures.....	211
Figure 10.1: Preparation of the TCLP samples.....	216
Figure 10.2: Rotary extractor machine	216
Figure 10.3: Atomic adsorption spectrometer	217

ACRONYMS AND ABBREVIATIONS

Alkali-activated Ternary Blended Filler	ATBF
Alumina Ferric Oxide Monosulphate (Ettringite)	AFm
Alumina Ferric Oxide Trisulphate (Ettringite)	AFt
Asphalt Concrete	AC
Binary Blended Filler	BBF
Calcium Carbide Residue	CCR
Calcium Hydroxide (Portlandite)	CH
Calcium Silicate Hydrate	CSH
Centipoise	cP
Cold Bitumen Emulsion Mixture	CBEM
Cold Mix Asphalt	CMA
Cold Rolled Asphalt	CRA
Degrees Celsius	°C
Dense Bitumen Macadam	DBM
Energy Dispersive X-ray Fluorescence	EDXRF
Fatigue Life	N _f
Flue Gas Desulphurisation Gypsum	FGD
Fluid Catalytic Cracking Catalyst	FC3R
Four-point Bending	4PB
Ground Granulated Blast-Furnace Slag	GGBS

Hot Mix Asphalt	HMA
Indirect Tensile Stiffness Modulus	ITSM
Initial Bitumen Emulsion Content	IBEC
Limestone Filler	LF
Liverpool Centre for Material Technology	LCMT
Mega Pascal	MPa
Micromtere	μm
Modified Bitumen Emulsion	MBE
Nano-meter	Nm
Normal Bitumen Emulsion	NBE
Ordinary Portland Cement	OPC
Optimum Bitumen Emulsion Content	OBEC
Optimum Pre-wetting Water Content	OPWC
Optimum Total Liquid Content at Compaction	OTLC
Paper Sludge Ash	PSA
Particle Size	PS
Particle Size Distribution	PSD
Proportional Rut Depth	PRD _{AIR}
Pulverised Fly Ash	PFA
Scanning Electron Microscopy	SEM
Secondary Cementitious Filler	SCF
Sewage Sludge Fly Ash	SSFA

Silica Fume	SF
Stiffness Modulus Ratio	SMR
Ternary Blended Filler	TBF
Toxicity Characteristics Leaching Procedure	TCLP
U.S. Environmental Protection Agency	USEPA
Warm Mix Asphalt	WMA
Waste Fly Ash	WFA
Wheel-tracking Slope	WTS _{AIR}
X-ray Diffraction	XRD

Chapter 1: Introduction

1.1 Overview

Roads play an essential role in the economic and social development of all countries. As such, roads are designed to withstand the stresses and strains induced by traffic loads and changing / challenging environmental conditions throughout their service life, without any disruption to operation. Asphalt pavements are the major structural load-carrying element of roads comprising superimposed layers above the subsoil, their job being primarily to distribute traffic loads to subgrade levels. Of paramount importance regarding pavement structures is that stresses induced by wheel loads, should not exceed the bearing capacity of the subgrade, this is achieved by minimising transmitted stresses throughout the pavement's structural layers.

A typical asphalt pavement must provide the following (Mathew and Krishna Rao, 2007):

- Adequate distribution of wheel load stress to the subgrade soil such that no deformation occurs.
- The ability to withstand all types of stresses.
- Sufficient skid resistance.
- Acceptable surface riding quality.
- Low noise from moving vehicles.
- Long service life with low cost of maintenance.

Hot mix asphalt (HMA) is the most common material used to construct asphalt pavements. It is prepared, laid and compacted at elevated temperatures ranging from 110 to 180°C (Su et al, 2009). Due to these relatively high temperatures during production, large amounts of fuel are needed to heat the aggregates and bitumen. As a consequence, a substantial proportion of pollutant gases are generated and emitted during the manufacturing process (Capitão et al,

2012). Rubio et al (2012) stated that one of the main sources of pollution within the road industry is the HMA manufacturing sector, this contributing to global warming. Health and safety issues due to fumes and dust during production, add another disadvantage to the uses of HMA. All these raise the necessity for more economic and sustainable pavement material alternatives.

From the viewpoint of developing more environmentally friendly and sustainable asphalt pavement construction practices, cold mix asphalt (CMA) technology has gained the attention of the road pavement industry in that many researchers have tried to develop such a mixture. Due to its environmental, economic and safety advantages, cold bitumen emulsion mixture (CBEM) has emerged as the most common type of CMA.

1.2 Benefits of CBEM

Cold bitumen emulsion mixture (CBEM) is the result of scientific studies aiming to reduce energy consumption and greenhouse emissions while improving cost effectiveness. CBEM is considered to have the following benefits:

1. It is an environmentally friendly product as no heat is required during its production and construction because CBEM is a water-based system: there is no environmental footprint attributed to it. CO₂ emissions during the manufacture of CBEM are approximately 14% of those produced by HMA (Kennedy, 1997). It eliminates dust emissions because there is no need to heat the aggregate.
2. No need of heat reduces the cost of CBEM by minimizing the energy used. The production of one tonne of CBEM costs about 13% of the energy needed for a conventional hot mix (le Bouteiller, 2010).
3. A reduction in the potential exposure of workers to fuel emissions, fumes and other chemical gases. Workers in a HMA job site are usually exposed to 0.1 to 2 mg/m³ of

bitumen fumes, which contain 10 to 200 ng/m³ of benzo(a)pyrene toxic gas (Chauhan et al, 2010).

4. It extends the paving season, as there is no threat of a critical loss of temperature. It is workable over a range of air temperatures and can be laid in wet or humid conditions. CBEM can also be stockpiled and hauled over long distances with no need for insulated trucks (Needham, 1996).
5. It maximises the use of recycled asphalt pavement, waste and by-product materials, which increases cost effectiveness.
6. It eliminates the problems associated with the heating process such as binder hardening through oxidation during the storage and construction stages (Al-Busaltan, 2012). The probability of producing waste from the CBEM construction process is limited, due to the elimination of the need to heat it (Al-Busaltan, 2012).

1.3 Drawbacks of CBEM and Problem Statement

Despite CBEM having so many advantages with respect to environmental, economic and safety issues, there are some shortfalls apparent during its stages of production and service life performance that make it inferior to HMA. These shortfalls form a barrier to use as a structural layer (Oruc et al, 2013). Consequently, its application has been restricted to preventive maintenance of pavements. The main drawbacks of CBEM, as stated by previous studies and applications (Thanaya, 2003; Al-Hdabi, 2014; Dulaimi, 2017), can be summarized as follows:

1. Poor early life strength due to the presence of water meaning that a long curing time is required for the trapped water to evaporate and achieve its ultimate strength. Laboratory and field studies have been conducted by the Chevron Research Company to evaluate the performance of CBEM in California. They concluded that between 2 to 24 months

are needed to obtain full curing of CBEM in the field, this dependent on the constituents of the mixture and the weather conditions (Leech, 1994).

2. High air voids content in compacted mixtures.
3. Inadequate aggregate coating percentage due to large and non-uniformly distribution bitumen droplets in the emulsion.
4. High water sensitivity, giving low early resistance to rainfall.
5. Adding cement and additives improves the performance of CBEM, but this substantially increases the cost of production.
6. Standards and specifications for CMA are not available.

The research problem tackled in this thesis was as a result of a critical appraisal of the literature. A number of unclear, or unresolved issues and knowledge gaps related to CBEM performance were identified, as summarized in the following paragraphs.

There are several parameters affecting the performance of bitumen emulsion such as the source of bitumen, type and amount of emulsifier, type of equipment used in its manufacture and particle size in the emulsion. Bitumen particle size is one of the vital parameters influencing the breaking behaviour of bitumen emulsions (Rayner and Marchal, 1991). As the bitumen droplets reduced, the interfacial area between the bitumen and the water increased. An increase in the surface area leads to an increase in the number of contact points and the capacity for emulsifier adsorption at the bitumen-water interface, thereby accelerating the breaking process (Needham, 1996). In contrast, the larger the particle size distribution, the more free emulsifier in the water phase. This will rapidly attach to the aggregate surface and prevent the binder from breaking onto the aggregate (Marchal et al, 1993). This in turn, leads to coalescence of the bitumen droplets away from the aggregate meaning that a poor binding matrix is formed. In addition, the larger the particle size, the less stable the emulsion. Larger particles are more

prone to settlement, which can result in an increase in particle size during storage (Needham, 1996).

Most of the previous studies in the literature have shown that the performance of CBEMs can be improved by using cement to absorb trapped water in the mixture through the hydration process (Thanaya, 2003; Oruc et al, 2007; Niazi and Jalili, 2009; Al-Hdabi et al, 2014a; Fang et al, 2016a). However, using cement in relatively high percentages, increases costs and cement demand worldwide, this consequently increasing CO₂ emissions.

1.4 Aim and Objectives of Research

The present study primarily aims to improve the mechanical performance of CBEM by addressing two issues pertaining to bitumen emulsion and curing time of CBEM. This will involve: i) reducing the size of the bitumen droplets and producing a more uniform emulsion and ii) enhancing the curing time of the new CBEM by replacing conventional limestone filler (LF) with a new secondary cementitious filler (SCF) with low CO₂ emissions. The new bitumen emulsion will be developed by reducing the bitumen droplet size using an ultrasound technique. Smaller droplets lead to an increase of the surface area per unit volume, thus increasing the area of the aggregates coated by the bitumen binder. The new SCF will absorb the trapped water in the CBEM through the hydration process and produce hydration products which working in parallel with the bitumen binder to form a cohesive mixture. This improves the performance of the CBEM in terms of mechanical properties, such as stiffness modulus, resistance to rutting and fatigue. The research outcomes ought to eliminate the restrictions imposed by road engineers on the use of such mixtures in road surface layers, due to the earlier said shortfalls; weak early strength and long curing time.

The novel factors in this research include:

1. The production of a sub-micron bitumen emulsion, using a new ultrasound technique which has never been applied before in the asphalt pavement domain.
2. The conversion of waste materials; low calcium sewage sludge fly ash (SSFA), flue gas desulphurisation (FGD) gypsum and calcium carbide residue (CCR), into a high value, secondary cementitious filler (SCF), adopting new LJMU activation techniques.
3. The application of the bitumen emulsion modified by ultrasound technology, and the new SCF, as replacements for conventional materials, to produce a high performance CBEM suitable for road surfacing.

The aim of the research will be achieved through the following objectives:

1. An upgrade of the properties of conventional bitumen emulsion, using a novel ultrasound technique, to reduce the bitumen droplet size of the said emulsion to a sub-micron level. This technical development will improve the characteristics and performance of the bitumen emulsion in the mixture and produce better interlocking between the mix contents.
2. Selection of the optimum ultrasonic irradiation time to ensure that the bitumen emulsion is dispersed and approaching a monodisperse state.
3. Specification of the characteristics of the upgraded bitumen emulsion in terms of viscosity, droplet size and droplet size distribution.
4. Selection of candidate waste materials, namely SSFA, FGD and CCR, to produce SCF to replace the limestone filler in conventional CBEM, and study their physical, chemical, mineralogical and morphology properties. Comparison of these to ordinary Portland cement (OPC) to predict their potential for use as cementitious and/or pozzolanic materials, individually and/or collectively.

5. Carrying out laboratory work on the said waste materials aiming to activate them mechanically and chemically, using grinding energy and chemical activation techniques, respectively.
6. Production and optimisation of SCF, made from 4 and 5 above, by blending the selected waste materials with OPC in different proportions, using binary and ternary blending procedures. Indirect tensile stiffness modulus (ITSM) was used as an indicator of improvement in the performance of the CBEMs containing the new filler.
7. Understanding the development in the ITSM of the new CBEM by using scanning electron microscopy (SEM) and X-ray diffraction (XRD) analysis to investigate changes in the microstructure of pastes bonding in the CBEM matrix at different curing ages (3, 7, 14 and 28 days).
8. Investigation of environmental issues by conducting a Toxicity Characteristic Leaching Procedure (TCLP) test on the waste materials, new cementitious filler and the newly developed CBEM, to analyse the leachate for heavy metal concentrations.
9. Complete a laboratory study on the performance of the new CBEM, containing the new modified bitumen emulsion and the new SCF, to specify its mechanical and durability properties in terms of ITSM, resistance to permanent deformation, resistance to fatigue cracking, temperature susceptibility, water sensitivity and ageing, using Liverpool Centre of Materials Technology (LCMT) lab at LJMU complying with BS EN codes of practice.
10. Conducting a critical analysis and discussion on the importance of the new products and their use in the pavement industry.

1.5 Research Significance

Developing a CBEM with high early age strength, strong resistance to water ingress and with minimal time delay requirements before structural loading, would be considered as a breakthrough in CBEM research. First time, worldwide application of a new technology - ultrasound technology - to produce bitumen emulsion, can improve its properties which in turn, can increase the performance efficacy of bitumen emulsion in pavement construction.

Using a sustainable filler derived from the candidate waste materials in combination with cement, provides enhanced properties for CBEMs and offers a potentially positive effect on sustainability by reducing the need for cement in CBEMs. The current research will contribute to the wider utilization of CBEMs in the construction of highway and pavement material, facilitating positive environmental and economic impacts. The use of a high percentage of SSFA when producing CBEMs would also provide the benefit of minimising the volume of waste disposed to landfill.

1.6 Thesis Structure

This thesis is organised into eleven chapters as follows:

- **Chapter 1:** includes the background to the research topic, and the advantages and disadvantages of using CBEMs in road construction. The research aim and objectives and the significance of the research are also presented in this chapter.
- **Chapter 2:** presents an intensive literature review of the research topic, including reviews on bitumen emulsion, cold asphalt technology, with more detail on CBEMs and ultrasound techniques as applied in emulsification practices.

- **Chapter 3:** summarises the methodology followed to accomplish the objectives of this research. The experimental procedures to characterise the bitumen emulsion and the selected raw materials are presented together in this chapter with the mix design and the test methods chosen for development of the CBEM.
- **Chapter 4:** provides the results of the ultrasound technology treatment process of the bitumen emulsion used to obtain the optimum upgraded bitumen emulsion. This chapter also presents an investigation on the properties of the newly upgraded emulsion and its performance in the CBEM compared to the conventional CBEM.
- **Chapter 5:** provides the detailed results of the mechanical, physical and chemical properties of the selected waste materials, compared to LF and OPC. The effect of applying activation techniques on the performance of these materials is also presented. This chapter also includes optimisation of the constituents of a binary blended filler after combined application of the activation techniques.
- **Chapter 6:** addresses and discusses the experimental results of the optimisation process for the ternary blends used to develop the new secondary cementitious filler. The results for the CBEM in terms of ITSM are also compared with those of CBEMs containing LF and OPC individually.
- **Chapter 7:** deals with the mineralogy and microstructure of the developed CBEM using XRD and SEM microanalysis tools. This will provide an understanding of the improvements in the performance of the new cold mixture in terms of ITSM, water sensitivity, rutting and fatigue resistance.
- **Chapter 8:** includes the development of a novel surface course CBEM, incorporating both the modified bitumen emulsion and the developed secondary cementitious filler. This chapter includes an evaluation of the newly developed CBEM in terms of ITSM and its durability properties i.e. water sensitivity and ageing.

- **Chapter 9:** provides the findings of the mechanical performance of the developed CBEM in terms of resistance to permanent deformation and fatigue resistance.
- **Chapter 10:** details the environmental investigation on heavy metal concentrations in the waste materials, new secondary cementitious filler and new CBEM.
- **Chapter 11:** contains the conclusions derived from the findings of this study. Recommendations for future works are also reported.

Chapter 2: Literature Review

2.1 Introduction

A comprehensive literature review, describing the background of the current study is presented in this chapter. It includes three sections, the first providing a general overview of cold mix asphalt (CMA) practice and summaries of attempts to enhance the performance of cold bitumen emulsion mixtures (CBEMs). The second section covers the most important aspects of bitumen emulsion technology. The last section reviews the ultrasound technology used in different emulsification applications such as food, cleaning products, cosmetics, pharmaceutical and biomedical manufacture.

2.2 Cold Mix Asphalt (CMA) Overview

2.2.1 Classification of Asphalt Mixtures

Asphalt mixtures are composite materials composed of graded mineral aggregates stuck together by a bitumen binder. The type and proportions of the constituents of an asphalt mixture, will determine the quality, performance and serviceability of the resulting asphalt mixture (Jakarn, 2012). There are two main types of asphalt mixtures classified according to the proportion and aggregate size distribution, namely continuously graded and gap graded. Continuously graded mixtures have various sizes of aggregate. The voids formed by the coarse aggregates are filled up by fine aggregates, bitumen and filler. This strengthening the aggregate skeleton (Roberts et al, 1991). An example of a continuously graded mixture is asphalt concrete (AC). It is typically used for constructing surface courses on lightly trafficked pavements, binder and base courses in major roads. The range of AC mixtures varies from 4 mm, fine graded, surface course to 32 mm, heavy duty AC. The difference between these types is based

on the proportions of coarse aggregate, fine aggregate, filler and bitumen (European Committee for Standardization, 2016b).

In gap graded mixtures, the gradating of aggregates is not continuous. This creates more air voids because of the lack of small particles to fill in the voids between the larger particles during compaction (Read, 1996). The structural strength of gap graded mixtures is based on the mortar of sand, bitumen and filler. As such, continuously graded mixtures offer better deformation resistance than gap graded mixtures.

Depending on the mixing temperature and energy consumed in the process of heating, asphalt mixtures are divided into three different types as described below (Vaitkus et al, 2009).

2.2.1.1 Hot Mix Asphalt (HMA)

Hot mix technology is most commonly used to produce road pavement materials, accounting for around 90% of the total mixes produced, because of its flexibility, weather resistance and ability to repel water. It is manufactured in a central mixing plant where the asphalt and aggregates are heated to a temperature between 150 and 190°C (based on the hardness grade of the bitumen), proportioned correctly and mixed. The completed paving mixture is transported by trucks to the paving site, spread by a mechanical spreader in a smooth layer then compacted by rollers while still hot. Soon after the material has cooled to the ambient temperature, the pavement is ready to open to traffic (Read and Whiteoak, 2003).

However, the production process of HMA is considered a substantial source of carbon emissions, these having a serious impact on the environment (U.S. Environmental Protection Agency (USEPA), 2011). Health hazards are created due to gas emissions from the heating process, the risk of fire and burns from melting bitumen. The annual production of a typical asphalt plant is approximately 200,000 tonnes of HMA, which in turn produces 13 tonnes of

carbon monoxide (CO), 5 tonnes of volatile organic compounds, 2.9 tonnes of nitrogen oxides, 0.65 tonnes of total hazardous air pollutants and 0.4 tonnes of sulphur oxides, as estimated by U.S. Environmental Protection Agency (USEPA) (2000).

2.2.1.2 Warm Mix Asphalt (WMA)

Warm Mix Asphalt (WMA) technology allows asphalt mixtures to be produced and spread at significantly lower temperatures than HMA. With this technology, mixing and compacting temperatures can be reduced around 20 to 40°C lower than that required for HMA without affecting the mix quality (Rubio et al, 2012). While there are numerous WMA technologies in use around the world, the most common technologies used to reduce bitumen viscosity are the use of organic additives, chemical additives and water-based or water-containing foaming processes (Zaumanis, 2010). Lowering the temperature during production reduces the energy required and thus fuel consumption. It also decreases the plant's carbon footprint thereby improving working conditions at the plant and paving site (European Asphalt Pavement Association, 2010). WMA can also be hauled over longer distances and has an extended paving season as it cools at a lower rate. However, there is still a certain reticence when it comes to use these mixtures as they are still at the experimentation and standardization stage of development (Zaumanis, 2010).

2.2.1.3 Cold Mix Asphalt

Cold mix asphalt (CMA) is a versatile and sustainable alternative to HMA as it is mixed, applied and compacted at ambient temperature without heating (Jenkins, 2000). It is a combination of graded mineral aggregate and emulsified, or cutback asphalt, and additives. There are several factors driving the development of CMA, including its environmental impact, energy savings and cost effectiveness. From the viewpoint of energy input, CMA manufacturing consumes much less energy than HMA. The manufacture of one tonne of CMA

requires 13% of the energy used to manufacture the same amount of HMA (le Bouteiller, 2010). The CO₂ emissions from preparing CMA are approximately 14% of those produced by HMA production.

Although the advantages of CMA are very attractive with respect to environmental, economic and safety issues, there are some shortfalls resulting from the poor performance of such mixtures that make it inferior to HMA. These shortfalls are apparent in the manufacturing stages and service life performance (Thanaya, 2003).

2.2.2 Practices Associated with the Manufacture of Cold Mix Asphalt (CMA)

Over the last century, it has been established that CMA has several advantages over conventional HMA in terms of sustainability and energy savings, as it produces almost no emissions as discussed in the previous section. As such, many efforts have been made by researchers and producers to improve these mixtures to increase their competitiveness and potential utilization (Gómez-Mejide and Pérez, 2014). These efforts have led to several CMA practices in use around the world, as detailed below.

2.2.2.1 Cold Lay Macadam

In this type of CMA, the bitumen used is liquefied by adding a solvent or flux oil (cutback emulsion). Flux oil is a non-volatile fraction of petroleum used to dilute bitumen to a more useful consistency. The performance of these mixtures is governed by the evaporation of flux oil from the mixture, this depending on flux volatility and weather conditions. These mixtures are often used as surface dressings, macadam mixtures and temporary fill material in reinstatement work which has suffered from low stiffness as a result of the presence of flux (Robinson, 1997).

There are some drawbacks associated with these mixtures including that the solvents used are considered pollutants, flammable and usually expensive. As a result of their environmental impact, the use of such mixtures has been restricted (Leech, 1994).

2.2.2.2 Foamed Asphalt

This technology was first developed in 1956 by Prof. Ladis H. Csanyi at Iowa State University, USA. It is manufactured using a foamed bitumen which is produced by injecting water into hot bitumen. The ensuing steam is trapped by thousands of tiny bitumen bubbles resulting in an increase in the volume of the bitumen and a temporary decrease in viscosity. Due to the expansion in volume, the aggregates will be coated at a lower temperature during the foamed state. Further developments have subsequently enhanced the production of this, one type of these mixtures carried out by Mobile Oil Australia in 1968, by adding cold water instead of steam, creating a simpler and more economic production method (Muthen, 1998; Ebels, 2008).

Another development made in the mid-1990s by Wirtgen, was when both water and air were injected into the hot bitumen in an expansion chamber. Compressed air with 1 to 5% water by mass of bitumen, was injected into hot bitumen (140 to 180°C), which converted the water into vapour, generating tiny bitumen bubbles (Kuna, 2015). After the air escapes, the foam collapses leaving a bitumen residue with properties similar to the original bitumen, to coat the aggregate. The main feature of this technology is that a small ratio of water, normally about 2% by bitumen mass, is required meaning that foamed bitumen can be opened to traffic almost immediately. It remains workable for longer and can be stockpiled for later use (Wirtgen, 2004).

2.2.2.3 Grave Emulsion

Grave emulsion was first produced in France and subject to specification in 1974 (Needham, 1996). It refers to emulsion stabilized aggregate applications, in which the bitumen emulsion

is mixed with pre-wetted aggregate. In France, grave emulsion is used in warm regions because of its water sensitivity. It has a lower binder content (3 to 3.5%), which allows partial coating of the aggregate compared to other types of CMA.

Grave emulsion could be a cost effective replacement to traditional HMAs, especially in remote areas where the nearest hot mix plant is some distance away. These mixtures are favoured as base and surface courses (Thanaya, 2003).

2.2.2.4 Cold Bitumen Emulsion Mixture (CBEM)

CBEM is the most popular type of CMA, using bitumen emulsion as a binder (Thanaya, 2003). It consists mainly of graded mineral aggregate, bitumen emulsion, filler and water. CBEM technology allows mixing, laying and compaction of a mixture with no heat. Contrary to HMA, CBEM experiences some drawbacks including low early life strength, high air voids and long curing times, needing 2 to 24 months to reach its ultimate strength. Accordingly, applications of CBEM have been limited to low/medium trafficked roads, footways and reinstatements work (Leech, 1994; Read and Whiteoak, 2003; Ojum, 2015). Since CBEM is highly sensitive to rainfall at early stages of construction, it is rarely used as a structural pavement layer, particularly in countries with cold, humid and wet conditions like the UK (Doyle et al, 2013). CBEMs show evolution properties, especially during early life, where the initial cohesion is low and builds up progressively, as reported by Serfass et al (2004). In its early life, it exhibits unusual behaviours which are governed by a group of factors, such as the existence of water, reactivity resulting from aggregate-binder film coalescence and cohesion build-up. Thanaya (2003) demonstrated inadequate aggregate coating percentages due to an incompatibility between coarse aggregates and emulsion, as the emulsion is flocculated on the fines portion. CBEMs can also experience problems with binder drainage and binder stripping during storage and compaction because of the low viscosity of the bitumen emulsion (Thanaya, 2003).

2.2.3 CBEM Developments

CBEM is considered to be of a low quality in comparison to HMA, mainly in terms of its mechanical properties, the prolonged period required for curing to achieve an optimal performance and its poor strength at early ages (Dulaimi et al, 2017). Because of this, studies have been implemented to investigate and understand the behaviour of CBEMs and to enhance its poor performance by applying different preparation approaches and incorporating various types of materials.

2.2.3.1 Compaction Improvement

The mechanical performance of CBEMs is directly affected by compaction as adequate compaction is required to achieve optimal performance. Various laboratory compaction methods such as Marshall Compaction, static compaction, vibratory compaction and gyratory compaction have all been used in previous studies to investigate the effect of compaction on their mechanical properties (Needham, 1996; Thanaya, 2003; Niazi and Jalili, 2009; Oke, 2011; Miljković and Radenberg, 2016). Brown and Needham (2000) found that as compaction increased, the degree of emulsion coalescence also increased when using granite aggregate with a 20 mm dense bitumen mixture (DBM) specification. The specification limits of air voids for CBEMs can be achieved by adopting heavy compaction (120 revolution, 240 kPa, 2° angle of gyration) rather than medium compaction (80 revolution, 240 kPa, 2° angle of gyration), as demonstrated by Thanaya (2003). His results also showed that target air void contents of compacted CBEMs (5 to 10%), could be attained by applying 240 gyrations, this categorised as extra heavy compaction. The application of heavy compaction is important to ensure that the emulsion breaks and that the mix achieves adequate strength (Thanaya, 2007). Serfass et al (2004) proved that increasing compaction influences the mechanical properties, as seen in Figure 2.1.

Different studies have discussed the influence of fluid content on the compaction of CBEMs, as the compaction process is complicated due to the presence of both water and bitumen phases. The applied stress due to compaction, has a role in improving the coalescence of bitumen droplets by breaking the narrow gap of the aqueous phase between them (Miljković and Radenberg, 2016). This helps the interface between the bitumen droplets and the aggregate to develop, thus affecting the entire emulsion breaking process. The majority of studies suggest applying heavy compaction to ensure that the emulsion sets, achieves the correct volumetric properties and thereby proper mechanical properties (Khalid and Eta, 1996; Thanaya, 2003; Serfass et al, 2004).

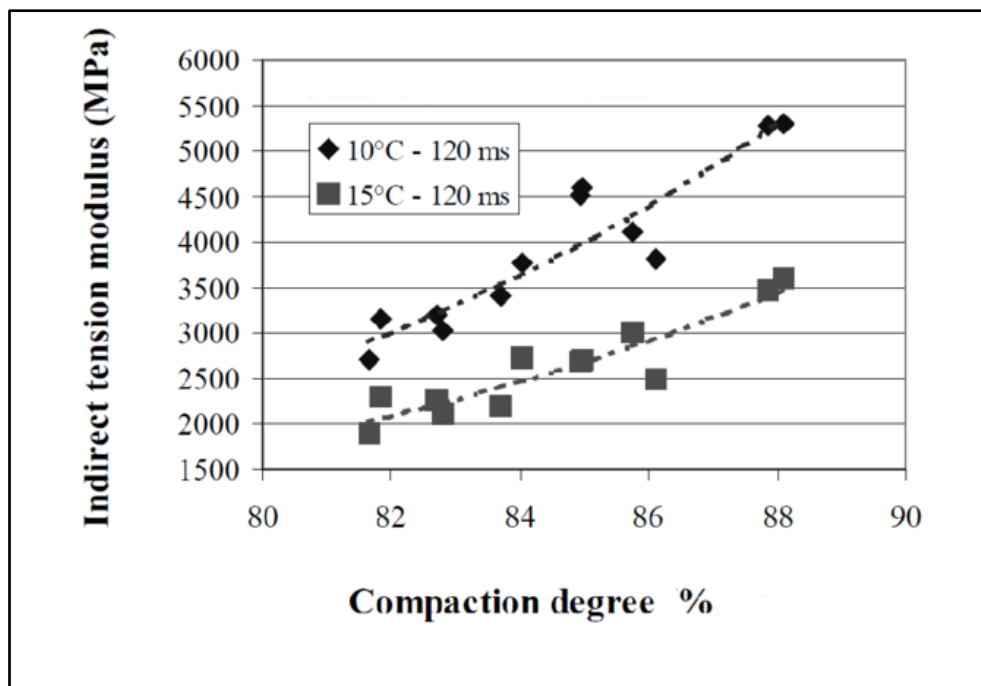


Figure 2.1: The effect of compaction degree on stiffness modulus (Serfass et al, 2004)

2.2.3.2 Improvements by incorporating Fibre Reinforcement & Polymers

The strength and bonding of asphalt mixtures can be improved by adding fibre reinforcement (Ye et al, 2009). The mechanical properties of fibre-reinforced, dense-graded, emulsified asphalt mixtures have been investigated by de S. Bueno et al (2003). Three percentages, 0.1%,

0.25% and 0.5%, of staple polypropylene fibres of 10, 20 and 40 mm, were added to the mixtures. The results indicated that the inclusion of fibres reduces dry density, Marshall Stability and mixture resilient moduli, compared to the mixture with no fibres. Abtahi et al (2010) explained that the role of fibre reinforcement is to increase the tensile strength of the resulting mixtures and extend the strain resistance to fatigue cracking and permanent deformation. However, there are some factors that affect the performance of asphalt mixtures with fibres such as type and content, diameter, length and surface texture (Hesami et al, 2014). An experimental study conducted by Ferrotti et al (2014) examined the characteristics of a high performance CBEM reinforced by three types of fibres, namely cellulose, glass-cellulose and nylon-polyester cellulose, at two percentages, 0.15% and 0.3%, by weight of aggregate. The samples were examined at different curing times; 1, 7, 14 and 28 days, under wet and dry conditions. The results revealed that the mix with 0.15% cellulose fibres showed a comparable, or even better performance than that of the conventional mixture (with no fibres).

Chavez-Valencia et al (2007) addressed the effect of polymer modified emulsion on the compressive strength of CBEMs. In this study, polyvinyl acetate emulsion was added to a rapid setting bitumen emulsion, to enhance the compressive strength of the CBEM. Two types of CBEM were prepared; the first whereby aggregates were coated with a film of asphalt-polyvinyl acetate binder, and the second, the aggregate mixed with a diluted polyvinyl acetate-emulsion to cover them with the polymer. The results revealed that the second type offered a 31% improvement in compressive strength due to the improvement in void contents. Another recent study carried out by Xu et al (2015), was to develop a new AC-13 asphalt mixture using a specially developed, polymer modified emulsifier. It was concluded that the developed mixture met the performance specification requirements in terms of moisture susceptibility and high and low temperature crack resistance, along with an improvement in permanent deformation resistance.

2.2.3.3 Improvements by incorporating Cement

Cement is a very fine, powdery substance that if mixed with other non-cohesive particles in the presence of water, gives a hardened mass. Cement setting and hardening are a result of the hydration process, a chemical reaction between the cement compounds and water, yielding very strong and durable binding materials (O'Flaherty, 2007). Ordinary Portland cement (OPC) is widely used as a replacement to limestone filler (LF) in CBEMs (Niazi and Jalili, 2009; Du, 2015). The incorporation of cement in asphalt concrete mixtures is not a new concept. OPC has been used as a full replacement of conventional filler in warm mix asphalts in order to avoid binder stripping from the pre-dried aggregate. It has also been used to improve the coating of wet aggregate with bitumen or tar (Transport Road Research Laboratory, 1969).

A series of three pioneer studies were conducted by Terrell and Wang (1971), Schmidt et al (1973) and Head (1974), looking at the influence of cement on the resilient modulus of treated CBEMs. Their results revealed that the addition of up to 3% cement accelerated the rate of development of resilient modulus in the early stages of curing, reaching up to 200%, depending on the type of emulsion.

As well as this, the incorporation of cement into CBEMs increased the stiffness modulus, permanent deformation resistance, fatigue cracking resistance (at initial strain below 200 microstrain) and enhanced the moisture sensitivity (Needham, 1996). Milton and Earland (1999) demonstrated that cement could be used either as a primary binder or as a supplementary binder to work as an adhesion agent or assist the enhancement of the short term properties of compacted mixtures. The addition of cement is of substantial value, producing outstanding creep performance and high stiffness modulus in laboratory samples, even after immersion in water.

A further study carried out by Thanaya (2003) investigated the effect of using 1 to 2%, rapid-hardening cement on the mechanical properties of CBEMs. The results showed a significant improvement in strength, resistance to rutting and fatigue at early ages. Oruc et al (2006) and Oruc et al (2007) carried out work to assess the mechanical properties of emulsified asphalt mixtures containing 0 to 6% OPC replacement for mineral filler. The results revealed significant improvements in the mechanical properties with higher OPC content, as seen in Figure 2.2, which led them to propose using cement modified asphalt emulsion mixtures when constructing structural layers. They also stated that with no cement, CBEMs perform poorly and are very sensitive to moisture.

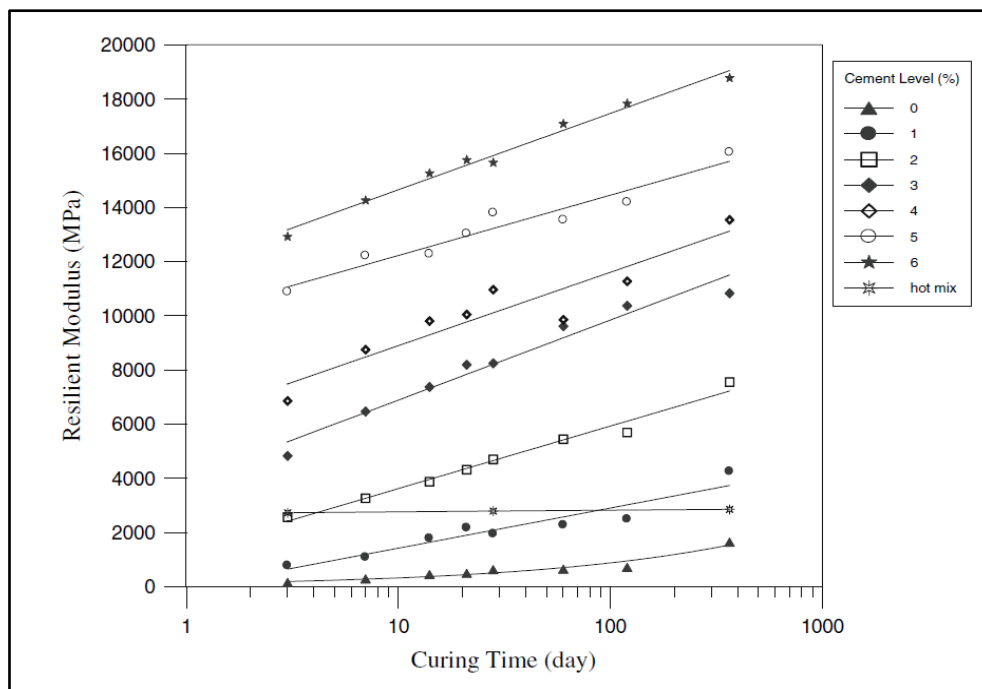


Figure 2.2: Effect of incorporating cement on resilient modulus of the CBEMs (Oruc et al, 2007)

Wang and Sha (2010) also indicated that the micro-hardness of the interface of aggregate and cement emulsion mortar, is influenced by the fineness of cement and mineral filler. A study conducted by Bocci et al (2011) on the effect of temperature on stiffness evolution during the curing stage of CBEM treated with OPC, lead them to deduce that the rate of evaporation of

water increases with an increase in curing temperature, due to the existence of hydraulic material. They also established that treated CBEM has lower thermal sensitivity compared to HMA, meaning that these mixtures experience less distortion and rutting during hot seasons.

CBEMs with various contents of cement have been examined by García et al (2013) using the Marshall stability test and when cured at different humidity levels; 35, 70 and 90% relative humidity (RH). The results showed that samples cured at 90% RH hardened more slowly than samples cured at low RH. Their results also revealed that the combination of cement and asphalt emulsion resulted in a material which had beneficial properties for both asphalt and concrete. They demonstrated that cement causes changes in the pH of the emulsion which leads to it breaking quickly, as seen in Figure 2.3. Wang et al (2013) have studied the influence of pH and water loss on emulsion stability, as caused by cement hydration, finding that the chemical stability of cationic emulsions is strongly influenced by pH value. By increasing the pH value, the charge and cationic emulsifiers on bitumen droplets are rapidly broken down, leading to fast flocculation and coalescence of the emulsion.

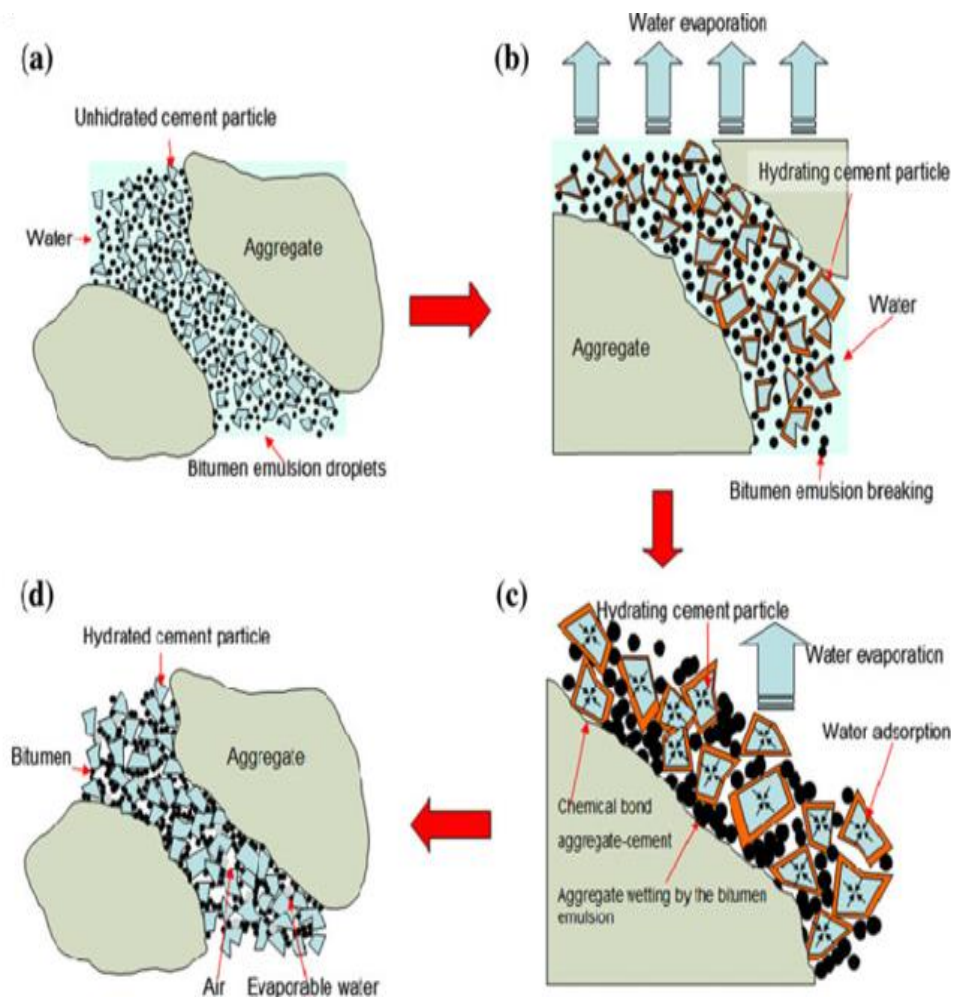


Figure 2.3: Schematic diagram representing the hardening process of an asphalt-emulsion composite (García et al, 2013)

A new cement treated CBEM, made with a gap grading, was developed by Al-Hdabi et al (2014a), using OPC as a full replacement of conventional mineral filler. They investigated the mechanical properties and water damage resistance of the developed mixture, the results showing significant improvements in mechanical properties, water damage resistance and temperature susceptibility. A study carried out by Fang et al (2016a) aimed at accelerating the improvement of mechanical properties of CBEMs by using rapid hardening cement. They found that the improvements in the mechanical properties of CBEM incorporating calcium

sulpho-aluminate and calcium aluminate cement after one day of curing, were comparable to those containing OPC but achieved after one week of curing.

From previous studies, it can be seen that cement has been widely used to enhance the properties of CBEMs. However, the production process of cement, consumes a massive amount of energy which creates a negative impact on the environment (Schneider et al, 2011), responsible for 5% of total global carbon dioxide emissions (O'Rourke et al, 2009). Accordingly, researchers and industrial companies are paying a great deal of attention to the use of waste and by-product materials as a replacement, or partial replacement, for cement (Ravikumar et al, 2010).

2.2.3.4 Improvements by incorporating Waste and By-product Materials

The use of waste or by-product materials as a filler replacement in the road construction industry, particularly in the manufacture of CBEMs, facilitates economic and ecological gains as these materials have low, or no, manufacturing costs and the reuse of these materials will reduce the need for expensive disposal. These materials are technically classified into two types depending on their reactivity; hydraulic and pozzolanic materials. Hydraulic materials react with water and generate cementitious products, while pozzolanic materials do not react with water as they do not have any cementitious properties but when mixed with cement or any other cementitious materials, they will react to form cementitious products.

Several studies have been conducted to investigate the use of waste and industrial by-product materials to replace LF in conventional CBEMs. In a study carried out by Thanaya (2003), different waste materials were introduced to CBEMs to improve their mechanical properties. It was established that red porphyry sand and synthetic aggregates made from sintering quarry fines and crushed glass, can easily be incorporated into CBEMs as they will offer satisfactory stiffness values.

In the same research, Thanaya (2003) found a risk if using steel slag as it leads to an expansion in volume in wet conditions. Later, Thanaya et al (2006) used pulverized fly ash (PFA) as a filler in CBEMs at full curing conditions. The results here showed that the CBEMs' stiffness was comparable to a hot mix, confirming its suitability for use.

Recently, paper sludge ash (PSA) waste cementitious materials were added to cold graded emulsified asphalt mixtures by Al-Busaltan et al (2012). The results revealed that the stiffness modulus, resistance to permanent deformation and water susceptibility were improved specifically when more than 50% of the new cementitious materials were used as a replacement for limestone filler. A laboratory study using a waste domestic fly ash, namely LJMUF-A1, was conducted by Al Nageim et al (2012). This material was used as a replacement for conventional limestone filler and was found to generate a second binder from the hydration process between LJMUF-A1 and the trapped water.

Al-Hdabi et al (2013) conducted a study to improve the properties of gap graded, cold rolled asphalt (CRA) which included a waste fly ash (WFA) as a filler replacement, also adding a high silica by-product material as an activator. The results showed a promising enhancement to the mechanical properties of the CRA in terms of moisture damage resistance, stiffness modulus and uniaxial creep tests. Dulaimi et al (2016c) developed a binary blended filler material, produced from high calcium fly ash and high silica-alumina material, namely fluid catalytic cracking catalyst (FC3R). It was found that using such materials provides improvements in microstructural integrity thereby providing fast-curing, cold asphalt concrete for binder course mixtures. Improvements in the mechanical properties of CBEMs using binary and ternary blended fillers (BBF and TBF), has been investigated by Nassar et al (2016). The BBF consisted of fly ash and ground granulated blast-furnace slag (GGBS), silica fume (SF) added to the BBF to produce TBF. The results showed that the TBF achieved more

improvements in mechanical and durability properties in comparison to BBF. The addition of SF has been found to accelerate the generation of hydration products.

More recently, a new, fast curing and environmentally friendly CBEM for binder courses was developed by Dulaimi et al (2017). A waste alkaline NaOH solution was used to activate the binary blended filler to generate an alkali-activated, binary blended filler. Substantial improvements were achieved regarding mechanical properties and water sensitivity in the developed CBEM.

2.2.4 Curing of CBEMs

Curing conditions have a critical impact on the performance of CBEM, its strength and stiffness, as reported in the literature (Needham, 1996; Thanaya, 2003; Oruc et al, 2007; Bocci et al, 2011). Specific curing times are required for CBEMs to build up their ultimate mechanical properties, as seen in Figure 2.4 (Bocci et al, 2011). The evolution process in ITSM values includes breaking of the emulsion, loss of moisture and hydration of cementitious materials when treating CBEMs with cement/cementitious materials (García et al, 2013).

Jenkins (2000) characterised the curing process in three ways; water loss over evaporation, particle charge repulsion and pore pressure induced flow paths. The reduction in moisture content results in an increase in the strength of the mix. The curing process itself is affected by several parameters, as reported by Jenkins and Twagira (2008). These include climatic parameters i.e. temperature, humidity and wind, aggregate gradation and properties, type and thickness of the layer, initial water content, binder content, filler type, drainage conditions and traffic loads.

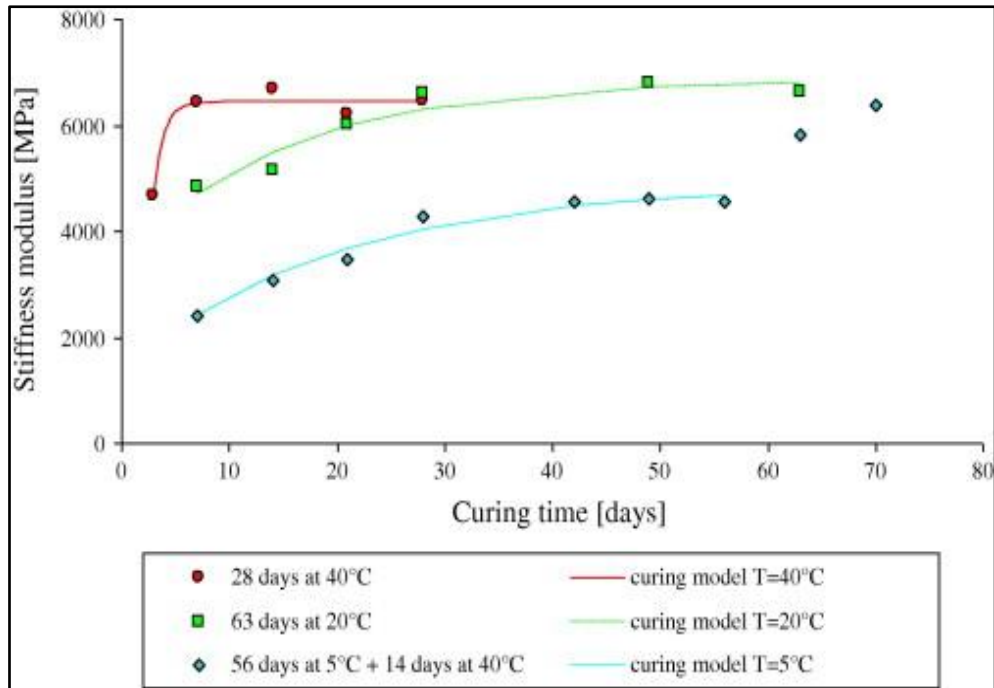


Figure 2.4: ITSM evolution as a function of curing time and temperature (Bocci et al, 2011)

Kim et al (2010) showed that the strength gained by CBEMs is directly related to moisture loss, this being obvious at higher temperatures over time. This is true when the CBEM includes inert LF, while in the case of an active filler such as cement, the story is different as the hydration process requires the existence of water. Excessive evaporation due to high temperature, can hinder the full potential of the cement hydration process, as confirmed by Bocci et al (2011). Their results showed that specimens subjected to a high curing temperature, had less resistance to moisture damage, attributing this behaviour to the lack of uniform density of hardened cement at high curing temperatures. This resulted in weaker regions in the microstructure of CBEM, as indicated by Rovnaník (2010).

With most laboratory curing protocols used by previous researchers, common curing temperatures are 20°C and 40°C. The performance of CBEMs is considerably improved when both curing temperature and time are increased: 14 days curing at 20°C is more or less comparable to 7 days curing at 40°C (Bocci et al, 2002). Serfass et al (2004) assessed and

compared different curing procedures, proposing an accelerated curing of 14 days at 35°C to be suitable for road engineers, this in line with the view that curing at temperatures higher than 50°C dries the samples too quickly causing premature failure. Cardone et al (2015) investigated the curing process of CBEMs treated with cement by analysing the influence of cement dosage and curing temperature (20°C and 40°C) on moisture loss and evolution of complex modulus. Their findings revealed that the increase in stiffness of the mixtures was controlled by moisture loss through the evaporation process, as higher temperatures accelerated the curing process.

2.3 Bitumen Emulsion Technology

The early part of the 20th century witnessed the creation of bitumen emulsion production and application in road construction (James, 2006). Today, this technology has gained worldwide attention due to the low temperature required for application, hence reducing energy consumption and greenhouse gas emissions. Regardless of the application, bitumen should behave as a liquid to increase workability and facilitate the mixing process. This can be achieved by reducing its viscosity using four main methods: bitumen heating, bitumen fluxing with flux oil (cutback bitumen), bitumen foaming (foamed bitumen) and bitumen emulsification (bitumen emulsion) (Read and Whiteoak, 2003).

Emulsions are a class of dispersion systems consisting of two immiscible liquids, one of which is usually water (Akzo Nobel, 2008). According to James (2006) and Akzo Nobel (2008), emulsions can be classified into three categories which depend on the nature of the dispersed phase: i) oil-in-water (O/W) in which the dispersed phase is an oily liquid and the continuous phase is water; ii) water-in-oil (W/O) in which the continuous phase is oil and the dispersed phase is water, and iii) multiple phase emulsion in which the dispersed droplets themselves contain smaller globules of a third phase, usually the same liquid as the continuous phase.

In the case of bitumen emulsion, the bitumen is dispersed in a continuous water phase as minute droplets of 0.1 to 50 μm diameter, stabilized by an emulsifier. The emulsifier keeps the bitumen droplets in permanent suspension by supplying them with electrostatic charges (Read and Whiteoak, 2003). A diagram of typical bitumen emulsion particle size distribution is shown in Figure 2.5. The particle size distribution of a bitumen emulsion is affected by its constituents and the manufacturing parameters at the plant (Gingras et al, 2005). Hu et al (2009) stated that particle size distribution not only affects physical properties such as viscosity and storage stability of the emulsion, but is key for interactions with cement in bitumen emulsion bound

asphalt mixtures. Therefore, smaller particle size leads to improve performance in both mixture and spray applications (Salomon, 2006). Accordingly, the ability to control particle size distribution during the emulsification process influences the properties of the emulsion.

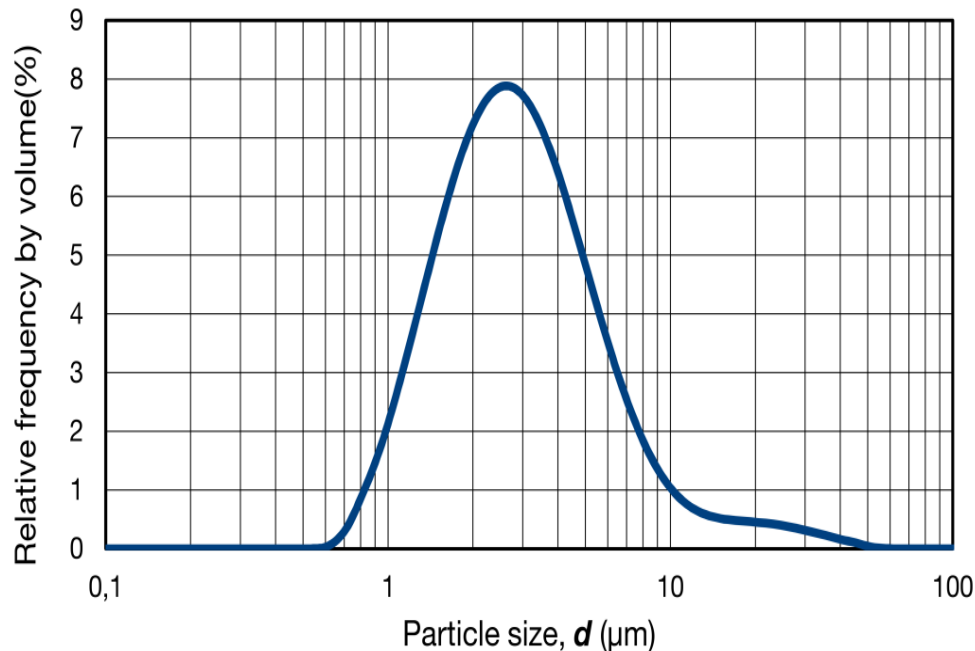


Figure 2.5: Typical particle size diagram of bitumen emulsion droplets (Miljković, 2014)

2.3.1 The Benefits of using Bitumen Emulsion

The use of bitumen emulsions results in the following benefits:

- High viscosity bitumen is retained in a form which can be handled and applied at low temperatures.
- The possibility of thermal degradation of the binder is minimised because of the low temperature of application and storage.
- It has ‘built-in’ wetting and adhesion properties.
- It improves safety when used in pavement construction because it is applied at a low temperature, minimising fume and burn hazards.

- Since bitumen emulsion does not need heat, there are no issues regarding flammability during its storage, transportation and paving.
- It reduces the use of energy as no heat is required during application.
- It possesses anti-stripping properties.

2.3.2 Composition of Bitumen Emulsions

2.3.2.1 Bitumen and Water

Bitumen is the basic component of a bitumen emulsion; it makes up between 50 and 75% of the emulsion. The grade, or hardness of a bitumen, significantly affects the finished emulsion. Most emulsions are made with bitumen in the range of 40 to 250 penetration (Salomon, 2006). Occasionally, climatic conditions may influence the type of base bitumen to be used as low viscous base bitumen is suitable for colder climates and vice versa (James, 2006). That aside, compatibility of the emulsifying agent with the bitumen is crucial to produce a stable emulsion. Bitumen is a colloid composed of large hydrocarbon molecules (Dulaimi, 2017). The interactions of these molecules are complex, which makes it almost impossible to predict precisely the behaviour of the bitumen to be emulsified; quality control is necessary during the manufacture of bitumen emulsion.

Water is the second largest ingredient in a bitumen emulsion, comprising 25 to 50% of the emulsion (James, 2006), contributing to the desired properties of the finished product. It may contain minerals that positively or negatively affect the production of stable emulsions, for example, magnesium and calcium ions are beneficial for the formation of a stable cationic emulsion, while they can be harmful in anionic emulsions. As such, impure water should not be used in emulsion manufacture as it results in an imbalance of the components of the emulsion components, which adversely affects the properties of the final product. However, pure drinking water might not be an option in the manufacture of bitumen emulsions.

Water is a polar medium comprising of ionic molecules such as H_3O^+ , OH^- and H^+ , as well as the polar water molecule itself. Therefore, when mixing water and bitumen under normal circumstances, the compound will separate quickly after mixing. This separation happens because the molecules in the polar medium tend to connect to each other to eliminate positive and negative charge regions. In order to achieve stability, an emulsifier should therefore be added.

2.3.2.2 Emulsifiers

Emulsifiers, or surfactants, are surface-active agents which are considered the most important component required to produce a homogeneous emulsion. They make up between 0.1 and 2.5% of a bitumen emulsion and can be defined as a water-soluble chemical whose existence in a solution significantly changes the properties of the solvent and the surface it contacts (Asphalt Institute, 2008). The properties of the bitumen emulsion are highly dependent on the properties and the contents of the emulsifier. A large interfacial area between water and bitumen phases will be created during the production of bitumen emulsion; approximately $500 \text{ m}^2/\text{l}$ (Boussad and Martin, 1996). The essential roles of an emulsifier are as follows (Read and Whiteoak, 2003):

- Facilitates bitumen dispersion in water by reducing the interfacial energy between the bitumen and water phases.
- Keeps the bitumen droplets in permanent suspension by forming a barrier between the water and bitumen.
- Provides each bitumen droplet with an electrical charge.
- Enhances the mechanical properties of the emulsion such as the tendency to settle and adhesivity.

A typical emulsifier has two groups of molecules: a hydrophilic (water-loving) ‘head’ group and a hydrophobic (oil-loving) ‘tail’ group (James, 2006). The tail group comprises a long hydrocarbon chain (R), consisting of 8 to 22 atoms, which orients towards the oily bitumen phase, while the head group orients towards the water phase.

Chemical surface agents can be classified into three types according to their dissociation characteristics in the water. These are:

I. Cationic Emulsifiers

Typically, these emulsifiers are acidic systems ($\text{pH} < 7$). The electrovalent and polar head group are positively charged and imparts a positive charge to the surfaces of the bitumen droplets. A typical example of this kind of emulsifier is octadecyl ammonium chloride ($\text{CH}_3(\text{CH}_2)_{17}\text{NH}_3^+\text{Cl}^-$), which dissociates in water into positive $\text{CH}_3(\text{CH}_2)_{17}\text{NH}_3^+$ and anion chloride (Cl^-), as seen in Figure 2.6.



II. Anionic Emulsifiers

These emulsifiers are generally alkaline systems ($\text{pH} > 7$). The electrovalent and polar head group is negatively charged, imparting a negative charge to the surfaces of the bitumen droplets. An example of an anionic emulsifier is sodium stearate ($\text{CH}_3(\text{CH}_2)_{16}\text{COONa}$), which dissociates in water into negative stearate anions ($\text{CH}_3(\text{CH}_2)_{16} \text{COO}^-$) and positive sodium cations (Na^+).



III. Non-ionic Emulsifiers

In non-ionic emulsifiers, the hydrophilic head group is a covalent polar and dissolves without ionisation. Any charge on the bitumen emulsion droplets, is derived from ionic species in the bitumen itself. It is rarely used for road emulsions.

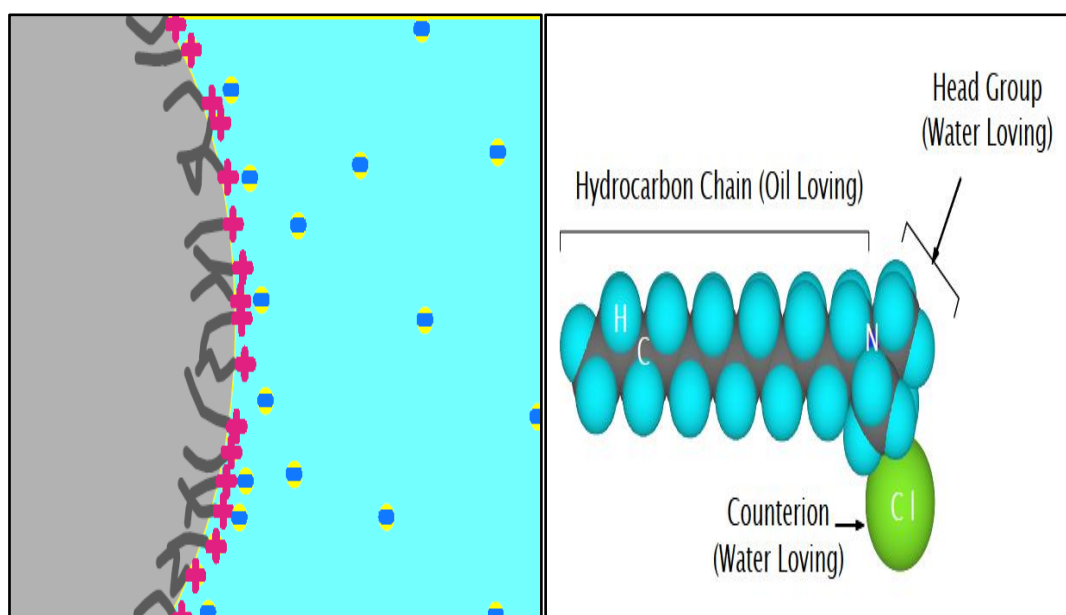


Figure 2.6: Schematic diagram of charges on a bitumen droplet and the structure of a cationic emulsifier (James, 2006)

2.3.2.3 Stabilizers

Due to insufficient desalting of crude oil, bitumen may contain salt which causes bitumen droplets to swell through osmosis by which water is pulled into the bitumen droplet. This phenomenon increases emulsion viscosity and affects its stability. Calcium chloride, or other soluble salts, is added at 0.05 to 0.2% into the water phase of the cationic emulsion to reduce the effect of water osmosis. Tri-sodium polyphosphate is used in anionic emulsions for the same purpose.

2.3.2.4 Solvents

Solvents may be added to bitumen emulsions to improve emulsification, minimize settlement, and enhance curing rates at low temperatures or to provide the right binder viscosity after curing (James, 2006). Solvents such as white spirit will improve coating ability, as reported by Thanaya (2003).

2.3.2.5 Sodium Tripolyphosphate

To improve the quality of the emulsion, sodium tripolyphosphate is included at 0.1% as a water softener in anionic emulsions which are sensitive to hard water (Akzo Nobel, 2008).

2.3.2.6 Thickeners

The task of these additives which are water soluble in the emulsion, is to increase the viscosity of the emulsion and decrease the escape of the emulsion in open graded mixes. They may be added at 0.02 to 0.20% to the water phase or to the finished emulsion. The type of thickener should be chosen carefully as it influences the breaking and adhesion of the emulsion (Akzo Nobel, 2008).

2.3.2.7 Adhesion Promoters

These additives are included in the emulsion to promote the adhesion of the bitumen to the aggregates, which in turn, reduces the risk of stripping. They can be added to the bitumen, or to the finished emulsion. Surface active amine compounds are often used as promoters (James, 2006).

2.3.2.8 Asphalt Peptizer

Many benefits can be gained by adding asphalt peptizer to the emulsion including; improvements in the quality of the emulsion by enhancing emulsifiability, creating smaller

droplets, decreasing settlement, increasing viscosity and improving adhesion (Thanaya, 2003). Regarding paving grade emulsions, the most common peptizers are styrene butadiene rubber, poly-chloroprene and natural rubber latex (James, 2006).

2.3.2.9 Latex

Latex is a water-based dispersion of polymer which is used to modify emulsions. Bitumen properties such as cohesion, crack resistance at low temperatures and resistance to flow at high temperatures, are improved when a polymer is added. However, considerable care should be taken when selecting the type of latex as it should be harmonized with the emulsion. Latex is available in cationic, non-ionic and anionic forms (Akzo Nobel, 2008).

2.3.3 Categories of Bitumen Emulsion

According to the sign of the charge on bitumen globules, bitumen emulsions are classified into four categories (Read and Whiteoak, 2003):

- Cationic bitumen emulsion
- Anionic bitumen emulsion
- Non-ionic bitumen emulsion
- Clay-stabilized bitumen emulsion

Cationic bitumen emulsion is commonly used in road construction. It has positive charges on bitumen globules, while the bitumen droplets of anionic emulsions have negative charges. Non-ionic emulsions include bitumen particles with neutral charges. Clay-stabilized emulsions are often emulsified by fine powders which are natural or processed clays, or bentonites.

Cationic emulsion, which is under consideration in this study, is more effective than anionic emulsion in terms of coating aggregates in all weather conditions. The positively charged

bitumen droplets in cationic emulsions are more attracted to negatively charged aggregates such as granite. However, there is no attraction between negatively charged anionic emulsifiers and the negatively charged surface of idealized granite (O'Flaherty, 2007). A non-ionic emulsion is rarely used in highway applications while clay-stabilised emulsions are used for industrial applications.

Bitumen emulsions are also classified into three groups according to their reactivity: i) Rapid setting (RS) emulsion sets quickly once in contact with clean aggregates of low surface area and is normally used in chip seals (surface dressing); ii) Medium setting (MS) emulsion usually sets less quickly than RS and can be mixed with aggregates with low surface area such as open graded mix, and iii) Slow setting (SS) emulsion, which mixes with reactive aggregates of high surface area (James, 2006).

2.3.4 Manufacturing Process of Bitumen Emulsions

When producing emulsion, it is necessary to keep the viscosity of the bitumen at a suitable level for emulsification. As such, it is usually heated to between 120 and 180°C, corresponding to a viscosity of 0.2 Pa.s (2 poise) (Sjoblom, 2005). Most emulsifiers are either unstable or have a very short lifespan at these temperatures. Therefore, the common practice in bitumen emulsification is to mix the emulsifier into the water phase (Miljković, 2014). To avoid boiling the water and exceeding the emulsifier thermal stability demands, the temperature of the water phase is adjusted so that the temperature of the resultant emulsion is less than 90°C (Read and Whiteoak, 2003). However, in practice, this varies between 45°C and 60°C, as reported by Miljković (2014).

Two processes are usually used to manufacture bitumen emulsions; continuous or batch processing. Most bitumen emulsions are produced in a continuous processing plant which sees the controlled mixing of water, emulsifier and bitumen using a colloid mill. In the colloid mill,

the hot bitumen and the emulsifier solution are fed separately, but simultaneously, and a high shear action is produced by a high speed conical disc (rotor) (Read and Whiteoak, 2003). Depending on the geometrical properties of the mill and the desired particle size distribution, the revolution speed of a stationary part (stator) ranges from 1,000 to 10,000 min^{-1} . The typical clearance between rotor and stator is between 0.25 and 0.50 mm and is usually adjustable. The shear force applied by the colloid mill, helps to break up the bitumen and emulsifier mixture into small droplets, which assists in coating the bitumen globules with emulsifier and initiates electrical charges on said globules. The resulting electrostatic forces prevent the globules from coalescing (Read and Whiteoak, 2003).

In batch mixing, the colloid mill is replaced by a static mixer, initiating the globules from a highly turbulent flow. The required shear is generated from a series of baffles that result from pumping the bitumen at high speed. The batch process can be used to produce small volumes of emulsion (Read and Whiteoak, 2003). The manufacturing processes of cationic emulsions are demonstrated in Figure 2.7. They are very similar to anionic emulsion manufacturing processes.

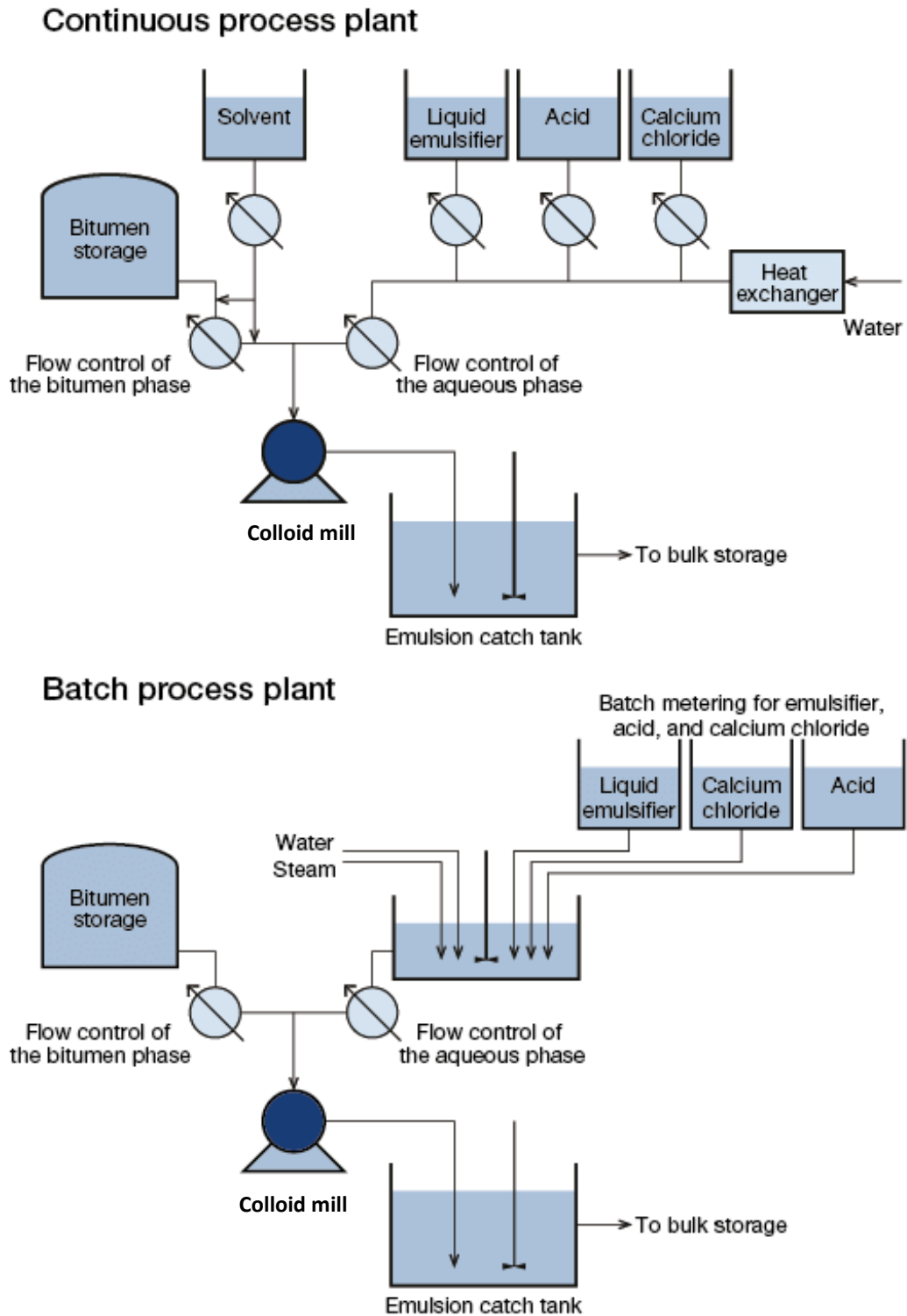


Figure 2.7: Schematic diagram illustrating continuous and batch process plants for manufacturing bitumen emulsions (Read and Whiteoak, 2003)

2.3.5 Properties of Bitumen Emulsions

The most important properties of bitumen emulsions are stability, viscosity, breaking and adhesivity (Read and Whiteoak, 2003). A typical emulsion will be stable under storage, transport and application conditions, but will break (separated from the aqueous solution and form a thin film cover materials) rapidly after application, leaving a binder with the properties of the original bitumen adhering to the aggregate. Although it is generally assumed that the bitumen recovered by the breaking of the emulsion is the same as the bitumen that was used to produce the emulsion, there are exceptions. The emulsifier used may modify the recovered bitumen, specifically, its surface-dependent properties such as adhesion. The properties of the recovered bitumen can be addressed by modifiers (Miljković, 2014).

2.3.5.1 Stability of Bitumen Emulsions

Emulsion stability is a measure of the ability of a particular emulsion to resist change to its properties over time. In a stable emulsion, the properties of the emulsion will change more slowly over time, various physical and chemical processes contributing to stability. Emulsion stability is very important in storage, transport and use (Dehghan, 2009). Several processes are involved when the system approaches a state of equilibrium. Typically, settlement, flocculation and coalescence take place simultaneously at fairly well defined rates, continuously changing the properties of the system.

- *Settlement*

Under normal circumstances, the grades of bitumen normally used in emulsions have a density that is slightly greater than that of the aqueous phase of the emulsion. Consequently, bitumen globules tend to separate and settle in the aqueous phase, resulting in a bitumen-rich lower layer and a bitumen-deficient upper layer (Read and Whiteoak, 2003). Bitumen emulsions can

be said to be stable in storage until this settlement starts (Thanaya, 2003). The two main factors that hinder or accelerate settlement are gravity and the repulsive/attractive forces between bitumen droplets, produced by the layers of emulsifier on the droplets.

Bitumen emulsions with low bitumen content and low viscosity are more prone to settlement. Bitumen emulsions with high bitumen content (between 67 and 70%), generally have fewer problems with storage stability than those with a low bitumen content (from 40 to 60%) (Sjoblom, 2005). This can be explained as most of the spaces in the former are filled by bitumen particles such that there is practically no room for settlement to occur, while the distance between the bitumen droplets in the latter is so large, that it is almost impossible to avoid settlement. However, bitumen emulsions with low bitumen content are widely used, thus some settlement must always be expected. This emphasises the importance of agitating the emulsion carefully before use.

One method of reducing settlement is to equalize the density of the two main constituents by adding a salt, for example calcium chloride, to the aqueous phase. Another way to reduce settlement is by reducing the mean particle size, or the range of particle sizes, as larger particles settle faster (Read and Whiteoak, 2003). The risk of settlement during pumping, transport and agitation is increased when the bitumen droplets are larger than approximately 10 μm as they are more sensitive to mechanical stress.

- *Flocculation and Coalescence*

Settlement represents the first stage of emulsion instability and is followed by flocculation and coalescence. Bitumen globules in emulsions have small charges from both the emulsifier and ionisable components in the bitumen itself. These small charges on the droplets provide an electrostatic barrier when they are close to each other. However, if two droplets do achieve

enough energy to overcome this barrier and get close, they adhere to each other, i.e. flocculate. Flocculation is defined as the aggregation of bitumen droplets (with no change in the original droplet size) into larger units. Flocculation can be reversed by agitating, diluting or adding more emulsifier.

Over time, the water layer between droplets in a floccule will become thinner and the droplets will coalesce. Coalescence is described as the process of thinning and disruption of the liquid film between the particles resulting in the fusion of two or more droplets (Akzo Nobel, 2008). This process is irreversible and eventually results in a complete separation of the emulsion into two distinct liquid phases. The process of flocculation and coalescence of a bitumen emulsion is illustrated in Figure 2.8.

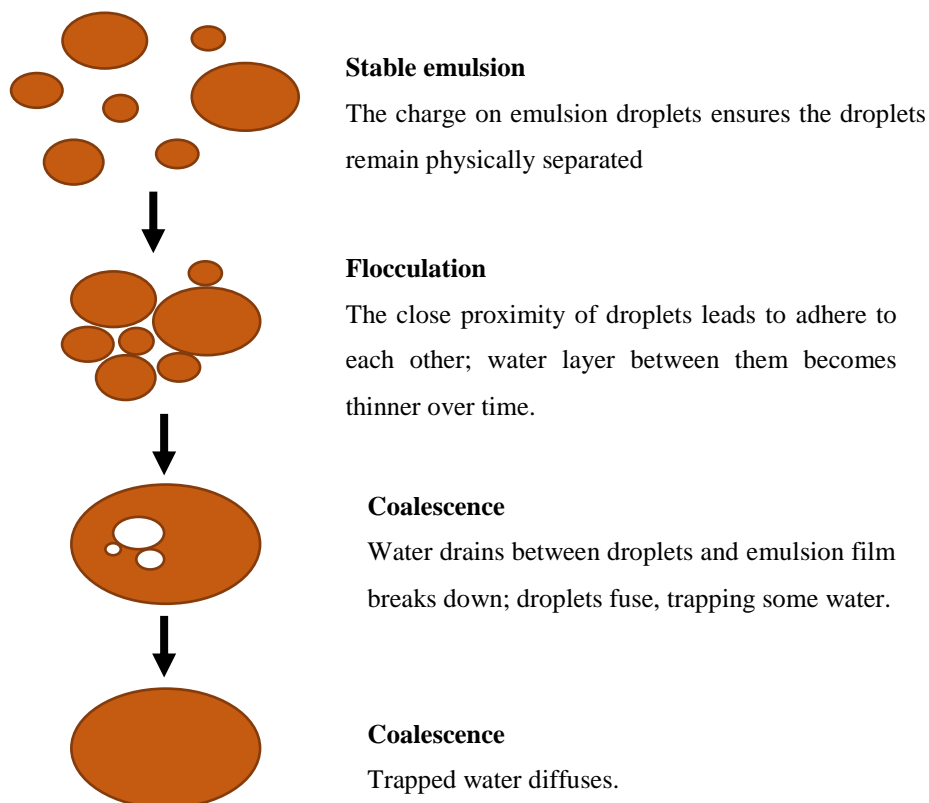


Figure 2.8: Schematic diagram illustrating the destabilising process of a bitumen emulsion

(Akzo Nobel, 2008)

2.3.5.2 Viscosity of Bitumen Emulsions

The viscosity of bitumen emulsions is of primary importance as they are almost always applied by spraying, either for surface dressing or when mixing with aggregates. It should be low enough to permit even spraying, but at the same time, high enough to prevent escape from the aggregate surface once it is sprayed and mixed (Sjoblom, 2005). The particle size distribution of the emulsion is dependent on the flow rate through the mill, especially when the bitumen content is higher than 65%. Particle size distribution and viscosity change as a result of packing bitumen globules relatively closely together.

Emulsions with a high concentration in the disperse phase (bitumen), seldom have Newtonian viscosity characteristics, i.e. apparent viscosity changes when the shear rate changes. Emulsion viscosity is fairly independent of bitumen viscosity and because of that, emulsions with hard bitumen (< 10 pen), which are easily poured at 10°C, can be manufactured (Read and Whiteoak, 2003). The effect of increasing bitumen concentrations at low level content is small. However, at high bitumen contents, a small increase in concentration can induce a dramatic alteration in viscosity, which may get out of control (Read and Whiteoak, 2003).

The viscosity of a bitumen emulsion is strongly dependent on aqueous phase composition (Sjoblom, 2005). The viscosity of conventional cationic emulsions can be increased by decreasing the acid content or increasing the emulsifier content. However, controlling the salt content in bitumen may produce an osmotic effect which will drag water inside the bitumen particles, resulting in an expansion of the particles and a decrease in the continuous water phase, this resulting in a rise in viscosity. This effect can be overcome by adding a small amount of a salt, for example calcium chloride, in the aqueous phase, this helping to decrease osmotic pressure. Special additives can also be used as viscosity modifiers (Read and Whiteoak, 2003; Sjoblom, 2005).

2.3.5.3 *Breaking of Bitumen Emulsions*

Bitumen emulsion should be converted to continuous bitumen-film coating aggregate particles to act as a binder in road materials. This requires separation from water, adherence to the aggregate surface and bonding of the aggregate particles (Needham, 1996). This process is described as breaking of the emulsion and it involves a number of steps as follows (Sjoblom, 2005):

- Destabilisation of the emulsion through adsorption of emulsifiers on the added mineral aggregate;
- Agglomeration of emulsion particles forming a solid, non-tacky and brittle material (a so called cheesy state);
- Coalescence of bitumen droplets resulting in increased stiffness of the bitumen;
- Complete water evaporation giving full adhesion to the aggregate surface and full strength of the asphalt mixture.

The breaking process varies depending on the type of application. In some applications, a fast-break is preferred, while in others, a delayed process is preferred. For example, in surface dressing applications, breaking should be as fast as possible, creating good adhesion to the aggregate. Conversely, the breaking process in bitumen emulsion bound asphalt mixtures must be delayed to allow enough time for transportation, application and compaction after the aggregates have been mixed with the bitumen emulsion. After compacting, breaking should occur as quickly as possible to produce the properties required by the layer to sustain traffic as soon as possible, preferably within hours rather than days (Sjoblom, 2005).

Different explanations of the breaking mechanism are described in the literature including breaking under the influence of the adsorption of emulsifiers, breaking due to evaporation of the water (drying) and breaking due to pH change.

➤ ***Breaking Due to Adsorption of Emulsifiers***

Emulsifier molecules are found in both the water and on the surface of the droplets in a bitumen emulsion. Some emulsifier ions form micelles and, in a stable emulsion, equilibrium exists, as shown in Figure 2.9. As soon as these emulsifier ions are adsorbed by oppositely charged mineral aggregates, this equilibrium will end. Therefore, the breaking rate of the emulsion depends on the adsorption rate of emulsifiers into the mineral aggregate, which is controlled by the surface area and chemical nature of the mineral aggregate (Thanaya, 2003). This starts the breaking process, as shown in Figure 2.10. A point is reached where the charge on the surface of the droplet is so depleted that rapid coalescence takes place. At the same time, the layer of emulsifier sticking to the aggregate will make the surface hydrophobic, promoting coating of the aggregate by the liberated hydrophobic bitumen. The emulsifier here is acting as an adhesion promoter. The adherence between the bitumen and the aggregate is just enough to squeeze the water from the system.

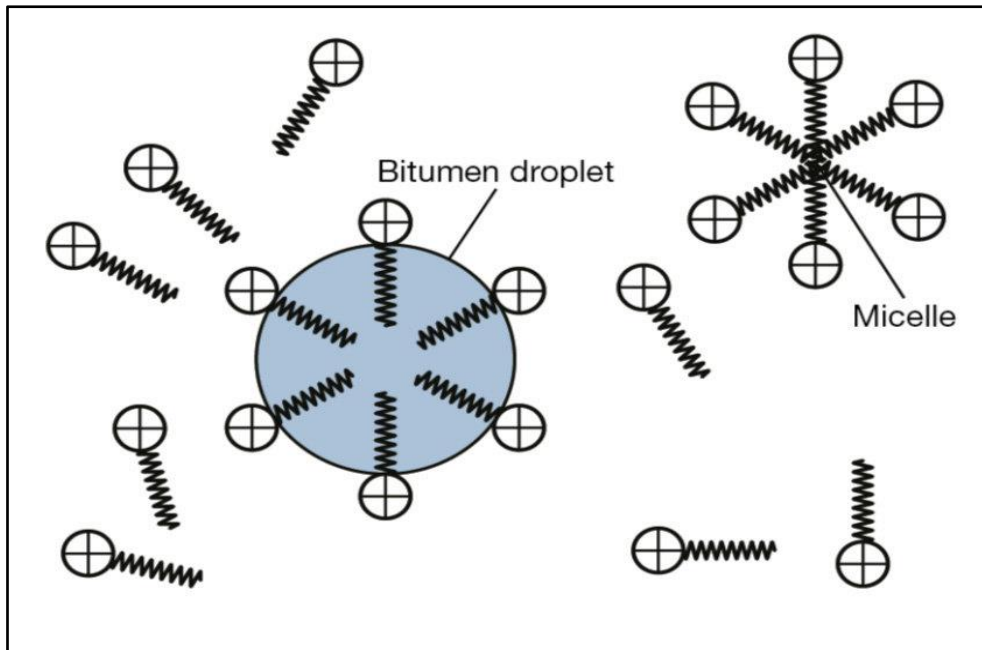


Figure 2.9: A schematic diagram illustrating emulsifier ions forming a micelle in a stable emulsion (Read and Whiteoak, 2003)

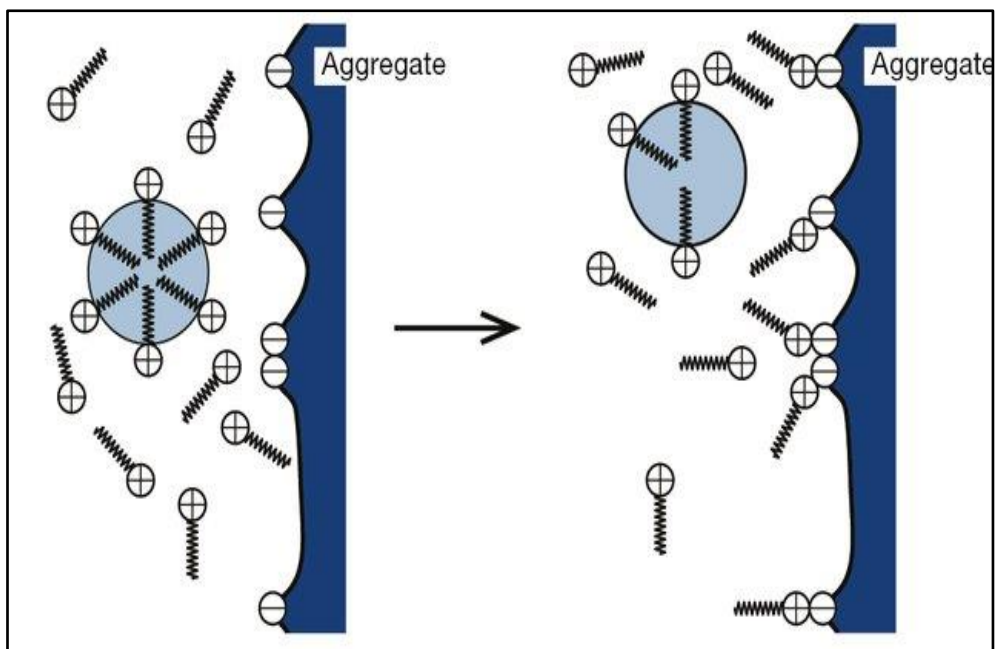


Figure 2.10: A schematic diagram illustrating the breaking process (Read and Whiteoak, 2003)

➤ ***Breaking Due to Water Evaporation***

The breaking of an emulsion is heavily influenced by the evaporation of water from the emulsion system. This, in turn, is influenced by environmental conditions such as temperature, humidity and wind velocity. Water evaporation resulting in an increase in the concentration of the bitumen droplets with more direct contact between droplets. As the bitumen droplets start merging, the interfacial area decreases. Emulsifiers spread from interfaces to the solution, forming emulsifier micelles. The process of water evaporation can take years as water can be trapped in closed pores within the bitumen this explaining why CMA continuous to gain strength even after many years.

➤ ***Breaking Due to pH Change***

The speed of the emulsion break is influenced by the type and concentration of emulsifying agent used in the manufacturing process (Das, 2008). Since emulsifier soaps are created by altering emulsifiers with acids or alkalis, the surface charge of the emulsifier depends on the pH. For example, fatty amines, known as cationic emulsifiers, are insoluble in water but soluble in acid. They are usually dissolved by hydrochloric acid (HCl) to obtain a water soluble soap. This soap is then blended with hot bitumen in a colloid mill to produce bitumen emulsion. This means that emulsifiers may lose their function soon after cationic emulsions come into contact with mineral aggregates, or cement particles, due to a rise in pH. When cement is blended with cationic emulsion, the pH can be reversed immediately. The stability and setting time of bitumen emulsions are usually evaluated using cement; however, it should be noted that some emulsifiers such as quaternary amines, do not lose their function when the pH is changed (Salomon, 2006).

In conclusion, it has been shown that cationic emulsions break chemically when in contact with aggregates with the aid of emulsifiers. Cationic emulsifiers work as adhesion and anti-stripping agents, the breaking mechanism being highly dependent on emulsifier adsorption and a rise in pH. For anionic emulsions, the breaking mostly depends on the evaporation of volatiles through the emulsion system. This takes longer, and less adhesion can be expected in comparison to cationic breaking mechanisms.

2.3.5.4 Adhesivity of Bitumen Emulsions

The amount of adhesion between the bitumen emulsion and aggregates is determined by how much surface area is coated in emulsion. In all applications using bitumen, it is essential that the bitumen adheres to the surface of the aggregate. This will not be achieved unless the aggregate surface is slightly damp to ensure easy distribution of the emulsion over the aggregate surface. According to Read and Whiteoak (2003), the adhesion, or bonding quality between emulsion and aggregate, is influenced by several factors:

- The type and amount of emulsifier.
- The grade of bitumen and its components.
- The pH of the emulsifier solution.
- The particle size distribution of the bitumen droplets in the emulsion.
- The type of aggregate.

The appropriate selection of an emulsifier can improve the situation since certain cationic emulsifiers displace water from the surface and promote good adhesion between the bitumen and the aggregate. Cationic emulsifiers are preferable for acidic aggregate surfaces such as granite and quartzite, while anionic emulsifiers are appropriate for basic aggregates like

limestone or basalt. That said, cationic emulsions have a good affinity with all types of aggregate, as shown by various studies.

2.3.6 Applications of Bitumen Emulsions

As a result of the development of CBEM technology and the demand for bitumen emulsions for different applications, the consumption of bitumen emulsion is rising. Worldwide emulsion production is estimated to be around 12 million tonnes, of which 30% is manufactured in the USA and 10% in France (Querol Solà, 2013). These two countries produce the most bitumen emulsion for road applications in secondary and rural networks with medium to low traffic (Corroler, 2010).

Bitumen emulsions that were produced in the early 1900s were mainly used for dust control and other spray applications. Today, they are successfully used over a wide range of road construction and pavement preservation projects, such as cold mix asphalt, soil stabilisation, slip coats, protective coats, slurry seals and fog seals. Typical applications of bitumen emulsions with different breaking rates are summarised in Table 2.1.

Table 2.1: Bitumen emulsions applications with different breaking rates (James, 2006)

<i>Application</i>	<i>Breaking or setting rate</i>		
	Rapid	Medium	Slow
<i>Plant mixes</i>			
<i>Open graded</i>		√	
<i>Dense graded</i>			√
<i>RAP mixes</i>		√	√
<i>Stockpile mix</i>		√	
<i>Pre-coated chips</i>		√	√
<i>Mix paving</i>			
<i>Open graded</i>		√	
<i>Slurry seal</i>			√
<i>Slurry for Cape seal</i>			√
<i>Micro-surfacing</i>			√
<i>In-place mixes</i>			
<i>RAP mixes</i>		√	√
<i>Dense graded</i>			√
<i>Soil stabilisation</i>			√
<i>Spray applications</i>			
<i>Chip seal</i>	√		
<i>Fog seal</i>	√	√	
<i>Tack coat</i>		√	√
<i>Prime coat</i>			√
<i>Dust palliative</i>			√
<i>Penetration macadam</i>	√		

2.4 Ultrasonic Emulsification

The range of human hearing is between 20 Hz and 20 kHz. Sound waves which have higher frequencies than those which humans can hear (> 20 kHz), are termed as ultrasonic. The upper limit of the frequency of ultrasound has not been clearly identified but is usually considered to be 5 MHz in gases and 500 MHz in liquids and solids. The application of ultrasound within this large frequency range can generally be divided into two areas. The first area includes low amplitude (higher frequency) propagation, commonly known as low power (high frequency) waves, between 2 to 10 MHz; this is used in medical scanning, chemical analysis and the study of relaxation phenomena. The second area is that of high energy (low frequency) waves referred to as “powerful ultrasound”, between 20 kHz and 100 kHz, used for cleaning, plastic welding and, more recently, to effect chemical reactivity (Kuldiloke, 2002).

Emulsification was one of the first applications to use powerful ultrasound, the first related patent dating back more than fifty years (Swiss Patent, 1944). Since then, many scientists and industrialists have used various types of ultrasound devices to produce different types of emulsions. Ultrasonic emulsification is a very effective processing method for producing dispersions and emulsions with small particle sizes (sub-micron). It has been used extensively in industry including applications related to food, paint, pharmaceuticals, cosmetics, cleaning products and agriculture, to generate stable emulsions. Such emulsions are often more stable than those produced conventionally and often require little emulsifier. Smaller droplet sizes that lie within a narrow size distribution, are obtained by ultrasonic emulsification (Miljković, 2014).

2.4.1 Mechanisms of Ultrasound

A reduction in particle size during the ultrasonic process is mainly due to the mechanical effect of ultrasonic cavitation. When a liquid is sonicating at high intensity, sound waves that

propagate into liquid media create alternating high pressure (compression) and low pressure (rarefaction) cycles rates depending on the frequency (Hielscher, 2005). During low pressure cycles, small bubbles in the liquid will be created by high intensity ultrasound waves. These bubbles grow over several cycles until they no longer absorb energy. They then collapse violently during high pressure cycles, causing powerful shock waves which radiate throughout the solution, thereby breaking the dispersed liquid, as seen in Figure 2.11. This phenomenon is known as cavitation and is characterized by intense local heating ($5000\text{ }^{\circ}\text{K}$), significant heating and cooling rates ($> 10^9\text{ }^{\circ}\text{K}/\text{sec}$), high pressures (1000 atm) and liquid jet streams (400 km/h) (Hielscher, 2005). A twostep mechanism has been proposed for ultrasound emulsification (Canselier et al, 2002). In the first step, a combination of interfacial waves and instability result in the eruption of dispersed phase droplets into the continuous phase. The second step consists of breaking droplets up via cavitation near the interface.

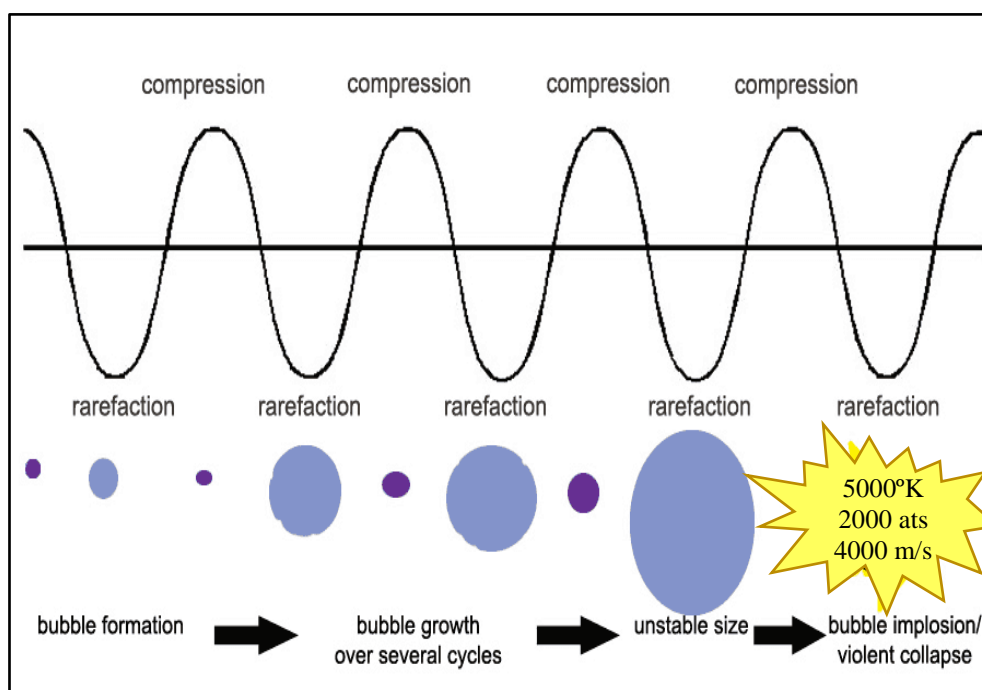


Figure 2.11: Schematic diagram of growth and collapse of a bubble in acoustic cavitation process (Hielscher, 2005)

2.4.2 Ultrasonic Process Parameters

2.4.2.1 Frequency

Using the appropriate frequency is considered to be an important, extrinsic-control parameter for the production of ultrasonic-assisted, sub-micron emulsions. The recent literature shows that a frequency range of 20 to 24 kHz is regularly used as it is found effective for the initiation of cavitation (Amani et al, 2010; Chalothorn and Warisnoicharoen, 2012; Kaltsa et al, 2013). Low frequencies are preferred for the production of high-power waves (Bermúdez-Aguirre et al, 2011), the power (P) generated inversely related to the square of the frequency (f), as given in the following Equation:

$$P \propto \frac{1}{f^2} \quad (2.1)$$

The relation above indicates that high power ultrasonic waves can be generated at lower frequencies. As the frequency increases, the time available for the expansion and collapse of bubbles decreases, reducing the extent of cavitation (Feng and Yang, 2011). At higher frequencies (>100 kHz), the cavitation threshold increases, this making the sonication process less efficient as additional power is required to initiate the cavitation process (Santos et al, 2008).

2.4.2.2 Treatment Time

The length of ultrasonic treatment time has a profound effect on droplet size. Increasing treatment time leads to an increase in the amount of energy available to disrupt droplets, this decreasing the mean droplet diameter. Salvia-Trujillo et al (2013) studied the influence of sonication time on the average diameter of a droplet of lemongrass oil–alginate Nano-emulsion. Increasing treatment time gradually decreased the droplet diameter, resulting in a final average droplet diameter of 4.31 ± 0.18 nm after 180 seconds of treatment.

Basil oil nano-emulsion (oil–surfactant ratio of 1:1) was examined at different ultrasonic treatment times by Ghosh et al (2013). In that study, the droplet diameter decreased from 57.75 to 41.15 nm when sonication time increased from 5 to 15 minutes. Similarly, Leong et al (2009) formulated 15% sunflower oil nano-emulsions with 5.6% sodium dodecyl sulphate and 13.6% polyethylene glycol, using a glass batch cell with 5, 10, 15 and 20 minutes residence time. The average droplet diameter decreased gradually with an increase in time, from approximately 100 nm at 5 minutes to 40 nm at 20 minutes.

Up to a certain limit, increasing the residence time leads to a decrease in the emulsion droplet diameter. Above that optimum limit (threshold limit), any further increase in ultrasonic residence time (energy), has the reverse effect on droplet diameter (Maali and Mosavian, 2013).

2.4.2.3 Temperature and Viscosity

Series of explosions and implosions in an emulsion sample during the cavitation process create high temperatures and pressure. The overall temperature of the liquid increases over time as a result of heating cycles that occur at the microscale bubble interface (due to cavitation). The increase in temperature due to cavitation, results in a reduction in the viscosity of the dispersed and continuous phases of the emulsion, thereby lowering the interfacial tension and Laplace pressure (Canselier et al, 2002; Jafari et al, 2008). Consequently, less energy is required for the emulsification and production of sub-micron emulsions. Although cavitation processes increase with a rise in temperature (as the number of nuclei increase), vapour pressure also increases, thereby reducing the intensity of the acoustic shock waves and damping the cavitation bubbles (Canselier et al, 2002; Jafari et al, 2008). Therefore, there is an optimum temperature at which the viscosity is low enough to improve cavitation bubble formation, while still being low enough to avert the impact of dampening.

The dynamic agitation and shear stress produced in a fluid when placed under high intensity sound fields, affects its fluid properties, specifically, the viscosity. Newtonian fluids usually preserve their characteristics, but dilatant and thixotropic fluids tend to either stiffen or become less viscous, respectively (Ensminger, 1986).

2.5 Summary

Although comprehensive works have been carried out across different topics related to CBEMs, to date, the problems relating to CBEM curing time, low early strength, mechanical properties and durability have still not been fully addressed. Therefore, improving CBEMs by addressing the above issues would be a breakthrough for CBEM practice. Although bitumen droplet size affects many of the emulsion properties that are critical to achieving success in application and service, there is no single study worldwide which has investigated the effect of reducing the particle size using ultrasonic waves. Most of the studies in the literature have shown that the performance of CBEMs can be improved using cement as a replacement for conventional limestone filler. However, this would increase the cost and demand for cement, and produce more CO₂ emissions. Therefore, developing alternative cementitious fillers made from waste and by-product materials, will have a positive impact on sustainability by reducing the need for cement in CBEMs.

Chapter 3: Research Methodology, Materials and Mix Design

3.1 Introduction

The main aim of this research is to develop a novel, high performance, cold mix asphalt with mechanical and durability properties similar to those of traditional hot mix asphalts used for road surfacing. This aim will be achieved by modifying bitumen emulsion using an innovative technology and developing a new secondary cementitious filler from industrial waste or by-product materials. This chapter consists of three main parts, the first summarizing the testing methods that were used. The second provides the essential characteristics of the candidate materials used in this study: limestone filler (LF), ordinary Portland cement (OPC), sewage sludge fly ash (SSFA), flue gas desulphurisation (FGD) gypsum and calcium carbide residue (CCR). The final part presents the mix design procedure and the selected gradation, mixing, compacting and curing of the cold bitumen emulsion mixtures (CBEMs).

3.2 Methodology

The methodology involves four main stages: the first stage comprises a comprehensive literature review about cold mix asphalt technology, bitumen emulsion and ultrasound technology used for emulsification. The second stage details the modification of the bitumen emulsion using a novel technology. The characteristics of the modified bitumen emulsion are specified, the optimization of the modification technology described. The aim is to manufacture a cold bitumen emulsion mixture (CBEM) which incorporates the modified bitumen emulsion, with optimal mechanical performance, in terms of indirect tensile stiffness modulus (ITSM). The third stage covers the development of a new secondary cementitious filler (SCF) by executing mineralogical and morphological analysis of the candidate materials to identify their

pozzolanic or hydraulic properties. Optimization of the mix design, with different types and dosages of the selected materials on the ITSM of the CBEMs, was also implemented during the third stage. The last stage includes developing the novel CBEM, incorporating both the modified bitumen emulsion and the developed SCF. Extensive evaluations of the microstructure, durability and mechanical performance in terms of permanent deformation and fatigue resistance of the developed CBEM, will be detailed. A schematic diagram of the entire methodology is summarized in Figure 3.1.

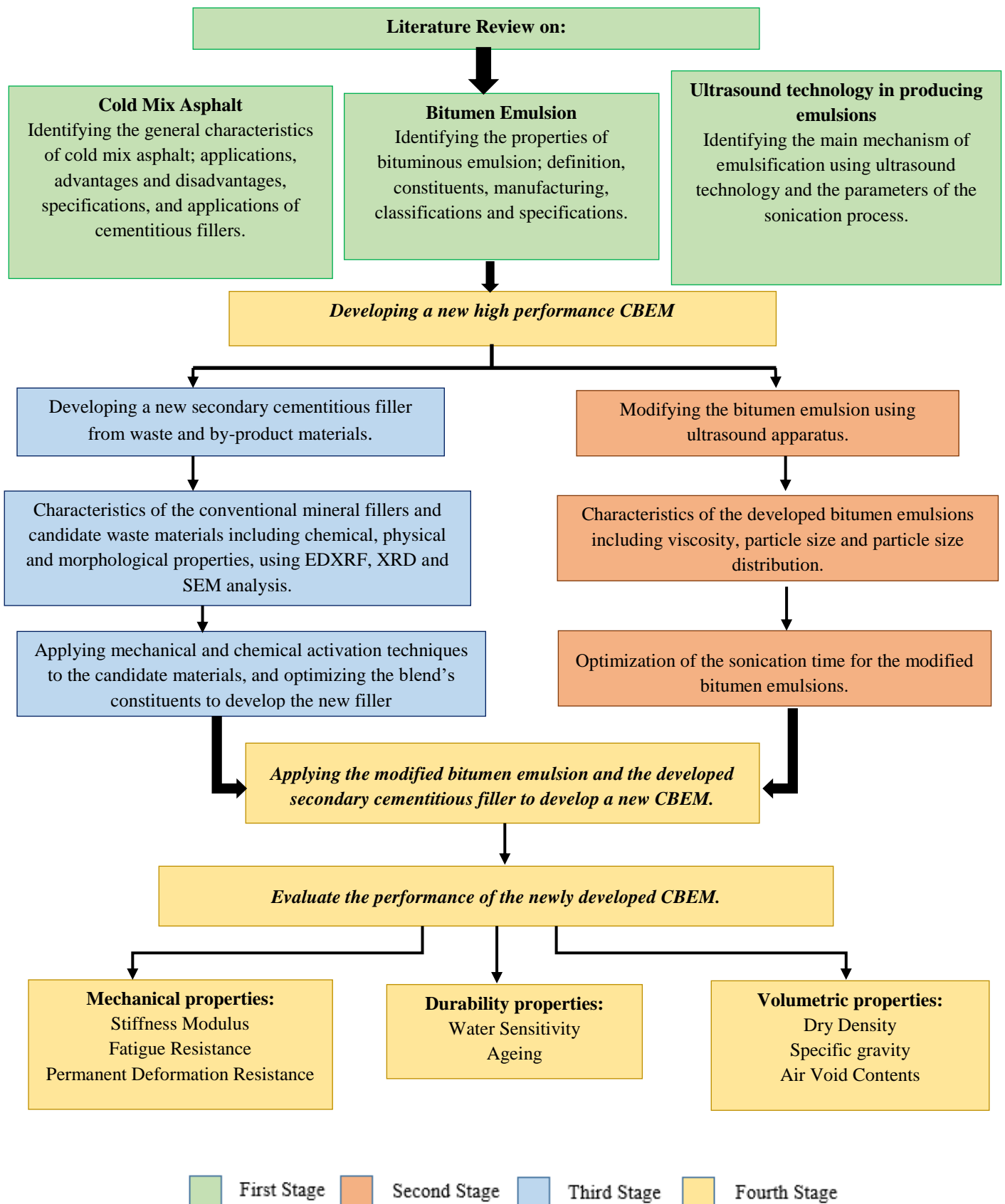


Figure 3.1: Research methodology flow chart

3.3 Programme of Laboratory Experiments and Testing Equipment

3.3.1 Characterisation of the Bitumen Emulsion

In this study, the upgrade of the bitumen emulsion will be achieved by reducing the particle size of the bitumen droplets to a sub-micron level. Ultrasound technology is one of the fast growing technologies in recent years, having a range of applications, especially in the food and pharmaceutical industries, as a novel delivery system for drugs and lipophilic materials such as flavours, colours and fatty acids (Mao et al, 2009). This technology has never been applied in the bitumen emulsion domain. Ultrasonic apparatus purchased by Liverpool Centre of Materials Technology (LCMT) has been used during this study to produce, for the first time, a novel, sub-micro, bitumen emulsion. The following laboratory study approach was adopted to identify the characteristics of the developed bitumen emulsion.

3.3.1.1 Ultrasonic Apparatus

A Dr Hielscher series, Model UP 400S (400 Watts, 24 kHz) was used in this study. It is a probe system consisting of a generator, ultrasonic converter (transducer), metal horn and probe (Santos et al, 2008). The ultrasound generator schematic diagram is shown in Figure 3.2. The heart of the converter is a lead zirconate titanate piezoelectric quartz crystal that can expand and contract under an alternating current. This type of ultrasonic apparatus is commonly used to produce sub-micron emulsions. Electrical waves are produced by the generator of a specific frequency (normally 24 kHz), while the ultrasonic transducers convert electrical oscillations into mechanical vibrations of a similar frequency (Santos et al, 2008). In the form of acoustic waves, the generated mechanical vibrations are amplified and further propagated through a probe attached to the horn. When the probe is immersed in a liquid sample, the ultrasonic waves are transmitted into the sample. These sinusoidal waves apply pressure (Pa), known as acoustic

pressure, on the sample and are dependent on time (t), frequency (f) and the maximum pressure amplitude ($P_{a, \max}$) of the wave (Patist and Bates, 2011).

$$P_a = P_{a, \max} \sin(2\pi ft) \quad (3.1)$$

$P_{a, \max}$ of the wave is directly proportional to the power input of the transducer. Acoustic streaming is the predominant phenomenon at lower amplitudes, while acoustic cavitation is initiated at higher amplitudes (Patist and Bates, 2011).

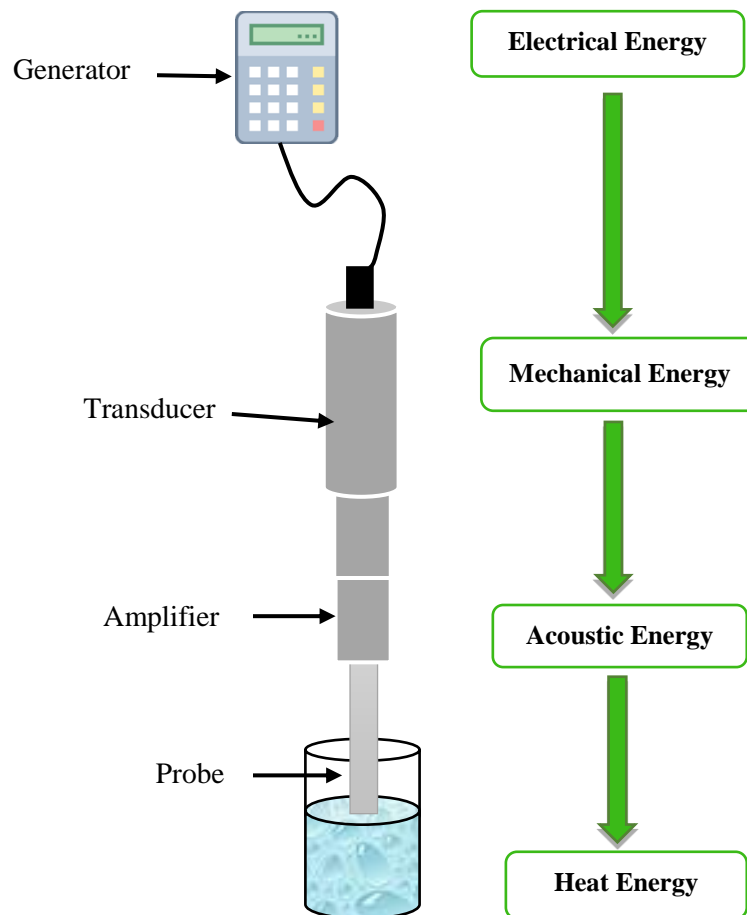


Figure 3.2: Ultrasonic set-up and the sequence of energy transformation at different levels of operation

3.3.1.2 Viscosity Measurement

Viscosity can be defined as the resistance to flow of a fluid. This test was conducted according to BS EN 13302 (European Committee for Standardization, 2018a), using a rotating spindle apparatus, as shown in Figure 3.3. The apparatus used in this study is a Brookfield DV-II+ Pro Viscometer, which consists of two parts: a head unit with a motor and a spindle that is driven by the motor. In principle, the DV-II+ Pro operates by means of a disk shape spindle that is immersed in a liquid sample measuring the resistance of the substance at a selected known speed. The resistance results are the measurement of the viscosity according to the flow characteristics of the reference spindle. The instrument calculates the results and displays the viscosity that is reported in centipoise (cP) using the following formula:

$$\text{Full Scale Viscosity Range (cP)} = \text{TK} * \text{SMC} * \frac{10,000}{\text{RPM}} \quad (3.2)$$

where:

TK= DV-II+Pro Torque Constant (for the RV model = 1) and SMC= Spindle Multiplier Constant.

The viscosity for all the bitumen emulsion samples, treated at different sonication times, was measured at ambient temperature, along with the normal (untreated) emulsion sample for comparison purposes. The viscosity result for each sample is the average of three measurements.



Figure 3.3: Viscometer used to measure the viscosity of the emulsion

3.3.1.3 Particle Size and Particle Size Distribution in Bitumen Emulsions

Particle size and particle size distribution are important variables as they can substantially impact viscosity, stability and the overall performance of the emulsion. They are governed by the formulation of the emulsion, raw materials and the instrument used to manufacture the emulsion (Baumgardner, 2006). There are two main types of equipment used to measure particle size and particle size distribution, namely the Electrozone Method developed by Coulter and Laser Light Scattering. Laser Light Scattering is based on the diffraction patterns of laser light emerging from particle dispersion. After a complicated calculation method which uses the optical properties of the particles under assessment, particle size distribution can be determined (Needham, 1996).

In this study, a Beckman Coulter Laser Diffraction Particle Size Analyser LS 13 320 with Variable Speed Fluid Module (VFM) (Figure 3.4), was used to measure the particle size

distribution (PSD) by volume percentage of the bitumen emulsion droplets for quality control. This instrument uses reverse Fourier optics incorporated in a patented fibre optic spatial filter system and a binocular lens system. According to Beckman (2016), this helps the analyser to optimize light scattering measurements through the widest dynamic range, from 40 nm to 2,000 μm , in a single scan in aqueous liquid mode. To prepare the samples of the bitumen emulsion, distilled water which was made acidic ($\text{pH} = 2.5 - 3.0$) with hydrochloric acid and was used to dilute the bitumen emulsion sample to 50:50. The diluted suspension was then added drop by drop to the VEM to a suitable obscuration. An average of five consecutive runs was recorded as a measurement of each particle size.



Figure 3.4: Laser diffraction particle size distribution analyser

3.3.2 Characterisation of the Candidate Mineral Fillers

The main aim of conducting the following experimental analytical techniques is to investigate the physical and chemical characteristics of the selected materials, as well as explain the relationship between the physico-chemical structures of the materials under study. This

investigation will identify similarities to OPC, as well as unpack their behaviour in the CBEM, individually or collectively, with OPC powder.

3.3.2.1 Energy Dispersive X-ray Fluorescence (EDXRF)

In this study, the composition of the elements comprising the selected filler materials (major oxides and trace elements) was analysed using the Shimadzu EDX 720 energy dispersive X-ray fluorescence spectrometer (Figure 3.5). This equipment performs qualitative and quantitative element analysis and is ideal for non-destructive applications. It works by applying X-rays to the sample and analysing the re-emitted characteristic fluorescent X-ray.



Figure 3.5: Energy dispersive X-ray fluorescence (EDXRF) spectrometer

3.3.2.2 X-ray Diffraction (XRD)

X-ray diffraction relies on the dual wave/particle nature of X-rays to obtain information about the structure of crystalline materials. The primary use of this technique is the identification and characterization of compounds according to their diffraction pattern. The X-ray beam is

targeted at a sample in a powder state, and the pattern of the diffracted rays recorded. The intensity and the angle of the diffracted X-ray beam are analysed after encountering a plane of atoms in the material under analysis (Alizadeh, 2009). A Rigaku Miniflex Diffractometer with CuK X-ray radiation, voltage 30 kV, current 15 mA, scanning speed of 2.0 deg/min in continuous scan mode, with an aluminium sample holder (Figure 3.6), was used to identify the phase composition for the candidate waste materials. Patterns were identified by comparison with standard patterns for different compounds available in the powder diffraction file database.



Figure 3.6: Rigaku Miniflex X-ray Diffractometer

3.3.2.3 Scanning Electron Microscopy (SEM)

Scanning Electron Microscopes (SEM) use a focused beam of high energy electrons to generate a variety of signals at the surface of solid specimens. They are used to investigate the microstructure of particles and the surface characterization of materials. A Quanta 200 Scanning Electron Microscope (Figure 3.7), was used to view images of the materials under

study. To increase conductivity, the specimens were coated with a thin layer of gold or palladium, using an auto fine sputter coater. Test conditions included an SEM resolution of 3 to 4 nm, high vacuum and a test voltage of 5 to 25 kV.



Figure 3.7: Quanta 200 scanning electron microscope

3.3.2.4 Laser Particle Size Diffractometer

The same apparatus as described in subsection 3.3.1.3, was used to measure the particle size distribution (PSD) for the materials under study.

3.3.2.5 pH Value Measurement

The pH value can be defined as the concentration of hydrogen ions (H^+) in a solution. A solution with a high concentration of H^+ has a low pH, while a high pH indicates the solution has a low concentration of H^+ . Hydraulic and pozzolanic materials are pH dependent and thus, the measurement of the pH value is a crucial test to control for different reactions which may occur. The pH value should not be lower than 8 for materials used to produce cementitious

materials, as recommended by BS EN 450-1 (European Committee for Standardization, 2012a). To measure the pH value for the selected mineral fillers, a pH meter was calibrated using a standard buffer solution prior to the test. Suspensions of water with the selected fillers (1 part by mass with 5 parts distilled water), were stirred for 30 minutes, the pH measured at lab temperature using the instrument shown in Figure 3.8.



Figure 3.8: pH meter

3.3.2.6 Particle Density

The particle density of the selected mineral fillers was measured by an automatic gas expansion multi-pycnometer, shown in Figure 3.9. Solubility issues, which might be encountered with a liquid pycnometer, have been eliminated. The dry sample was weighed, placed in the sample cell and degassed by purging with a flow of dry helium gas by vacuum. The sample cell was then pressurised to approximately 117 kPa, the value recorded. Following this, the selector valve was rotated to allow the gas to be extended into the reference, this lower pressure was also recorded. The volume of the sample was determined accurately from these two

measurements, using the volume-pressure relationship known as Boyle's law which is expressed as follows:

$$P_i V_i = P_f V_f \quad (3.3)$$

Where P_i and V_i are the initial pressure and initial volume respectively, while P_f and V_f are the final pressure and final volume, respectively.



Figure 3.9: Multi-pycnometer used for measuring the density of fillers

3.3.2.7 Standard Consistency

The standard consistency of a cement paste is defined as that consistency which permits a standard plunger to penetrate to a point 5 to 7 mm from the bottom of the mould. The standard consistency of the selected filler materials (LF, OPC, SSFA, FGD and CCR), was examined using Vicat apparatus (Figure 3.10). Different trials of pastes, with varying percentages of water for a filler sample, were prepared and tested according to BS EN 196-3 (European

Committee for Standardization, 2016c). The standard consistency, 6 ± 2 mm penetration from the bottom of the Vicat mould, was measured using the following equation:

$$\text{Standard consistency \%} = \frac{\text{Weight of water added}}{\text{Weight of cement}} \times 100 \quad (3.4)$$



Figure 3.10: Vicat apparatus

3.3.2.8 Heavy Metal Concentrations

Pavement layers which include waste materials, are responsible for the chronic emission of pollutants, especially heavy metals which are believed to be of specific ecological, biological and health significance (Halim et al, 2003). These layers are in direct contact with both surface and underground water, this which increasing the potential for metal pollutants dispersal into underground water supplies thus inducing the contamination of soil (Modarres et al, 2015). High concentrations of heavy metals can generate risks for human health because of chronic

toxicity (Halim et al, 2003). Such elements include lead (Pb), copper (Cu), nickel (Ni), cadmium (Cd), zinc (Zn), strontium (Sr) and chromium (Cr).

In this study, the leaching of these elements was determined using a Toxicity Characteristics Leaching Procedure (TCLP) test which will be described in detail in Chapter 10. This method has been adopted by several researchers such as Xue et al (2009) and Modarres et al (2015), to determine heavy metals leaching from CBEMs. An atomic adsorption spectrometer (Figure 3.11) was used to conduct the measurements.



Figure 3.11: Atomic adsorption spectrophotometer

3.3.3 Characterisation of the Developed CBEMs

To identify the performance of asphalt pavement mixtures, there are three main properties to consider: mechanical properties, durability and volumetric properties. To date, there is no specific procedure to follow to design CBEMs, testing protocols or specifications as is the case for HMA (Nassar et al, 2016). Therefore, HMA test methods have been routinely used by

researchers to characterize CBEMs with some amendments to cover compatibility of properties under relevant testing temperature, curing and conditioning times. The tests used in this study to investigate the properties of the CBEMs, are listed in Table 3.1.

Table 3.1: Tests used to specify the properties of CBEMs

Properties	Tests	Standard Specification
Mechanical Properties	Indirect Tensile Stiffness Modulus (ITSM) on cylindrical specimens	BS EN 12697-26: 2018
	Fatigue Test (four-point bending test) on prismatic specimens	BS EN 12697-24, Annex D: 2018
	Wheel Track Test on a slab sample	BS EN 12697-22: 2003
Durability	Water Susceptibility	BS EN 12697-12: 2018
	Ageing Test	SHRP A-003A
Volumetric Properties	Dry Bulk Density	BS EN 12697-6: 2012
	Air Void Contents	BS EN 12697-8: 2018

3.3.3.1 Mechanical Properties

Three types of tests were conducted to evaluate the mechanical properties of the proposed CBEMs which incorporate modified bitumen emulsion and cementitious materials, individually and collectively.

- ***Indirect Tensile Stiffness Modulus (ITSM)***

Stiffness Modulus can be defined as uniaxial stress divided by corresponding strain. It is considered an indicator of adequate structural design because it is related to the capacity of individual pavement layers to spread traffic loads to the layer underneath. The stiffness

modulus of CBEM is highly dependent on the temperature and frequency of loading (Read and Whiteoak, 2003). The indirect tensile stiffness modulus test comprising diametric pulsed loads on a cylindrical specimen is widely used to evaluate the stiffness modulus of asphalt mixtures because it is simple, quickly conducted and non-destructive. This allows repeat tests on the same specimens at different curing ages to avoid variability in the mixtures and to derive reliable results for stiffness evaluation (Nassar, 2016).

Many researchers have used this test as an indicative test to rank CBEMs (Thanaya, 2003; Oke, 2011; Al-Busaltan et al, 2012; Al-Hdabi et al, 2013; Ojum, 2015; Dulaimi, 2017). The measurements of stiffness can also be used as an indicator of the mixture's susceptibility to temperature, water damage and ageing (Sunarjono, 2008).

ITSM was carried out according to BS EN 12697-26 (European Committee for Standardization, 2018b) using Cooper Research Technology HYD-25 testing apparatus, seen in Figure 3.12. In the test, the sample was exposed to five transient load pulses across its vertical axis, the resulting indirect deformation along the horizontal axis measured using Linear Variable Differential Transducers (LVDTs). The measurements were repeated along two orthogonal orientations, the average ITSM values calculated using the following equation:

$$\text{ITSM} = \frac{L}{D \times t} \times (v + 0.27) \quad (3.5)$$

where

ITSM: indirect tensile stiffness modulus (MPa)

L: vertical load (N)

D: horizontal deformation (mm)

t: the mean thickness of the specimen (mm)

v: Poisson's ratio for the asphalt at the test temperature

The test was implemented at 20°C as per published Standards. To ensure that the samples were at the required temperature, the specimens were conditioned at 20°C in a temperature-controlled chamber for at least 4 hours prior to the test. Table 3.2 summarizes the test parameters.

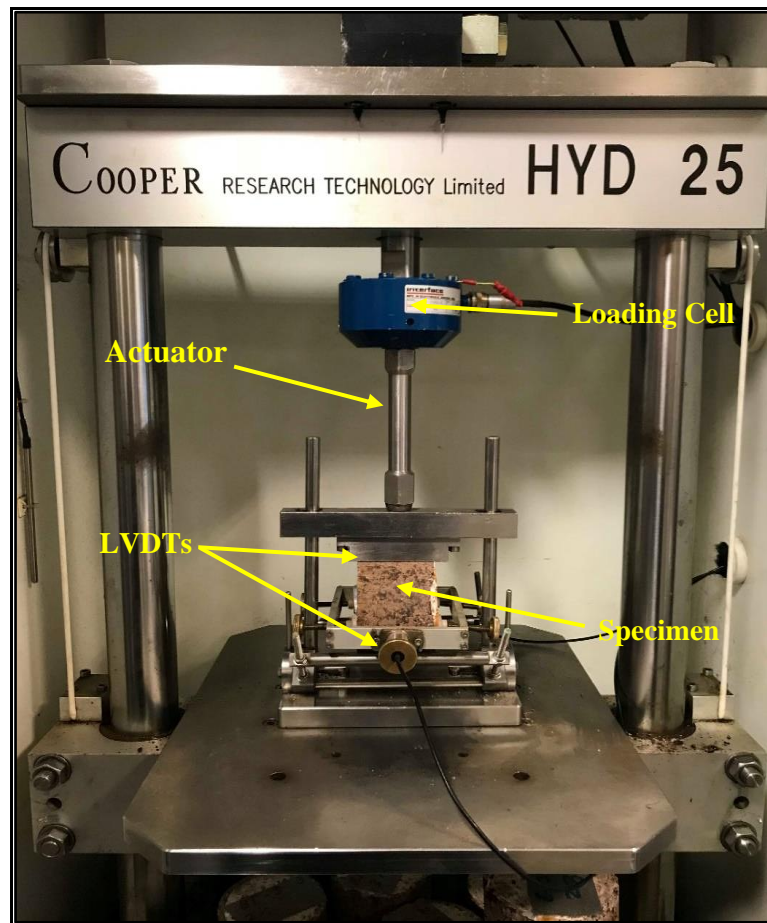


Figure 3.12: ITSM test using Cooper Research Technology HYD 25 apparatus

Table 3.2: ITSM test conditions

<i>Parameter</i>	<i>Range</i>
<i>Specimen diameter (mm)</i>	100 ± 3
<i>Rise time (ms)</i>	124 ± 4
<i>No. of conditioning pulses</i>	5
<i>Loading time (s)</i>	3-300
<i>Transient peak horizontal deformation (µm)</i>	5
<i>Poisson's ratio</i>	0.35
<i>No. of test pulses</i>	5
<i>Test temperature (°C)</i>	20 ± 0.5
<i>Specimen thickness</i>	63 ± 3
<i>Marshall Compaction (blows/face)</i>	50
<i>Specimen temperature conditioning</i>	4 hours before testing

- ***Fatigue Cracking Resistance***

Fatigue cracking has traditionally considered to be the most common, and major type of asphalt pavement degradation, appearing as a series of interconnected cracks when the pavement experiences repeated traffic loading. A number of factors can lead to fatigue cracking of asphalt pavements including continued traffic loading, variations in temperature, a lack of strength and compaction of the base, or of the subgrade, which induces stress higher than the tensile strength of the asphalt (Read, 1996). As tensile strains are repeated, fatigue cracking develops in two stages: the crack initiation stage during which micro-cracks coalesce to generate macro-cracks, and the crack propagation stage during which the macro-cracks grow under additional application of tensile strains (Read and Whiteoak, 2003).

In this study, a four-point bending test (4PB) (Figure 3.13), was used to examine the fatigue crack resistance for the asphalt mixtures according to BS EN 12697-24 (European Committee for Standardization, 2018d). The device used is capable of clamping specimens in a bending frame to provide horizontal translation and rotational freedom at all supports. When cyclic bending is applied, the two inner clamps are loaded in the vertical direction while the perpendicular position of the outer clamps is fixed. Constant movement will be created with constant strain between the inner loading points.

All tests were conducted at 20°C and a frequency of 10 Hz, under a sinusoidal waveform in controlled strain mode, on shaped prismatic specimens measuring 400 × 50 × 50 mm (Table 3.3). The prismatic specimens were cut from a slab and had dimensions length: 400 mm, width: 305 mm and thickness: 50 mm. These were compacted using a Cooper Technology roller compactor machine (Figure 3.14), following BS EN 12697-33 (European Committee for Standardization, 2003a). In general, fatigue life is defined as the number of cycles of loading that a material withstands before failure (Fatemi et al, 2001). In this research, fatigue life (N_f) is considered to be the number of cycles required to reach a 50% reduction in the material stiffness modulus. The relationship between fatigue life and different strain levels, i.e. 100, 125 and 150 microstrain, have been investigated for both developed and conventional mixtures. Linear regression analysis was then applied to the natural logarithm of N_f and the natural logarithm of the initial strain amplitude (ϵ), to obtain the fatigue line. The shape of the fatigue line can be depicted using the equation below:

$$\ln N_f = A_0 + A_1 \ln \epsilon \quad (3.6)$$

where

A_0 : the intercept with the y-axis

A_1 : the slope of the fatigue line

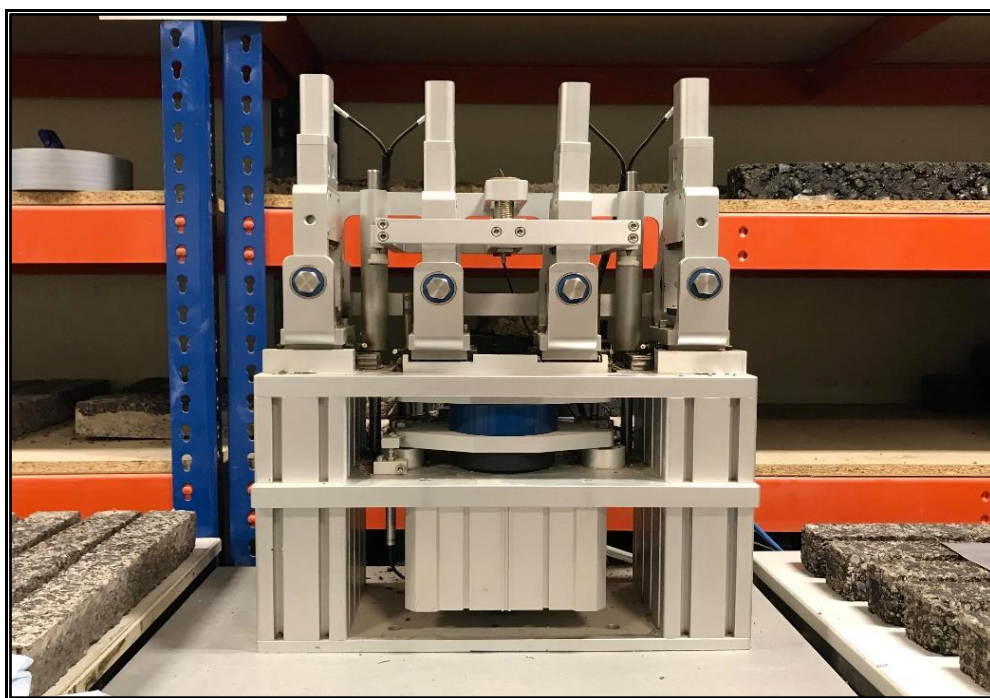


Figure 3.13: Configuration of the four-point load fatigue test (4PB)

Table 3.3: Four-point fatigue test conditions

<i>Parameter</i>	<i>Range</i>
<i>Control mode</i>	Constant strain
<i>Test temperature (°C)</i>	20 ± 1
<i>Specimen dimensions (mm)</i>	400 × 50 × 50
<i>Frequency (Hz)</i>	10
<i>Microstrain</i>	100 -150
<i>Initial stiffness end value</i>	50%



Figure 3.14: Roller compactor equipment

- ***Permanent Deformation Resistance***

Permanent deformation (rutting) is a longitudinal depression in the wheel path due to the repeated traffic loading. It is the most important distress mechanism in flexible pavements, exacerbated by increased tyre pressure and axle loads. The accumulation of permanent deformations in one or more layers of the pavement structure, eventually results in a distorted pavement surface. Many different approaches and devices have been developed to imitate the effect of a wheel rolling over the surface of an asphaltic layer. The wheel tracking test is one of these devices, used by several researchers to investigate permanent deformation in asphalt mixtures (Bodin et al, 2009; Ma et al, 2015; Dulaimi et al, 2016c; Shanbara et al, 2018).

In this research work, the wheel tracking test was used to assess the resistance of both the conventional and developed mixtures to permanent deformation and to demonstrate their susceptibility to failure under loading. The test was carried out to simulate, as much as possible, field conditions to establish the mechanisms of failure of the CBEMs under controlled conditions (Ojum, 2015).

The test was conducted in accordance with BS EN 12697-22 (European Committee for Standardization, 2003b) using a small model HYCZ-5, wheel tracking device (Figure 3.15) which is normally used to evaluate rutting resistance at moderate to very heavily stressed sites, according to BS EN 13108 (European Committee for Standardization, 2016a). Two temperatures, 45°C and 60°C, were used to conduct the test using a temperature controlled chamber; Table 3.4 details the test parameters. During the test, a rubber tyre with a 50 mm contact width, was applied to the centre of the slab sample, in a forward and backward mode of motion, at a speed of 42 passes/minute. The vertical displacement of the sample along the wheel path was measured by a Linear Variable Differential Transformer (LVDT). The tests were performed with five specimens per mix type.

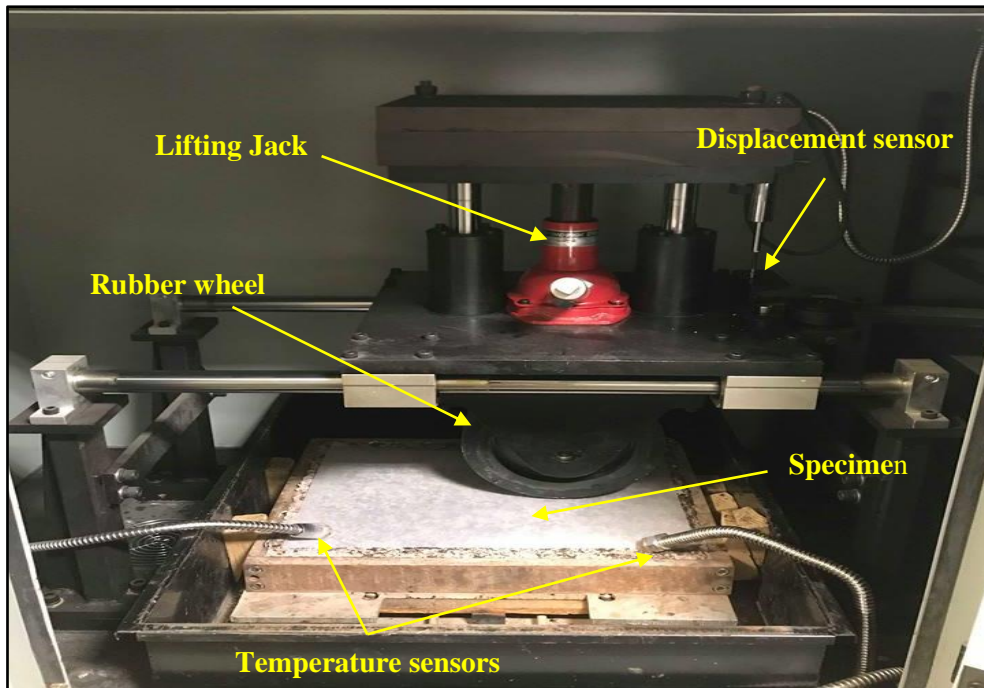


Figure 3.15: Wheel tracking apparatus

Table 3.4: Wheel tracking test conditions

<i>Parameter</i>	<i>Range</i>
<i>Tyre outside diameter (mm)</i>	200-205
<i>Tyre width (mm)</i>	50 ± 5
<i>Trolley travel distance (mm)</i>	230 ± 10
<i>Trolley travel speed (time/min)</i>	42 ± 1
<i>Contact pressure (MPa)</i>	0.7 ± 0.05
<i>Poisson's ratio</i>	0.35
<i>No. of conditioning cycles</i>	5
<i>No. of test cycles</i>	10000
<i>Test temperature (°C)</i>	45 & 60
<i>Compaction</i>	Roller compactor
<i>Specimen temperature conditioning</i>	4 hours before testing

To evaluate the resistance to permanent deformation of the mixtures, two parameters were calculated:

- PRD_{AIR} representing the proportional depth of the rut after 10,000 cycles (%).
- WTS_{AIR} representing the tangent of the angle slope of the rut depth increase (mm/cycles) using the formula below:

$$WTS_{AIR} = \frac{d_{10000} - d_{5000}}{5} \quad (3.7)$$

where

d_{5000} and d_{10000} are the depths of the rut after 5,000 and 10,000 loading cycles, respectively, (mm).

3.3.3.2 Durability Tests

The durability of asphalt pavements can be described as its ability to maintain its structure, provide satisfactory performance and long term service under increasingly demanding conditions. Because water sensitivity and ageing have a profound effect on the mechanical properties of asphalts, the durability of the fabricated mixtures has been evaluated in terms of these.

- **Water Sensitivity Test**

Moisture may be a key factor in the degradation of asphalt pavements. [The integrity of asphalts can be degraded through three mechanisms: a lack of stiffness and cohesion of bitumen film, inadequate adhesion between the asphalt and the aggregate, and deterioration of the aggregate itself. Bitumen is stripped away when the aggregate absorbs water, this leading to premature asphalt distress and may eventually lead to failure of the pavement.

In this research, the stiffness modulus ratio (SMR) was used to evaluate the water sensitivity of both the conventional and developed asphalt mixtures in accordance with BS EN 12697-12 (European Committee for Standardization, 2018c). The specimens for testing were divided into two sets, each set consisting of three samples which were manufactured using a Marshall hammer. The first set was for the unconditional (dry) test in which the specimens were left in their moulds for 24 hours before being extruded. Following this, they were kept in the lab at 20°C for 7 days then tested for ITSM at 20°C. The second set was prepared for the conditional (wet) test in which the specimens were extruded from moulds after 24 hours, stored in the lab at 20°C for 4 days and then conditioned as follows (Figure 3.16):

- Placed in a vacuum container filled with distilled water and partially saturated under the effect of 6.7 kPa vacuum, for 30 minutes at 20°C.
- Immersed for the next 30 minutes, after carefully releasing the pressure from the vacuum container, to avoid damage to the samples from expansion.
- Soaked in a water bath at $40\pm 1^\circ\text{C}$ for 3 days.

Thereafter, the conditioned samples were tested for ITSM at 20°C, the water sensitivity evaluated in terms of SMR, the percentage of stiffness modulus after conditioning over stiffness modulus before conditioning.

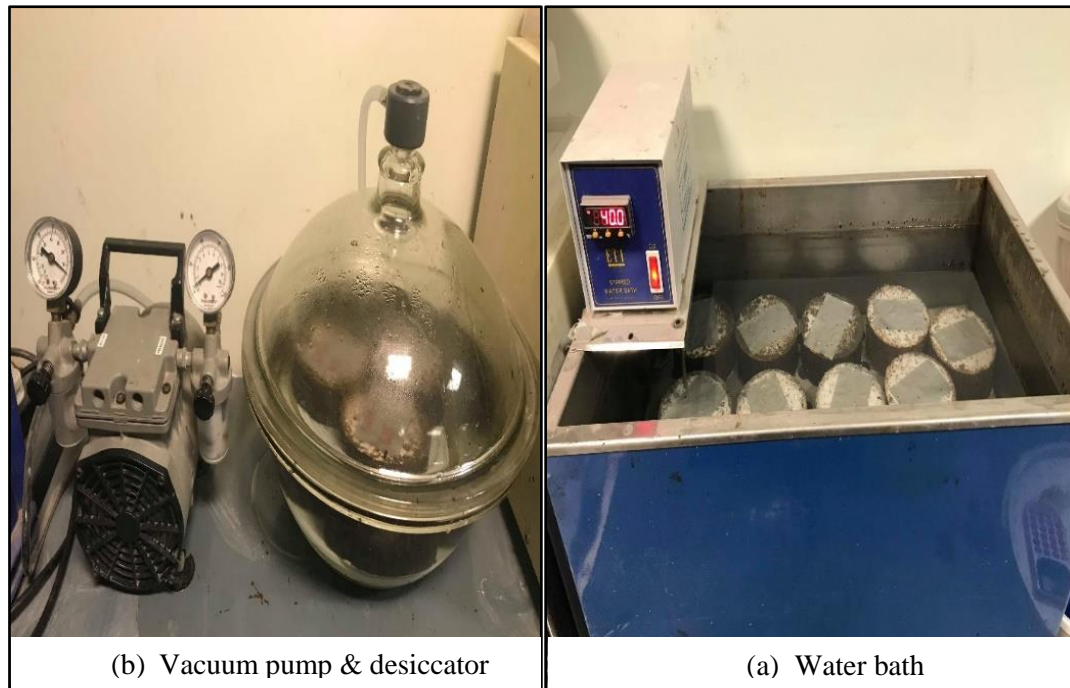


Figure 3.16: Water sensitivity instruments

- ***Ageing Test***

The term ageing can be used to describe the change in the rheological properties of bitumen binders/mixtures due to the changes in chemical composition during construction and its service life period (Sirin et al, 2018). In general, bitumen ageing occurs in two stages: short term ageing which takes place as a result of heating the binder during the production and construction process, and long term ageing due to oxidation over time throughout the service life of the pavement. Short term ageing does not occur in CBEMs because no heat is applied during the production process.

In this research, long term ageing for the new asphalt mixtures was assessed by adopting the long term oven ageing method as recommended by the Strategy Highway Research Program (SHRP) A003A. In this method, compacted specimens are cured in an oven at 85°C for 2 to 5 days to simulate 5 to 10 years of bitumen ageing in the field (Kliwer et al, 1995).

This test was conducted on two types of group samples, the unconditioned and conditioned groups. The samples in the first group were subjected to normal curing at lab temperatures, while the samples in the second group were exposed to oven curing at 85°C for 5 days, to simulate the age hardening effect over 10 years. The ITSM was then measured for both groups of samples in accordance with BS EN 12697-26 (European Committee for Standardization, 2018b) at 20°C to assess the hardening ageing in terms of the Stiffness Modulus Ratio (SMR).

3.3.3.3 Volumetric Properties

The volumetric properties of the conventional and the developed bituminous mixtures were calculated following the Asphalt Cold Mix Manual (MS-14) adopted by the Asphalt Institute (1989). Such properties can be calculated as follows:

$$\text{Wet Density} = \frac{\text{Weight in air}}{\text{SSD Weight} - \text{Weight in water}} \quad (3.8)$$

$$\text{Dry Density} = \frac{(100 + \text{RBC})}{100 + \text{RBC} + \text{W}} \times \text{Wet Density} \quad (3.9)$$

$$\text{SG}_{\text{max}} = \frac{100}{\frac{\text{CA}}{\text{SG}_{\text{CA}}} + \frac{\text{FA}}{\text{SG}_{\text{FA}}} + \frac{\text{F}}{\text{SG}_{\text{F}}} + \frac{\text{B}}{\text{SG}_{\text{B}}}} \quad (3.10)$$

$$\text{Air Voids} = \left(1 - \frac{\text{Dry Density}}{\text{SG}_{\text{max}}}\right) \times 100\% \quad (3.11)$$

where:

SSD: weight of the sample in the saturated surface dry condition,

RBC: residual bitumen content,

W: water content at testing time,

SG_{max} : maximum specific gravity for the mixture,

CA: percentage of coarse aggregate,

FA: percentage of fine aggregate,

F: percentage of filler,

B: percentage of bitumen.

3.4 Materials

3.4.1 Mineral Aggregate

Both the fine and coarse aggregates used in this study are of crushed granite obtained from Carnsew Quarry at Mabe, Penryn, UK (operated by Colas). These materials are used for producing asphalt pavement mixtures. The aggregates were completely dried in an oven at 110°C, refilled and sieved according to BS EN 933-1 (European Committee for Standardization, 2012b). The fractions were then recombined to achieve the gradation required to manufacture the mixtures. The physical properties of the fine and coarse aggregates with conventional limestone filler are listed in Table 3.5.

Table 3.5: Physical characteristics of the granite aggregate

Material	Property	Value
<i>Coarse aggregate</i>	Bulk particle density (Mg/m ³)	2.60
	Apparent particle density (Mg/m ³)	2.66
	Water absorption (%)	0.8
<i>Fine aggregate</i>	Bulk particle density (Mg/m ³)	2.52
	Apparent particle density (Mg/m ³)	2.58
	Water absorption (%)	1.6
<i>Conventional mineral filler</i>	Particle density (Mg/m ³)	2.64

3.4.2 Bitumen & Bitumen Emulsion

A slow setting cationic bitumen emulsion (C50B4), comprising 50% residual bitumen designed for use in road pavement and general maintenance applications, was used to prepare the conventional and new CBEMs. This type of emulsion is called Cold Asphalt Binder (CAB50) based on 40/60 penetration grade base bitumen and is supplied by Jobling Purser, Newcastle, UK. The reason for choosing this type of bitumen emulsion is its high stability and high adhesion, as recommended by Nikolaides (1994) and Thanaya (2003).

For comparison purposes, the hot asphalt mixtures were produced using two bitumen grades of 100/150 pen and 40/60 pen. The relevant properties of the selected bitumen and bitumen emulsion are presented in Table 3.6.

Table 3.6: Properties of bitumen & bitumen emulsion

Material	Property	Value
	Type	Cationic
	Appearance	Black to dark brown liquid
Bitumen Emulsion	Base bitumen (penetration)	40-60
	Bitumen content (%)	50
	Boiling Point (°C)	100
	Relative Density at 15°C (g/ml)	1.07
	Appearance	Black
Bitumen 40/60	Penetration at 25°C	49
	Softening point, °C	51.5
	Density at 25°C	1.02
	Appearance	Black
Bitumen 100/150	Penetration at 25°C	131
	Softening point (°C)	43.5
	Density at 25°C	1.05

3.4.3 Mineral Fillers

The term mineral filler typically refers to the fine mineral particles passed through a 0.063 mm sieve. Mineral fillers have two functions in asphalt mixtures. Firstly, they act as part of the mineral aggregate by filling the voids between the coarser particles in the mixture and becoming part of the load bearing framework. Secondly, the extremely fine particles will be located in the asphalt films resulting in a high consistency binder matrix called mastic that coat and bind the coarser aggregate particles to each other. The use of industrial waste and by-product materials as replacements for conventional limestone filler and ordinary Portland cement to improve the properties and performance of CBEMs, has been investigated repeatedly. In addition to enhancing the performance of CBEMs, incorporating such materials could achieve economic and environmental gains in terms of reducing CO₂ emissions and reducing the impact on landfills.

In this study, an extensive investigation was conducted to assess the suitability of different types of waste and by-product materials to use as secondary cementitious fillers (SCFs). The materials selected for this study are limestone filler (LF), ordinary Portland cement (OPC), sewage sludge fly ash (SSFA), flue gas desulphurisation (FGD) gypsum and calcium carbide residue (CCR), as shown in Figure 3.17. The most important physical, chemical, mineralogical and morphological characteristics for the candidate materials were identified to investigate and evaluate their full potential. The details of their properties are presented in the next chapter.

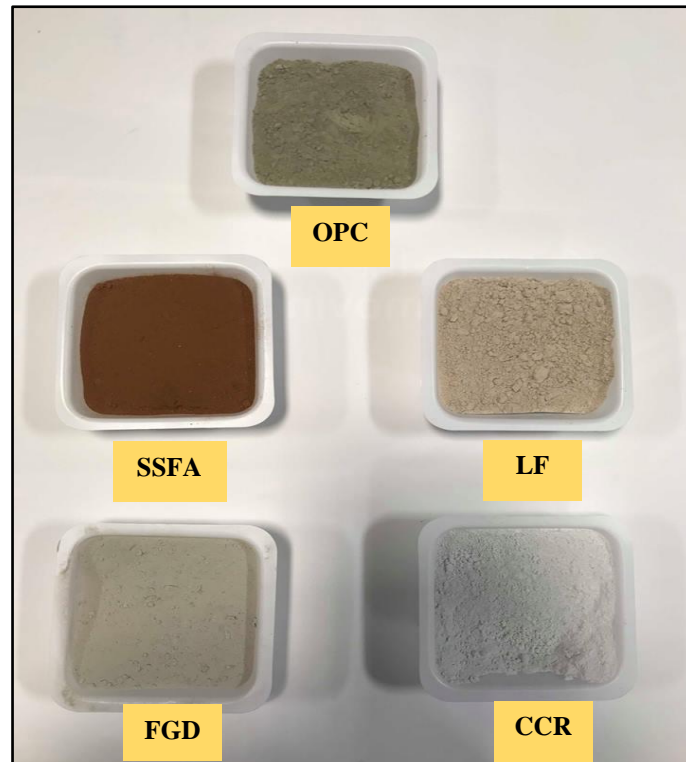


Figure 3.17: Selected mineral fillers

3.5 Mix Design

To date, there is no universally accepted mix design procedure for CBEMs. However, the Asphalt Institute (1989) recommends the most widely used method and the basis for developing some procedures by various authorities and researchers, e.g. Jenkins (2000) and Thanaya (2003), but with some modifications. In this research, the Marshall Method for Emulsified Asphalt Aggregate Cold Mixture Design (MS-14) adopted by the Asphalt Institute (1989) was used to design the CBEMs mixtures. In this method, the indirect tensile stiffness modulus (ITSM) test was used as an alternative to the Marshall test. The design method for preparing and producing samples is detailed below.

3.5.1 Selection of Aggregate Gradation

Aggregate grading is one of the most influential characteristics when determining how an asphalt pavement will perform (Teklu, 2015). The maximum aggregate size in the MS-14 method is specified to be 25 mm or less. A variety of types of aggregate have been suggested for use such as crushed stone, rock, gravel, sand, silty sand, sandy gravel, slag, reclaimed aggregate and ore tailings. A close graded surface course with 10 mm grading was selected for this study complying with the standard BS EN 13108-1 (European Committee for Standardization, 2016a). Aggregate grading is given in Table 3.7 and shown in Figure 3.18. This selection was made in order to ensure an appropriate interlock between the aggregate particles in the mixtures as recommended by (European Committee for Standardization, 2016b). It is suitable for all pavement layers and for all traffic conditions.

Table 3.7: Aggregate gradation for AC10 surface course

Test sieve aperture size (mm)	% by mass passing range	% by mass passing mid
14	100	100
10	100	100
6.3	62-68	65
2	25-31	28
1	14-26	20
0.063	6	6

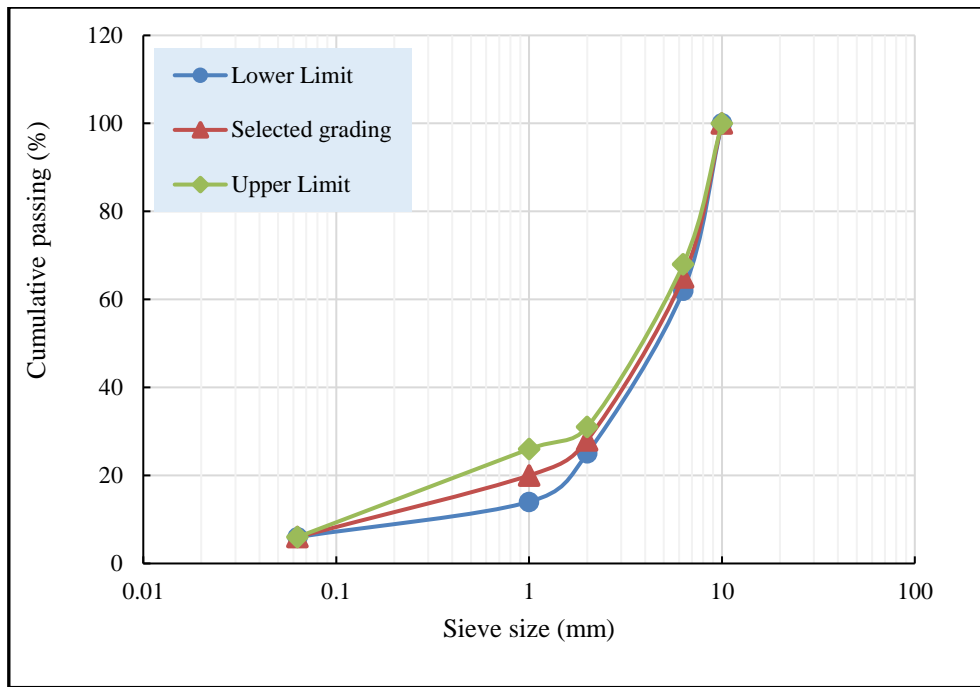


Figure 3.18: The gradation of AC 10 close-graded surface course

3.5.2 Determination of Initial Bitumen Emulsion Content (IBEC)

The initial residual bitumen content (P) for producing CBEMs was calculated using the empirical equation suggested by MS-14. This equation is as follows:

$$P = (0.05A + 0.1B + 0.5C) \times 0.7 \quad (3.12)$$

where

P: the percentage of initial residual bitumen content by the total weight of dried aggregate.

A: the percentage of aggregate retained on a 2.36 mm sieve.

B: the percentage of aggregate passing through a 2.36 mm sieve but retained on a 0.075 mm sieve.

C: the percentage of aggregate passing through a 0.075 mm sieve.

Some modifications were made in line with common practice in the UK by which sieve 2.36 mm was replaced by a 2 mm sieve, and sieve 0.075 mm replaced by a 0.063 mm sieve. The

value of P for the selected grading mixture was calculated to be 6.16%. The initial bitumen emulsion content (IBEC) was determined by dividing P by the percentage of bitumen content in the emulsion as below:

$$\text{IBEC (\%)} = \frac{P}{X} \quad (3.13)$$

where

X: the bitumen content of the emulsion which is 50%

IBEC = 6.16 / 0.5 = 12.32% of aggregate weight.

3.5.3 Determination of Optimum Pre-Wetting Water Content (OPWC)

The coating of aggregates by the bitumen emulsion is essentially controlled by the pre-wetting water content. Insufficient pre-wetting water leads to fine particles balling in the bitumen, resulting in an undesirable coating. When there is adequate pre-wetting water, this will help to facilitate a uniform distribution of bitumen emulsion on the aggregate surface, achieving a better coating (Thanaya, 2003). Thom (2009) stated that aggregates need to be wetted to ensure appropriate binder coating. The function of pre-wetting water is to lubricate aggregates and activate the surface charges on the aggregate particles before adding bitumen emulsion (Ojum, 2015).

The coating test, as recommended by the Asphalt Institute (1989), was conducted to determine the OPWC. Different samples of aggregate and emulsion mixes were prepared, keeping the same quantity of bitumen emulsion content (as calculated by equation 3.13), while varying the water content. Five percentages of pre-wetting water content, 2.5%, 3%, 3.5%, 4% and 4.5% of the total weight of aggregate, were investigated to indicate the lowest pre-wetting water content at which the maximum coating of aggregates occurs, making the mixture neither too

sloppy nor too stiff. By visual assessment, 3% was selected as the OPWC, as seen in Figure 3.19.

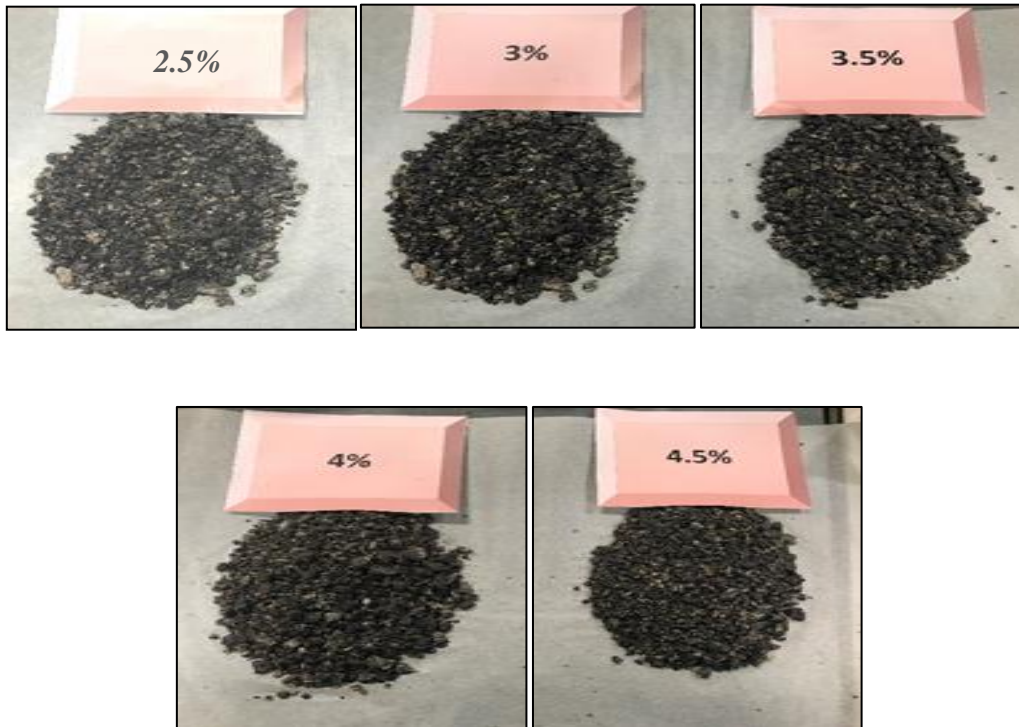


Figure 3.19: Percentages of pre-wetting water content

3.5.4 Determination of the Optimum Total Liquid Content at Compaction (OTLC)

The compaction of specimens is strongly influenced by the percentage of water used. A high percentage of water results in dissipated compaction effort, low density and unsatisfactory mechanical properties, while low workability of the mixture is the result of low water content. As such, optimizing the water content during compaction will improve the desired properties of the mixture.

The OPWC by coating test was 3% by total weight of aggregate, the IBEC 12.32%, as measured in the previous sections, meaning that the total liquid content was 15.32%. According to MS-14, different water contents at compaction (the loose mixtures were prepared at 15.32%

and compacted with different water contents in 1% steps by air drying) were investigated as Marshall's specimens. This gives an indication of the optimum water content at the level of compaction at which the dry density of the sample is at a maximum.

To find the OTLC at compaction, five percentages of total liquid content were investigated: 15.32%, 14.32%, 13.32%, 12.32% and 11.32%. The water content for each mix was measured prior to compaction, after leaving the loose mixtures for various periods to reduce the total liquid content. Afterwards, 50 blows per face of specimen, were applied using a Marshall Hammer. The dry density was then calculated according to MS-14 (Asphalt Institute, 1989). Figure 3.20 shows that 12.32% was the optimum percentage of total liquid content giving the highest dry density. Every single point in Figure 3.20, represents the average of three specimens' results.

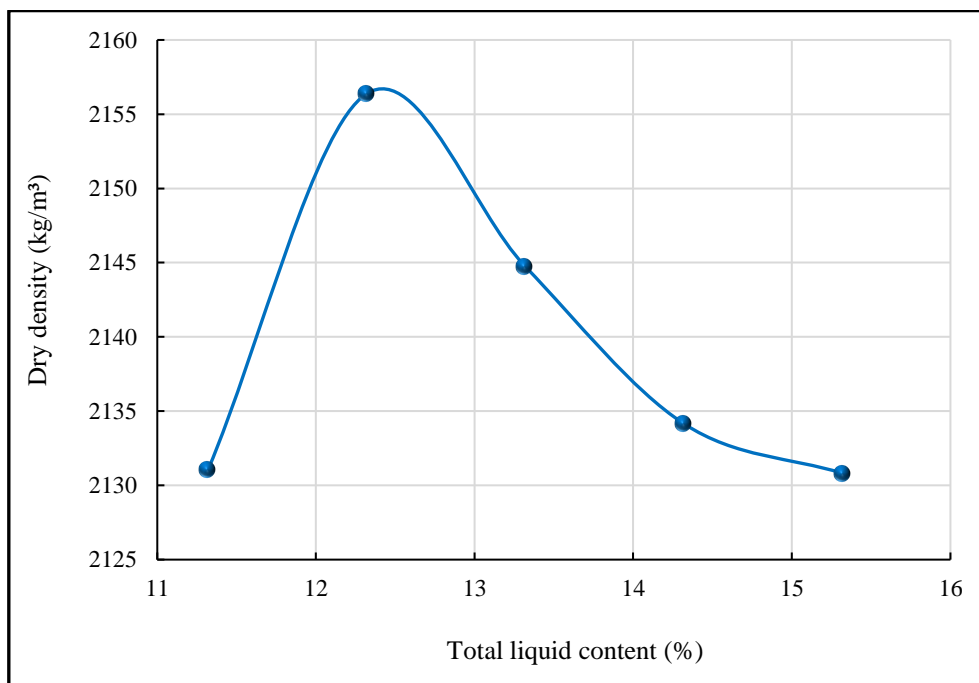


Figure 3.20: The percentage of optimum liquid content

3.5.5 Determination of the Optimum Bitumen Emulsion Content (OBEC)

Above and below the determined initial bitumen emulsion content, Marshall's specimens were prepared with different bitumen emulsion contents, while keeping the value of the total liquid content at 15.32%. The optimum residual bitumen emulsion content was obtained by measuring the ITSM for dry and soaked samples, as seen in Figure 3.21. It was observed that the optimum residual bitumen was 6.2% of the total weight of aggregate (12.4% bitumen emulsion content) for soaked samples, while for dry samples, the ITSM decreased when increasing the residual bitumen content. However, 12.5% bitumen emulsion content was rounded and considered to be the optimum emulsion content because the wet condition is the governing case.

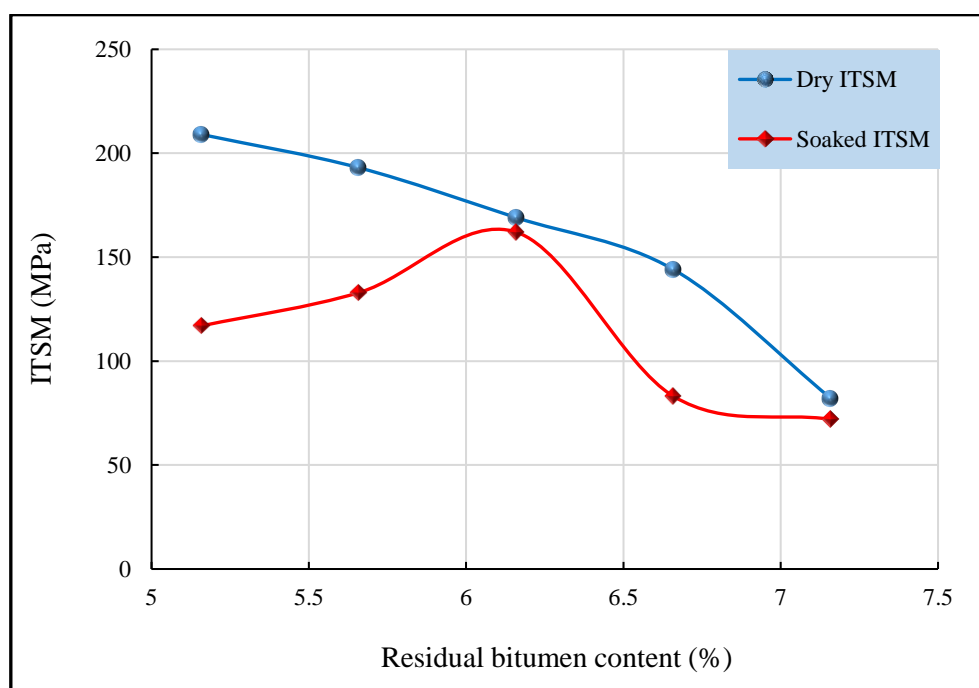


Figure 3.21: The percentage of optimum residual bitumen content

3.5.6 Preparation of Samples

All the CBEMs were prepared according to the method outlined by the Asphalt Institute (1989). The aggregate and filler materials, with the specified pre-wetting water content (3%), were

placed into the mixing bowl of a Hobart mixer (Figure 3.22a) and mixed for 60 seconds at low speed. The bitumen emulsion (12.5%) was then added gradually over the next 30 seconds, the mixing continuing for the next 90 seconds at the same speed. A Marshall Hammer (Figure 3.22b), was used to compact the 100 mm diameter samples with 50 blows to each face. Finally, the specimens were left inside their moulds for 24 hours, then extruded using a hydraulic de-moulding machine.

For comparison purposes, two types of hot mix asphalt with two different bitumen grades were prepared: an AC 10, close graded surface course with a soft bitumen 100/150 pen and an AC 10, close graded surface course with a harden bitumen 40/60 pen. According to PD 6691 (European Committee for Standardization, 2016b) for AC 10 close graded surface courses, 5.2% optimum binder content by weight of aggregate was added. The mixing temperature for the 100/150 and 40/60 AC 10 surface course was 150 to 160°C and 160 to 170°C, respectively. The compaction method and the number of blows applied for the HMAs were the same as CBEMs.

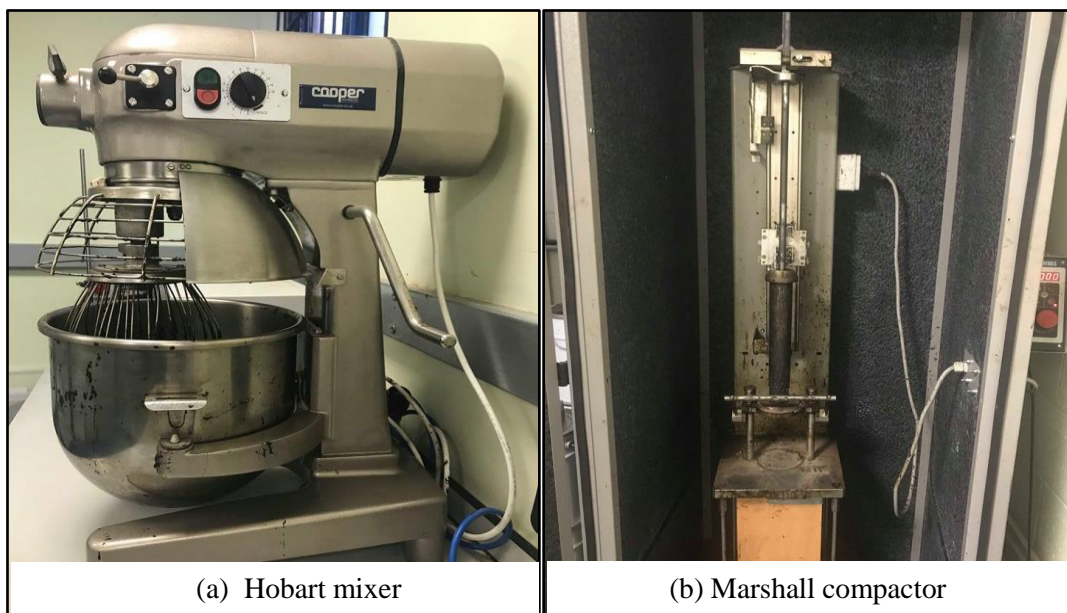


Figure 3.22: Steps of preparing samples of CBEMs

3.5.7 The Curing Regime for the CBEMs Samples

Curing of CBEMs can be defined as the process whereby the mixture loses water through evaporation. The strength gained by the CBEM is strongly related to moisture loss (Lee et al, 1983). The performance of the cold mixes improved markedly by increasing the curing temperature and time as reported by Bocci et al (2002). Previous researchers such as Thanaya (2003), Al-Busaltan et al (2012) and Al-Hdabi et al (2013) have used high temperature curing regimes e.g. 40°C for CBEMs due to the weak early strength of such mixtures.

In this research work, a room temperature of 20°C was adopted as the normal curing temperature for all the prepared mixtures when testing for ITSM. This regime was followed in order to mimic the production, laying and compaction of such mixtures in field conditions and also avert any premature ageing of the bitumen (Serfass et al, 2004; Khalid and Monney, 2009; Ojum et al, 2014). The earliest stage of curing started when the samples were in their moulds for 24 hours before extrusion. The samples were then kept at lab temperature until testing at different curing ages i.e. 3, 7, 14, 28, 90 and 180 days.

3.6 Summary

To summarise, the testing programme in this study can be divided into different stages of experimental works as follows:

- Experimental work to modify the bitumen emulsion and specify its characteristics in terms of viscosity, particle size, particle size distribution and performance of CBEMs containing the modified bitumen emulsion.
- Experiments used to identify the physical and chemical characteristics of the selected candidate materials for producing SCF. The output at this stage is to select a group of three waste materials, SSFA, FGD and CCR, which were involved in further experimental works.
- Optimisation stages for the production of SCF where binary blending optimisation using SSFA and OPC, and ternary blending optimisation using SSFA, OPC and CCR, were carried out. Investigation of the effects of mechanical activation (grinding) with FGD as a grinding aid agent, was also carried out. Optimisation was carried out in terms of compressive strength for the paste and indirect tensile stiffness modulus for the CBEMs.
- The investigation of hydration kinetics for both the conventional LF paste and the new SCF, was carried out using XRD and SEM analyses. The output at this stage was an explanation of the reasons behind the development in strength of the CBEM containing the new filler.
- Investigations of the durability and mechanical characteristics of the developed CBEM incorporating both the modified bitumen emulsion and the new SCF, were conducted in terms of water sensitivity, age-hardening, resistance to permanent deformation and fatigue resistance.

Chapter 4: Application of a New Technology - Ultrasound Technology - in Bitumen Emulsion

4.1 Introduction

Bitumen emulsion technology is an environmentally attractive method which minimizes costs and energy consumption. It can be defined as a two phase system where bitumen globules (dispersed phase) are suspended in water (continuous phase) by the effect of electrostatic charges supplied by an emulsifier (Read and Whiteoak, 2003). Bitumen emulsions are usually produced using colloid mills by forcing a mixture of molten bitumen and water through a rotating rotor and stator discs under the action of centrifugal forces. The diameter of bitumen droplets typically ranges between 0.1 and 50 μm . There are several factors affecting the particle size in bitumen emulsions, related to its components and the operating conditions of the manufacturing plant (Gingras et al, 2005).

Bitumen emulsions have different applications in the pavement industry such as surface dressing, prime and tack coats, bond coat, chip seals, micro-surfacing and cold asphalt mixtures. Regardless of its application, there are four essential physical parameters controlling the overall performance of bitumen emulsions: viscosity, stability, coating and breaking. These parameters are strongly affected by the bitumen particle size distribution (PSD) which also plays a significant role in the interactive bond between the cement and bitumen emulsion in the asphalt mixture (Hu et al, 2009). Macro emulsions are inherently in an unbalanced state, attempting to achieve a state of equilibrium over time through sedimentation, flocculation and coalescence. As a result of these destabilising processes, the droplet size distribution will alter, this eventually leading to complete separation of the phases (Sjoblom, 2001). Emulsions with

small globule size are more kinetically stable against sedimentation because of the increase in the repulsive forces between the particles due to the absorbed layer of surfactant and also the movement of the droplets due to gravitational forces is hindered by their neighbours; thereby given sufficient time before separate into their phases. This leads to an increase in the repulsive forces between particles, reducing the effect of destabilising actions (Tadros et al, 2004). In general, smaller particle size produces noticeable enhancements in the performance of bitumen emulsion in both mix and spray applications (Deneuvillers and Samanos, 2000).

Recently, interest has grown in the development of technological processes for the production of bitumen emulsion in order to control its physical and performance properties by adjusting the particle size and particle size distribution during the manufacturing process. Currently, ultrasound technology is the most promising and is applied in various industrial sectors, offering several improvements in performance compared to normal manufacturing processes. This study has therefore investigated, for the first time, the influence of ultrasound technology on the operational characteristics and performance of a bitumen emulsion, by changing the particle size and particle size distribution of the bitumen droplets. This has had an outstanding influence on the viscosity of the new emulsion (ultrasonic emulsion) as can be seen in section 4.3.

4.2 Sonication Treatment of the Bitumen Emulsion

Ultrasound has been shown its ability to produce emulsions with smaller particle sizes thanks to the cavitation phenomenon responsible for ultrasonically induced effects (Jayasooriya et al, 2004). The propagation of acoustic waves through aqueous media causes pressure fluctuations in simple sound waves which result in the formation and violent collapse of small bubbles during the expansion cycles. This breaks coarse particles down into smaller sizes.

In this study, a pre-prepared, cationic bitumen emulsion (C50A4), containing 50% residual bitumen content with macroscale bitumen droplets, was subject to ultrasonic agitation treatment using a high power ultrasonic device. A probe system ultrasonic processor manufactured by Hielscher Ultrasound Technology, Model UP 400S (Figure 4.1), was used to modify the bitumen emulsion. The horn tip of a 22 mm diameter cylindrical titanium probe was dipped in the conventional bitumen emulsion, the sonication process was then turned on to the highest power (100% amplitude), at a constant frequency of 24 kHz.

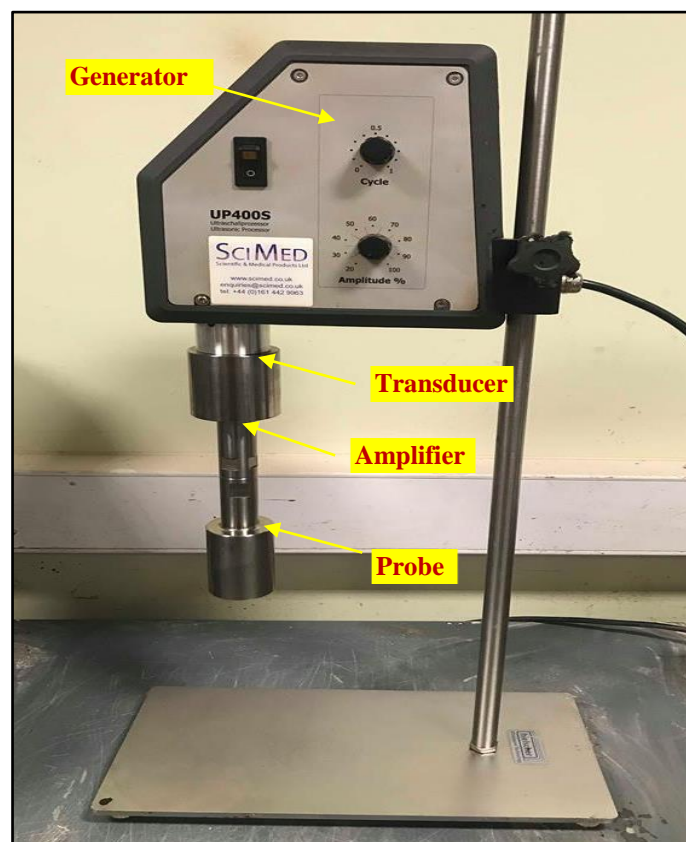


Figure 4.1: Ultrasound apparatus

Sonication time has a profound impact on the resulting droplet size. As treatment time increases, the amount of energy used to disintegrate the droplets also increases, this decreasing the particle diameter. Salvia-Trujillo et al (2013) conducted a study to investigate the effect of ultrasound processing parameters on the characteristics of lemon grass oil-alginate nano-

emulsions. Their results demonstrated that an increase in sonication time led to a decrease in droplet diameter. Similarly, Tang et al (2013) studied the effect of sonication processing time on the size of aspirin nano-emulsions. He deduced that the average particle diameter reduced as sonication treatment time increased up to 60 seconds; after that time, no changes in particle size occurred. Prolonging treatment above a certain limit, the optimum limit, is counter-productive (Maali and Mosavian, 2013). As such, in this study, the length of sonication treatment time was changed from 5 to 60 minutes in order to assess the effect of ultrasonic process time on the physical and performance characteristics of the treated emulsion. All experiments were carried out in a 500 ml plastic beaker at room temperature, in triplicate.

As the field of emitted sound is usually heterogeneous in ultrasound instruments, it is important to recirculate the emulsion sample so that all bitumen droplets experience the same shear rate and achieve a reasonably uniform particle size distribution. During the sonication process, the temperature of the treated emulsion was raised gradually because of the cavitation phenomenon. A digital thermometer was put on the side of the beaker to measure the temperature of the emulsion sample at the end of treatment. Figure 4.2 shows the elevation in temperature by the increase in processing time. The temperature at 0 to 20 minutes sonication processing time, increased linearly by approximately 275% compared to the normal (untreated) sample. After 20 minutes, the elevation in temperature was only 7% up to 60 minutes treatment. At the beginning of the sonication process, a violent turbulence in the emulsion sample was noticed, this accompanied by a loud sound which was attributed to the occurrence of cavitation. As the treatment time increased, the processing action became much steadier and calmer. This explains the considerable elevation in the sample's temperature at the beginning of treatment. In order to eliminate the impact of temperature rise on the properties of the treated bitumen emulsion, all treatments were performed in a cold water bath.

The influence of ultrasound treatment on the physical characteristics of the processed bitumen emulsion was investigated in terms of viscosity, particle size and particle size distribution. The threshold treatment time was selected in light of the results of the latter properties. The performance of the treated (modified) bitumen emulsion in CBEMs was evaluated and compared to CBEMs made with untreated (normal) bitumen emulsion.

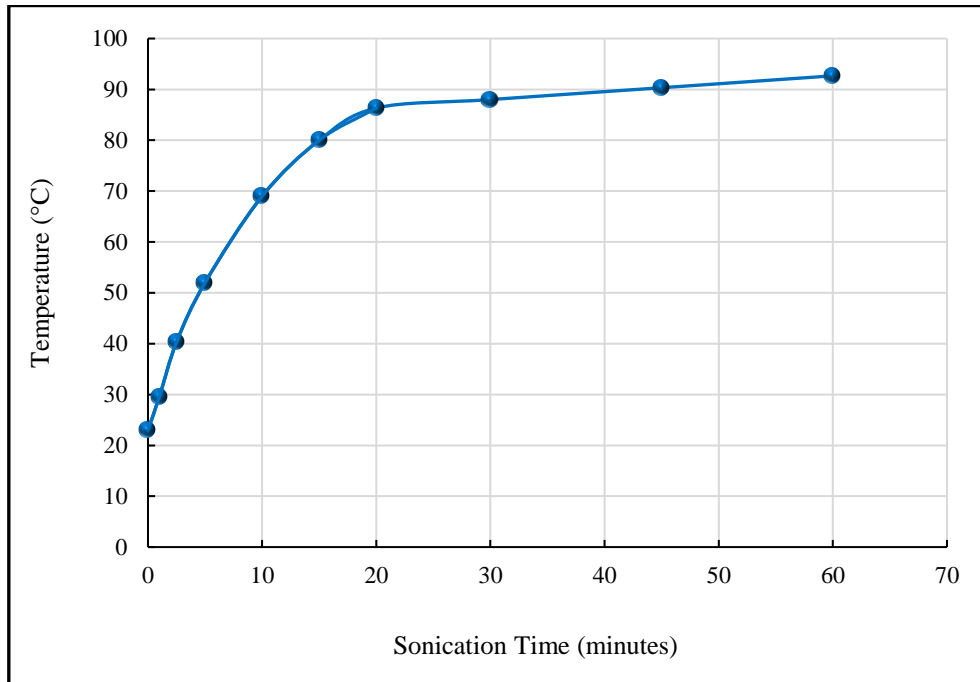


Figure 4.2: Effect of sonication treatment time on temperature

4.3 Viscosity Measurements

The viscosity of the treated bitumen emulsion samples was measured using a Brookfield DV-II+ Pro Viscometer, in accordance with BS EN 13302 (European Committee for Standardization, 2018a). All experiments were carried out in 600 ml glass beakers, at lab temperatures and in triplicate. Ultrasonic processing and other high shear treatments such as high pressure homogenization, have been reported to affect the flow behaviour of hydro-colloid dispersions due to the reduction in their molecular weight (Marcotte et al, 2001). The

degradation of the macromolecules is considered 'mechano-chemical' in nature, as stated by Striegel (2003).

From the results shown in Figure 4.3, the viscosity of the emulsions initially decreased with increasing treatment time, which indicates that samples exhibited shear-thinning behaviour at these ultrasonic duration levels. The reduction in the viscosity at 7 minutes treatment, was approximately 28% compared to the normal sample. Similar findings were presented by Wang et al (2006) in that the effect of ultrasonic treatment on petroleum coke oil slurry is not limited to simply decreasing the apparent viscosity, but also markedly improves its stability. Another study conducted by Kaltsa et al (2014) found that increasing the time or amplitude reduces the viscosity and droplet size in olive oil model emulsions containing xanthan, while also improving its stability. This reduction can be explained by the fact that when applying ultrasonic waves, the bitumen emulsion was more dispersed as the diameters of the bitumen droplets had decreased. Consequently, the amount of emulsifier adsorbed on the surface of the bitumen droplet decreased, i.e. the total bitumen-water interfacial surface area increased while the emulsifier film thickness decreased. Following this stage, sonicated bitumen emulsion will reach a mono-disperse state where the viscosity has decreased compared to that of the normal emulsion. Several researchers working on the physico-chemical characteristics of emulsions have found that the increase in the thickness of an emulsifier in an emulsion, leads to an increase in its viscosity (Napper, 1983; Karpenko and Gureev, 1998).

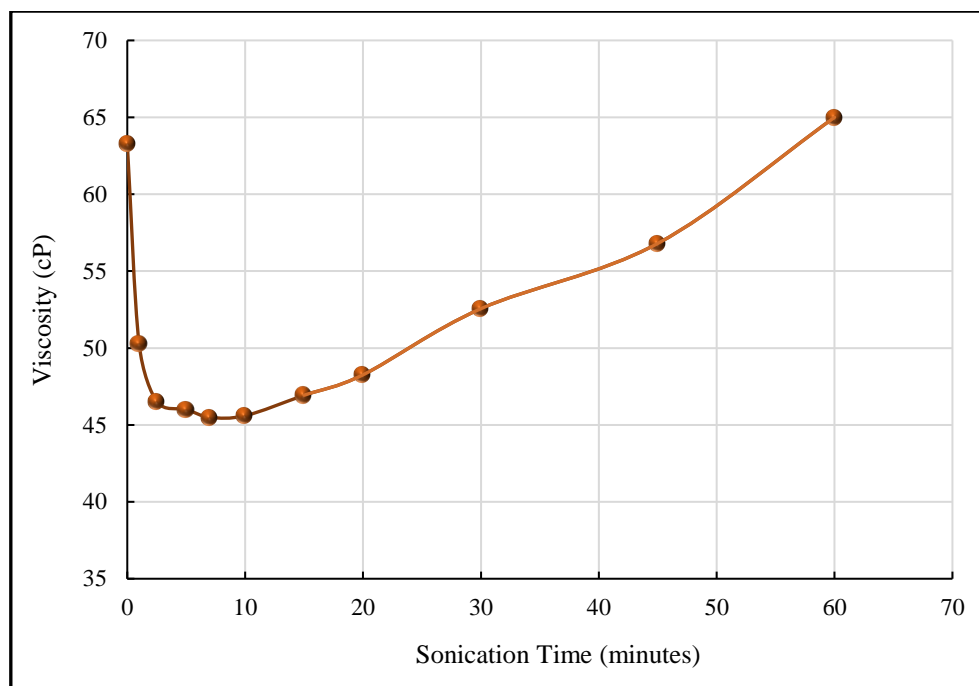


Figure 4.3: Effect of sonication time on the viscosity of treated bitumen emulsions

After 10 minutes of sonication, viscosity increases gradually. As treatment time increases, dispersion and coagulation of the bitumen droplets start to compete because the temperature has risen due to the vigorous mechanical mixing of the emulsion (over-processing). Coagulation of the bitumen globules will occur after a certain period of sonication treatment because of the increase in the number of globules, leading to increasing collisions through Brownian motions. The coalescence of bitumen particles will occur when the amount of emulsifier at the interface drops to a level where it loses its function as a barrier to prevent contact and coalescence of droplets. Therefore, the optimal time for ultrasound treatment should be used to avoid shear-induced coalescence and to prepare a more monodispersed bitumen emulsion with lower viscosity.

4.4 Droplet Size Measurements

Particle size (PS) and particle size distribution (PSD) were characterized by a Beckman Coulter Laser Diffraction Particle Size Analyser LS 13 320 apparatus, for different lengths of ultrasonic

treatment. Five measurements were carried out for each sample at lab temperature, using three samples for each treatment time. PSD was presented as a volume percentage vs. droplet diameter. The most commonly used metrics when describing particle size distributions are D-Values (D_{10} , D_{50} & D_{90}) which are the intercepts for 10%, 50% and 90% of the cumulative mass. . In addition, the width or ‘span’ of the PSD was calculated from the following equation:

$$\text{Span} = \frac{[D_{90} - D_{10}]}{D_{50}} \quad (4.1)$$

where

D_{50} : is the size in microns that splits the distribution with half above and half below this diameter.

D_{10} : is the diameter at which 10% of the sample's mass is comprised of particles with a diameter less than this value.

D_{90} : is the diameter at which 90% of the sample's mass is comprised of particles with a diameter less than this value

Figure 4.4 shows the differential PSD for all bitumen emulsion samples treated with different sonication durations, while Figure 4.5 presents the cumulative PSD. The emulsion samples were treated for 5, 7, 10, 12.5, 15, 20, 30, 45 and 60 minutes and their PSDs compared with the PSD of the normal sample. The results show that the diameters of the particles decreased on an increase in sonication time. An explanation for this is that as the treatment time increased, the applied energy also increased leading to more intensive cavitation and the production of smaller particles. These differences were more obvious in the case of D_{10} , D_{50} and D_{90} , as seen in Table 2.1. This Table also demonstrates how the width of distribution became closer with increasing treatment time. 7 minutes sonication treatment gives approximately 85% reduction in D_{50} , 86% reduction in D_{10} and 90% reduction in D_{90} , compared to the normal sample. In

addition, the PSD became narrower by approximately 40% when compared with before sonication treatment.

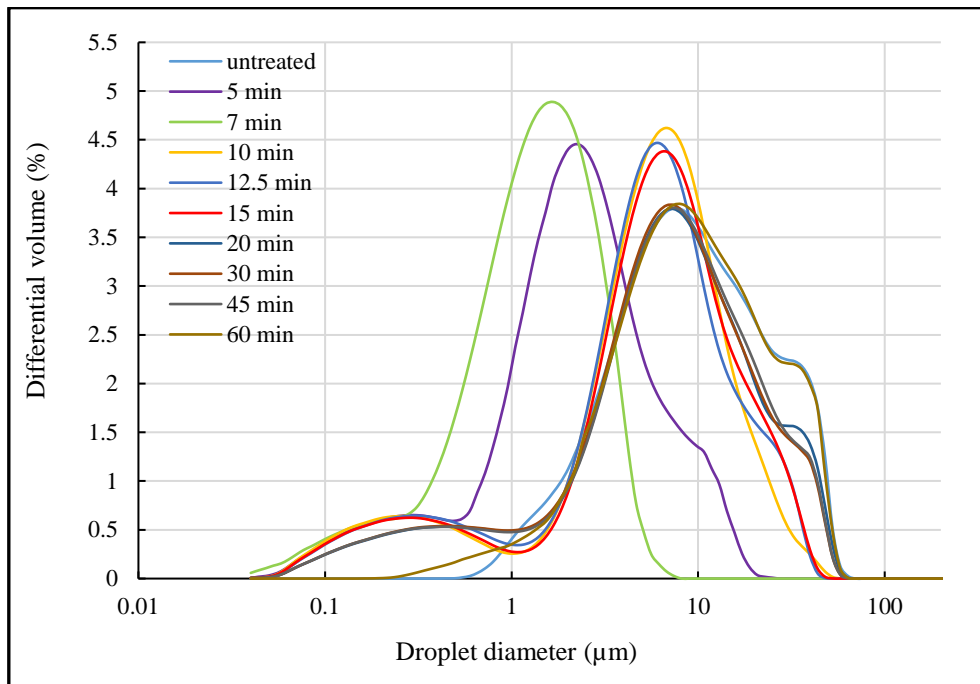


Figure 4.4: Effect of sonication time on PSD

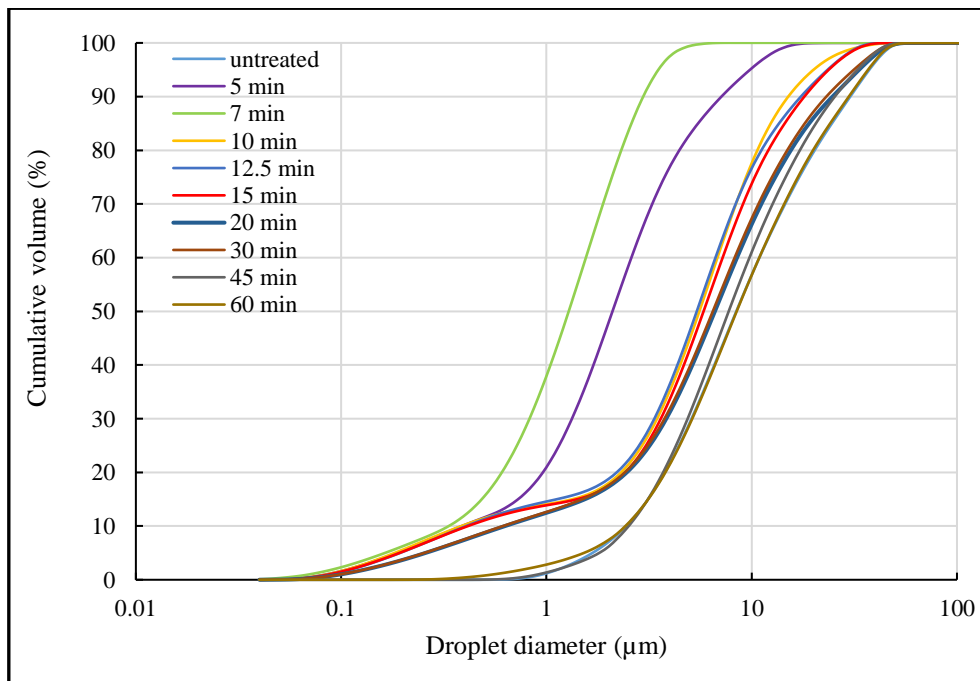


Figure 4.5: Effect of sonication time on cumulative distribution

Table 4.1: Effect of sonication time on PS

<i>Treatment time (min.)</i>	<i>D10 (μm)</i>	<i>D50 (μm)</i>	<i>D90 (μm)</i>	<i>Span</i>
0	2.423	8.146	30.068	3.393
5	0.375	2.207	7.421	3.192
7	0.341	1.261	2.919	2.044
10	0.375	5.609	15.651	2.723
12.5	0.412	5.609	17.181	2.989
15	0.412	6.158	18.861	2.995
20	0.598	6.760	24.951	3.602
30	0.598	6.760	24.951	3.602
45	2.423	7.421	27.391	3.364
60	2.423	8.943	30.068	3.091

However, this is apparently limited to a specific duration (7 minutes); after that, PS starts to increase. This phenomenon, where the particle size increases with an increase in input energy, can be referred to as “over-processing” as stated by Desrumaux and Marcand (2002). This can be attributed to poorer functioning of the emulsifiers and an increase in Brownian motion, hence a higher probability of collision and coalescence with higher energy input. In these conditions, the droplet size distribution of the emulsion, is a result of the competition between two opposite processes; droplet disruption and drop-drop coalescence. A fresh interface is created whenever a droplet is formed from the disruption of an original droplet. Between its formation and its subsequent encounter with other droplets, some surfactant will be adsorbed onto this fresh interface. If the timescale of collision is shorter than the timescale of adsorption, the fresh interface of the newly formed droplets will not be fully covered with surfactant, such conditions leading to coalescence. Since the newly formed droplets are not completely covered

by the surfactant, a higher rate of collision represents a greater coalescence rate, leading to an increase in the droplet size (over-processing).

From the PS and PSD results above, it is clear that 7 minutes represents the optimum time (threshold time) for sonication treatment of bitumen emulsion to achieve smaller PS and more uniform PSD.

4.5 Application of Modified Bitumen Emulsion in CBEMs

4.5.1 CBEM incorporating Limestone Filler (LF)

The performance of the CBEMs made using sonicated bitumen emulsions, was evaluated in terms of indirect tensile stiffness modulus (ITSM) and air void contents. An asphalt concrete, AC 10 mm, close graded surface course, was selected based on BS EN 13108 (European Committee for Standardization, 2016a), to prepare the control CBEM containing conventional LF and normal bitumen emulsion (NBE). A HMA with two grades of bitumen, 100/150 and 40/60 pen bitumen, were prepared for comparison purposes. The preparation method was previously presented in Chapter 3 (section 3.5.6). The control mixtures were stored at 20°C and subjected to ITSM testing at 3, 7, 14, 28, 90 and 180 days.

The behaviour of the cold asphalt mixtures is unusual compared to the control hot mixes, especially at an early age. A combination of several factors leads to this behaviour including the existence of water, binder film coalescence and cohesion, and the reaction between the aggregate and emulsion (Serfass et al, 2004). Figure 4.6 illustrates the performance of these mixtures at different curing times, showing that the control CBEM displays low strength during its early life but gains strength progressively over time, with an increasing rate of water evaporation. The development in the ITSM value for the control CBEM mainly occurred during the first 28 days. However, these values are relatively low compared to the target ITSM value for 100/150 (1500 MPa) and 40/60 HMA (4000 MPa) (Al-Busaltan, 2012; Nassar, 2016;

Shanbara et al, 2018). It is worth mentioning that even though the ITSM test is a non-destructive test, three samples of CBEM-LF were fabricated for each curing time due to the inability of the specimens to withstand testing. In contrast to the CBEM, neither grade of hot mix showed any noticeable change in its performance over time.

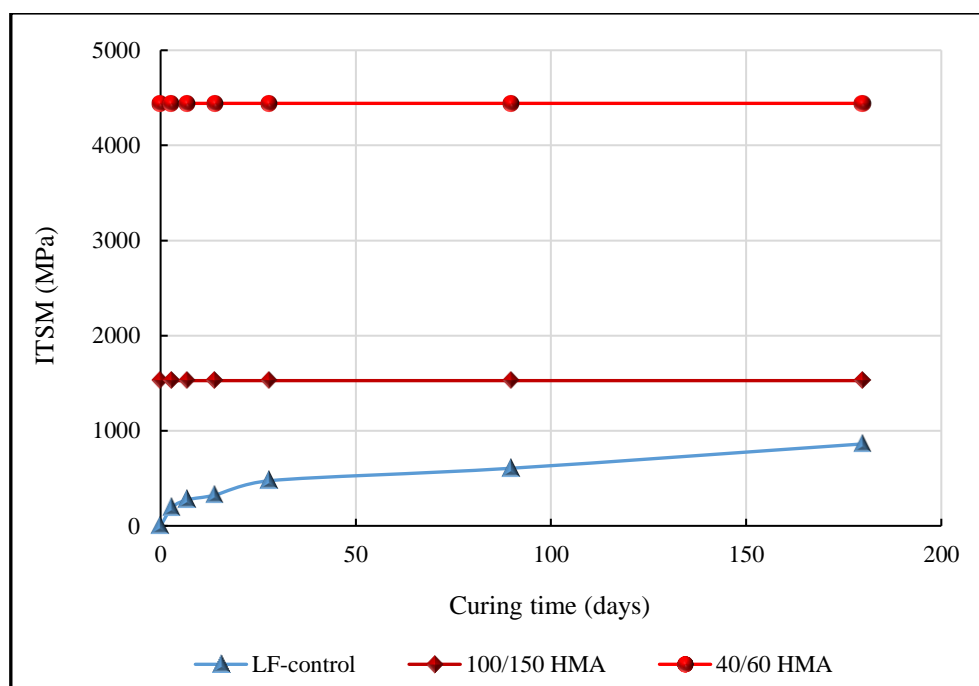


Figure 4.6: Development ITSM values of the control CBEM containing LF

CBEMs made from LF and treated bitumen emulsion subject to a range of sonication times (5, 7, 10, 12.5, 15 and 20 minutes), were tested and compared with the control CBEM and HMAs at various curing ages. The results of ITSM testing for the prepared specimens after 3 days age are presented in Figure 4.7, where 0 time refers to the control CBEM including NBE. The results show that 7 minutes sonication treatment achieved the best ITSM value over other treatment times. The improvement in ITSM at 3 days of age for CBEM made from 7 minutes treated emulsion, is approximately 70% in comparison to the mix with NBE at the same age. This improvement is most probably due to the greater specific surface area provided by smaller particles in the sonicated bitumen emulsion which achieved a better coating quality between

the aggregates and bitumen binder. As the sonication time increased over 7 minutes, ITSM values decreased gradually. This can be attributed to recoalescence of the newly formed bitumen droplets due to them being insufficiently covered with surfactant. This also explains the increase in emulsion viscosity, as discussed in Figure 4.3.

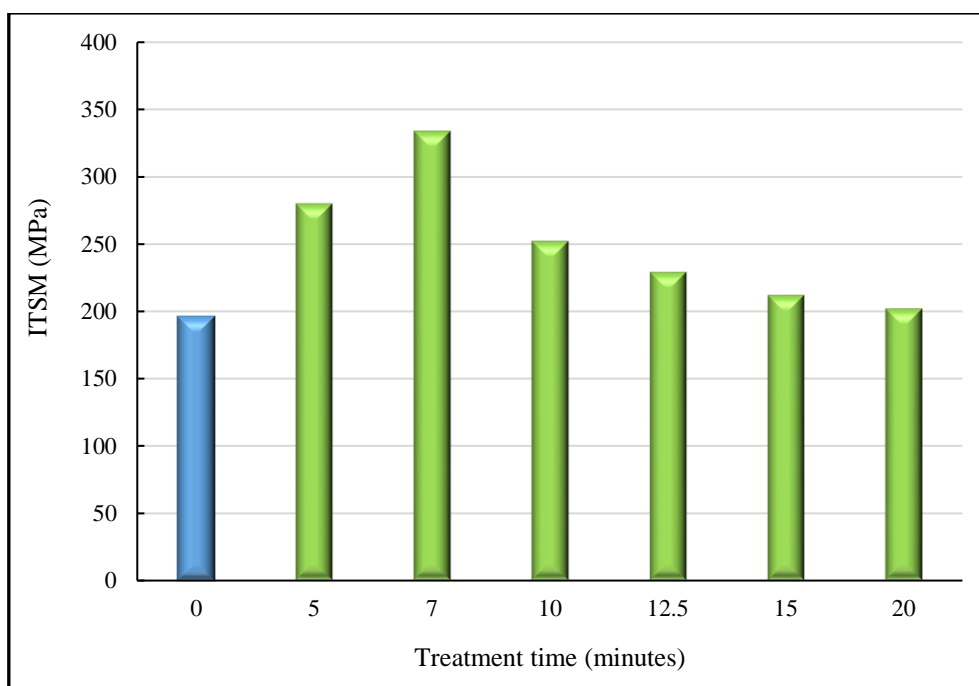


Figure 4.7: Effect of sonication time on the ITSM of CBEMs at 3 days

From the results above, it is clear that 7 minutes represents the optimum time (threshold time) for the sonication treatment of the bitumen emulsion used in this study. Accordingly, this treatment time was selected to prepare a modified bitumen emulsion (MBE) with smaller PS and more uniform PSD, to be used to develop a new CBEM.

The CBEM with 7 minutes-MBE at different curing ages, was subjected to ITSM testing and compared with the control mixes, as seen in Figure 4.8. Similar to the control CBEM with NBE, the 7 minutes treated CBEM gained the most improvement in ITSM during the first 28 days, compared to longer age spans.

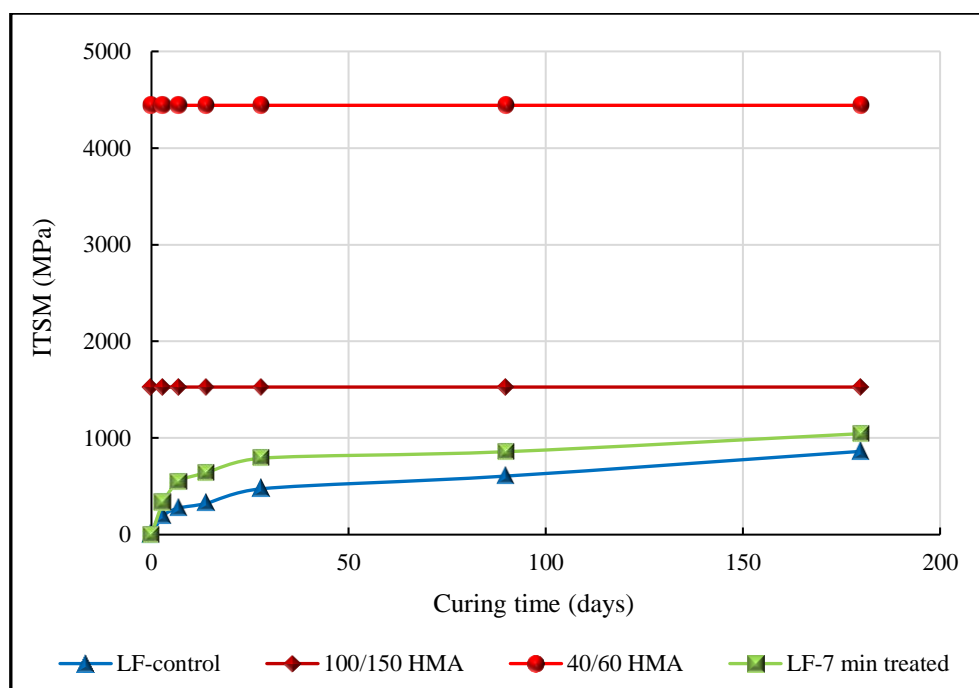


Figure 4.8: ITSM values of 7 minutes treated CBEM with curing times

The volumetric properties of the Marshall specimens in terms of air void contents, were measured in accordance with the Asphalt Institute (1989) recommendations after 3 days of curing. Table 4.2 presents the results of the measured air void contents for CBEMs made from sonicated bitumen emulsion and NBE for comparison purposes. All CBEMs with sonicated bitumen emulsions, showed lower air void contents than the control mixture with NBE. However, the mixture with 7 minutes MBE has the lowest air void contents, approximately 33% compared to the conventional CBEM-LF with NBE. This is related to lower viscosity and smaller bitumen particles of the 7 minutes MBE which provided a better coating for the aggregates, which in turn, facilitated the compaction effort of the mixture. This is also reflected in the better performance of the CBEM mixture with 7 minutes sonicated emulsion after three days curing age, as shown in Figure 4.9. The mixtures made from bitumen emulsion with longer treatment durations (longer than 7 minutes) have higher air void contents in comparison with other mixtures made from emulsions sonicated at 5 minutes and 7 minutes. This is

explained by recoalescence of the bitumen droplets in the emulsions sonicated for more than 7 minutes, thereby reducing the surface area of the droplets which adversely affects the ability of bitumen film to coat the aggregates and consequently, the compaction quality of the mixture. Although this ultrasound technology appears to be very promising in enhancing the properties of CBEM, the mechanical performance of the cold mixes measured in terms of ITSM is still poor compared to traditional hot asphalt mixtures. Consequently, in common with other researchers (Al-Hdabi, 2014; Nassar, 2016; Dulaimi, 2017), ordinary Portland cement (OPC) was used to substitute conventional limestone mineral filler (LF) as explained in the next section, in an attempt to improve the performance of the CBEM.

Table 4.2: Air void contents of CBEMs with treated and untreated bitumen emulsions

Sonication duration (min)	Air Void Content (%)
0	12.23
5	9.81
7	8.25
10	10.25
12.5	10.49
15	10.62
20	11.55
100/150 HMA	3.85
40/60 HMA	3.53

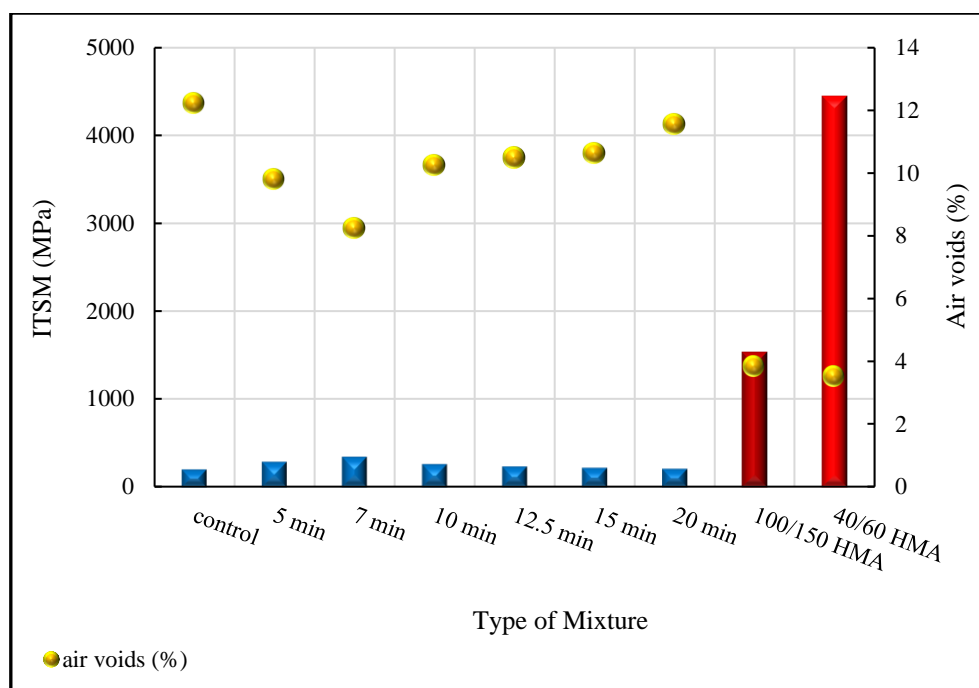


Figure 4.9: Air void contents and ITSM of CBEMs at 3 days with different treated emulsions

4.5.2 CBEM incorporating Ordinary Portland Cement (OPC)

Hydraulic binders such as cement, have been incorporated in cold asphalt mixtures by many researchers in order to overcome their shortcomings and upgrade their mechanical characteristics, as described in Chapter 2. Cold mixes including OPC, showed improvement in their strength, resistance to rutting and resistance to fatigue at early ages (Al-Busaltan, 2012; Al-Hdabi, 2014; Nassar, 2016; Dulaimi, 2017). As such, the second step in the development of the new CBEM in this study, is to replace conventional LF with the following percentages of OPC: 0%, 1%, 3% and 6%, by total weight of dried aggregate. The mixtures with said percentages of OPC were first made with NBE and subject to ITSM testing at different curing ages (3, 7, 14 and 28 days). Figure 4.10 shows that the use of OPC as a filler replacement substantially increases the ITSM value of CBEMs, approaching their ultimate value when LF is fully replaced by OPC. The stiffness modulus of CBEM containing 6% OPC, increased by approximately 17 times in comparison with conventional CBEM-LF at just 3 days. The CBEM

containing 6% OPC had twice the ITSM value of 100/150 HMA at 3 days of age, while its ITSM value is close to that of 40/60 HMA after nearly 10 days, as shown in Figure 4.11. It is obvious that the increasing rate of stiffness modulus of the CBEM containing 6% OPC at early ages, was comparatively higher than at other ages. The reasons behind this improvement are the formation of cementitious bonds and the consumption of trapped water induced by the hydration process of OPC, which leads to a loss in moisture from the mixtures. This improvement in the ITSM overcomes deficiencies associated with CBEMs-LF, namely low early life strength and a long curing time. Therefore, total substitution of conventional LF by OPC (6%) is recommended to achieve the targeted improvements in CBEMs.

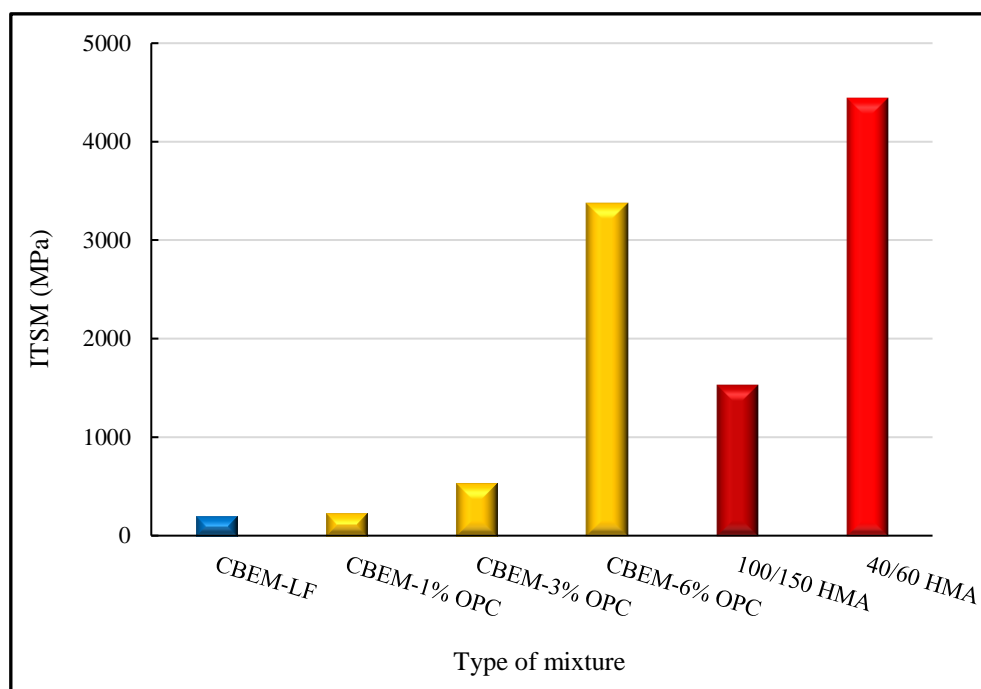


Figure 4.10: Influence of OPC replacement on ITSM values in CBEMs at 3 days

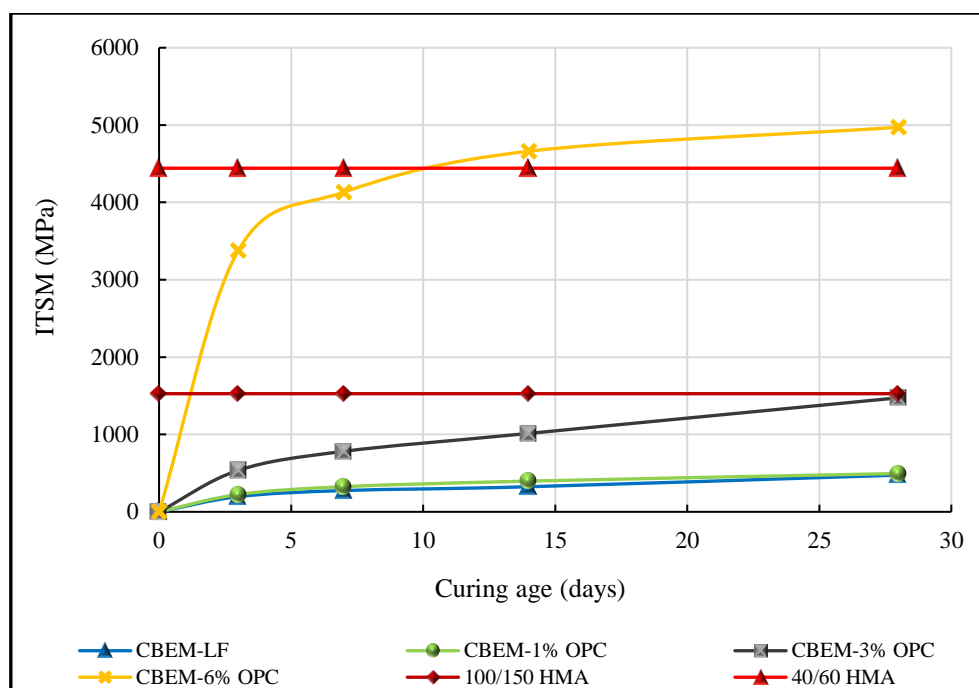


Figure 4.11: ITSM values of OPC mixtures at different curing times

The performance of CBEM made from 6% OPC and MBE, was investigated in terms of ITSM testing and compared to the same mixture containing NBE. The results at 3 days of curing are given in Figure 4.12. It is clear from this figure that MBE improved the ITSM value for the CBEM-OPC by around 11%, compared to the same mixture including NBE. Also, the CBEM-OPC with MBE reached the same ITSM value as for 40/60 HMA at 7 days, as shown in Figure 4.13. This development is explained by:

- i. The presence of OPC in the CBEM accelerating breaking of the cationic bitumen emulsion as it increases the pH because of the alkaline nature of the cement paste. This leads to an increase in the dissociation rate of the emulsifier on the bitumen droplets, allowing the bitumen emulsion to flocculate and coalesce rapidly, as demonstrated by Wang et al (2013);
- ii. The loss of trapped water during the hydration process of the OPC, which is responsible for creating a cementitious bond between aggregates alongside the bitumen binder; and

- iii. The MBE provided a uniform coating of bitumen emulsion film for the aggregates, thus increasing compaction which reduces the air void contents, thereby improving its strength.

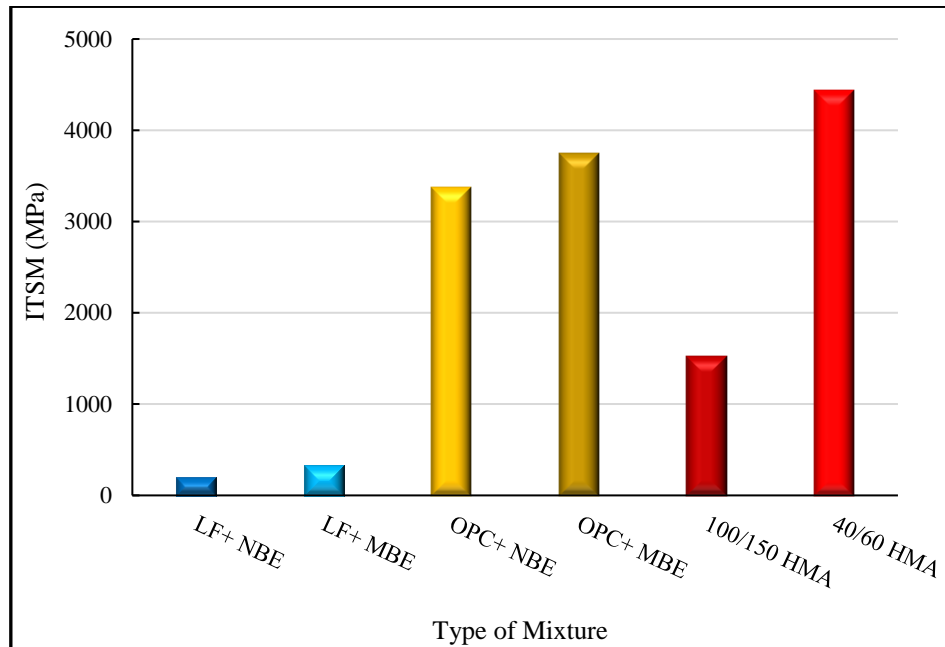


Figure 4.12: Influence of MBE on the ITSM value for CBEM-OPC at 3 days

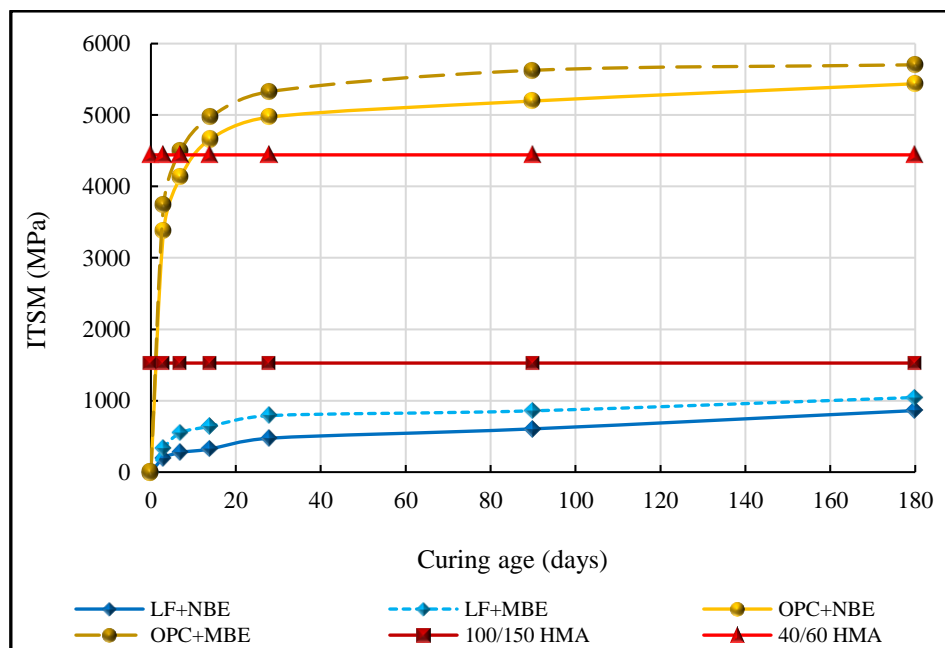


Figure 4.13: ITSM values for CBEM-OPC with MBE at different curing ages

Unfortunately, the use of OPC has economic and ecological shortcomings. The cement industry consumes a lot of energy and quarry materials thus contributing to CO₂ emissions. Therefore, the author of this thesis has decided to upgrade the performance of the CBEMs by developing a new secondary cementitious filler made from waste and by-product materials to work as an effective alternative to the OPC. The next chapter will cover the process development of the new filler.

4.6 Summary

This chapter has presented and described the modification process of the cationic bitumen emulsion (C50B4) by applying ultrasound technology using a Dr Hielschers device, Model UP 400S (400 Watts, 24 kHz), resulting in the production of a bitumen emulsion with lower viscosity and smaller uniformly distributed droplets (modified bitumen emulsion). The modified emulsion provides a better quality of coating on the aggregates in the mixture, facilitating increased compaction and reducing air void contents. This has been confirmed by the ITSM values of the modified CBEM when compared to conventional CBEM made with conventional emulsion. This chapter also included the performance enhancement of the CBEM by replacing conventional LF with OPC. A significant increase in ITSM results was reported with complete replacement of LF with OPC, especially in its early life. Further developments were achieved by producing a CBEM-OPC with modified bitumen emulsion. Higher stiffness moduli was achieved at different curing ages, in comparison to those mixtures employing normal emulsion, providing results comparable to those for 40/60 HMA. In conclusion, this innovative technology (sonicated bitumen emulsion and OPC) appears to be very promising in overcoming the shortcomings associated with the use of conventional emulsion and LF.

Chapter 5: Development of a New Secondary Cementitious Filler

5.1 Introduction

Many environmental and economic benefits have been achieved by producing cementitious materials from waste, or by-product materials, as alternatives to cement, in different types of concrete production (Mohammed et al, 2013). There are a variety of cementitious materials such as fly ashes, ground granulated blast-furnace slag and silica fume that can be used as construction materials, individually or collectively, with cement. Such materials show either pozzolanic or hydraulic behaviours (Snellings et al, 2012). Although there are considerable variations in their properties, different types of cementitious materials share the ability to take part in chemical reactions and form compounds that supplement cement hydration products (Snellings et al, 2012).

This chapter includes the results of the experimental works which identified the physical and chemical properties of commercial types of limestone filler (LF) and ordinary Portland cement (OPC), as well as the candidate waste materials used in this study to produce a new secondary cementitious filler (SCF) namely, sewage sludge fly ash (SSFA), flue gas desulphurisation (FGD) gypsum and calcium carbide residue (CCR). Initially, the mineralogy and the morphology of LF (commonly used as mineral filler in the production of asphalt concrete mixtures), OPC, SSFA, FGD and CCR were investigated. A comparison between the properties of the candidate materials to those of LF and OPC, was conducted to assess the suitability of these materials to develop a new cementitious filler. Following this, a laboratory investigation for the physico-chemical activation of SSFA by grinding with FGD and blending with OPC, was carried out.

5.2 Characterisation of the Selected Mineral Fillers

5.2.1 Limestone Filler (LF)

A commercial LF, supplied by Francis Flower Ltd, was used in this study. The chemical composition analysis of the LF using an EDXRF (described in Chapter 3, subsection 3.3.2.1), is presented in Table 5.1. The results show that the LF was mainly comprised of calcium oxide (CaO) and silicon dioxide (SiO₂). The main crystal peaks recognised in the X-ray diffraction pattern of the LF were calcite (CaCO₃) and quartz (SiO₂) (Figure 5.1). The pH value of the LF was 9.12. The particle size distribution (PSD) of the LF powder was also examined; 90% of the particles passed through sieve 76 µm, as demonstrated in Figure 5.2. In the SEM image, shown in Figure 5.3, the LF particles appear as irregular shapes with sharp angles. Although LF has a high content of CaO, approximately 73.712%, it is considered an inert material (no hydration occurs when in contact with water) because CaO exists in a non-hydrated state (pure calcium carbonate) (Speweik, 2011).

Table 5.1: The chemical composition of LF and OPC

Chemical Compounds	LF%	OPC%
<i>CaO</i>	73.712	64.488
<i>SiO₂</i>	16.937	24.862
<i>Al₂O₃</i>	0.029	1.247
<i>MgO</i>	0.977	1.519
<i>Fe₂O₃</i>	---	1.856
<i>SO₃</i>	0.100	2.805
<i>K₂O</i>	0.355	0.783
<i>TiO₂</i>	0.194	0.434
<i>Na₂O</i>	2.136	1.572
<i>P₂O₅</i>	0.250	---

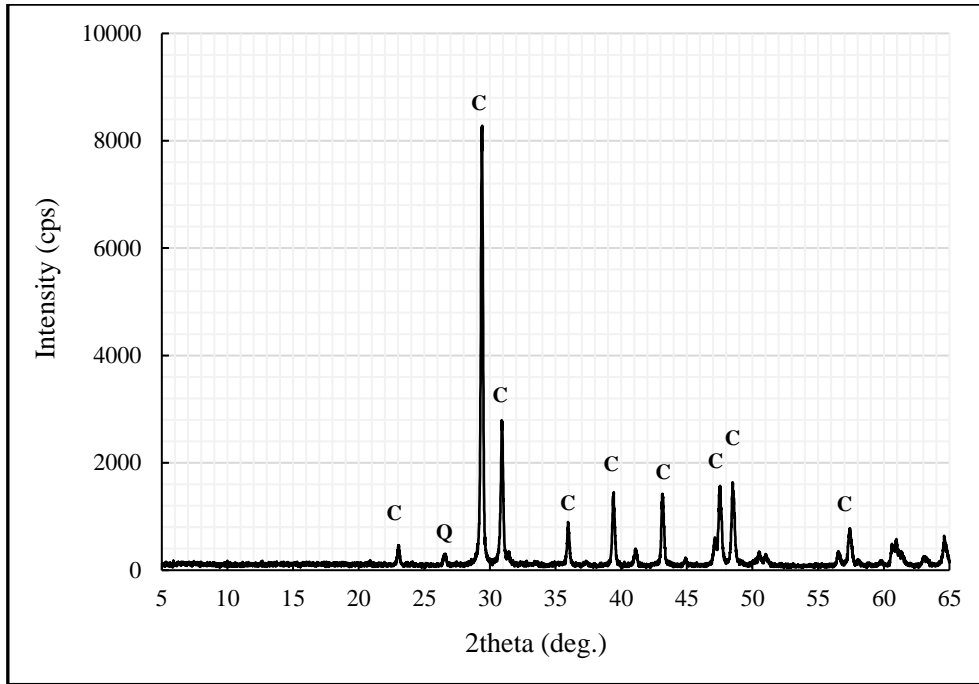


Figure 5.1: The XRD pattern for the LF powder (C= calcite, Q= quartz)

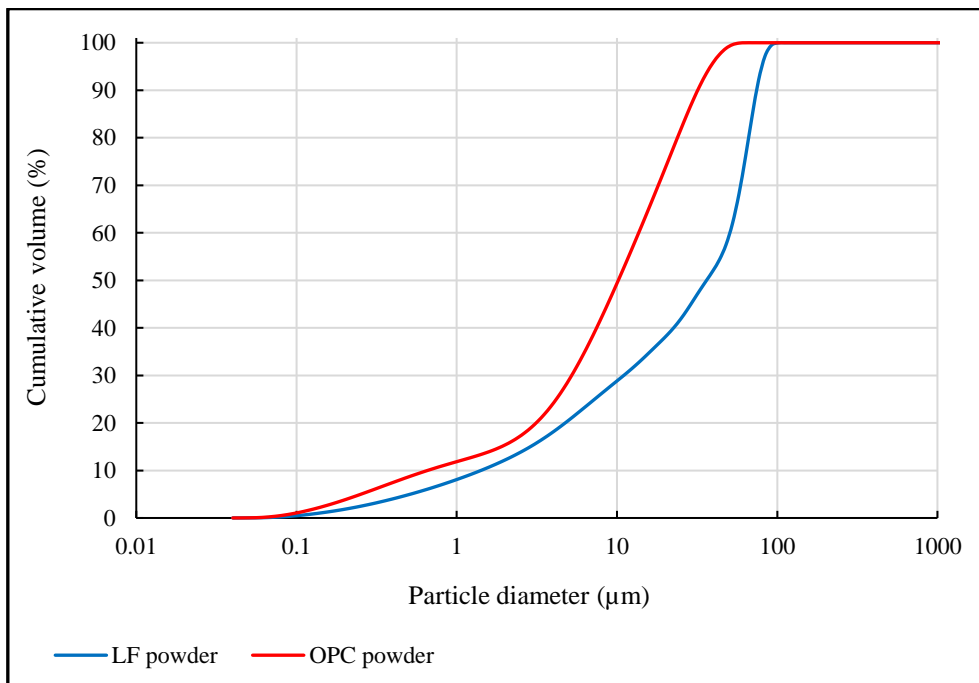


Figure 5.2: Particle size distribution of the LF and OPC

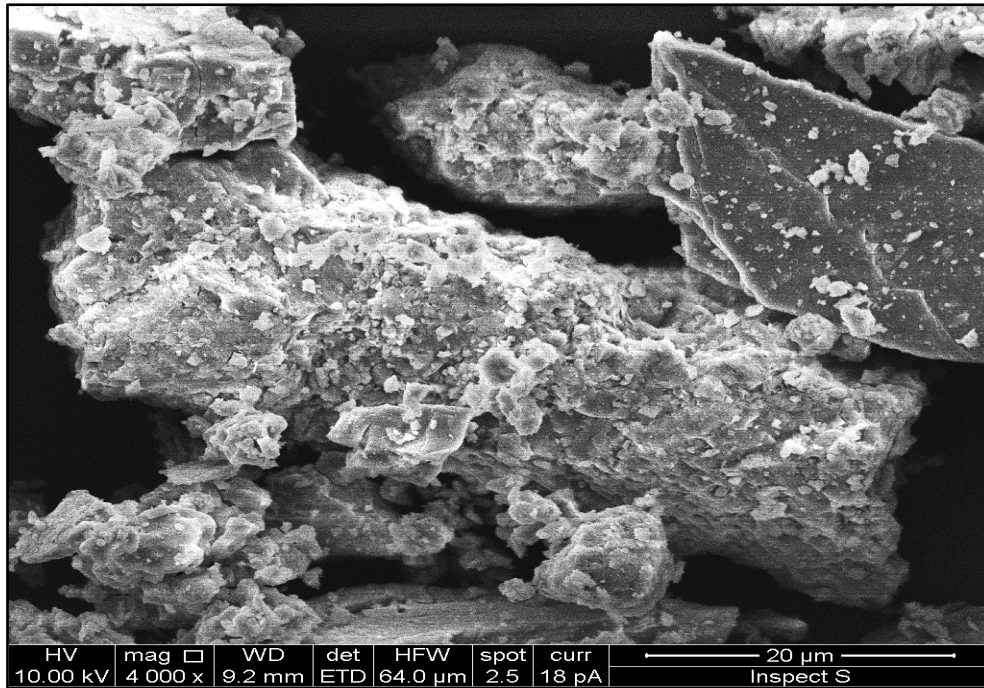


Figure 5.3: SEM image for dry powder LF

5.2.2 Ordinary Portland Cement (OPC)

A commercial ordinary Portland cement (OPC CEM-II/ A-L 42.5-N), manufactured by QUINN CEMENT, was used throughout this study. The chemical composition of the OPC measured using EDXRF, is reported in Table 5.1 above. It can be seen that it mainly consists of free lime (CaO) and SiO₂ which are responsible for the hydration process and gains in strength with longer curing time. These results are consistent with the chemical compositions of the same type of cement as analysed by Sadique et al (2012b), Dulaimi et al (2017) and Jafer et al (2018). The mineralogical configuration of the crystal particles in the powder form of OPC, obtained by XRD analysis, is illustrated in Figure 5.4. The diffraction patterns of OPC comprised calcite (CaCO₃), alite (3CaOSiO₂), belite (2CaOSiO₂), periclase (MgO) and ferrite (4CaOAl₂O₃.Fe₂O₃). The pH of the aqueous solution of the OPC was found to be 12.85 which helps to speed up the breaking of bitumen emulsion in the CBEM (Fang et al, 2016b). This OPC has finer particles than the LF, as seen in Figure 5.2 above. It is observed that the dominant

particle size almost fall below 30 μm . The fineness of OPC particles has an important effect on the hydration rate when exposed to water. This allows a higher reactivity reaction through the hydration process by increasing the surface area exposed to the hydration reaction, thus producing higher strength. The SEM micrograph of OPC in a dry powder state, shown in Figure 5.5, illustrates that the OPC particles have a variety of angular shapes, produced after grinding the clinker pellets.

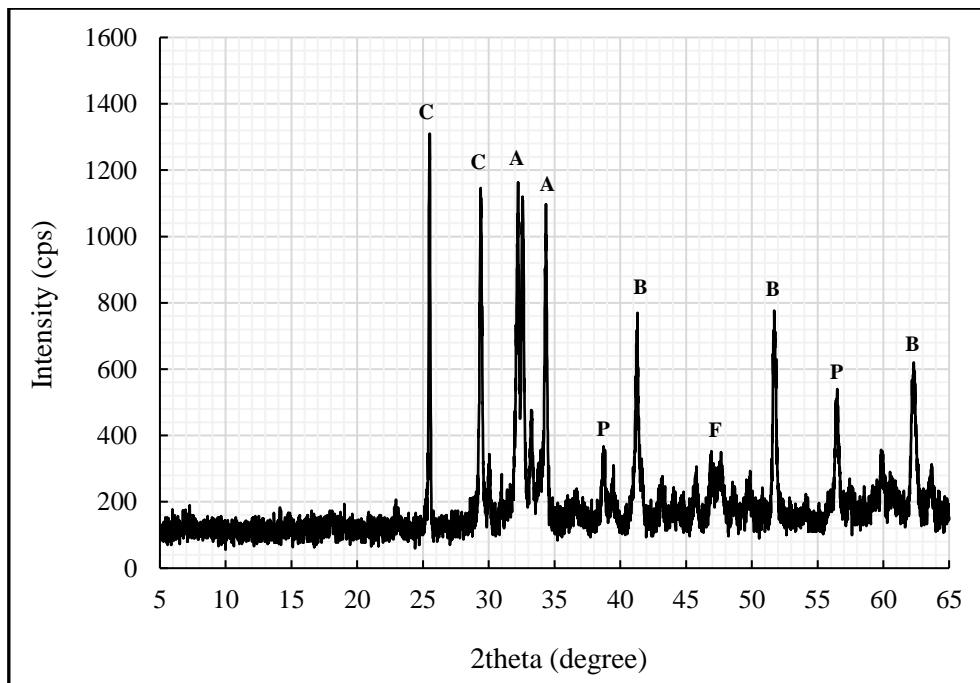


Figure 5.4: The XRD pattern diagram for the OPC (C= calcite, A= alite, B= belite, P= periclase, F= ferrite)

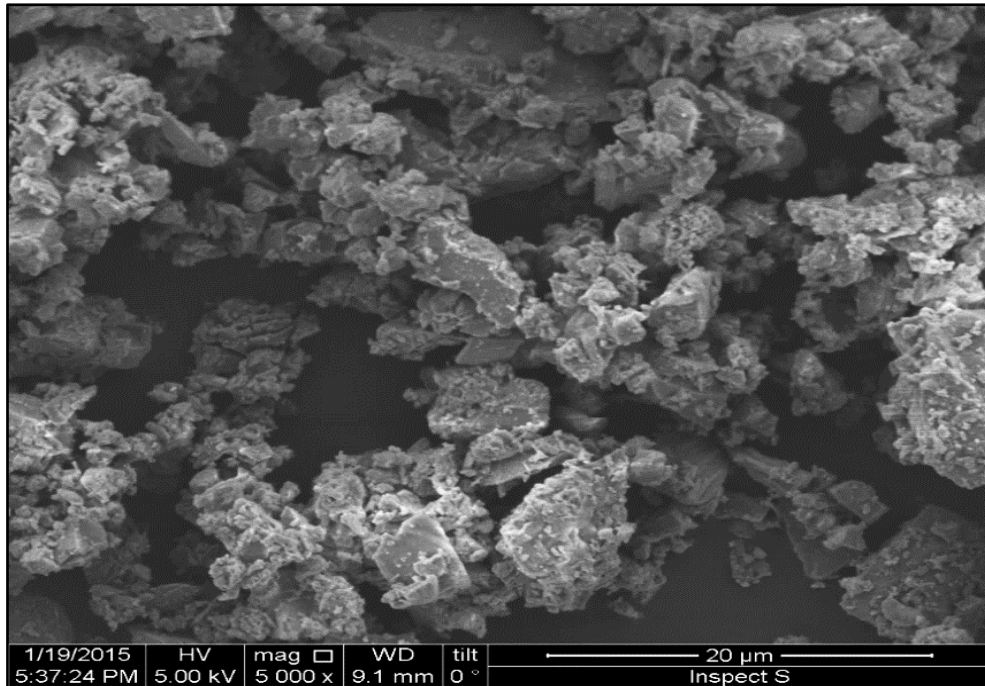


Figure 5.5: SEM image for dry powder OPC

5.2.3 Sewage Sludge Fly Ash (SSFA)

Sewage sludge refers to the residual, semi-solid material that is a result of sewage treatment and of waste water discharged from households and industries. Sewage sludge fly ash (SSFA) is dewatered sewage sludge which has been combusted through an incinerator.

The SSFA used in this study was supplied by the United Utilities Limited sewage sludge incineration system, Mersey Valley SPC, Widnes, UK. The digested sludge is pumped along the Mersey Valley Sludge Pipeline to Shell Green. At Shell Green, the sludge is dewatered through centrifuges to around 26% dry solids and then conveyed to sludge dryers. It is then fed into a fluidised bed incinerator which operates at between 800 and 900°C. Fly ash is then removed using an electrostatic precipitator where it is held in a silo for collection and then sent to landfill.

The chemical composition of the SSFA used in this study is shown in Table 5.2. The SSFA primarily consists of SiO_2 because of the use of sand in the fluidised combustion process. Iron oxide (Fe_2O_3) is also present in relatively high quantities as a result of the use of ferric chloride, or ferrous sulphate, as a flocculator making the SSFA a dark reddish-brown colour. A considerable amount of calcium oxide (CaO) is also present. X-ray diffraction analysis (Figure 5.6), shows that the dominant mineral phases of SSFA are quartz (SiO_2), hematite (Fe_2O_3), magnetite (Fe_3O_4) and whitlockite ($\text{Ca}_3(\text{PO}_4)_2$). The pH of the aqueous solution of the SSFA was found to be 8.29. The particle size distribution for the raw SSFA is presented in Figure 5.7 where it can be seen that the particles are much coarser than OPC particles, most of them between 5 to 84 μm , with a mean diameter of 36.33 μm . The SEM image is given in Figure 5.8, showing that the raw SSFA particles were rough, irregular in shape and contained some isolated and open pores which demand more water for paste samples than OPC.

Table 5.2: The chemical compositions of raw SSFA

Chemical Compounds	%
<i>CaO</i>	10.538
<i>SiO₂</i>	30.233
<i>Al₂O₃</i>	3.071
<i>MgO</i>	2.498
<i>Fe₂O₃</i>	15.236
<i>SO₃</i>	0.08
<i>K₂O</i>	1.285
<i>TiO₂</i>	1.189
<i>Na₂O</i>	1.512
<i>P₂O₅</i>	0.25

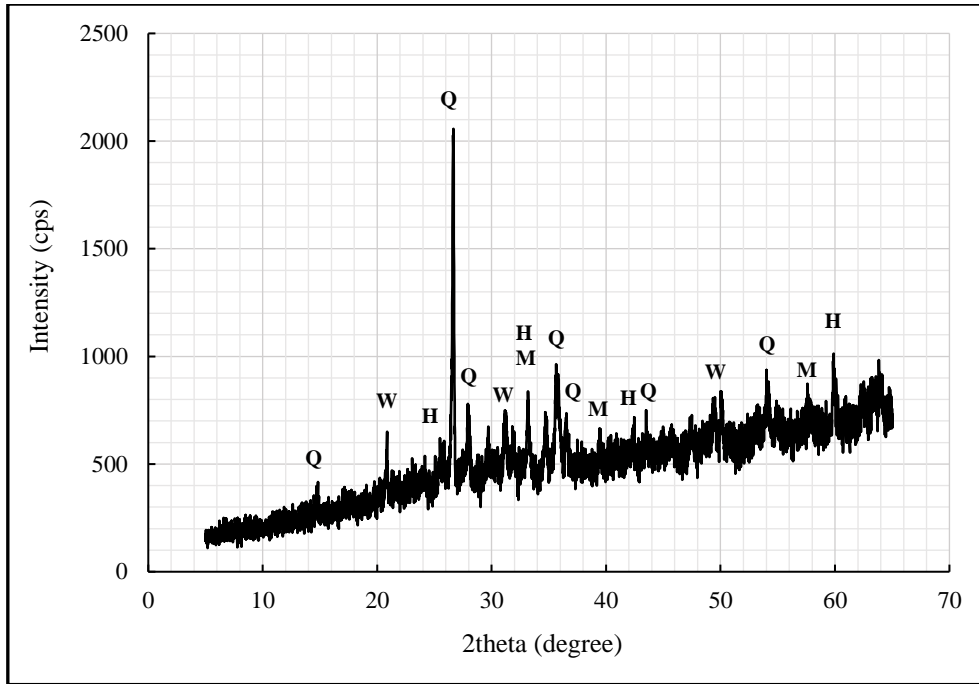


Figure 5.6: Mineralogy of the SSFA (Q= quartz, H= hematite, M= magnetite, W= whitlockite)

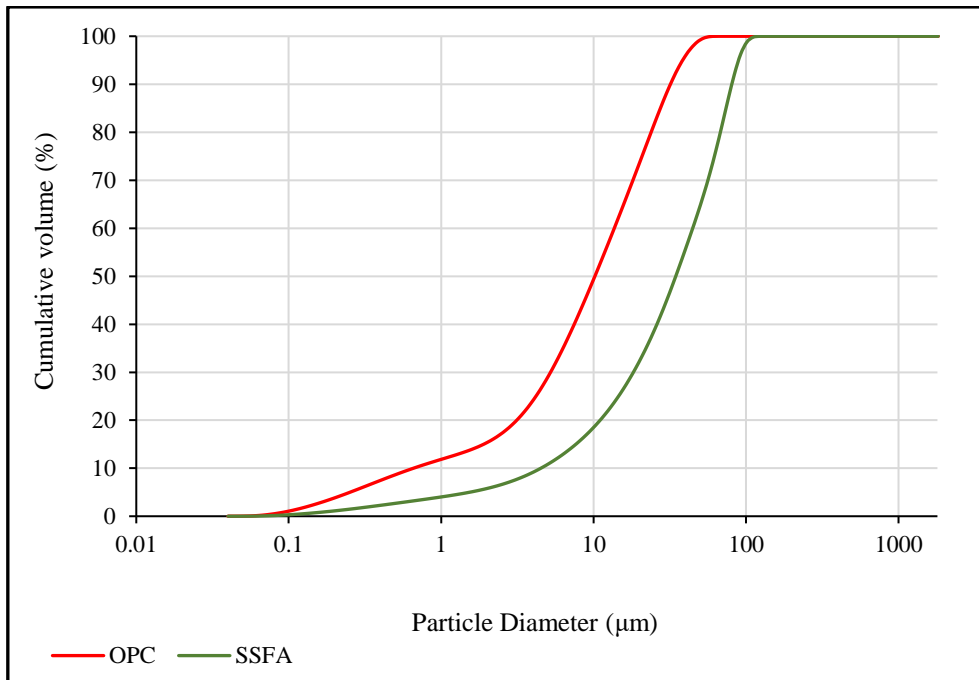


Figure 5.7: Particle size distribution of the SSFA powder

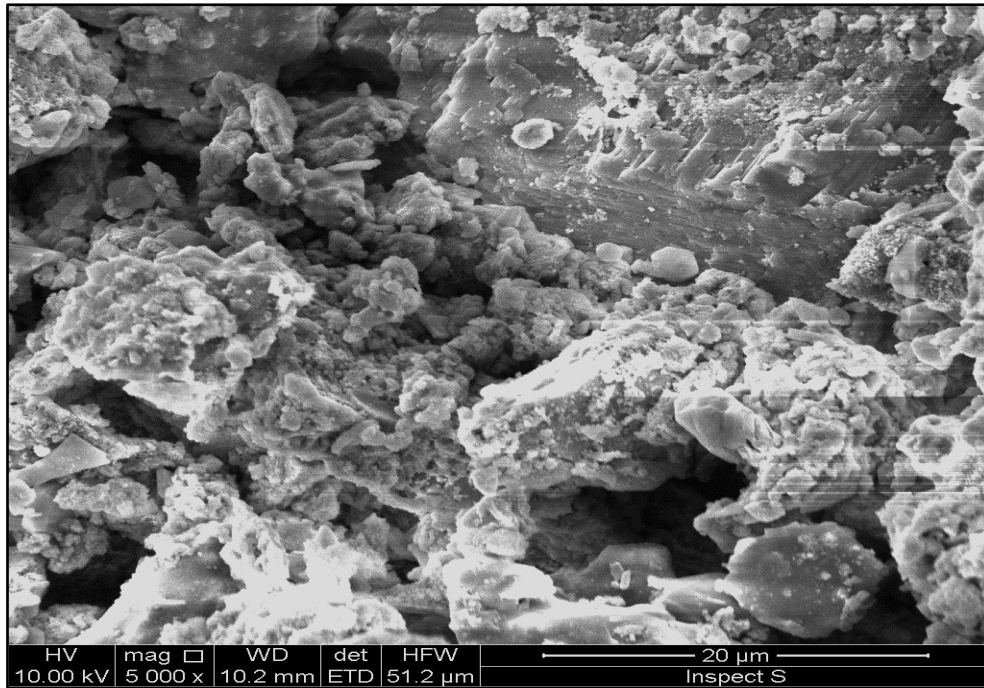


Figure 5.8: SEM image for dry powder SSFA

5.2.4 Flue Gas Desulphurisation (FGD) Gypsum

Flue gas desulphurisation is the technology commonly used to remove sulphur dioxide from flue gas in coal-fired power plants before being released into the atmosphere, thus reducing the environmental impact (Sadique et al, 2012a). There are two major processes commonly used for desulphurisation using CaO as an alkaline sorbent: wet type scrubbing and dry, or semi-dry scrubbing. The FGD gypsum used in this study was collected from a 4,000 MW coal-fired power station that used limestone slurry as a sorbent. Because the raw FGD was in a semi-dry state, it was dried at a temperature of $100\pm 5^{\circ}\text{C}$ for 24 hours before blending or conducting the EDXRF, XRD, SEM and PSD tests. The aqueous solution of FGD has a pH value of 12.3. The EDXRF analysis of the FGD, shown in Table 5.3, indicated that the major chemical compounds present were calcium oxide (CaO) and sulphate (SO_3), and a smaller amount of silica (SiO_2). Figure 5.9 illustrates the powder diffraction pattern of the FGD, mainly composed of calcium sulphate hemihydrate ($\text{CaSO}_4 \cdot 1/2\text{H}_2\text{O}$) in addition to calcium sulphate dehydrate

(CaSO₄.2H₂O) and quartz (SiO₂). The PSD of the FGD gypsum powder is shown in Figure 5.10 which shows that approximately 90% of the particles are smaller than 10 μm. FGD gypsum powder has regular crystal-shaped particles, as shown by the SEM micrograph in Figure 5.11.

Table 5.3: The chemical compositions of the FGD gypsum

Chemical Compounds	%
<i>CaO</i>	34.036
<i>SiO₂</i>	14.409
<i>MgO</i>	0.520
<i>SO₃</i>	33.335
<i>K₂O</i>	0.031
<i>TiO₂</i>	0.107
<i>Na₂O</i>	1.184
<i>P₂O₅</i>	0.250

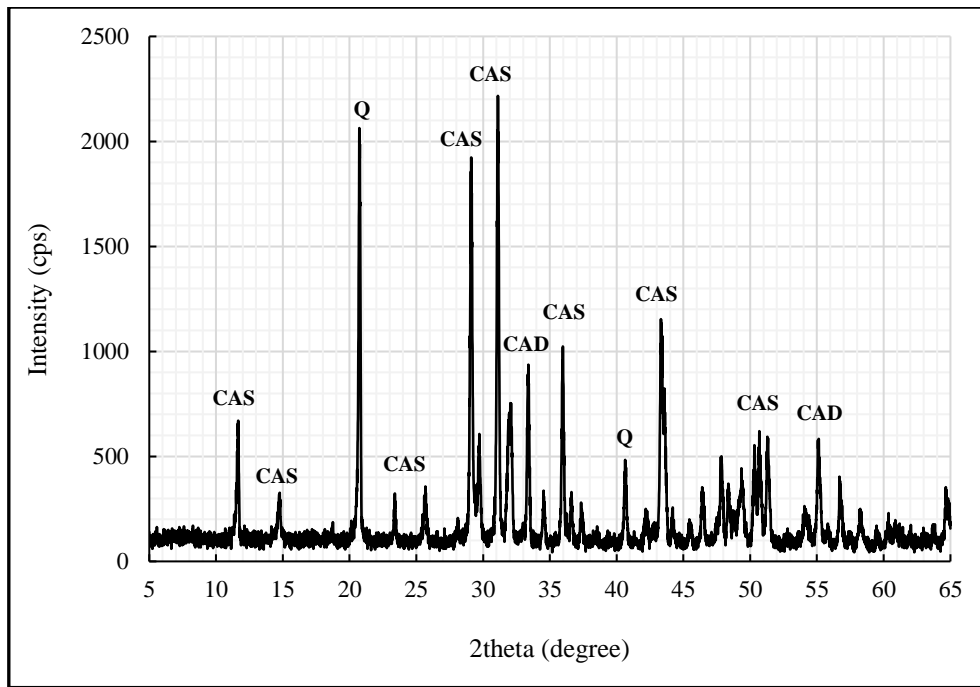


Figure 5.9: XRD patterns of the FGD gypsum (CAS= calcium sulphate hemihydrate, CAD= calcium sulphate dehydrates, Q= quartz)

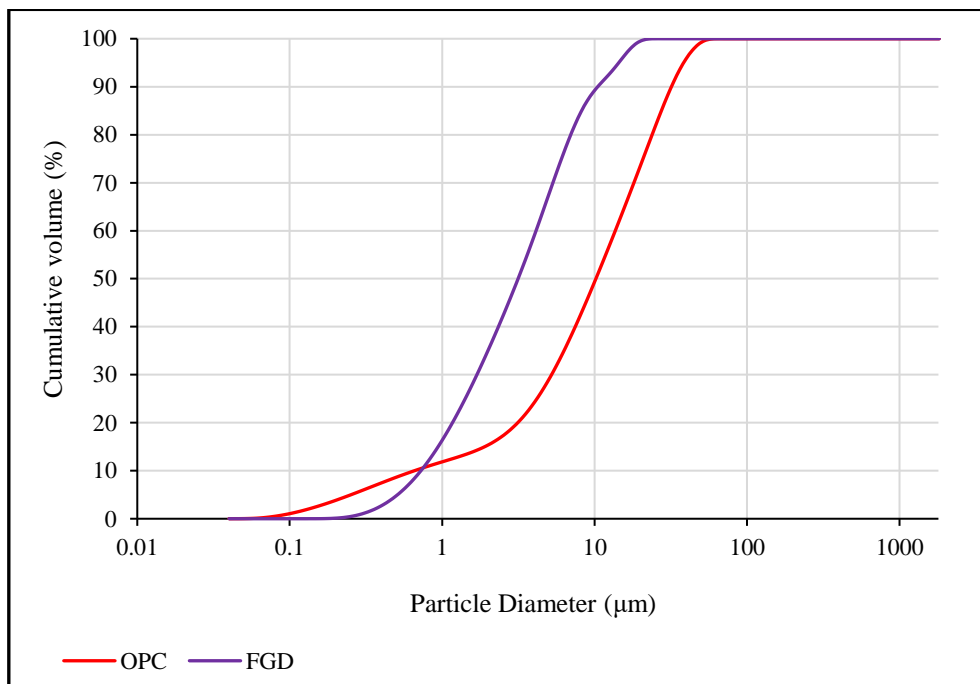


Figure 5.10: Particle size distribution of the FGD powder

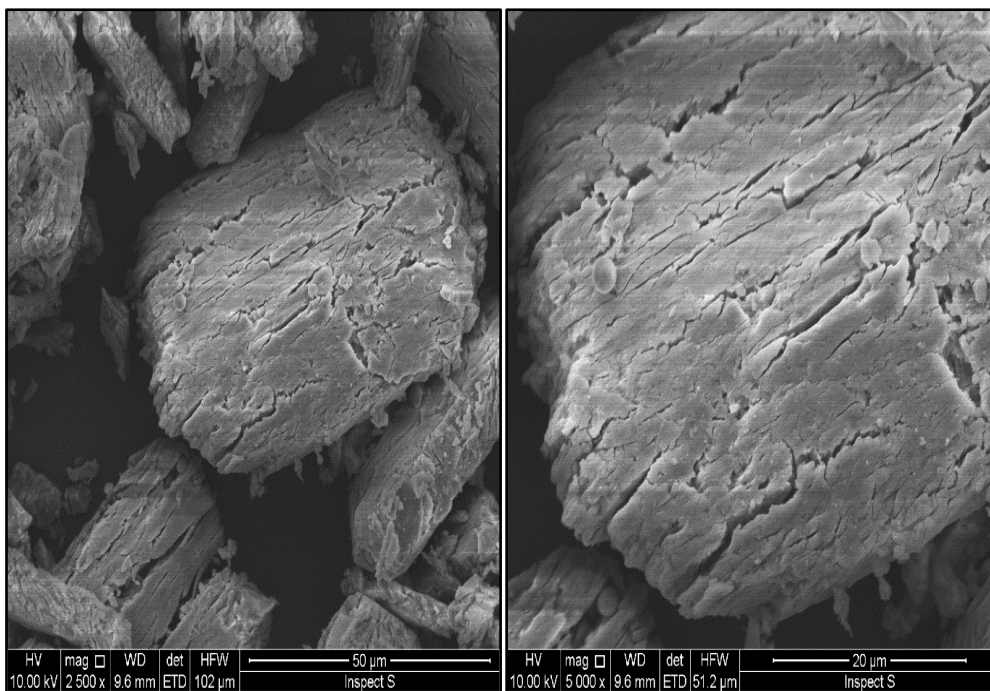


Figure 5.11: SEM image for dry powder FGD

5.2.5 Calcium Carbide Residue (CCR)

Calcium carbide residue (CCR), also called carbide slurry or lime slurry, is produced as a by-product of the industrial production of acetylene gas (Jaturapitakkul and Roongreung, 2003). In the production process, calcium carbide (CaC_2) is mixed with water to produce acetylene gas (C_2H_2), lime slurry ($\text{Ca}(\text{OH})_2$) and heat. The final product is a sludge in slurry form. After the high alkalinity water is fully discharged, the slurry transforms to a solid-state residue which makes disposal to landfills an expensive and difficult task. Globally, the production of acetylene gas was approximately 500,000 tonne in 2014, with a generation of approximately 1,423,000 tonne of CCR correspondingly as waste, and it is expected to grow by 3% until 2020 (Market Research Store, 2015).

The CCR used in this study was supplied by BOC UK & Ireland (a member of the Linde Group) dissolved acetylene plant, located in north east Lincolnshire, UK. When delivered, the material was in the form of large, wet blocks, making it necessary to break it into small pieces and oven

dry at $100\pm 5^\circ\text{C}$ for 24 hours. The resultant lumps were then pulverized using a mechanical grinder. In this study, it was found that 5 minutes of grinding, using a pestle and mortar grinder, achieved a finer grade, as seen in Figure 5.12. This was to take sustainability into consideration and avoid agglomeration due to excessive grinding. The average grain size (D_{50}) of the CCR ground for 5 minutes, was approximately $10\ \mu\text{m}$. The EDXRF analysis, seen in Table 5.4, reveals the presence of an impressive amount of calcium oxide in addition to some silica. The XRD profile of CCR (Figure 5.13), shows calcium hydroxide ($\text{Ca}(\text{OH})_2$) as the main component, in addition to small amounts of calcite (CaCO_3) and graphite (C), which were also reported in CCR studied by other researchers (Vichan and Rachan, 2013; Saldanha et al, 2018). The high alkalinity of this material ($\text{pH}=13$), could provide an ambient environment to activate the hydration process of the incorporated cementitious components, as stated by Al-Hdabi et al (2014b). From SEM photographs of CCR powder (Figure 5.14), it appears as a very coarse agglomeration of particles with irregular surfaces.

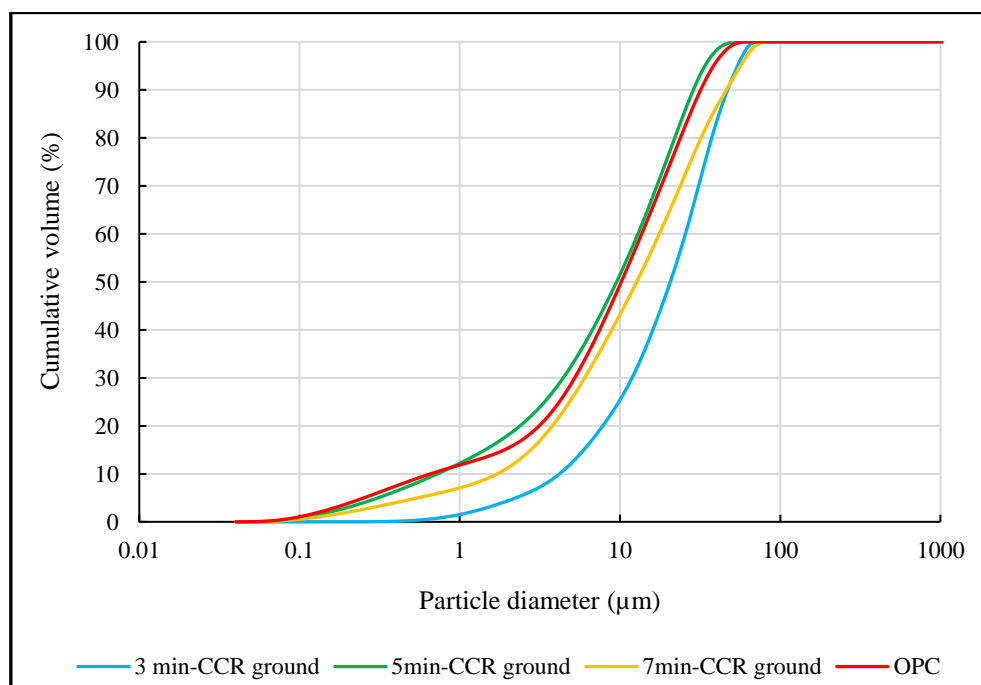


Figure 5.12: Particle size distribution of the CCR powder

Table 5.4: The chemical compositions of the CCR

<i>Chemical Compounds</i>	<i>%</i>
<i>CaO</i>	80.031
<i>SiO₂</i>	15.939
<i>MgO</i>	0.954
<i>SO₃</i>	0.619
<i>K₂O</i>	0.047
<i>TiO₂</i>	0.162
<i>Na₂O</i>	1.508

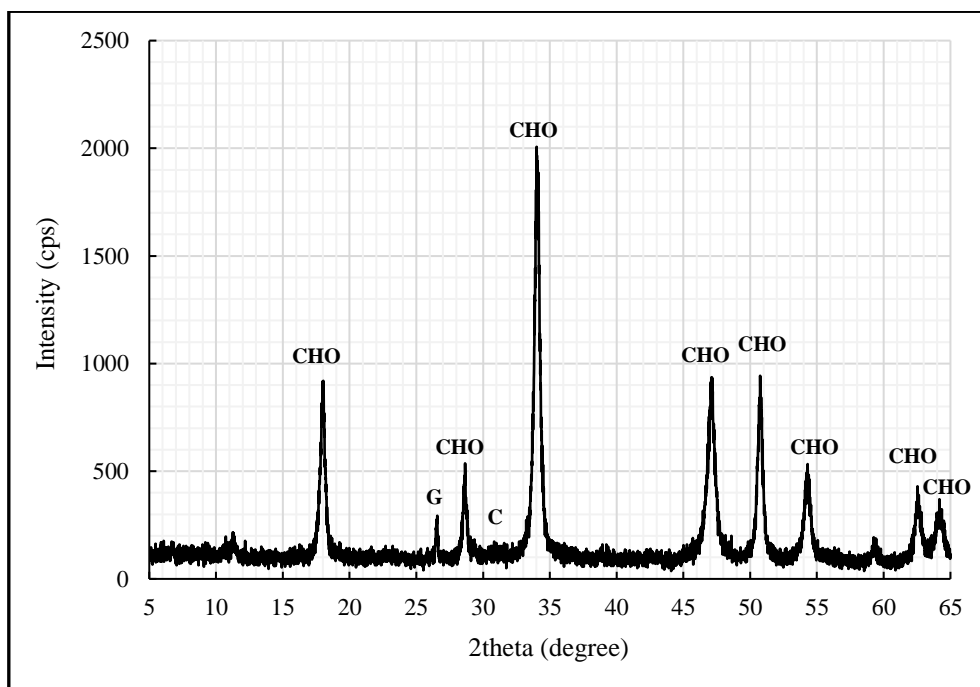


Figure 5.13: The XRD pattern of the CCR (CHO= calcium hydroxide, G= graphite, C= calcite)

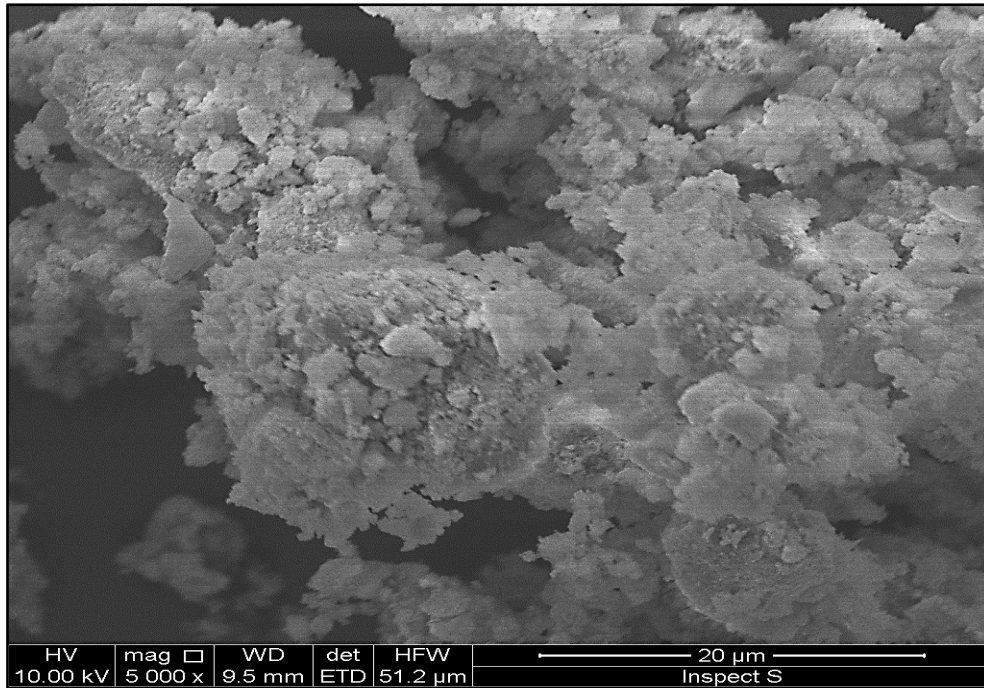


Figure 5.14: SEM image for dry powder CCR

5.3 Comparative Physical and Chemical Characteristics of the Selected Materials

The reason for identifying the physico-chemical properties of the selected materials in this research study was to assess their suitability and potential to develop a low cement content secondary cementitious filler (SCF) to be used as a full replacement of limestone filler in CBEM. Accordingly, a comparison was carried out to evaluate the chemical properties of the selected materials, including the oxide contents identified by EDXRF analyses, pH values and physical properties including PSD, density and consistency of the materials under study.

The chemical compositions of the conventional LF filler and OPC, along with the other materials selected for use, are summarised in Table 5.5. The chemical analysis of SSFA revealed a significant silica content indicating that this material is a pozzolanic, having the potential to be used to produce a cementitious material.

During cement manufacture, gypsum is added to cement clinker to act as both a retarder and grinding agent to stop the clustering of cement particles during the grinding process (Marchon and Flatt, 2016). Gypsum is also needed as a source of sulphate which reacts with hydrated lime and alumina to produce calcium sulpho-aluminate, also known as ettringite, which facilitates the development of early age strength (Puppala et al, 2015; Aïtcin, 2016). For that reason, the FGD gypsum for this study was used as a sulphate activator as well as a grinding aid, because it is composed mainly of calcium sulphate hemihydrate. The EDXRF analysis of CCR (Table 5.5) shows the presence of a high percentage of calcium oxide which is promising for use as a hydraulic activator for the SSFA to boost the hydration process in the presence of water in the CBEM. The chemical analysis also showed a high pH (13) for CCR, along with an acceptable amount of silica. These chemical properties are beneficial in accelerating the hydration reaction in the existence of pozzolanic materials while keeping a sufficient level of alkalinity for the hydration environment: the latter is necessary for hydration reaction continuity (Habert, 2014).

According to BS EN 197-1 (European Committee for Standardization, 2011), the clinker in OPC is a hydraulic material which contains at least two thirds by mass of calcium silicates ($3\text{CaO}\cdot\text{SiO}_2$ and $2\text{CaO}\cdot\text{SiO}_2$), the remainder consisting of other oxides such as aluminium oxide (Al_2O_3) and iron oxide (Fe_2O_3). BS EN 197-1 (European Committee for Standardization, 2011) also recommends that the ratio by mass of CaO/SiO_2 in cement shall not be less than 2.0, the magnesium oxide content (MgO) not exceeding 5% by mass. Regarding pozzolanicity, the specifications state that the amount of reactive silicon dioxide (SiO_2) in cement should not be less than 25% by mass. Table 5.6 illustrates the comparative chemical properties for the materials under study according to the British Standard. From this table, it can be seen that SSFA has more silica, aluminium and iron oxides than OPC, these playing an important role in the pozzolanic reaction. CCR has significantly more calcium oxide content than OPC which

supplements the hydration process. However, SSFA, FGD and CCR have not individually met all the requirements of the aforementioned standard; this will not influence the requirements if they are mixed in appropriate portions with OPC to produce a new SCF.

To increase pozzolanic reactivity, SSFA was ground to a PSD curve similar to, or finer than that of OPC. Based on the beneficial roles of blending (binary and ternary) over solo systems, to activate low calcium SSFA, a ternary system of SSFA, OPC, and calcium rich, high alkalinity CCR was proposed in this study. Therefore, the synergistic physico-chemical feature of the ternary system will allow the development of a new SCF comparable to OPC.

Table 5.5: Comparative chemical properties of the selected materials

Propertie	LF	OPC	SSFA	FGD	CCR
<i>CaO</i>	73.712	64.488	10.538	34.036	80.031
<i>SiO₂</i>	16.937	24.862	30.233	14.409	15.939
<i>Al₂O₃</i>	0.029	1.247	3.071	----	----
<i>MgO</i>	0.977	1.519	2.498	0.520	0.954
<i>Fe₂O₃</i>	----	1.856	15.236	----	----
<i>SO₃</i>	0.100	2.805	0.08	33.335	0.619
<i>K₂O</i>	0.355	0.783	1.285	0.031	0.047
<i>TiO₂</i>	0.194	0.434	1.189	0.107	0.162
<i>Na₂O</i>	2.136	1.572	1.512	1.184	1.508
<i>P₂O₅</i>	0.250	----	0.250	----	----
<i>pH</i>	9.1	12.8	8.3	12.3	13.0

Table 5.6: Comparative chemical properties of the selected materials in accordance with BS EN 197-1

Item	LF	OPC	SSFA	FGD	CCR
$CaO+SiO_2 \geq 67\%$	90.65	89.35	40.771*	48.445*	95.97
$(SiO_2+Al_2O_3+Fe_2O_3)\%$	16.97	27.965	48.54	14.409	15.939
$CaO/SiO_2 \geq 2$	4.35	2.59	0.348*	2.36	5.021
$MgO < 5\%$	0.977	1.519	2.498	0.520	0.954
$SiO_2 \geq 25\%$	16.937*	24.862	30.233	14.409*	15.939*

* Does not meet the standard requirements.

Particle size distribution of a filler plays a significant role in improving the packing of pores and producing a dense mixture (Brouwers, 2006). It has been established that a higher compressive strength can be achieved when finer particles of fly ash are used in concrete with cement (Kumar et al, 2008; Zhao et al, 2016). The overall particle size distributions of all selected materials are presented in Figure 5.15, their physical properties listed in Table 5.7. It can be seen that OPC and CCR, ground for 5 minutes, are closer to each other with CCR having slightly finer particles. Approximately 40% of SSFA particles in the region of 0.1 to 35 μm , have a coarser grading than LF, but the remainder of both curves are close. Therefore, grinding activation was required to increase the pozzolanic reactivity of the SSFA through reducing the grain size and increasing the specific surface area. This will be explained in the following section.

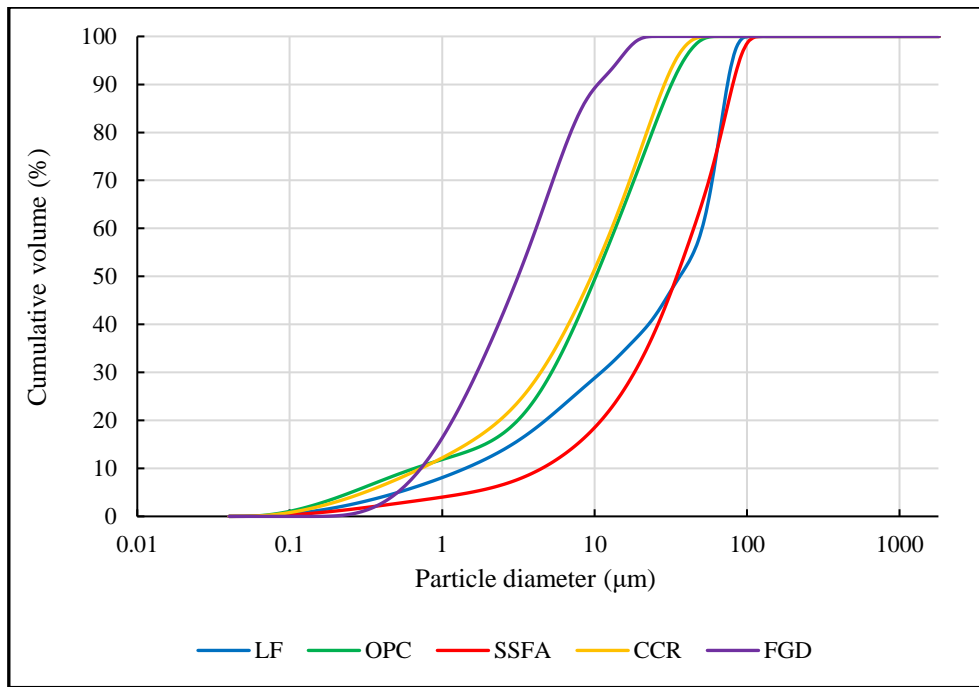


Figure 5.15: Comparison of the PSD's of the selected materials

Table 5.7: Comparison of the physical characteristics of the fillers

Item	LF	OPC	SSFA	FGD	CCR
D_{10} (μm)	1.555	0.722	4.113	0.796	0.720
D_{50} (μm)	36.235	10.777	36.33	3.457	9.817
D_{90} (μm)	76.419	33.008	83.890	10.773	30.068
Density (gm/cm^3)	2.784	3.100	0.273	2.550	0.162
Consistency (%)	23	27	88.75	nd	nd

5.4 Mechanical Activation of SSFA

Mechanical activation by means of grinding has been suggested as an effective method to improve the reactivity of cementitious materials (Kumar et al, 2008). The external dynamic forces which result from the comminution during grinding, leads to destabilisation of the

electronic bonding structure, making the solid open to the chemical reaction (Sadique et al, 2013). In the literature, different types of milling devices have been used for mechanical activation such as an attrition mill, a ball mill, an agitator mill, a jet mill and a vibro mill (Sekulić et al, 1999).

In this study, a mortar grinder RM 200, shown in Figure 5.16, was used to grind the SSFA for various time periods. This grinder has the ability to grind and homogenise powders, suspensions and pastes to a fineness size $< 10 \mu\text{m}$, operates with a low energy agitation of 250 W and has a bowl capacity of 700 ml. Grinding efficiency can be influenced by various factors including the initial particle size, softness and carbon content. In some cases, particles adhere to each other and agglomerate when applying prolonged grinding because of the action of strong chemical bond forces on particles with a metastable high state, thus reducing grinding efficacy (Juhasz, 1998; Sajedi and Razak, 2011). The reduction in grain size is not proportional to grinding time.



Figure 5.16: Mortar grinder

In order to control agglomeration and weaken the strength of the particles, an appropriate amount of additives have been used as a grinding aid, as specified by Lu and Wei (1992). Grinding aids help to enhance grinding efficiency by creating a repulsive force, a result of adsorbing the additives, on the surface of the particles, hence avoiding agglomeration. Likewise, Katsioti et al (2009) identified a benefit of grinding aids in that they partially neutralise surface charges and prevent agglomeration. The effectiveness of using FGD gypsum as a grinding aid has been examined by previous researchers. Sekulić et al (1999) found that incorporating 5% FGD gypsum into a system where clinker was replaced by 20% pulverised fly ash (PFA), increased its strength compared to the control mix. Sadique et al (2013) and Jafer et al (2018) also used 5% FGD gypsum by total mass of binder. In light of this, 5% FGD gypsum was used in the present study to assist grinding of SSFA. The optimum time for grinding was found to be 20 minutes. To evaluate the effect of grinding SSFA with and without FGD gypsum, physical, morphological and mineralogical properties were determined using analytical techniques.

The physical alteration of the grinding activation of SSFA is listed in Table 5.8. The effect of the grinding activation, along with the effect of using FGD gypsum on the PSD of SSFA, is illustrated in Figure 5.17. The fineness of the SSFA increased significantly when ground for 20 minutes without FGD gypsum. However, a significant improvement in the PSD was accomplished after using FGD gypsum as a grinding aid. The virgin SSFA particles ranged between 4 and 75 μm : after grinding activation and when using FGD, they were in the range of 0.4 to 20 μm . The median diameter (D_{50}) of the SSFA particles (Figure 5.18), decreased from 36.33 μm to 22.86 μm and 7.082 μm after grinding only and grinding with FGD, respectively. Sadique and Al-Nageim (2012) and Jafer et al (2018) reported similar findings by which the improvement achieved in the PSD was attributed to the fineness of the FGD and to the altered particle size distribution, along with the morphological modification caused by

the grinding energy and the FGD gypsum. It should be noted that grinding with FGD creates three peaks in the PSD of SSFA. This produces a gap gradation which is expected to have a critical impact on water requirements, the packing density and hydration behaviour of SSFA, as stated by Zhang et al (2011).

Table 5.8: Changes in physical properties after grinding activation

Material	D ₁₀ (µm)	D ₅₀ (µm)	D ₉₀ (µm)	Density (gm/cm ³)	Standard Consistency
<i>SSFA untreated</i>	4.113	36.33	74.6	0.273	88.75
<i>SSFA ground without FGD</i>	1.831	22.86	51.8	0.290	41.5
<i>SSFA ground with FGD</i>	0.435	7.082	19.19	0.305	40
<i>OPC</i>	0.722	10.777	33.008	3.100	27

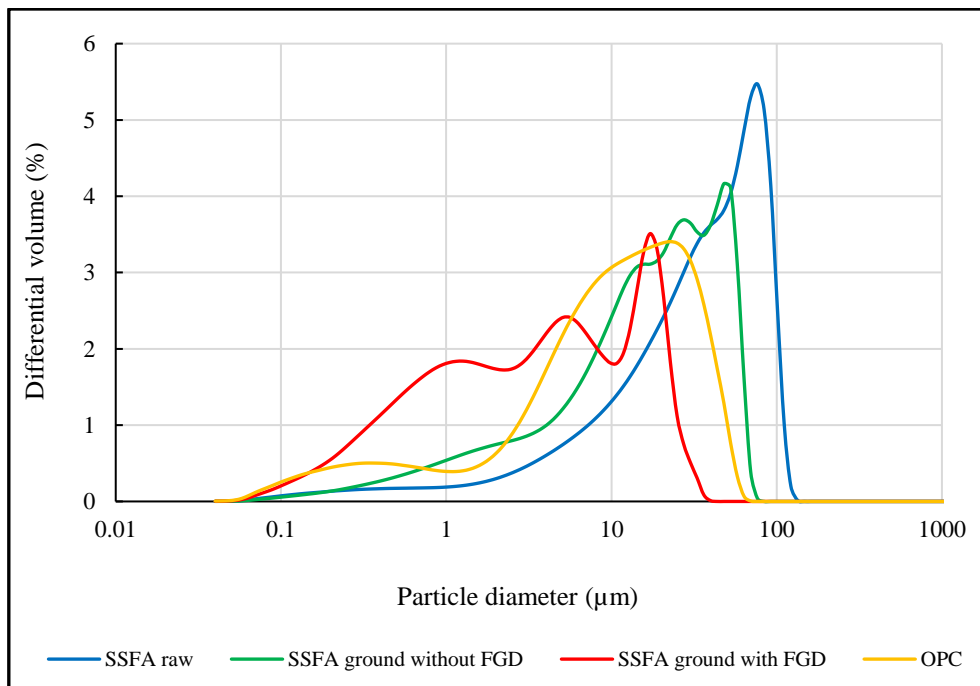


Figure 5.17: Comparative change in differential PSD when grinding SSFA using FGD gypsum

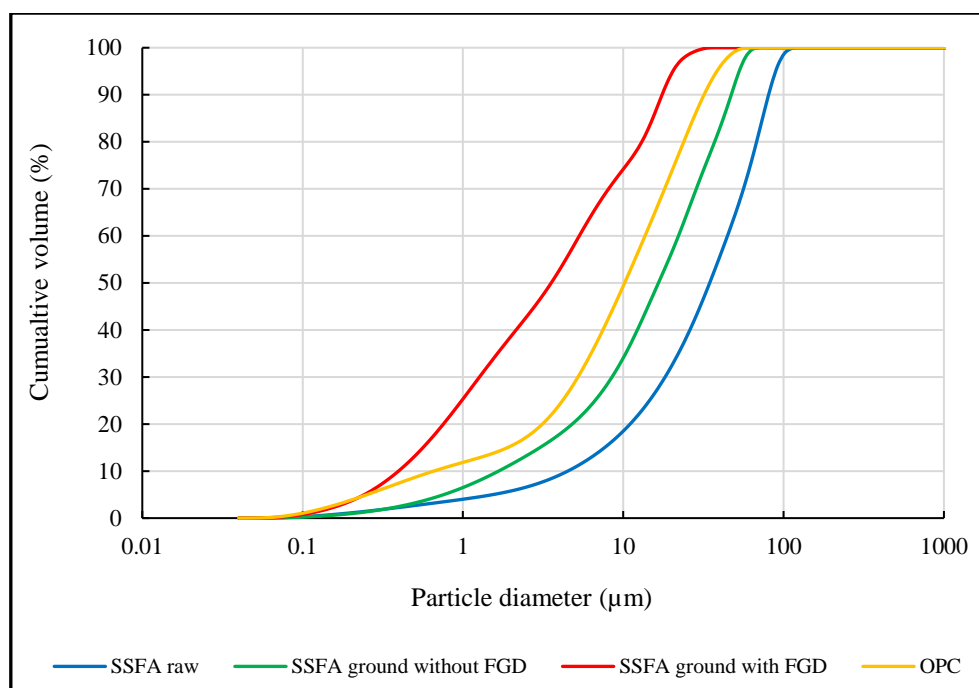


Figure 5.18: Comparative change in cumulative PSD when grinding SSFA using FGD gypsum

The XRD pattern of mechanically activated SSFA particles is illustrated in Figure 5.19. It can be seen that there is no significant change in the diffraction peaks of each angle for SSFA, without and with FGD gypsum, which means no new phase has been generated. The diffraction peak intensities of the quartz phase of SSFA with FGD gypsum, are weaker than those without FGD, broadening of the band and the relative crystallinity are decreased. This indicates that FGD gypsum has promoted the destruction of the crystal structure and increased the lattice defects and amorphous substances of the quartz phase via the grinding operation. These results correspond with the findings of Palaniandy and Azizli (2009) and Zhao et al (2015). Modifications in the morphology of the SSFA particles, before and after grinding with FGD gypsum, are shown in Figure 5.20. It can be concluded that the grinding operation has changed the microstructure through reforming the irregular shaped particles of SSFA into particles with a uniform continuous grain size mode. This helps the SSFA particles to chemically interact with other materials when water is added, reducing water demand and increasing reactivity.

Aydın et al (2010) claimed that the grinding operation breaks up large plerospheres (i.e. decreases porous particles) which reduces particle roughness, thus reducing water demand.

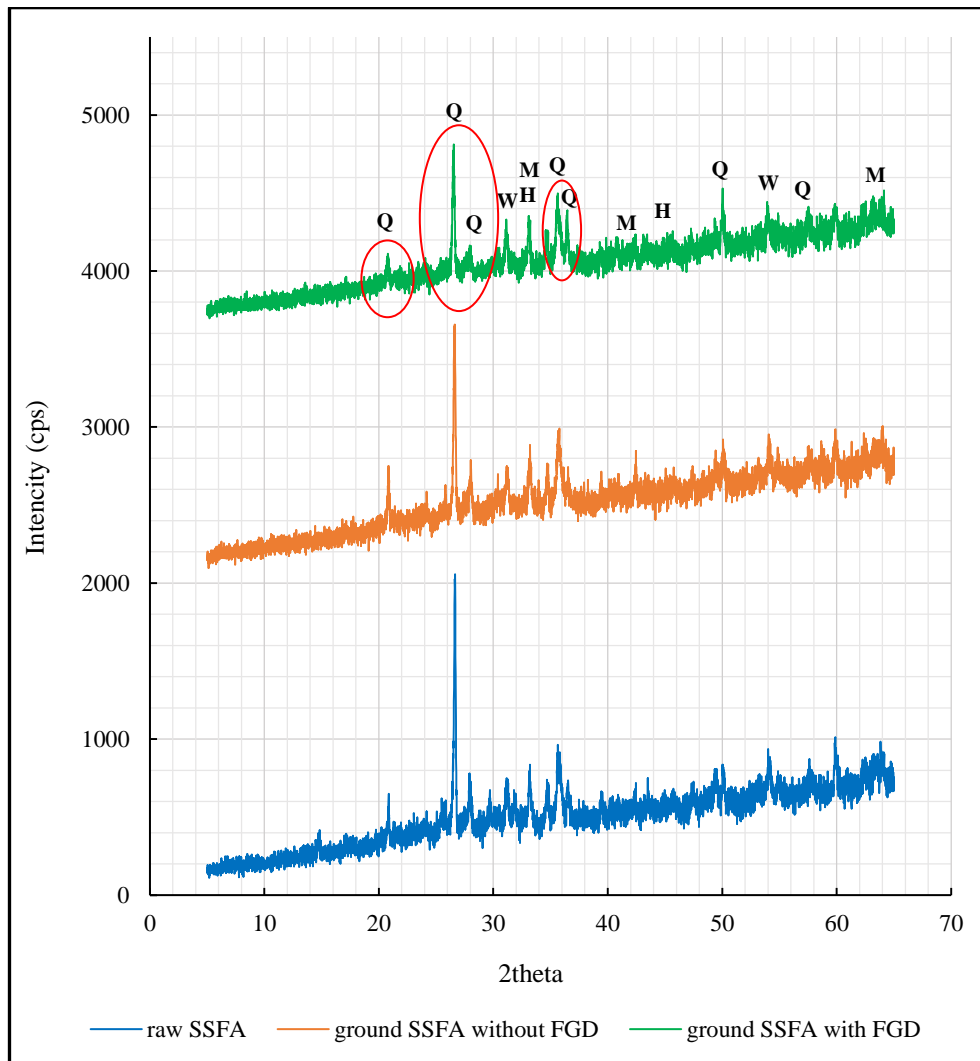


Figure 5.19: Comparative powder XRD for FGD and non-FGD assisted ground SSFA (Q= quartz, H= hematite, M= magnetite, W= whitlockite)

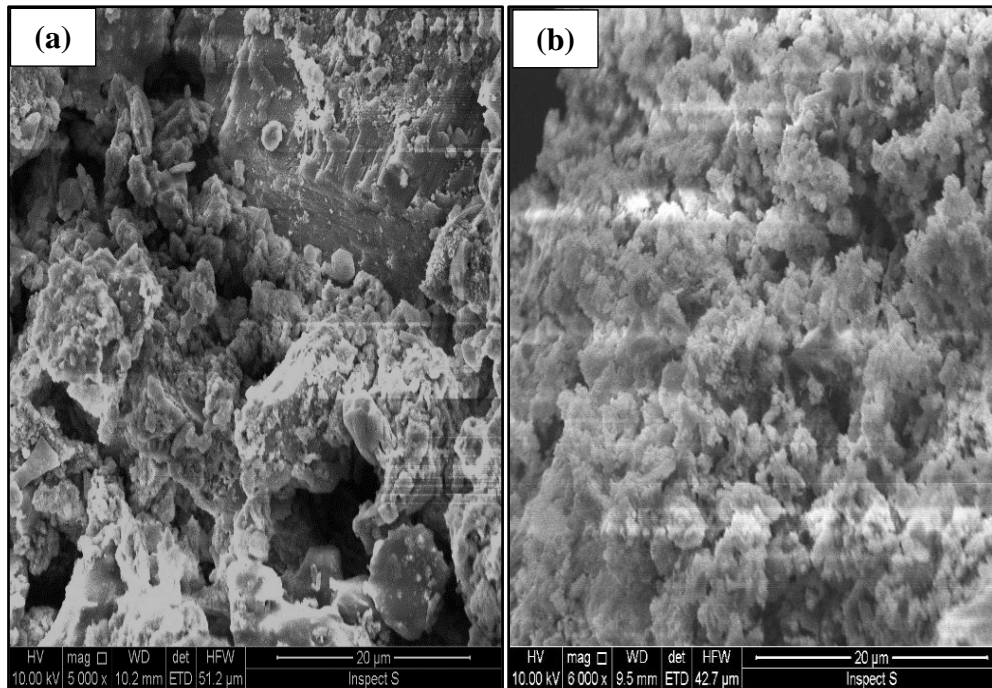


Figure 5.20: Microstructural change of SSFA dry particles (a) before grinding (b) after grinding with FGD gypsum

5.5 Physico-chemical Activation by Blending

Numerous researchers have investigated physico-chemical activation using binary and ternary blends with added cement (Winnefeld et al, 2010; Dulaimi et al, 2016c; Sadique and Coakley, 2016; Jafer et al, 2018). It is essential to investigate how soon added pozzolanic materials react with calcium hydroxide to generate hydration products. Regarding the blending process with water, homogeneous nucleation may happen between particles of different sizes, resulting in the development of a dense microstructure hardened product with higher durability (Sadique and Coakley, 2016).

In this research project, the second stage of development, the new SCF is binary blending optimisation by adding SSFA to the OPC with the aim of using SSFA in bulk (more than 50% of the total weight of binder). Prismatic paste specimens (40 × 40 × 160 mm) were prepared and cured in water at 20°C, as per designated periods of 3, 7, 14, 28, 56 and 90 days, following

the procedure contained in BS EN 197-1 (European Committee for Standardization, 2011). Compressive strength was measured according to the procedure detailed in BS EN 12390-3 (European Committee for Standardization, 2009). The paste specimens were mixed using a Hobart mixer. The cementitious materials and sand were added and mixed for 1 minute in a dry condition, water was then added over the next 30 seconds of mixing, the mixing continuing for a further 2 minutes at low speed. The specimens were extruded from the mould after 24 hours curing in the lab and subjected to curing by complete immersion in water. The compressive strength of the cubes was measured by applying 0.4 MPa/sec loading using a LJMU laboratory compressive test machine. The compressive strength value represents the average of four cubes prepared for each age of curing.

Initially, paste specimens of binary blended fillers (BBFs) consisting of raw (untreated) SSFA and OPC were prepared and cured for different periods of time: 3, 7, 14, 28, 56, and 90 days. The percentages of OPC were gradually decreased to evaluate the effect of increasing SSFA replacement on the compressive strength of the mixtures. The strength of different blends, focusing on the blends with low cement content (for economic and environmental reasons), were compared with the reference mix which included 100% OPC binder. The adopted sand to binder ratio was 2.25:1, the water/binder ratio 0.45. Their selection was based on the fact that these values achieved a high early age strength and high degree of workability as stated by Ban and Ramli (2010) and Sadique et al (2013). The details of the component matrix of the specimens are given in Table 5.9 and Table 5.10. The subsequent strength achieved by these mixtures at different curing ages are shown in Figure 5.21 and Figure 5.22 for the mixes shown in Table 5.9, while Figure 5.23 and Figure 5.24 show the strength achieved for the mixes reported in Table 5.10.

Table 5.9: Constituent matrix of the raw SSFA paste specimens

Type of Mix	OPC (%)	SSFA (%)
<i>Mix-OPC</i>	100	---
<i>Mix1</i>	75	25
<i>Mix2</i>	50	50
<i>Mix3</i>	40	60
<i>Mix4</i>	30	70
<i>Mix5</i>	25	75
<i>Mix6</i>	---	100

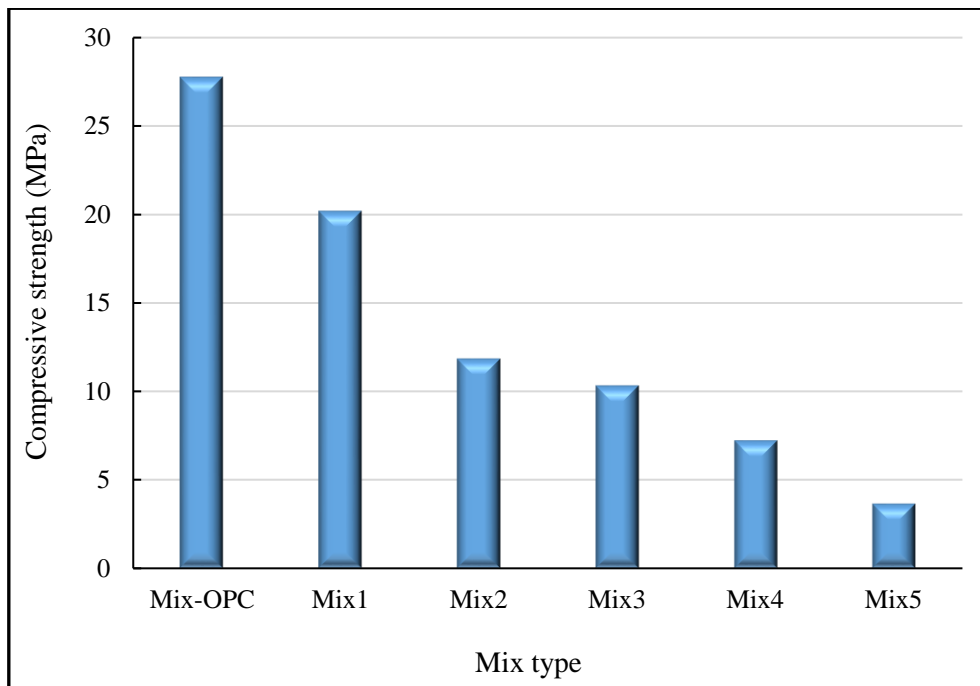


Figure 5.21: Influence of raw SSFA replacement on compressive strength at 3 days

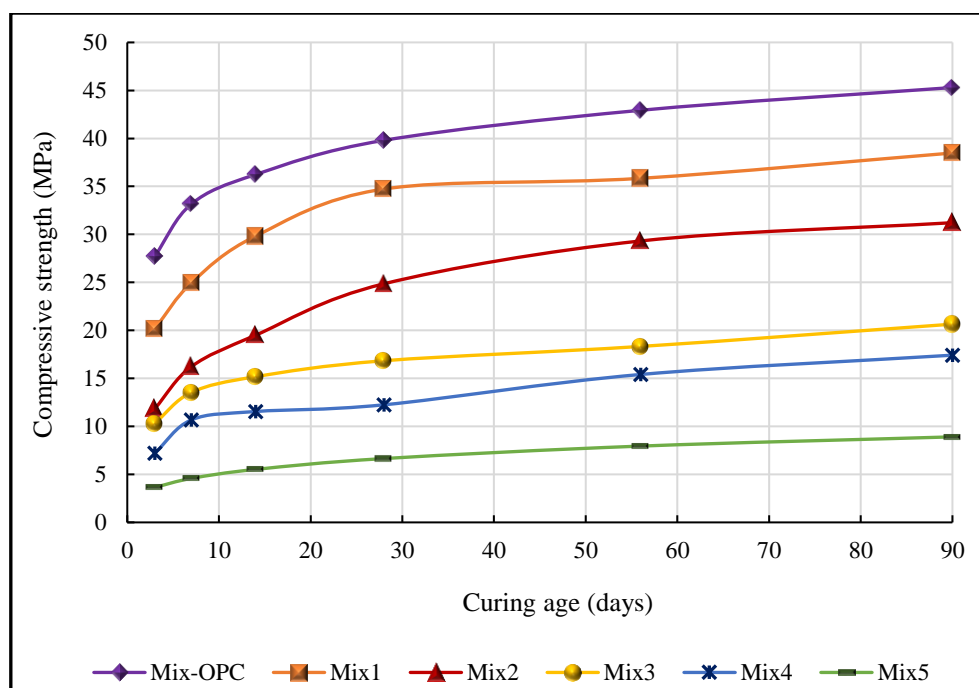


Figure 5.22: Effect of curing time of different raw SSFA replacements on compressive strength

It is apparent from Figure 5.21 and Figure 5.22 that the compressive strength of the specimens decreased with an increase in the percentage of SSFA. This can be attributed to the low CaO content in the SSFA and coarse particle size, as seen in Figure 5.7, which influences the hydraulic properties. In more detail, the reduction in the compressive strength of the mixture with 25% raw SSFA (Mix1) was 27% and 33% after 3 and 7 days of curing, respectively, compared to the reference 100% OPC mixture. For the other curing ages (14, 28, 56 and 90 days), the reduction in compressive strength ranged from 13% to 18%. The mixture with 75% raw SSFA (Mix5) shows a reduction in compressive strength ranging between 80% and 85% across all curing ages, compared with the reference mixture. It should be noted that both mixtures with 100% raw SSFA (Mix6) and 100% SSFA ground for 20 minutes with 5% FGD as a grinding aid (Mix12) achieved zero compressive strength because they disintegrated in water during the curing process. These results are in agreement with Chen et al (2013), who found that the flexural and compressive strengths of mortar samples decreased linearly with an

increase in the percentage of SSFA. They attributed this poor performance to the low CaO (free lime) content in the ash which affects the hydration process and also to the amount of water required to maintain workability of the SSFA. According to their study, the reduction in flexural and compressive strength for mixtures with 10% SSFA content, was less than 25% compared to samples without SSFA. A study conducted by Cyr et al (2007), also demonstrated that the compressive strength of mortar specimens was reduced after 28 days of curing when replacing between 25% and 50% of cement with sewage sludge ash, compared with reference mixtures. The effect of substituting 10% to 30% of cement by sewage sludge ash in mortars and high performance concretes, has been analysed by Fontes et al (2004). They concluded that substitution from 5% to 10% of sewage sludge ash meets all the requirements regarding mechanical properties.

Table 5.10: Constituent matrix of paste specimens of ground SSFA

Mix Type	OPC (%)	SSFA (%)	FGD gypsum (%)
<i>Mix-OPC</i>	100	---	---
<i>Mix7</i>	75	25	5
<i>Mix8</i>	50	50	5
<i>Mix9</i>	40	60	5
<i>Mix10</i>	30	70	5
<i>Mix11</i>	25	75	5
<i>Mix12</i>	---	100	5

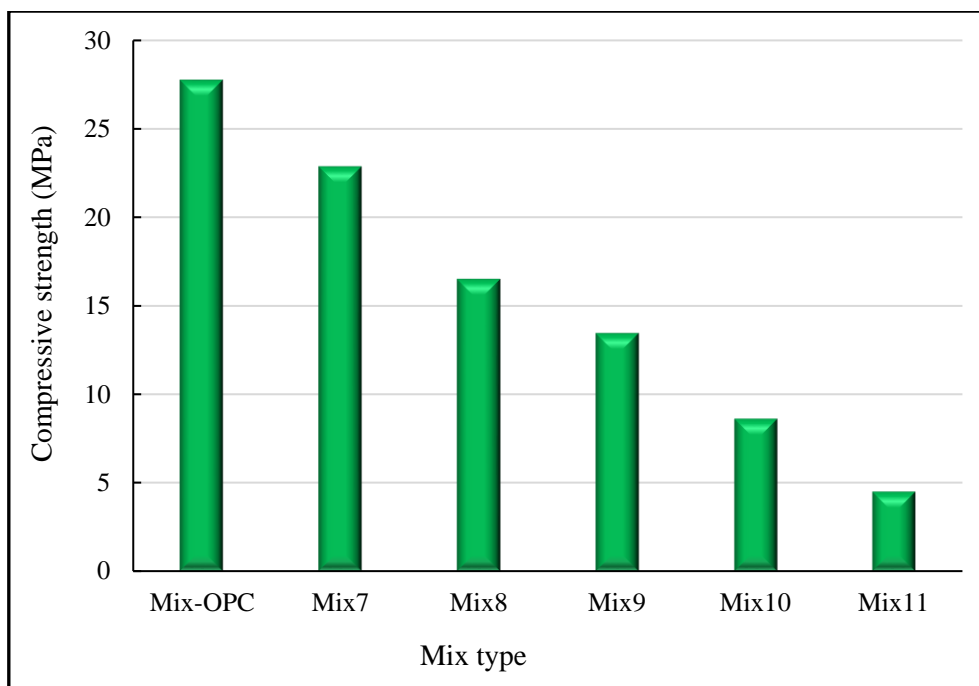


Figure 5.23: Influence of different percentages on compressive strength of ground SSFA with 5% FGD gypsum at 3 days

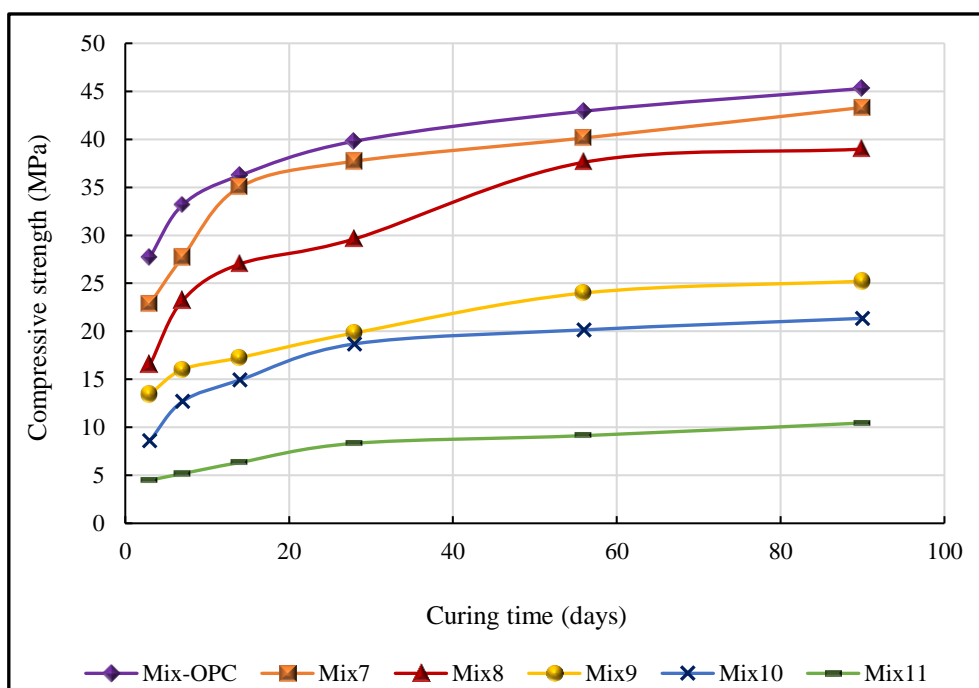


Figure 5.24: Effect of curing time on compressive strength for different percentages of ground SSFA with 5% FGD gypsum

Figure 5.23 and Figure 5.24 show that increasing the fineness of SSFA particles after grinding with 5% FGD gypsum (Figure 5.18), improved the compressive strength of samples with the same SSFA content. These improvements are due to the activation of the pozzolanic properties of the SSFA particles by breaking the glassy phases of non-amorphous silica when ground with FGD: these findings are in agreement with those of Pan et al (2003) and Donatello et al (2010). All mixtures showed improvements in compressive strength across all curing ages. The same trend of reductions in compressive strength with an increase in percentage of SSFA, can be observed.

To investigate the generation of the hydration products in the BBF (30% OPC + 70% SSFA treated with 5% FGD) when mixed with water, scanning electron microscopy (SEM) analysis was conducted on the paste samples of the aforementioned filler at 3 and 28 days (Figure 5.27 and Figure 5.28). The results were compared with those shown in Figure 5.25 and Figure 5.26 of OPC. A fibrous network structure formed in the OPC paste sample at 3 days (Figure 5.25), this identified as ettringite $[\text{Ca}_6\text{Al}_2(\text{SO}_4)_3(\text{OH})_{12}\cdot 26\text{H}_2\text{O}]$. Plate-like shaped portlandite $[\text{Ca}(\text{OH})_2]$ and amorphous phase calcium silicate hydrate (CHS) gel, a round and compact globule-like shape, are also present. As hydration proceeds, the CHS gel continues to grow in volume, filling the network structure, the cement paste structure becoming more dense during the later stages (Kourounis et al, 2007), as seen in Figure 5.26.

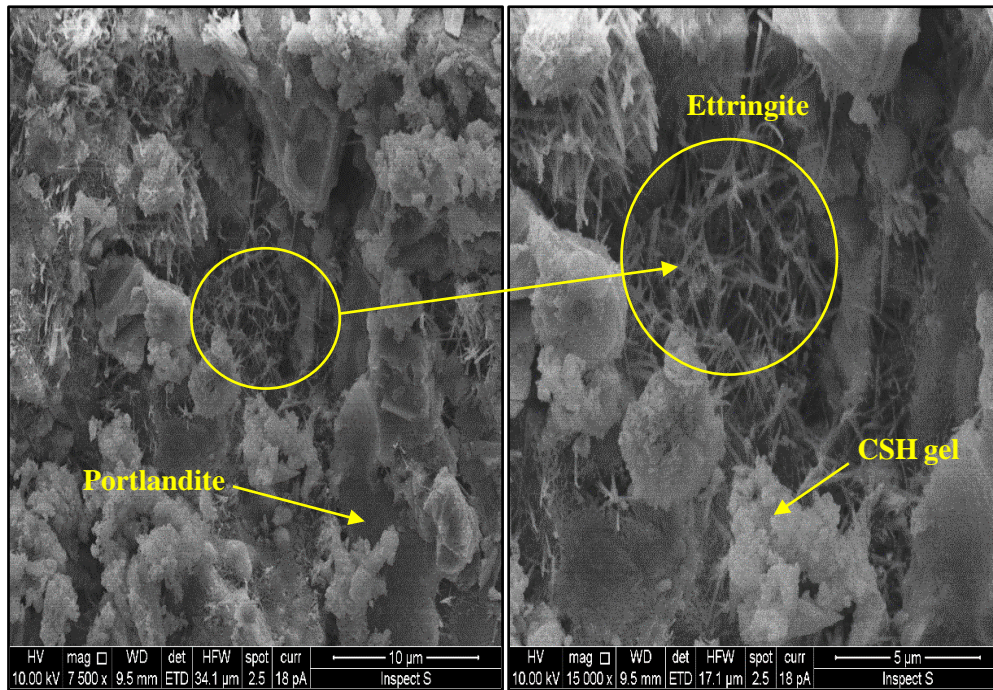


Figure 5.25: SEM images of the OPC paste at 3 days of age

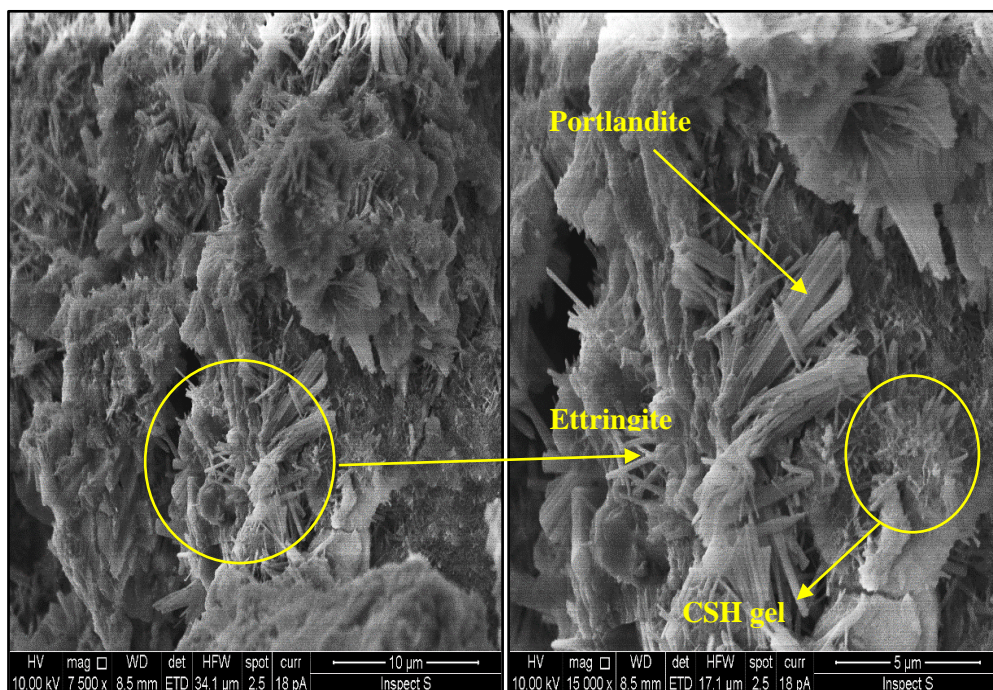


Figure 5.26: SEM images of the OPC paste at 28 days

A similar, but lower percentage of ettringite, is observed in the micrograph of the BBF paste at 3 days of curing (Figure 5.27), permeated by CSH gel. Figure 5.28 shows the progressive generation of CSH at 28 days. However, the hydration products in the structure of the BBF pastes were less than those for OPC; this is attributed to the reduction in production of tri-calcium silicate (C_3S) and di-calcium silicate (C_2S) due to a decrease in the amount of calcium oxide (CaO) and silicon dioxide (SiO_2) in the BBF. This will cause the paste mass to become weaker in compressive strength.

In conclusion, the density and compressive strength of the OPC and BBF pastes gradually increased with curing age, as evidenced by SEM observations.

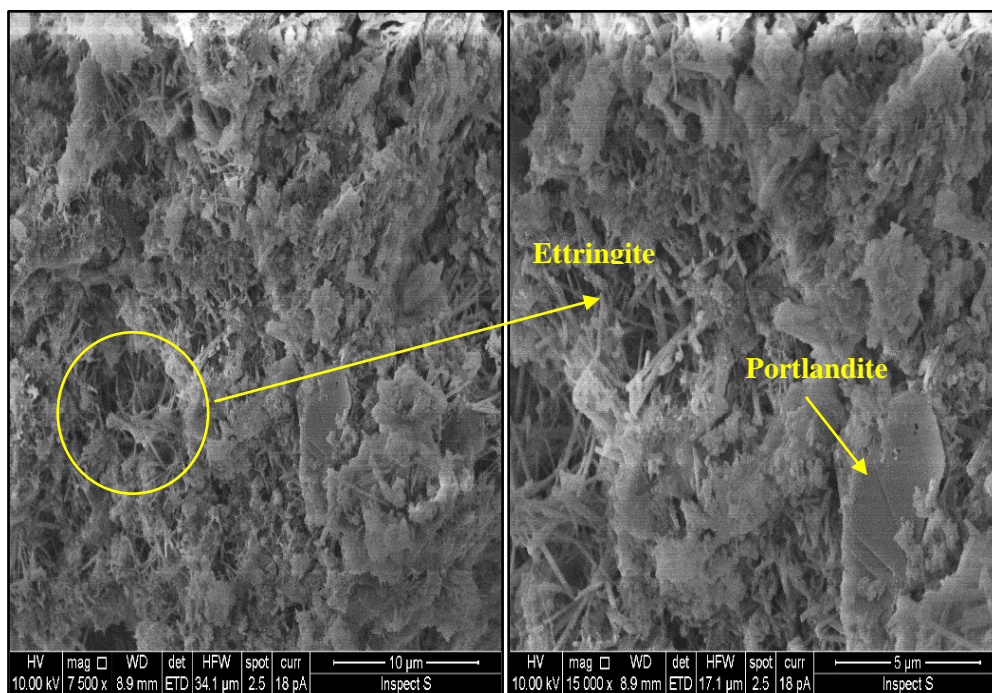


Figure 5.27: SEM images of the BBF paste at 3 days of age

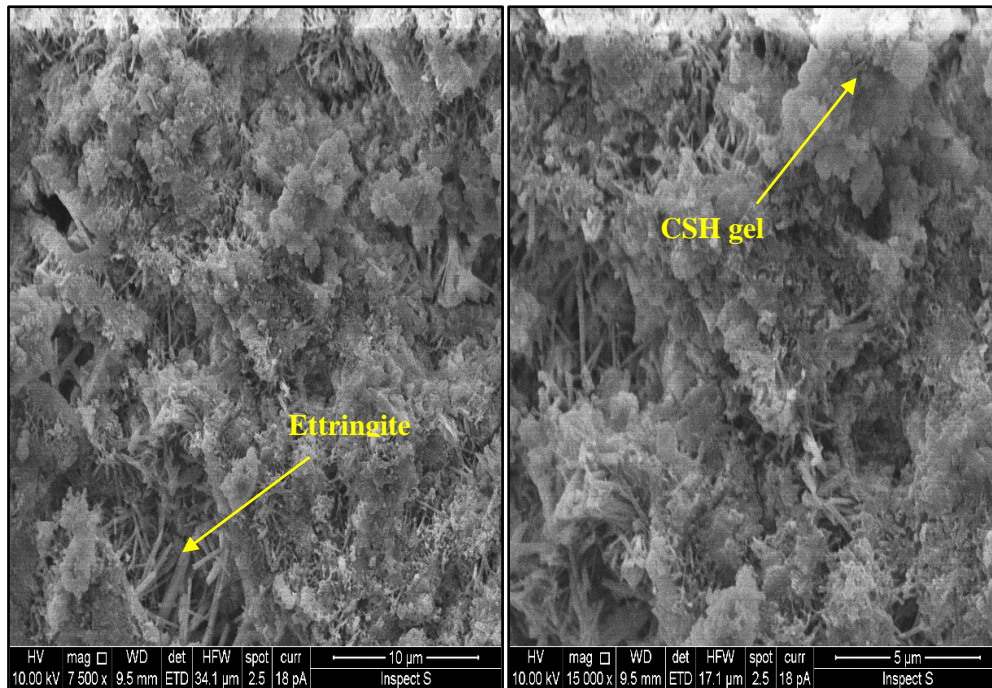


Figure 5.28: SEM images of the BBF paste at 28 days of age

As the aim of this study is to develop a new SCF with a high volume of SSFA to be used as an alternative to conventional LF in CBEMs, mixes with high percentages of treated SSFA (Mix8, Mix9 and Mix10) were selected for further investigation. The following section will present the analyses of the mechanical performance of the new CBEMs containing binary blended fillers (BBFs) in terms of indirect tensile stiffness modulus (ITSM) for ranking the strength of said CBEM mixtures. These will be then compared to conventional CBEM-LF, CBEM-OPC and traditional 100/150 HMA and 40/60 HMA.

5.6 CBEMs incorporating Binary Blended Filler (BBF)

In this section, the partial substitution of OPC by treated SSFA (ground with 5% FGD gypsum) in CBEMs, measuring 3% (Mix8), 3.6% (Mix9) and 4.2% (Mix10) by dried aggregate weight as shown in the previous section, was investigated and compared with conventional CBEM-LF. Figure 5.29 shows the effect of an increase in SSFA content on the performance of CBEM LF. Figure 5.29 shows the effect of an increase in SSFA content on the performance of CBEM LF in terms of indirect tensile stiffness modulus (ITSM) at 3 days age, Figure 5.30 showing the

ITSM values over a range of curing times: 3, 7, 14, and 28 days. It is clear that all the CBEMs treated with cement and SSFA give a better performance compared to conventional CBEM-LF. The CBEM containing 3% treated SSFA has an ITSM value close to that for 100/150 HMA at 3 days, while the mixtures with 3.6% and 4.2% treated SSFA performed better than 100/150 HMA after 7 and 28 days, respectively. However, all treated CBEMs have ITSM values less than 40/60 HMA for all curing ages. The delayed improvement in the ITSM of cement and SSFA treated CBEMs, clearly relates to slow hydration and pozzolanic reaction of SSFA. The same trend of reduction in the compressive strength has been observed in the previous section when increasing the substituted value of OPC by SSFA.

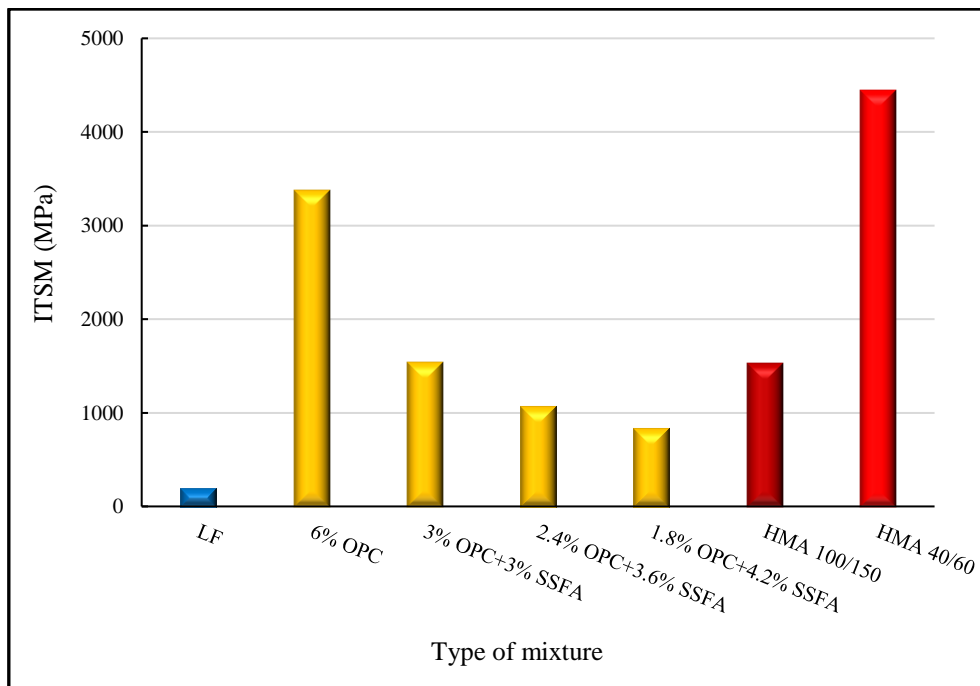


Figure 5.29: Effect of SSFA replacement on the ITSM of CBEMs at 3 days

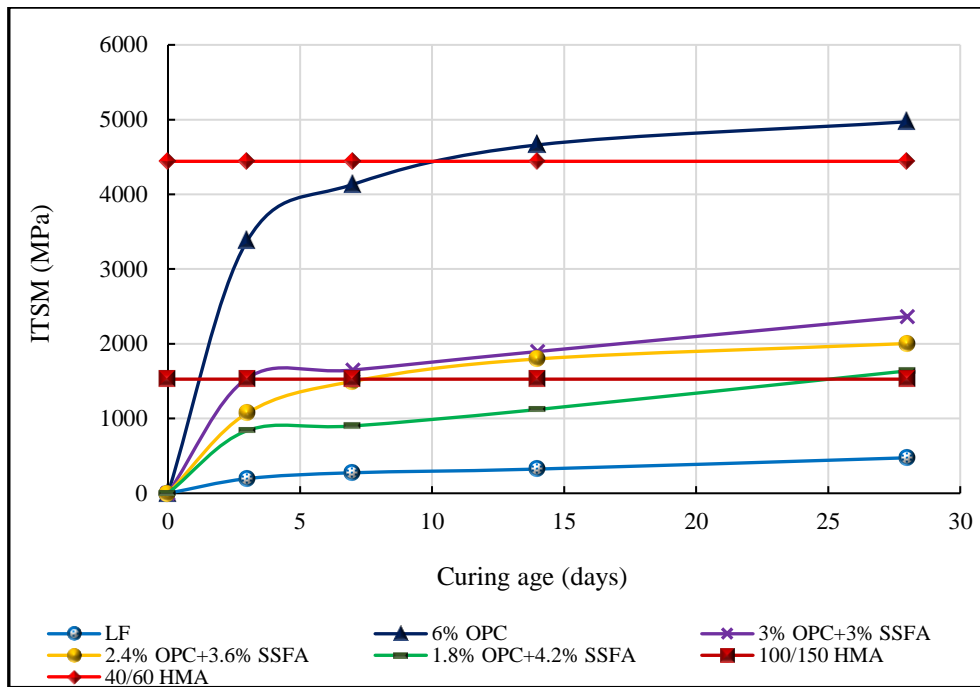


Figure 5.30: Effect of curing time on the ITSM of CBEMs

Further developments to the new SCF, using CCR as an alkaline activator due to its high alkalinity, as well as high calcium content will be presented in the next chapter, to achieve a CBEM with ITSM values comparable to HMA containing 100/150 and 40/60 pen bitumen. The latter have been produced using the European Committee for Standardization (2016b) for use in low, medium and heavily trafficked roads.

5.7 Summary

This chapter identified the physical and chemical characteristics of the specific types of waste materials used in this study, along with the reference fillers, limestone and OPC. The output of this chapter can be summarised as follows:

- From the comparative physico-chemical properties of the selected candidate materials to make the secondary cementitious filler, SSFA was identified as the main source of pozzolanic compounds, FGD gypsum as a grinding aid and sulphate activator to help breaking in the glassy phase of non-amorphous silica in the SSFA, and OPC as a hydraulic source.
- Large SSFA particles, in comparison with particle size distribution of OPC, have been found to be responsible for the negative effect on its pozzolanic reactivity during the hydration reaction. Ground SSFA improved in reactivity when subject to mechanical grinding activation; this has been confirmed by a slight enhancement in its compressive strength.
- Increasing the amount of SSFA in paste samples impacted inversely on the compressive strength of the paste samples. This has been attributed to the low CaO (free lime) content in SSFA, which in turn influences its hydraulic properties (Chen et al, 2013).
- In the binary blended filler, the use of treated SSFA with OPC resulted in a reduction in the stiffness modulus of the CBEMs. The mixture with 1.8% OPC and 4.2% SSFA has the lowest strength compared to the other substitution percentages of SSFA. However, this mixture has performed better than conventional CBEM-LF over different curing ages.

Chapter 6: Further Development of the New Secondary Cementitious

Filler

6.1 Introduction

This chapter presents the further development of the new secondary cementitious filler (SCF), explained in Chapter 5, to produce a CBEM with indirect tensile stiffness modulus (ITSM) comparable to HMA. The newly developed filler is made from waste and by-product materials including sewage sludge fly ash (SSFA), flue gas desulphurisation (FGD) gypsum and calcium carbide residue (CCR), in combination with OPC. As the development of a new SCF incorporating a high volume of SSFA is one of the aims of this research work, a binary blended filler (BBF) with 4.2% SSFA and 1.8% OPC by the total weight of the dried aggregate, was selected for further development by adding CCR to produce a ternary blended filler (TBF).

6.2 CBEMs incorporating a Ternary Blended Filler (TBF1)

Further activation of the BBF, which was produced from the stage outlined in Chapter 5, was carried out using a waste calcium carbide residue (CCR). The pH of the BBF produced in Chapter 5, is 9.8: this is a low value, therefore, CCR with a higher alkalinity was introduced to the BBF, to generate a new ternary blended filler (TBF1). CCR is a by-product of acetylene gas (C_2H_2) production through the hydrolysis of calcium carbide (CaC_2). The inclusion of a filler with an alkaline nature, such as CCR, increases the pH of the hydration mediums which in turn, improves breaking and dissolution in the glassy phase of pozzolanic materials (Shi and Day, 2000). An increase in alkalinity leads to an increase in coalescence of the bitumen emulsion, which gives faster-setting strength gains (Dulaimi, 2017).

CCR was used as a partial replacement for the BBF, introduced in five percentages: 1%, 2%, 3%, 4% and 5% by weight of dry aggregate, to identify the optimum composition in CBEMs which gives the maximum ITSM value in the CBEM at 3 days and comparable to 40/60 HMA. Figure 6.1 illustrates the positive impact of CCR when added to the BBF, a considerable increase in ITSM values when 1% of the BBF was replaced by CCR. At this point, a new TBF1 comprising 5% BBF + 1% CCR, was generated, this improving the ITSM value at 3 days by about 74%, compared to the ITSM value for the CBEM-BBF at the same age.

ITSM values for the CBEM-TBF1 at different curing times i.e. 3, 7, 14 and 28 days, are seen in Figure 6.2 where the addition of CCR to BBF results in a significant improvement in both early and long-term strength. The hydration and pozzolanic reaction processes in TBF1 can be explained as follows: the dissociation of $\text{Ca}(\text{OH})_2$ from CCR leads to an increase in the pH value of the medium. High alkalinity breaks the glassy phase of the pozzolanic material and dissolves the silica in SSFA in a manner similar to the reaction between a weak acid and a strong base (Bakharev et al, 1999; Shi and Day, 2000). The hydrous silica will then react with calcium ions liberated from the hydrolysis reaction of cement and create hydrated calcium silicate (CSH) which is responsible for the development of strength. Although there is a significant improvement in the performance of CBEM-TBF1 making it comparable to 100/150 HMA, it still performed lower than CBEM-OPC and 40/60 HMA. Therefore, another technique was adopted to facilitate the further improvement to the BBF, as explained in the following sections.

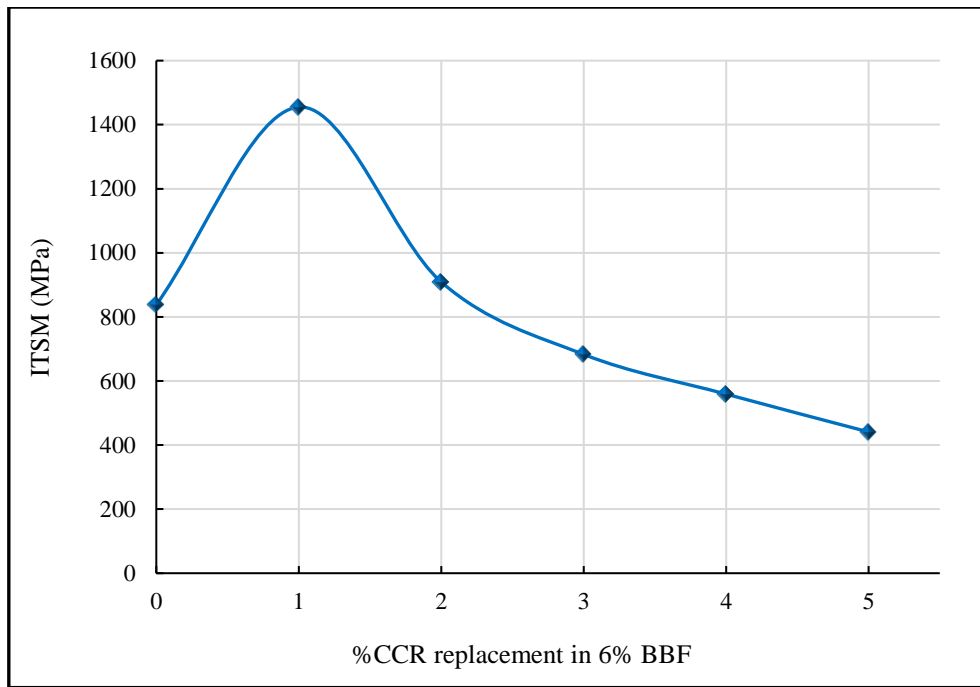


Figure 6.1: Effect of partial replacement of BBF with CCR on the ITSM of CBEMs at 3 days

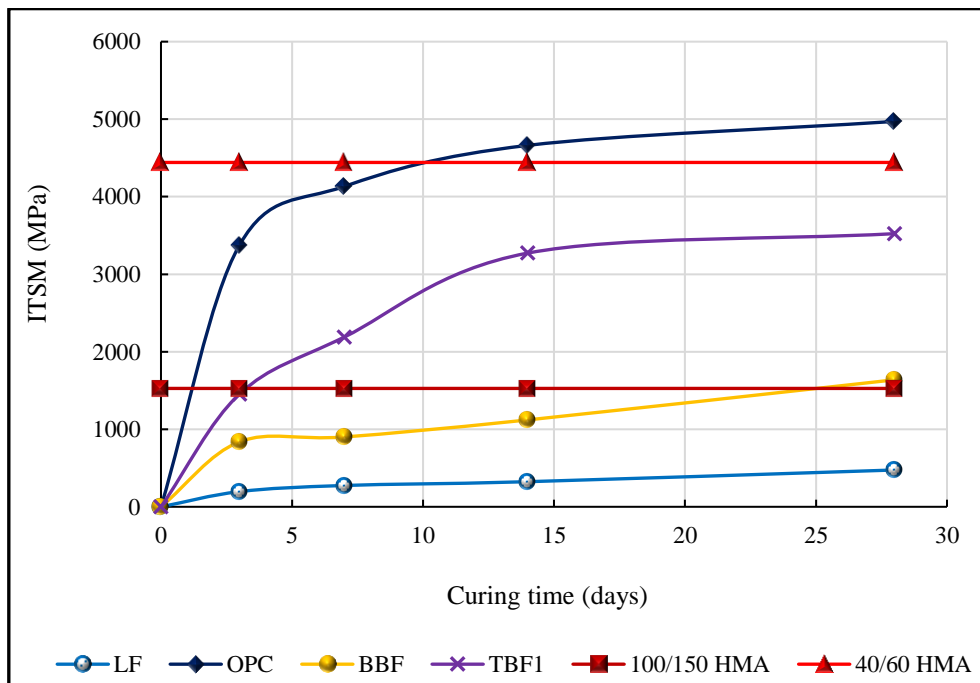


Figure 6.2: Influence of curing time on the ITSM of CBEM-TBF1

6.3 CBEMs incorporating a Second Ternary Blended Filler (TBF2)

This stage involves the addition of extra CCR to the BBF to facilitate further activation of the hydration process. In previous studies conducted by Al-Busaltan et al (2012) and Nassar (2016), a significant improvement was achieved in the mechanical and durability properties of CBEMs when adding silica fume (SF) as an extra filler (recommended filler content by the BS EN code plus extra SF). As both SF and CCR are very fine powders and both increase the pH of the mix, CBEM specimens were prepared by adding different percentages of CCR (0.5%, 1% and 2%) of the aggregate weight to 6% BBF to mark the optimum composition of filler to achieve the maximum ITSM of CBEM at 3 days. Figure 6.3 shows that there is a significant improvement in the ITSM results at 3 days when adding CCR. This improvement increased as CCR content in the filler increased, the maximum ITSM achieved when 2% of CCR was added to the BBF. An outstanding TBF2 was generated by adding 2% CCR to 6% BBF: the ITSM improved by approximately 199% in comparison to CBEM-BBF and 72% in comparison with CBEM-TBF1 at 3 days of curing.

The ITSM value of the CBEM-TBF2 was measured at different ages of curing; 3, 7, 14 and 28 days, to ascertain its performance over time. Figure 6.4 clearly shows that the addition of CCR to BBF, results in the significant development of the performance at all curing ages. CBEM-TBF2 produced a higher stiffness modulus than CBEM-LF, CBEM-TBF1, CBEM-BBF and 100/150 HMA over all curing times. It should be noted that at 14 and 28 days curing, the CBEM-TBF2 was comparable to 40/60 HMA and CBEM-OPC, respectively.

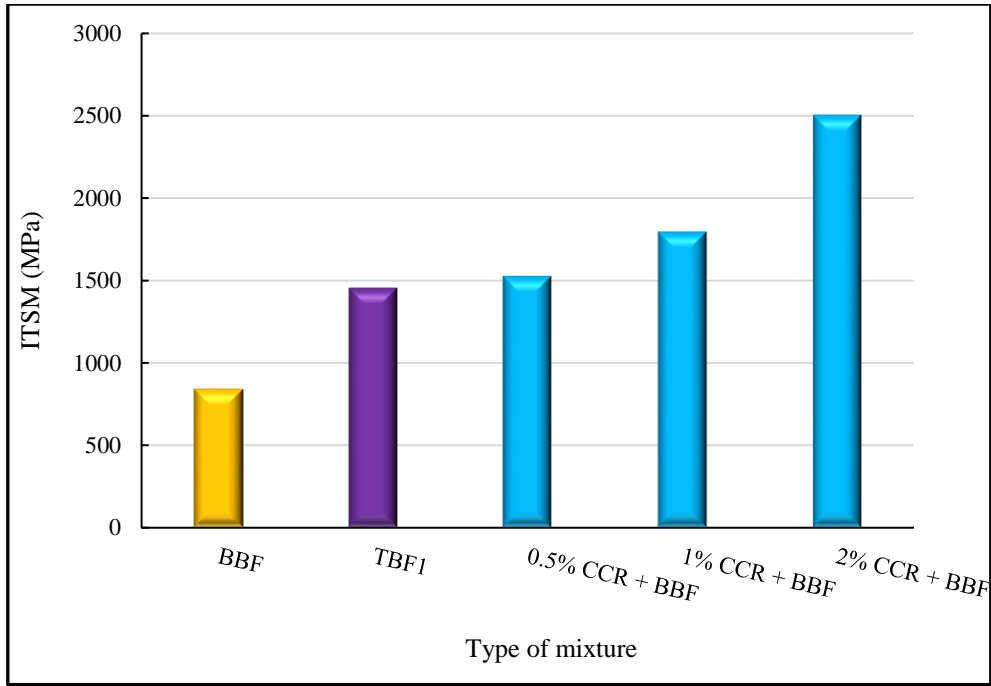


Figure 6.3: Effect of adding CCR to 6% BBF on the ITSM of CEBMs at 3 days

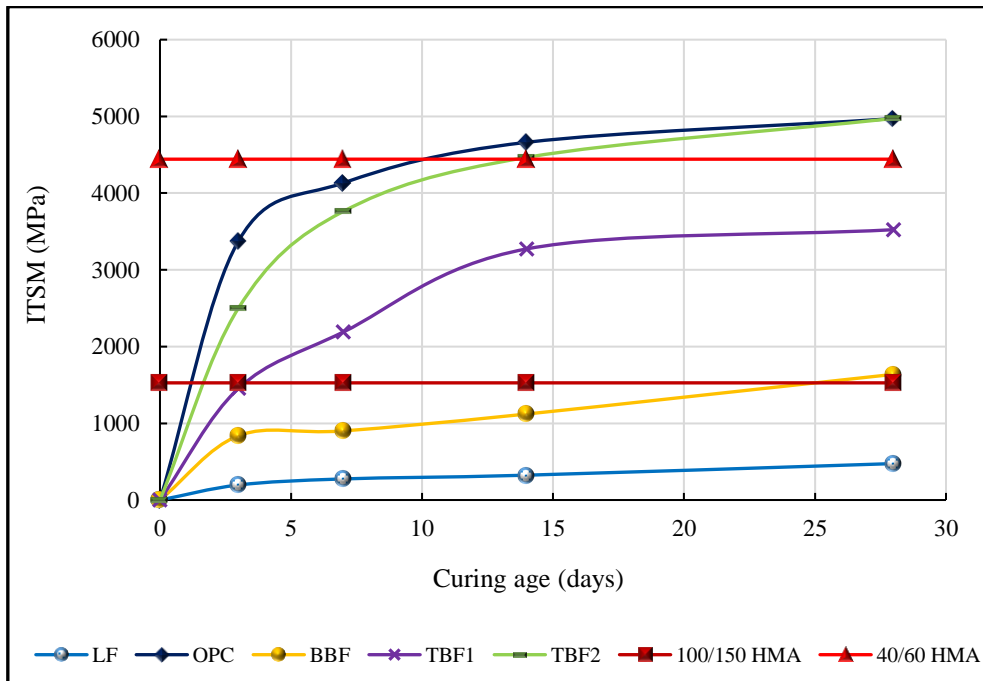


Figure 6.4: Effect of curing time on the ITSM of CBEM-TBF2

The further enhancement in ITSM for the CBEM-TBF2, in comparison with the other mixes shown in Figure 6.3 and Figure 6.4, can be explained as follows:

- The generation of hydration products within the CBEM in the existence of water was accelerated due to an enhancement in the hydraulic environment as supplied by the CCR solution in water. These hydraulic products produced a secondary binding material while simultaneously strengthening and reinforcing the main bitumen binder paste.
- The absorption of trapped water was improved due to the hydration process and the high absorbability of CCR to water, this a result of its morphology, high surface area and chemical phases.
- Coalescence of the bitumen emulsion was increased through an increase in the pH value on the addition of CCR.

6.4 CBEM incorporating Alkali-activated TBF2 (ATBF2)

The alkali activation of waste materials is a chemical process that assists the conversion of glassy structures (partially or totally amorphous and/or metastable) into very compact, well-cemented composites. Theoretically, any material consisting of silica and alumina can be alkali-activated. Silica, for example, starts to dissolve as soon as it comes into contact with an alkali solution (Comrie and Kriven, 2006). A range of chemicals that can be used as alkaline activating agents, such as sodium hydroxide (NaOH) and calcium hydroxide (Ca(OH)₂), have been discussed by Sajedi and Razak (2011).

With the aim of producing CBEM with ITSM results similar to those ITSM of the CBEM-OPC over different curing times from 3 to 28 days, a waste, high alkalinity, Ca(OH)₂ solution was used as an alkaline activator to increase the pH concentration of the hydration mediums to

improve breaking and dissolution in the glassy phases of the SSFA. This solution is discharged from the dewatering process of CCR and has a pH value of 13.8. The waste alkaline $\text{Ca}(\text{OH})_2$ solution was used as a total replacement of the 3% pre-wetting water content. This further development of the technology for producing a high strength CBEM is based on the work of Dulaimi (2017) who carried out a study to develop a new, fast-curing CBEM for binder courses, finding that activating a binary blended filler by using a waste alkaline NaOH solution, significantly improved its mechanical properties, water susceptibility and thermal sensitivity.

The specimens of the alkali-activated TBF2 (ATBF2) mixture were prepared, ITSM testing conducted at different curing times to investigate its strength. ITSM testing results for the CBEM-ATBF2 at 3 days, were compared with those for other developed and controls mixtures, as shown in Figure 6.5. Figure 6.6 shows the ITSM values for these mixtures over 3 to 28 days of curing. From Figure 6.5, a substantial increase in ITSM values is observed when replacing the pre-wetting water by the waste alkaline solution. The ITSM for CBEM-ATBF2 increased by approximately 41% compared to the same mixture with water for pre-wetting. The new mixture also surpassed conventional CBEM-LF and 100/150 HMA by 18 and 2.3 times, respectively. The ITSM value also exceeded the value for CBEM-OPC by 4.7% at 3 days age. The stiffness modulus for the CBEM-ATBF2 continued to increase over time as seen in Figure 6.6: it performed 4% better than 40/60 HMA at 7 days and 35% at 28 days. This represents an outstanding achievement from both environmental and economic perspectives.

The reason for the improvements in the ITSM of CBEM-ATBF2 in comparison with the previously optimised mixtures, is because of the addition of the highly alkaline activator which directly impacted on the reaction kinetics of the SSFA. Alkalis attack fly ash particles from outside to inside and induce them to continue to dissolve, meaning that the fly ash reactivity kinetics have become much faster in the new system.

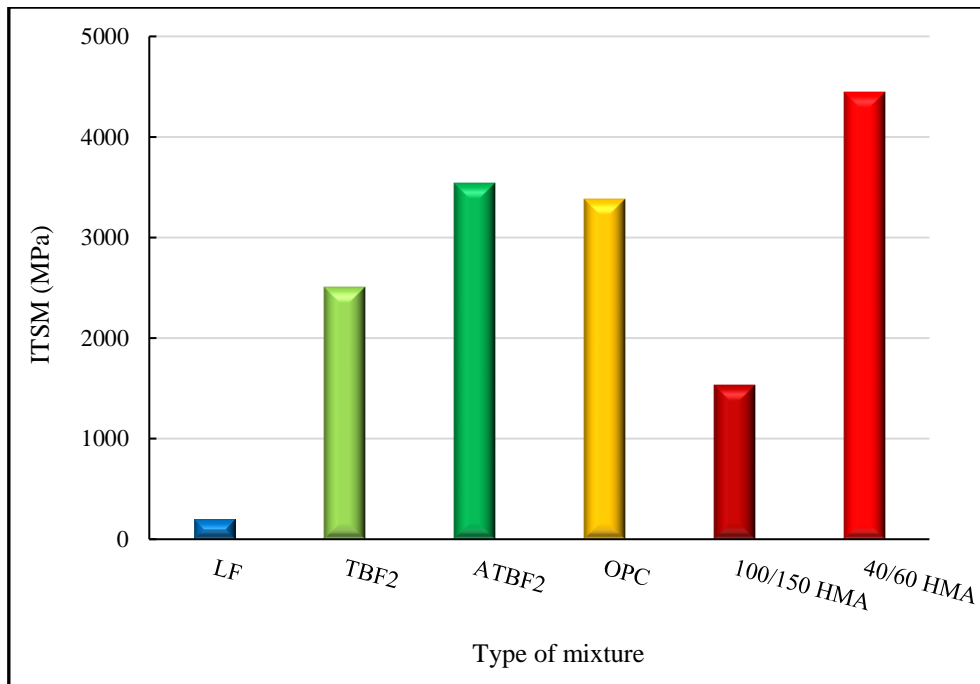


Figure 6.5: Stiffness development of CBEM-ATBF2 at 3 days of age

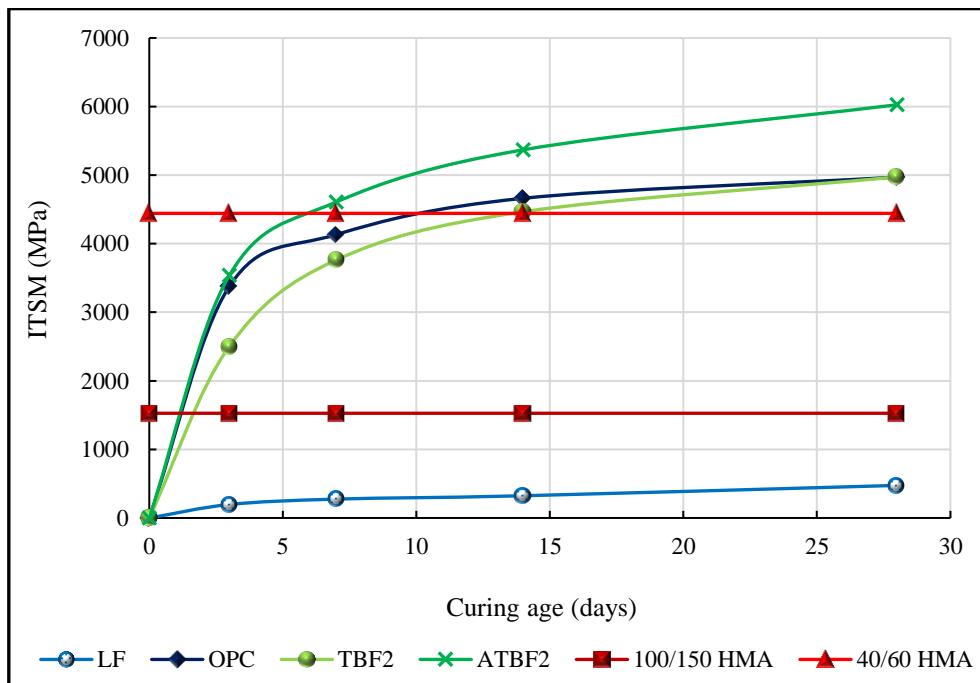


Figure 6.6: ITSM values of CBEM-ATBF2 at different curing ages

6.5 Water Loss in CBEMs

The removal of moisture from CBEMs and the breaking of bitumen emulsion, are the key factors that affect the stiffness of these mixtures (Needham, 1996). It is important therefore to track the water loss from CBEMs at various curing times. There are two sources of water in CBEMs: water in the bitumen emulsion and water added during mixing (pre-wetting water). In the current study, water loss was used as an indicator of water absorptivity, the hydration process and gains in the strength of CBEMs. To measure water loss, all mixtures were manufactured and left in their moulds for 24 hours before being extruded, then cured in the lab at 20°C throughout the investigation periods. Water loss was measured for each specimen by measuring the loss in mass at 1, 2, 3, 7, 14, 21 and 28 days.

The results of water loss for all studied mixtures are presented in Figure 6.7. It is clear that most of the water loss occurred during the first three days. Conventional CBEM-LF has the highest rate of water loss over the testing times. However, the water loss rate decreased for the mixtures including active fillers i.e. OPC, TBF2 and ATBF2. The latter had the lowest rate of water loss as most of the trapped water was absorbed by the active filler and consumed during the hydration process.

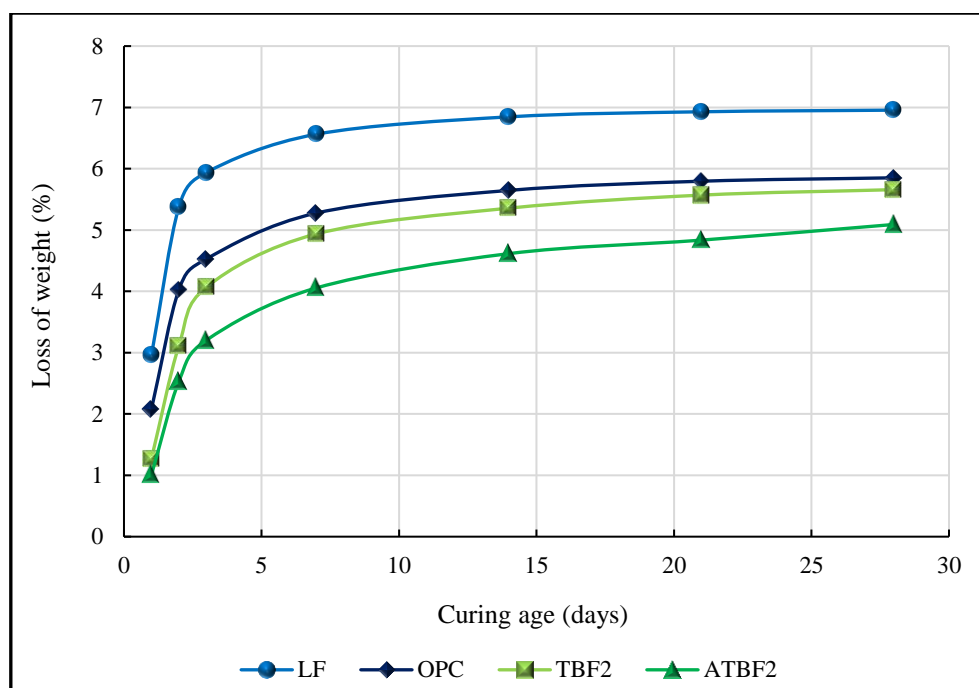


Figure 6.7: Water loss of CBEMs over different curing periods

6.6 Temperature Susceptibility of CBEMs

Using the ITSM test, temperature susceptibility was evaluated for all the optimised CBEMs and the HMAs at three different temperatures, 5, 20 and 45°C after 28 days curing. As illustrated in Figure 6.8, the stiffness modulus decreased with an increase in testing temperature. The curve of the slope in a semi-logarithmic plane, can represent thermal sensitivity by which the mixture with the higher change rate is identified as more susceptible to temperature. This trend is evident for 100/150 HMA, 40/60 HMA and CBEM-LF. However, the CBEMs with OPC, TBF2 and ATBF2 were only slightly influenced by testing temperature, which indicates that these mixtures are less susceptible to temperature change, especially high temperatures. For example, there was a stiffness reduction of only 40% when heating CBEM-ATBF2 from 5 to 45°C. In contrast, both 100/150 HMA and 40/60 HMA lost around 97% of their stiffness under the same conditions.

The stiffness performance of the new mixes at high temperatures is due to the presence of a secondary binder within the mix's internal microstructure, produced from the hydration of the SCF in the existence of water. This has facilitated an improvement in the interlocking of aggregate particles within the mass of the mixtures and enhanced the cohesion of the paste between the said aggregate particles. These mixtures benefit from being more thermally stable, have less susceptibility to high-temperature rutting and are less likely to suffer from cracking at lower temperatures. These results are in agreement with those obtained by other researchers (Bocci et al, 2002; Al-Hdabi et al, 2014a; Nassar, 2016).

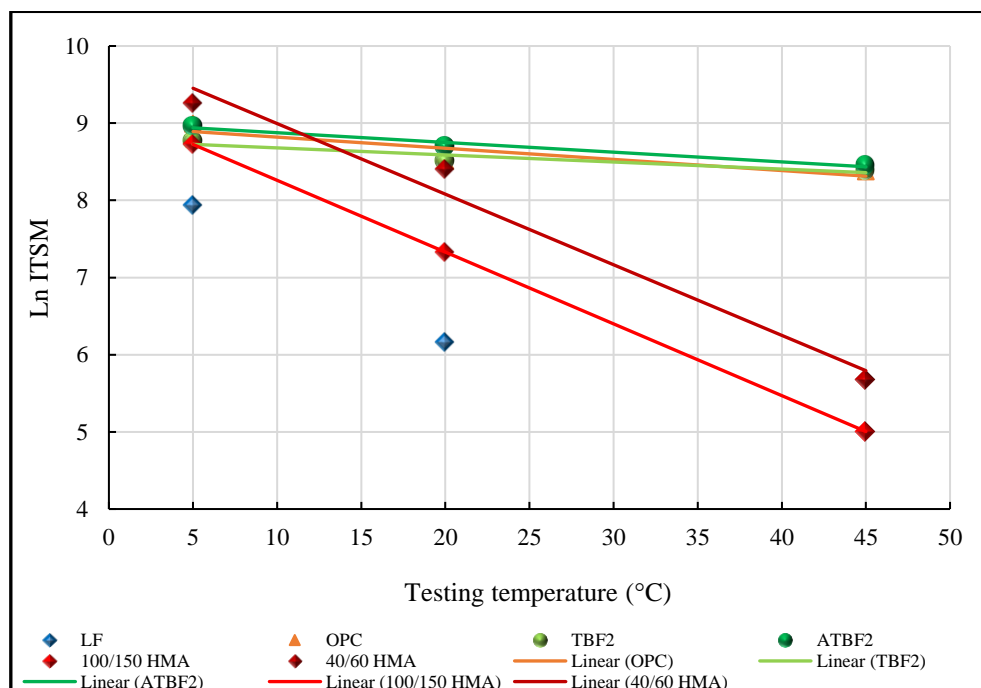


Figure 6.8: ITSM results at different testing temperatures

6.7 Summary

In this chapter, the mechanical performance of the studied mixtures, CBEM-BBF, CBEM-TBF1, CBEM-TBF2 and CBEM-ATBF2, was evaluated in terms of ITSM over different curing times. The conclusions can be summarised as:

- A significant improvement was achieved in the stiffness modulus of CBEMs when incorporating BBF and CCR (TBF2). This improvement is attributed to the hydration process occurring inside the treated CBEMs by which another cementitious binder has been created in the mixture through the hydration process.
- Further improvements were achieved by producing CBEM-ATBF2 by adding a waste alkaline solution to the CBEM-TBF2 as a full replacement of pre-wetting water. This mixture has mechanical properties comparable to the mixtures treated with OPC and traditional hot mixtures by ensuring advanced activation via the alkaline solution.
- The newly CBEM-TBF2 and CBEM-ATBF2 have shown less thermal susceptibility in comparison to the CBEM-LF and the two grades of bitumen hot mixtures.

In the next chapter, the reasons behind the improvements gained in the ITSM performance of the developed CBEM will be investigated by examining their chemical qualities and internal paste microstructure. This will be achieved using X-ray diffraction (XRD) analysis and scanning electron microscopy (SEM).

Chapter 7: The Microstructural Characterisation of the New Secondary Cementitious Filler

7.1 Introduction

Based on the findings of the previous chapter, CBEM-ATBF2 has been determined as the optimum mixture for potential use in road surfacing. The main source of this enhancement was due to the hydration process that occurred inside the mixture between the new secondary cementitious filler (SCF) and the trapped water in the compacted mass of the CBEM. The hydration products supplement the bitumen binder to produce a harder and denser mass because of the development of bonds and interlocking between particles.

This chapter reports the analysis of the internal composition and the microstructure of the new SCF, incorporating treated SSFA, OPC and CCR, and the waste alkali activator solution. X-ray diffraction (XRD) and scanning electron microscopy (SEM) are accepted as the most powerful techniques for investigating physico-chemical reactions upon hydration (Li et al, 2014). Accordingly, these tests were used to investigate the mineralogy and microstructure of the ATBF2 paste, at different curing ages, to identify the cementitious products generated from the hydration reaction. These results were compared with the conventional LF paste to underline the positive changes achieved by replacing LF with ATBF2, the results clarifying the reasons behind the improvements in ITSM performance presented in previous chapters.

7.2 X-ray Diffraction (XRD) Analysis

X-ray diffraction (XRD) is the most effective analytical technique used to investigate crystalline materials. The atoms, ions or molecules in all crystalline materials, are arranged in a regular manner as layers or planes, often determining the properties of these materials. Each

plane works as a semi-transparent mirror. When the wavelength of the X-ray is similar to the distance between planes, the X-ray is reflected such that the reflection angle is equal to the incidence angle, as seen in Figure 7.1. This behaviour is called ‘diffraction’, and is described by Bragg’s Law:

$$2d \sin \theta = n\lambda \quad (7.1)$$

where:

λ : the wavelength of the X-ray; d : the distance between planes in a crystal structure; θ : the incidence angle, and n : an integer.

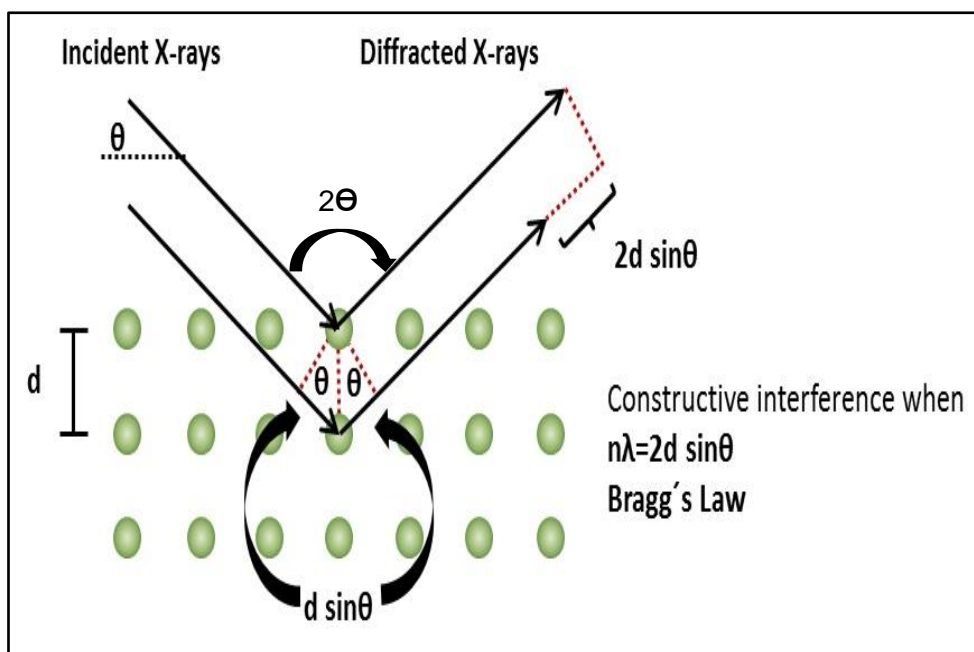


Figure 7.1: A schematic explanation of Bragg’s equation

The constructive interference of the diffracted X-ray beams occurs only if Bragg’s equation is satisfied. As such, X-rays scattered by the atoms in the plane of a periodic structure are in phase, diffraction occurring in the direction defined by the angle θ . The result of this measurement is plotted such that the X-ray intensity on the y-axis versus the angle 2θ (2θ is

defined as the angle between the incident and the diffracted beam) on the x-axis. Each XRD experiment has a set of diffracted intensities and angles at which they can be detected. This diffraction pattern can be thought of as a chemical fingerprint and can be identified by comparing it to a database of known patterns.

The XRD tool is commonly used to detect crystalline phases and various chemicals in cement pastes at different ages. The general features of reaction progression and cement hydrates using the XRD technique, have been discussed by Chatterjee (2001). In his study, it was demonstrated that unreacted phases such as calcite (CaCO_3), coexist with other reactants, in different proportions, at different ages. It has also been reported that the silicate phases, such as belite (Ca_2SiO_4) and alite (Ca_3SiO_5), lead to the production of calcium silicate hydrate (CSH), which is normally amorphous or inadequately crystalline, and portlandite (CH) which starts as a large hexagonal prism crystal plate. The result of aluminate and ferrite phase reactions in the presence of gypsum, is called ettringite (AFt) (alumina ferric oxide trisulphate). This is generated during the early hydration of cement and later converted to AFm (alumina ferric oxide monosulphate). Development of the hydration reaction of cement over time has been investigated by Esteves (2011) using XRD to identify the consumption of mineral phases and reductions in its crystalline nature. The mineral phases of a cementitious hydration reaction can be tracked using XRD by detecting new peak(s), disappearing peak(s), detecting changes (extension or reduction) in previous peak(s) and unchanged peak(s).

In this study, changes in the mineralogy of ATBF2 as a dry powder and a paste, along with LF dry powder and paste for comparison purposes, were tracked and analysed using XRD by recording the intensity of the material crystals exposed to various curing times (3, 7, 14 and 28 days). XRD patterns were assessed before and after mixing with water, to identify the formation and development of cementitious products such as the calcium silicate hydrate

(CSH) gel phase, ettringite in both AFt and AFm phases and portlandite (CH). This was achieved by using a Rigaku Miniflex diffractometer (Miniflex goniometer) (see Chapter 3, Figure 3.6), using a Wolfram cathode and an aluminium sample holder as an anode (Cu Ka), a voltage of 30 kV and current of 15 mA, registering from 3 to 60 with 2.0 deg/min scanning speed in a continuous mode. The ATBF2 and LF paste samples were prepared at the optimum liquid/filler ratio by hand mixing with a lab spatula and kept in cylinder moulds for 24 hours. The specimens were de-moulded and left to dry at lab temperature until the specified curing time. Prior to the XRD test, tiny pieces were snapped out from the paste sample at the due age and pulverized into powder. This was then sieved and placed on an aluminium holder, the surface flattened by a small lab spatula to ensure the X-ray beam hit the surface uniformly.

The XRD patterns for LF, before and after mixing with water at 3, 7, 14 and 28 days, are shown in Figure 7.2. It is clear that there is no noticeable change in the crystalline phases, i.e. calcite and quartz, in both powder state and after mixing with water, at different ages. These results confirm the expected inert state of LF as it did not interact with water to create new chemical phases, this explaining the low rate of increase in the ITSM of CBEM-LF.

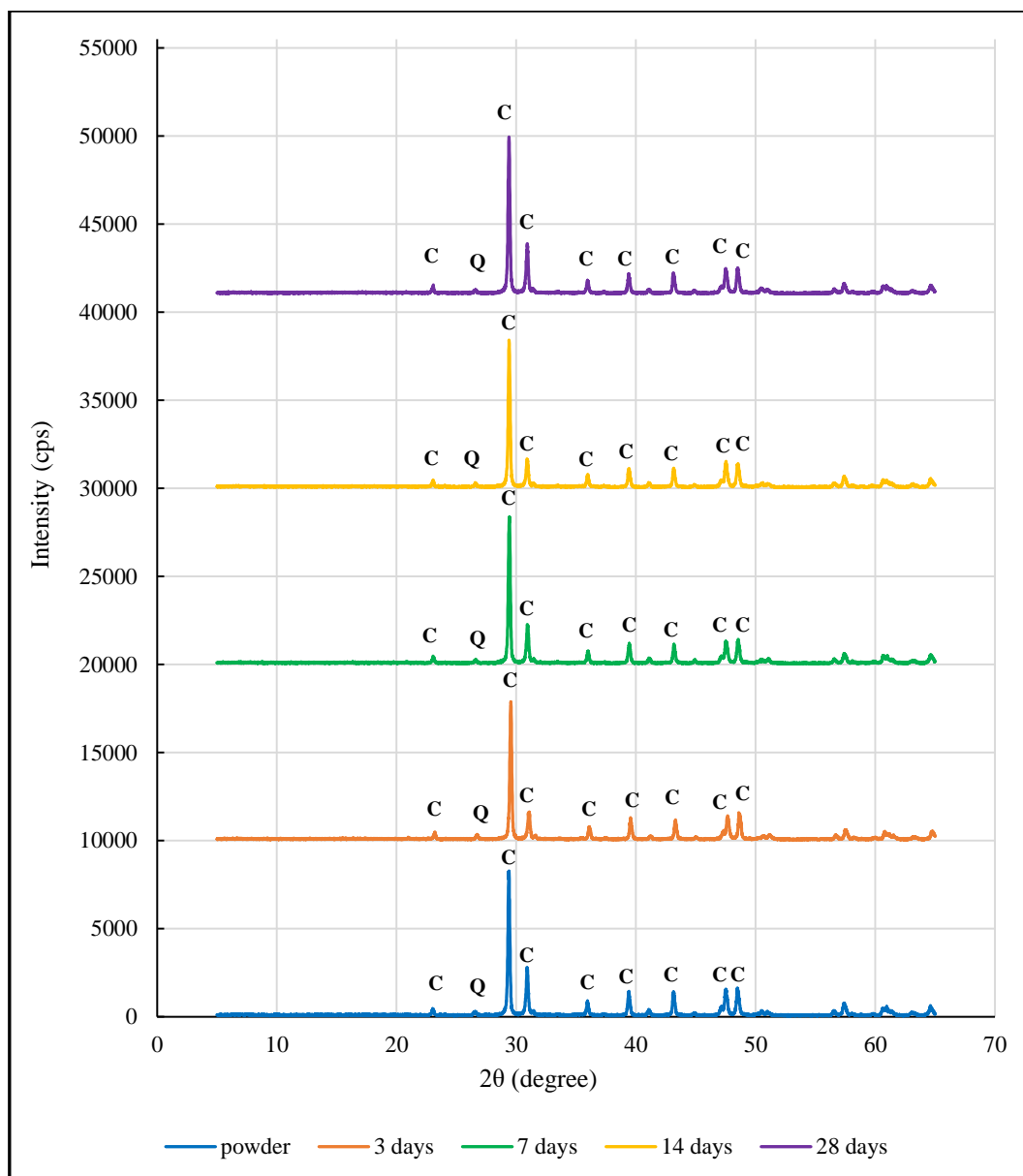


Figure 7.2: XRD spectra for the LF powder and paste at different ages (C= calcite, Q= quartz)

Figure 7.3 shows the mineralogical phases of the TBF2 powders and pastes after mixing with a calcium hydroxide waste solution to generate ATBF2 paste, and cured for 3, 7, 14 and 28 days. TBF2 in its dry state mainly consists of quartz, calcium hydroxide, alite, belite, hematite and magnetite. There are reductions in some peaks in comparison to the individual materials in FGD assisted ground SSFA (Figure 5.19), OPC (Figure 5.4) and CCR (Figure 5.13). The appearance of hydration products such as portlandite (CH), ettringite (AFt) and calcium silicate

hydrate (CSH), are evidence of the substantial hydration process over curing time. The continuous generation of these products indicates accelerated hydration and consecutive progressive developments in strength.

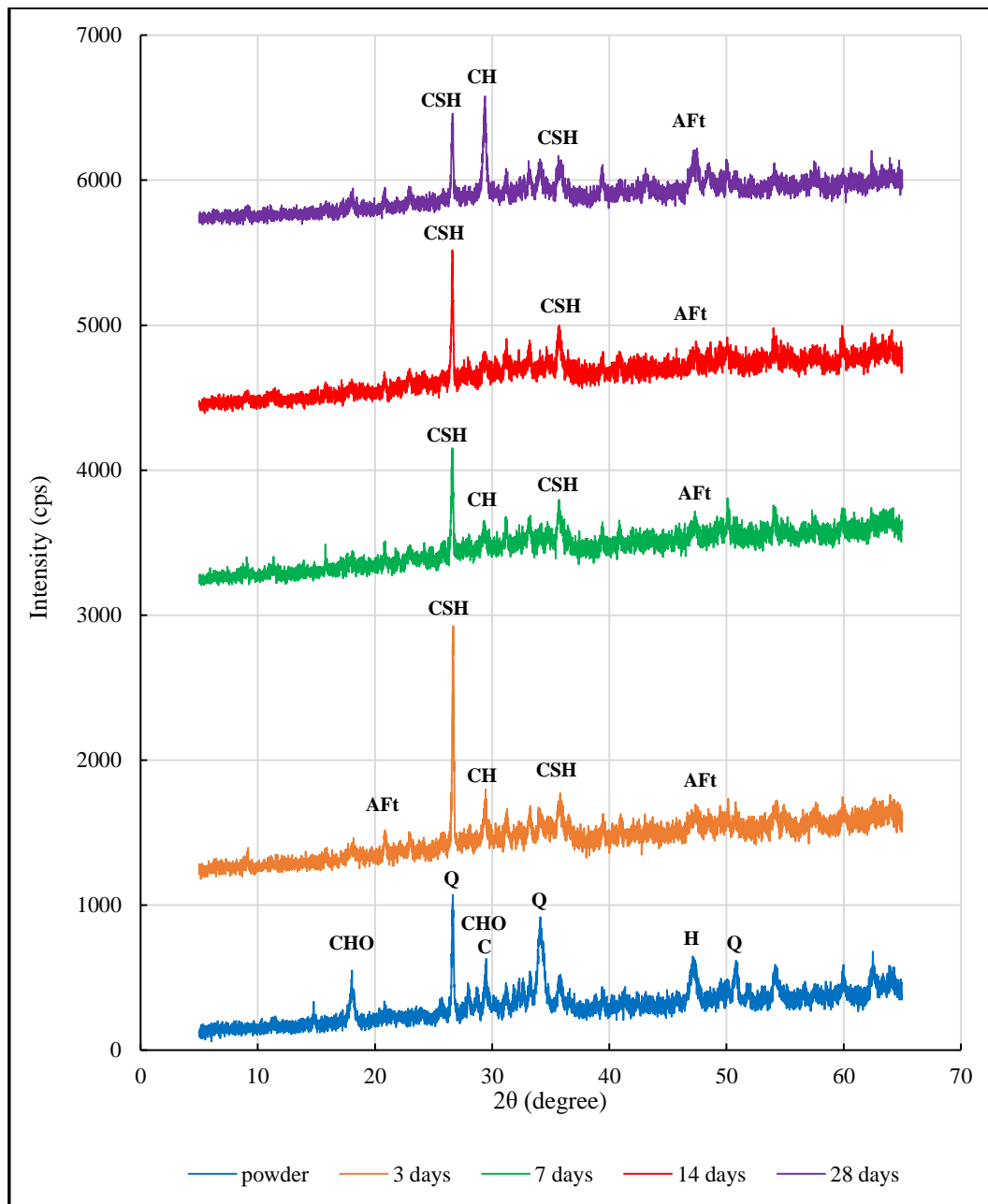


Figure 7.3: XRD spectra for the TBF2 powder and AATBF2 pastes at different ages (CHO= calcium hydroxide, Q= quartz, H= hematite, C= calcite, CH= portlandite, AFt= ettringite, CSH= calcium silicate hydrate)

Some of the mineral phases were consumed (calcium hydroxide, hematite, quartz) giving a reduction in crystallinity and new crystal hydrate peaks. In order to confirm the formation of hydration products, SEM was conducted to investigate the microstructure of the new filler over curing time. LF was also subject to SEM for comparison purposes, as explained in the following section.

7.3 Scanning Electron Microscopy (SEM) Analysis

Since scanning electron microscopy (SEM) was first commercialised around 40 years ago, it has undergone considerable development in that many different types of SEM are in use in different research and industrial applications. SEM has also been widely used in the cement industry to investigate the degree of hydration in cement pastes. The technique provides information about the surface topography and elemental composition of the hydrated phases of cement and other binders, providing high resolution, micrograph images (Rossen and Scrivener, 2017). Such images help to identify alterations in the microstructure over time (Jha and Sivapullaiah, 2016). When a sample is irradiated with a fine electron beam (electron probe), secondary electrons are emitted from the surface of the sample. The surface topography can be monitored by two dimensional scanning of the electron probe over the surface and ‘snapshotting’ an image from secondary electrons. Figure 7.4 shows the principle construction of SEM.

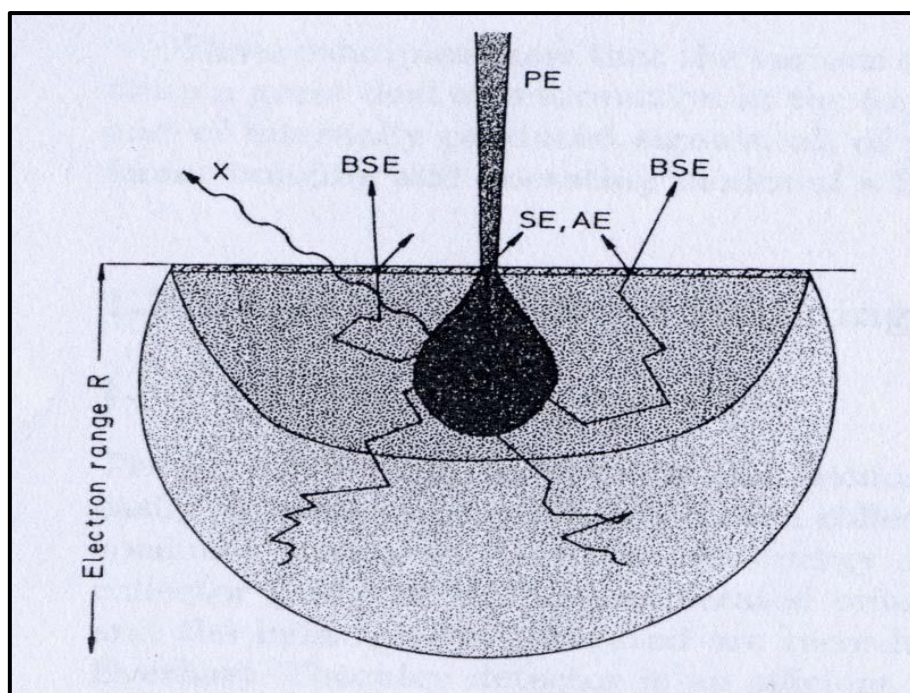


Figure 7.4: Secondary electrons (SE), backscattered electrons (BSE), Auger electrons (AE), and X-ray (X) in the diffusion cloud of electron range R for normal incidence of the primary electrons (PE) (El-Desawy, 2007)

Different phases of the hydrated cement can be seen in different forms in SEM images, e.g. ettringite (AFt), which is generated during early ages, can be seen as needle-like crystals. The calcium silicate hydrate (CSH) phase appears as a gel structure, while portlandite (CH) forms in a variety of shapes and sizes, starting as a large hexagonal prism crystal plate or large thin elongated crystal (Sarkar et al, 2001). Sarkar et al (2001) has discussed the efficacy of SEM in characterising the morphology and chemical compositions of the CSH phase, this being classified as the main product of cement hydration, primarily responsible for the strength in cementitious materials.

Accordingly, SEM was used in this study to explore the microstructure of TBF2 in a dry powder state and after mixing with the waste alkali solution (ATBF2 paste) over 3, 7, 14 and 28 days of curing. LF powder and pastes were also examined under the same conditions. SEM

observations were conducted to identify the development of the new binder using a Quanta 200 scanning electron microscope (see Chapter 3, Figure 3.7), with a probe current of 45 nA and counting time of 100 seconds, under a resolution of 3 to 4 nm, high vacuum and test voltage of 5 to 25 kV.

Samples for SEM were prepared in the same way as the XRD samples explained in section 7.2. Care needs to be taken in snapping pieces off from a sample so as not to touch the surface of the fracture to ensure that they truly represent the features of the material. SEM samples should be prepared to withstand a high vacuum and high energy beam of electrons and to be approximately $0.75 \times 0.75 \times 0.1$ cm in size. The samples were firmly mounted to aluminium specimen holders, or stubs, using conductive adhesive disks. Since the specimen chamber is a high vacuum, specimens were dried completely in a vacuum pump prior to observation. The specimens were then placed in an automatic, fine sputter coater to cover them with a thin layer of palladium to improve the spread of electrons and increase their electrical conductivity (Rêgo et al, 2015). Figure 7.5 shows SEM sample preparation.

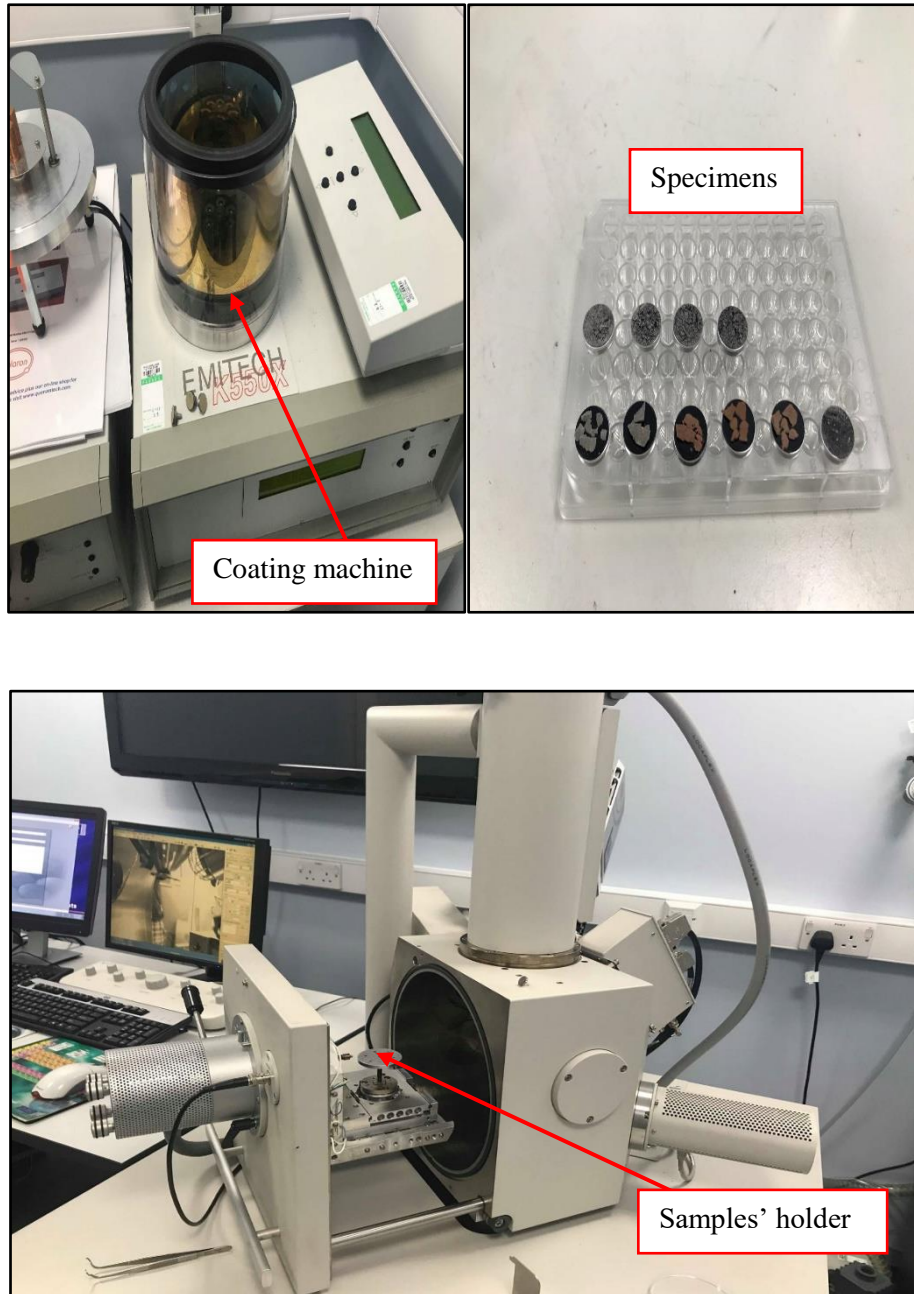


Figure 7.5: SEM samples preparation

The micrograph of the LF powder is presented in Figure 7.6, while Figure 7.7, Figure 7.8, Figure 7.9 and Figure 7.10 show the LF pastes at 3, 7, 14 and 28 days of curing, respectively. Figure 7.6 clearly reveals that the LF particles in a virgin powder state, have an irregular shape and that there is no sign of hydration of the LF pastes over different curing times: there are no considerable changes in the morphology at any age. Although the CBEM-LF showed a slight

improvement in ITSM value over curing time, this was due to the evaporation of trapped water. These results are in agreement with the ITSM results for the CBEM-LF presented in Chapter 4 (Figure 4.6), and the XRD analysis presented in the previous section.

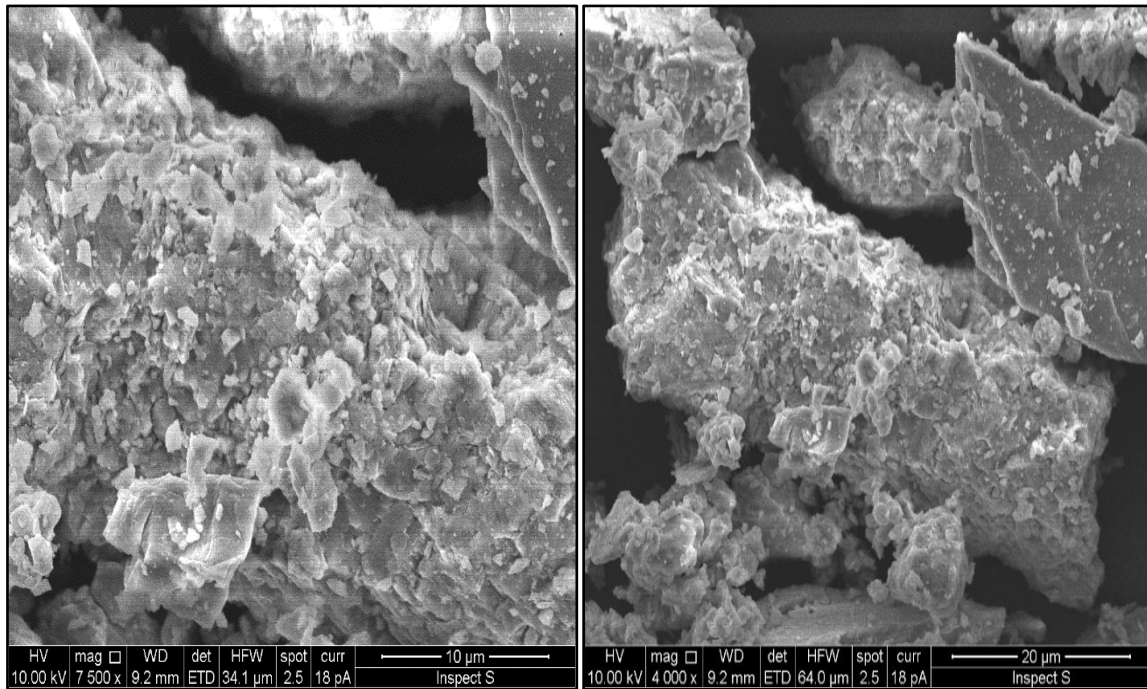


Figure 7.6: SEM images of the LF powder with 7500x and 4000x

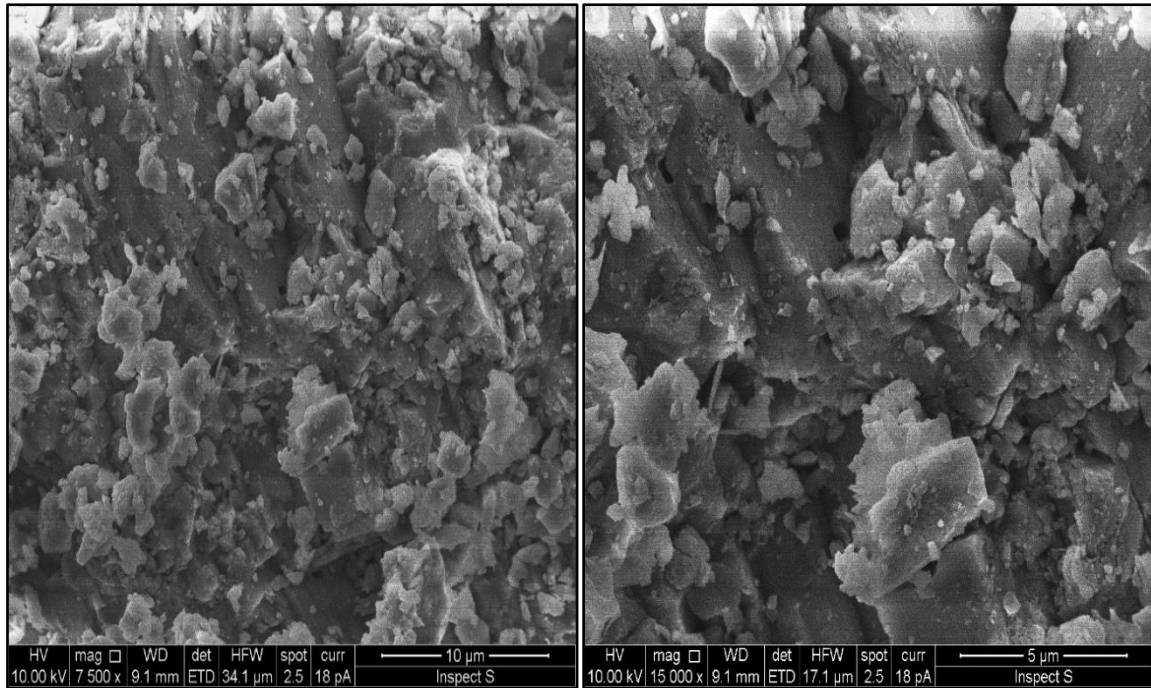


Figure 7.7: SEM images of the LF paste at 3 days of age

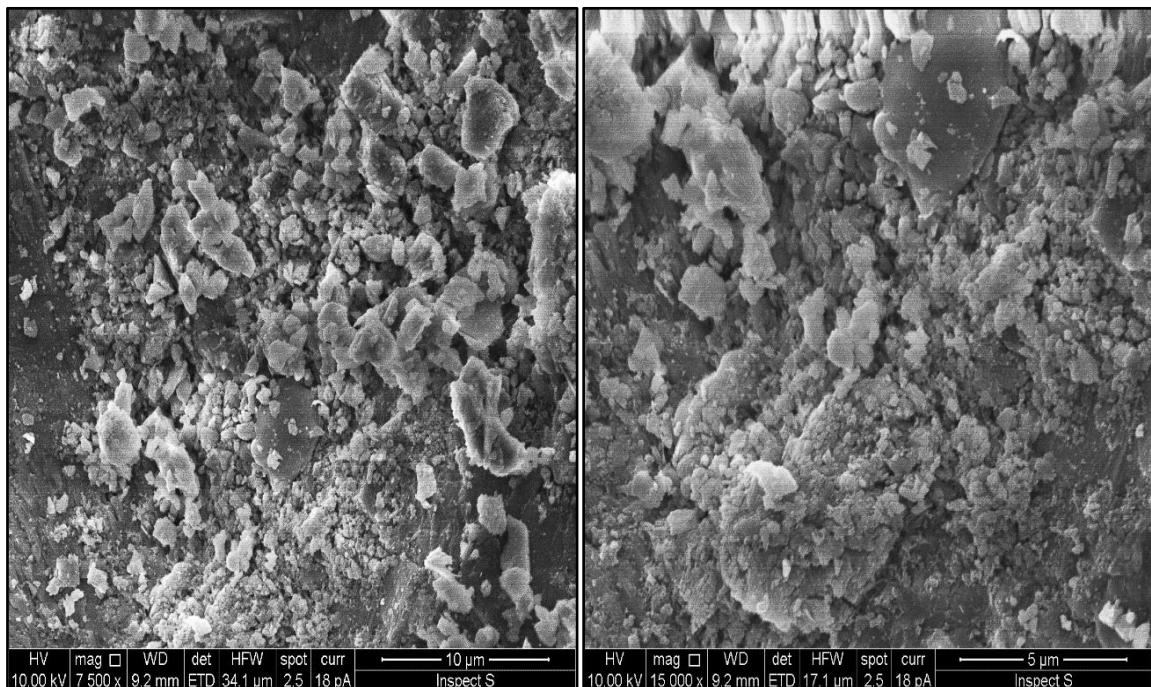


Figure 7.8: SEM images of the LF paste at 7 days of age

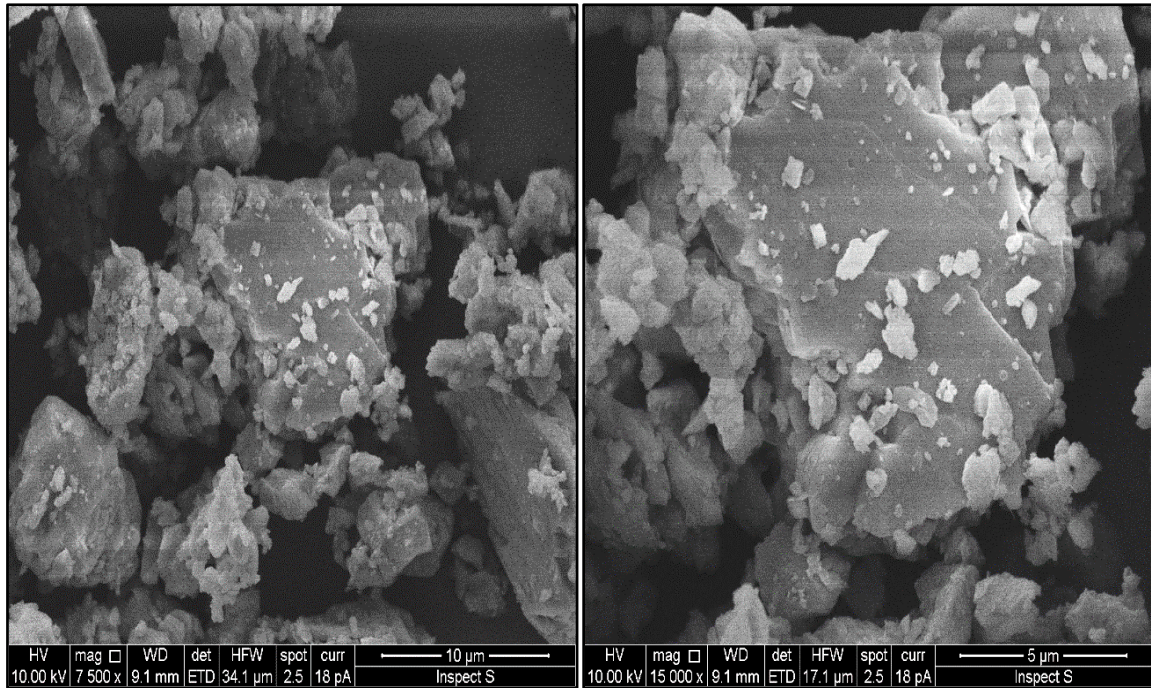


Figure 7.9: SEM images of the LF paste at 14 days of age

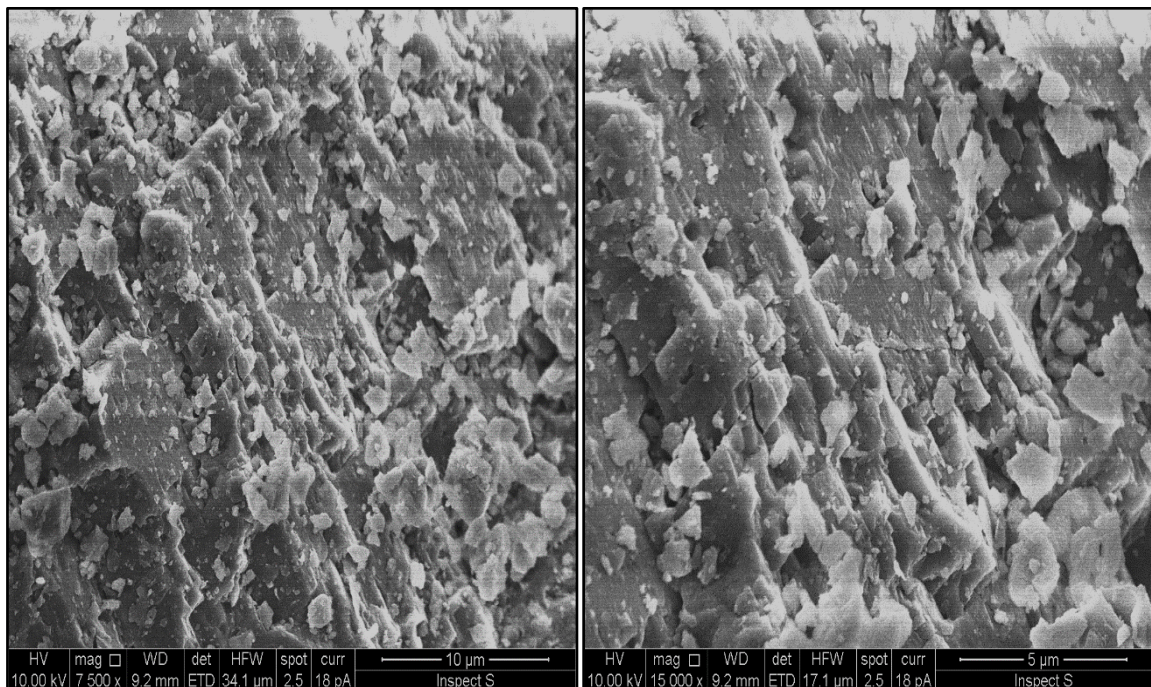


Figure 7.10: SEM images of the LF paste at 28 days

The microstructure of the TBF2 powder and the ATBF2 pastes at 3, 7, 14 and 28 days of curing, were investigated and are presented in Figure 7.11, Figure 7.12, Figure 7.13, Figure 7.14 and Figure 7.15. Figure 7.11 shows the morphology of TBF2, revealing the different characterisations of the blended cementitious materials, i.e. SSFA ground with FGD, OPC and CCR.

The SEM observations for the ATBF2 paste, after mixing with waste calcium hydroxide solution instead of water, reveal a dense microstructure which has increased substantially with time, especially between 3 and 7 days, this is in agreement with the increase in ITSM values during the same time period, as seen in Chapter 6 (Figure 6.6). The micrograph of the ATBF2 paste at 3 days of age (Figure 7.12), illustrates the generation of needle-like crystals, ettringite (AFt phase), a normal product of early cement hydration and a necessary and beneficial component of Portland cement systems. The amount of ettringite increases with an increase in the percentage of gypsum mixed with lime. The appearance of ettringite at an early age indicates a successful hydration reaction, the alkaline solution helping to accelerate this process by the breaking and dissolution of glassy phase of pozzolanic material (Shi and Day, 2000). Figure 7.13 displays the microstructure of the ATBF2 paste at 7 days, showing the beginnings of the formation of CSH gel, an essential product in the cement system as it is responsible for most of the engineering properties of the cement paste. This product constitutes approximately 70% of the total weight of the hydrated products, providing binding characteristics which contribute to its strength because these form a continuous layer that binds the original cement particles together into a cohesive whole (Feldman and Sereda, 1968).

After 14 days, (Figure 7.14) significant progress in the microstructure in terms of the structure's density and the appearance of flake-like particles of portlandite (CH), formed due to the lime hydration of C_3S and C_2S alongside ettringite and CSH can be seen in the ATBF2 paste. The

TBF2 particles have been replaced by hydration products, resulting in a reduction in the pore space apertures between particles and a dense packing of the binder.

In Figure 7.15 (samples tested at 28 days of curing), the surface area of the ATBF2 sample is enriched by CSH gel. The ettringite has become thicker, spreading out widely, covering most of the sample's surface area. Most of the ettringite is coated by cementitious gel which forms at this stage of curing. CH particles appear clearly in Figure 7.15 at this age of curing. The microstructure of the ATBF2 has become denser, its surface completely enriched by the hydrates. Similar alterations in the microstructure of the alkali-activated, binary blended cementitious filler, containing high calcium fly ash and fluid catalytic cracking catalyst residue activated by a waste alkaline NaOH solution, were reported by Dulaimi et al (2017).

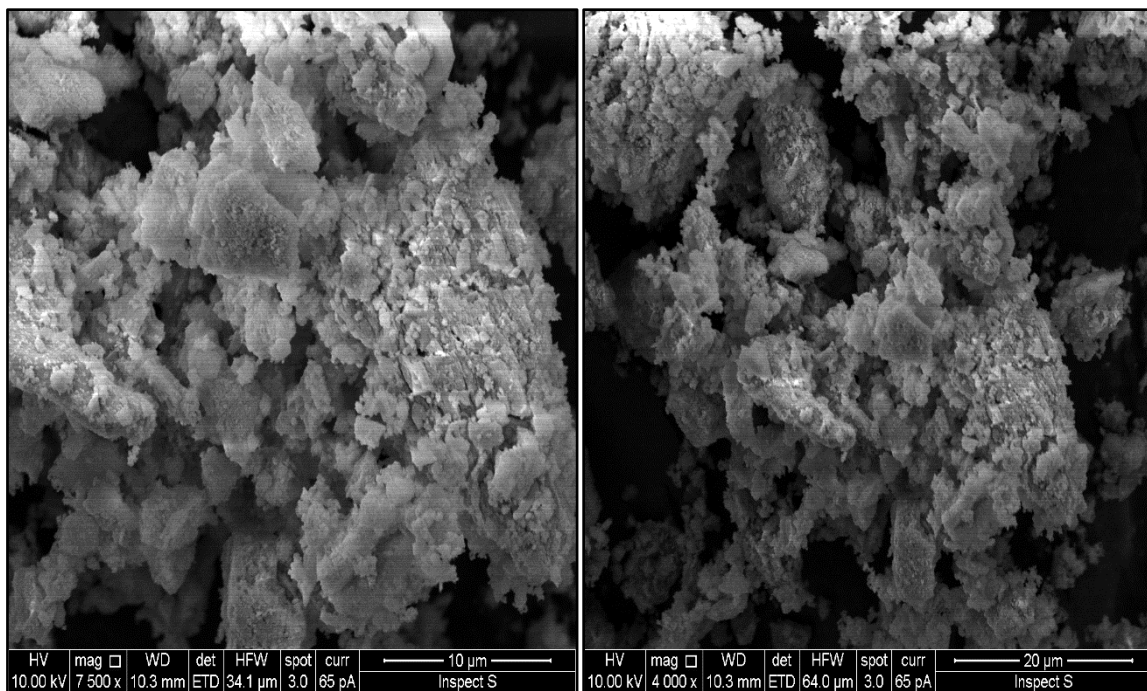


Figure 7.11: SEM images of the TBF2 powder

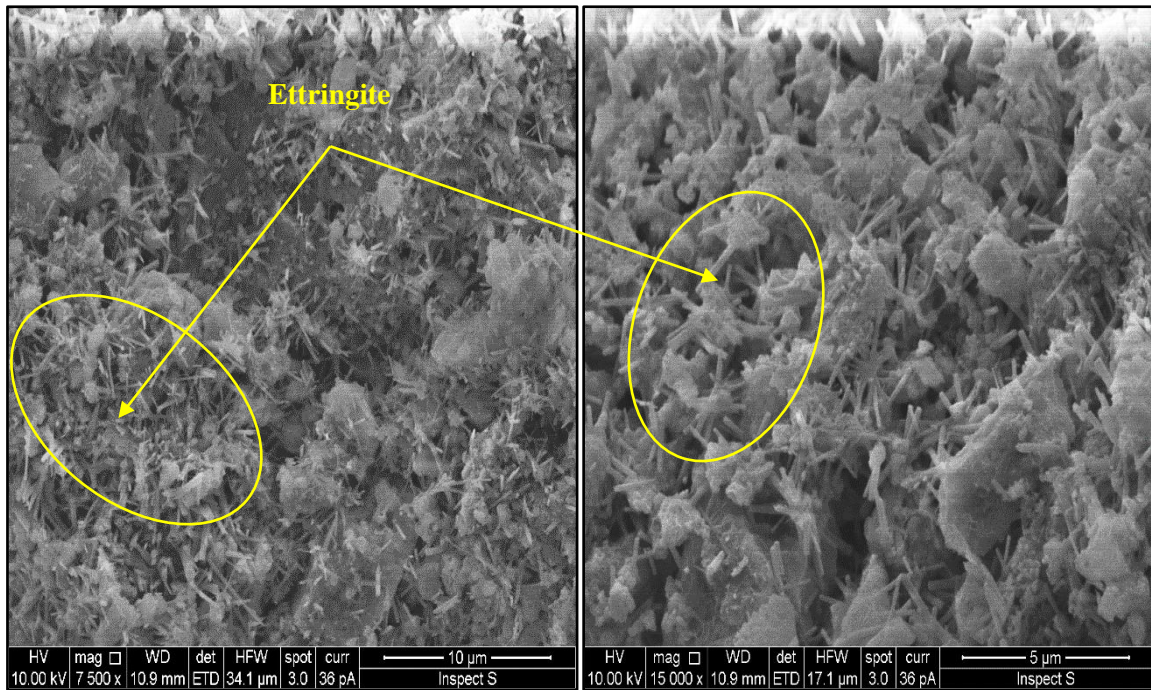


Figure 7.12: SEM images of ATBF2 paste at 3 days of age

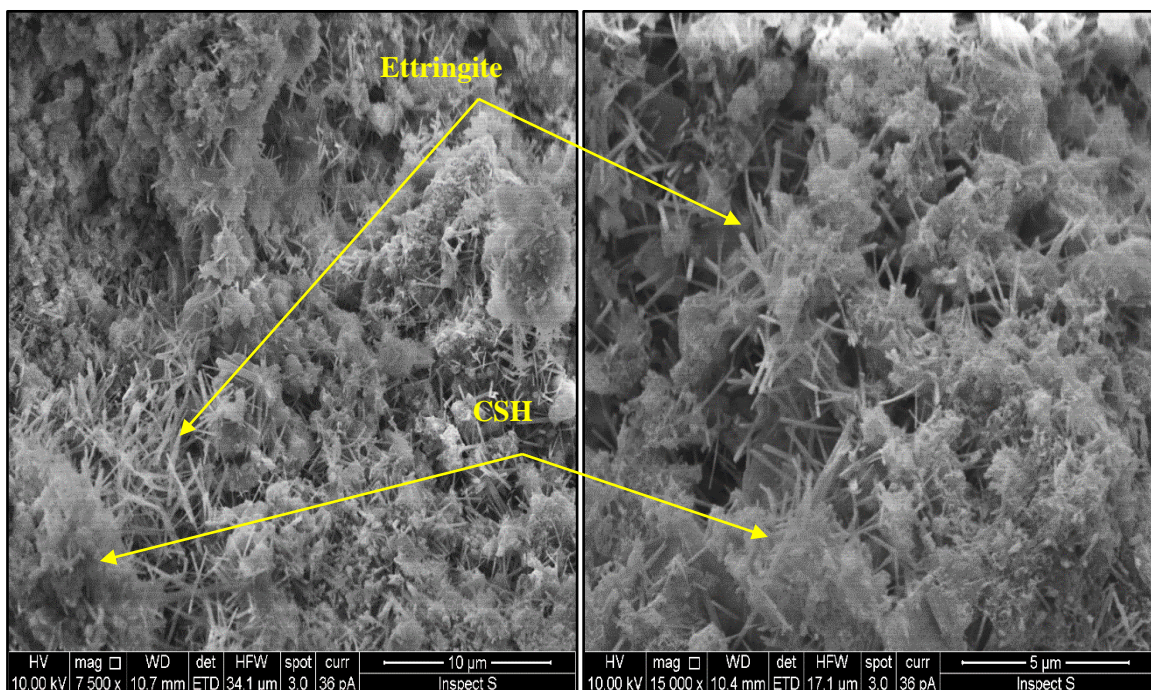


Figure 7.13: SEM images of ATBF2 paste at 7 days of age

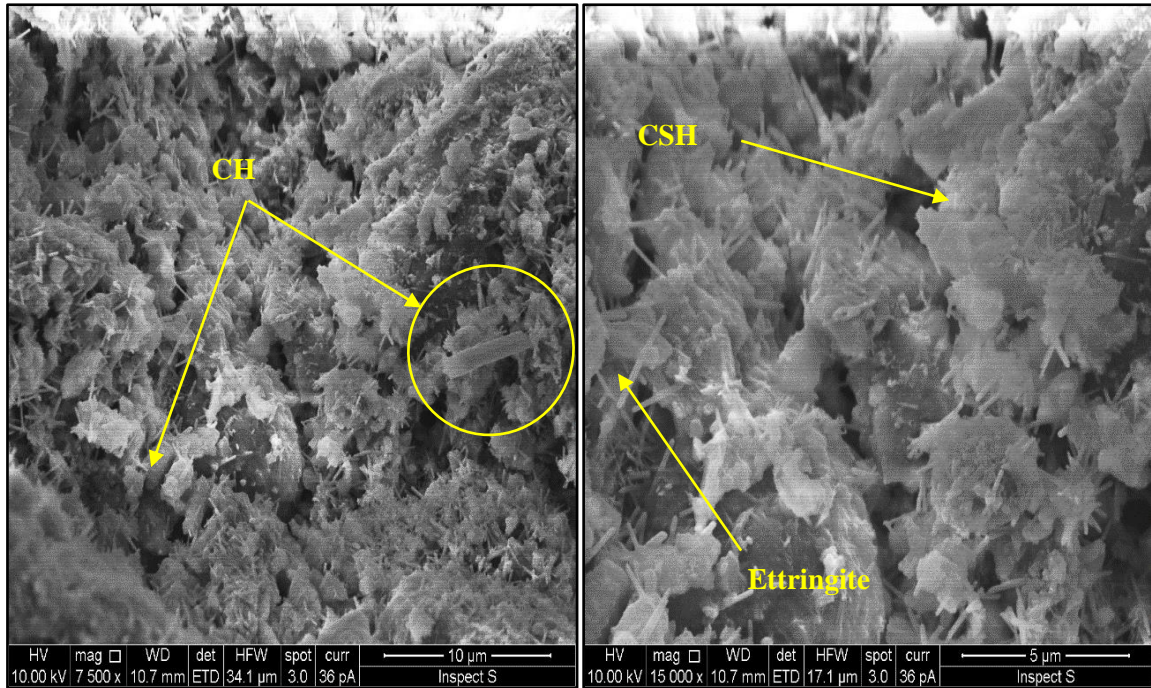


Figure 7.14: SEM images of ATBF2 paste at 14 days of age

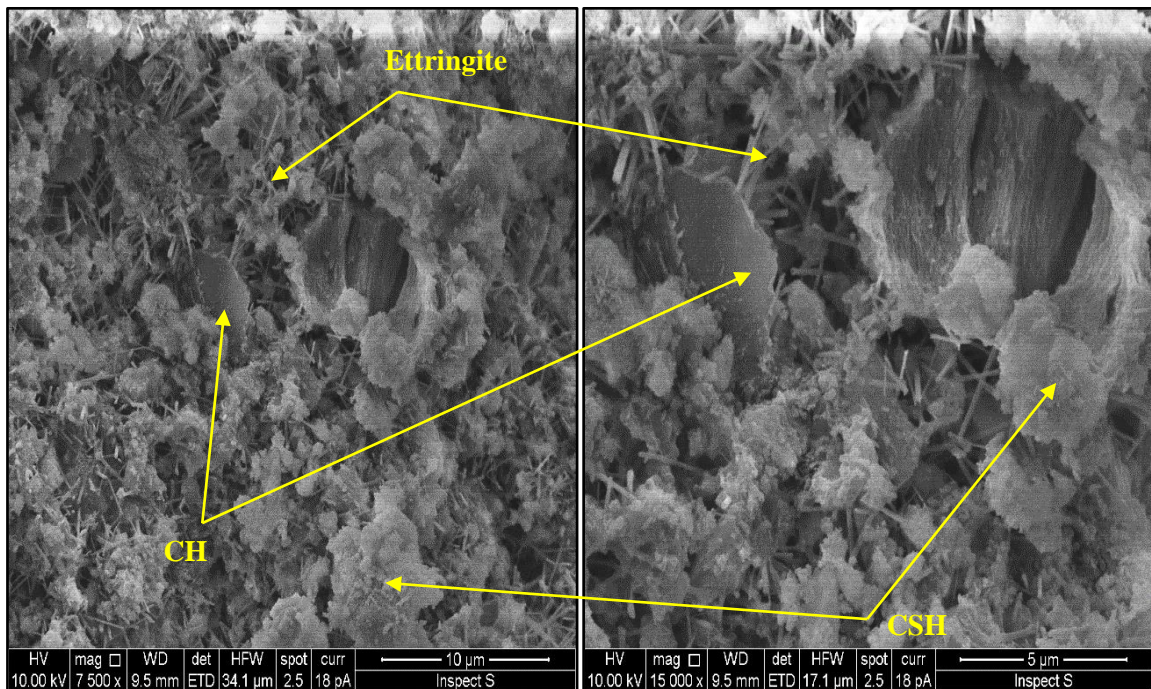


Figure 7.15: SEM images of ATBF2 paste at 28 days of age

The hydration products in the CBEM-ATBF2 are shown in Figure 7.16, where it can be seen that they are not affected when incorporated into the cold bitumen mixture (similar products to those shown in Figure 7.15 were generated). The two binders, the cementitious products and bitumen, are working together inside the CBEM-ATBF2 to generate an advanced CBEM, bound with visco-cohesion and interlocking-like bonding, giving substantial improvements in the ITSM with curing time, as described in Chapter 6.

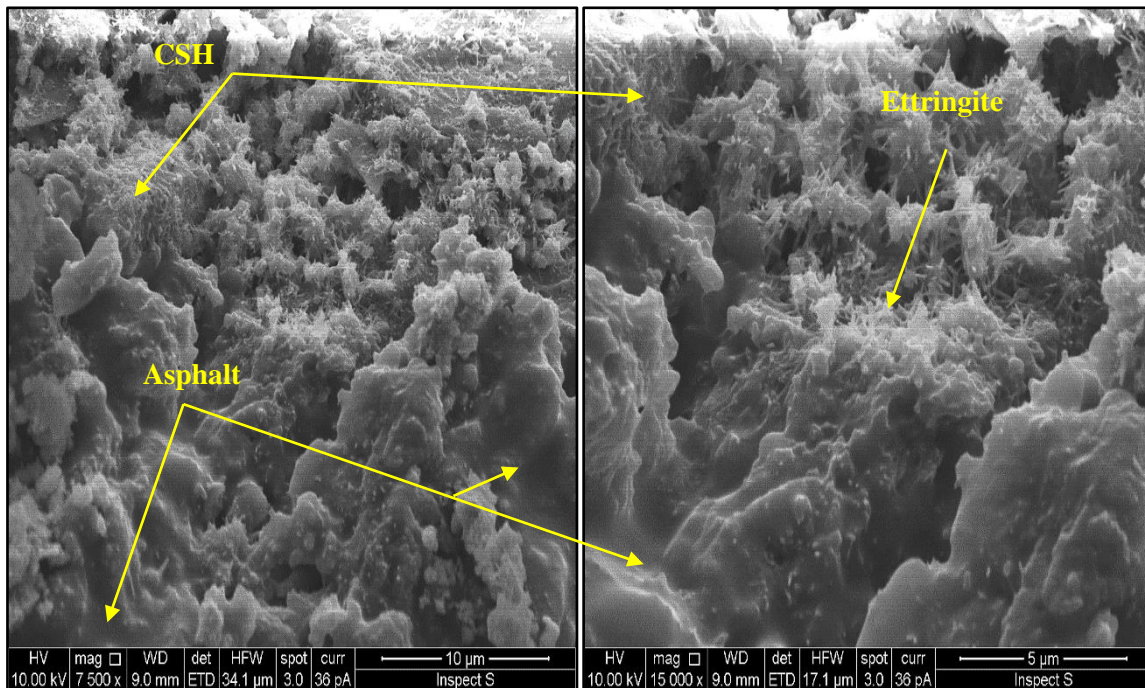


Figure 7.16: SEM images of the CBEM-ATBF2 at 28 days of age

7.4 Summary

The reasons for the successful improvements achieved in the indirect tensile stiffness modulus of the CBEM-ATBF2 mixture were explained in this chapter using XRD and SEM analyses. The results presented in this chapter were compared with those results obtained from samples of conventional LF. Pastes made from ATBF2 and LF were subjected to XRD analyses and SEM imaging at the same curing ages.

The most significant changes in the ATBF2 pastes, over the whole period of the 3 to 28 days of curing, happened due to the formation of ettringite, portlandite and CSH phases within the prepared samples. A very dense and compact microstructure was obtained when curing time increased. These findings strongly correlate with the improvement in ITSM of CBEM-ATBF2, due to absorption of the trapped water by the secondary cementitious filler through the hydration process, which results in hydraulic products that reinforce the mixture along with the main bitumen binder mastic.

Conversely, there were no changes over time in the morphology and microstructure of LF, this reflecting the inert state of the LF and explaining the low performance of CBEM containing LF.

Chapter 8: Development of a Novel High Performance CBEM

8.1 Introduction

This chapter reports the results of a laboratory study on the performance of CBEM which comprises both the new modified bitumen emulsion (MBE) and the developed secondary cementitious filler (SCF) in terms of i) indirect tensile stiffness modulus (ITSM) at different curing times, ii) water sensitivity and iii) long-term age hardening. It is predicted that the new mix will address the aim of this research work in overcoming the problems associated with the use of conventional CBEM, namely low strength at early ages and the amount of time required for curing, this ranging from 2 to 24 months, to develop its maximum strength. The performance of the CBEM-BBF, CBEM-TBF2 and CBEM-ATBF2 with MBE as per ITSM test results, was compared with the performance of the same mixtures made with normal bitumen emulsion (NBE). The ITSM results for the above mixes were also compared with CBEM-LF, CBEM-OPC, 100/150 HMA and 40/60 HMA. The durability of the control and the developed CBEMs with both emulsions, was also investigated.

8.2 CBEM incorporated BBF and MBE

The coating quality of the new MBE treated with ultrasound waves for 7 minutes, was evaluated in terms of its ITSM (CBEM-BBF with 4.2% ground SSFA + 1.8% OPC of the total weight of aggregate), at different curing times: 3, 7, 14, 28, 90 and 180 days. These results were compared with those of the same mixture, but with the NBE as described in Chapter 5 (section 5.6) and the results for CBEM-LF and CBEM-OPC, with both emulsions as described in Chapter 4 (sections 4.5.1 and 4.5.2).

The ITSM results of the CBEM-BBF containing MBE at 3 days are shown in Figure 8.1 where it can be seen that there is a significant increase in the stiffness modulus (around 25%) when replacing NBE with MBE. This mixture also achieved ITSM values greater than the CBEM-LF mixture with NBE and MBE by approximately 5 and 3 times, respectively. CBEM-BBF with MBE exceeded the performance of 100/150 HMA after 14 days, as seen in Figure 8.2. The highest rate of increase occurred in the first 28 days, this was followed by a slight rate of increment. This behaviour is similar to that of the control mixtures. However, the performance of the aforesaid mixture is still inferior to the OPC mixtures with NBE and MBE and to 40/60 HMA.

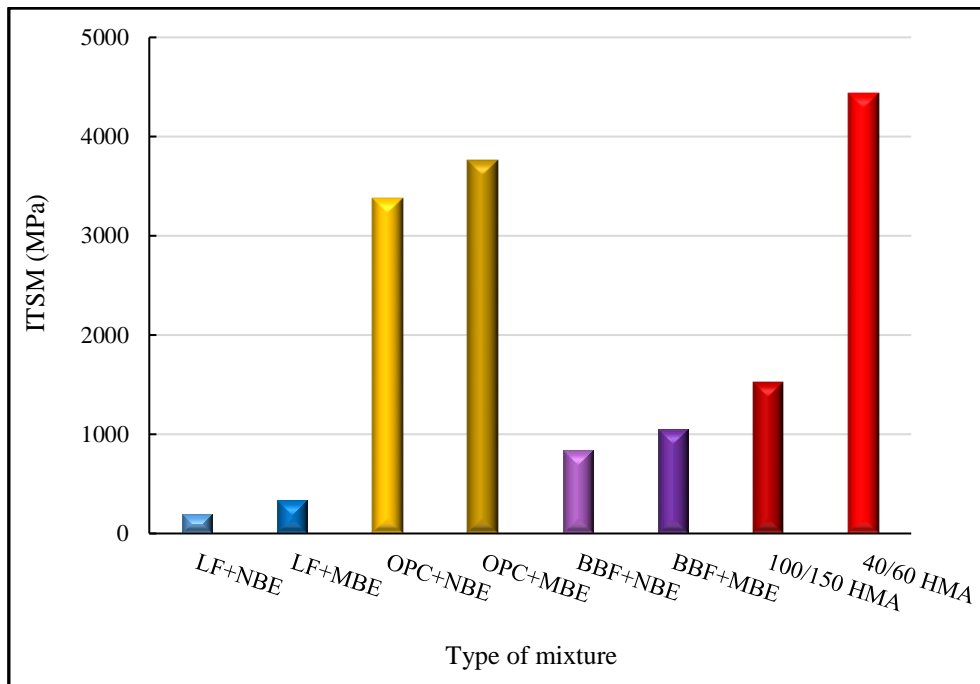


Figure 8.1: ITSM value of CBEM-BBF with MBE at 3 days of age

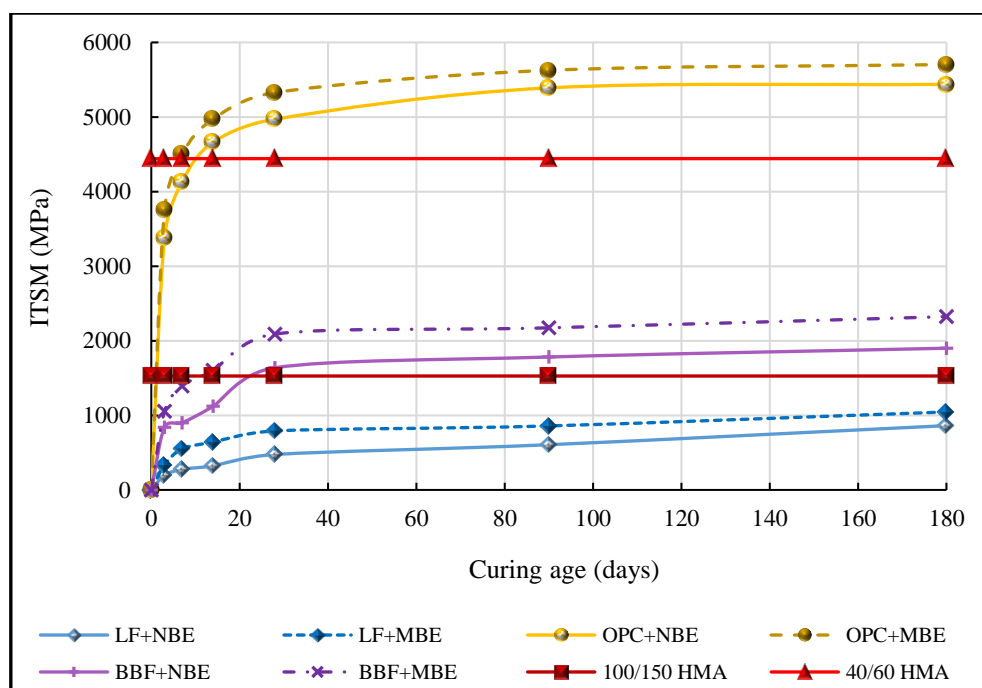


Figure 8.2: ITSM values of CBEM-BBF with MBE at different curing times

8.3 CBEM incorporating TBF2 and MBE

The ITSM results for CBEM-TBF2 (6% BBF + 2% CCR of the total weight of aggregate) at 3 days curing age, are presented in Figure 8.3. An outstanding increment in ITSM results has been achieved, compared to the same mixture made with NBE. It also has an ITSM value higher than conventional CBEMs-LF with NBE and MBE by approximately 16 and 9 times, respectively.

It should be noted that the ITSM value for CBEM-TBF2 with MBE, has exceeded those for 100/150 HMA at 3 days and 40/60 HMA at 7 days, as seen in Figure 8.4. The ITSM results reveal enhancements at early ages of curing, with limited further increases in ITSM values after that. This mixture performed significantly better than the CBEM-OPC with both emulsions, after 7 days age. However, at 3 days curing age, its performance was still below that of the OPC mixtures and 40/60 HMA. Therefore, to attain fast curing and have a high performance CBEM, MBE was incorporated into the CBEM-ATBF2, as presented in the next section.

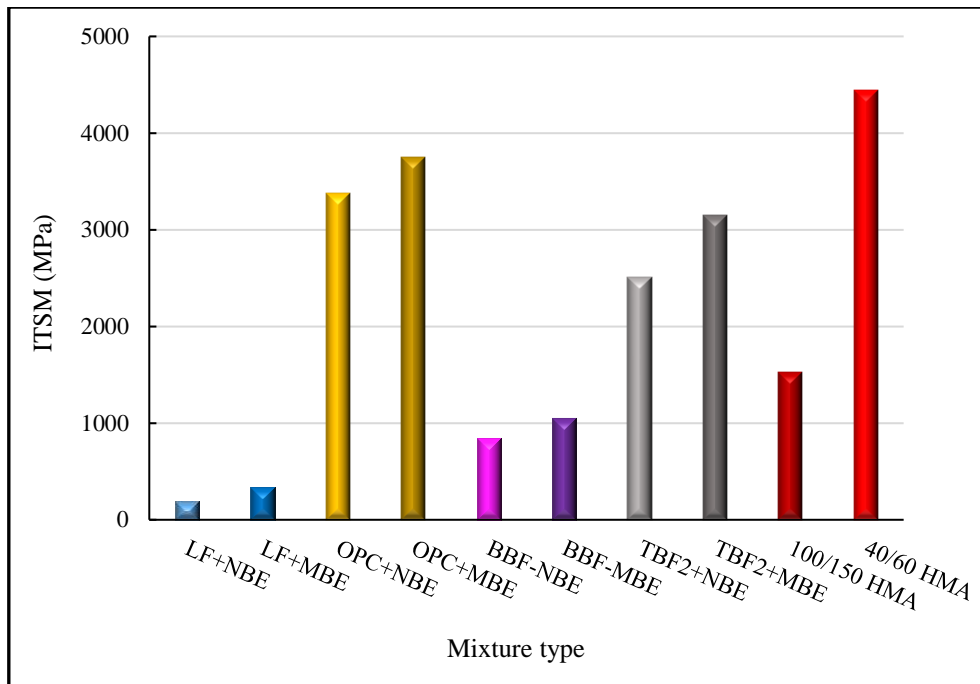


Figure 8.3: ITSM values of CBEM-TBF2 with MBE at 3 days curing

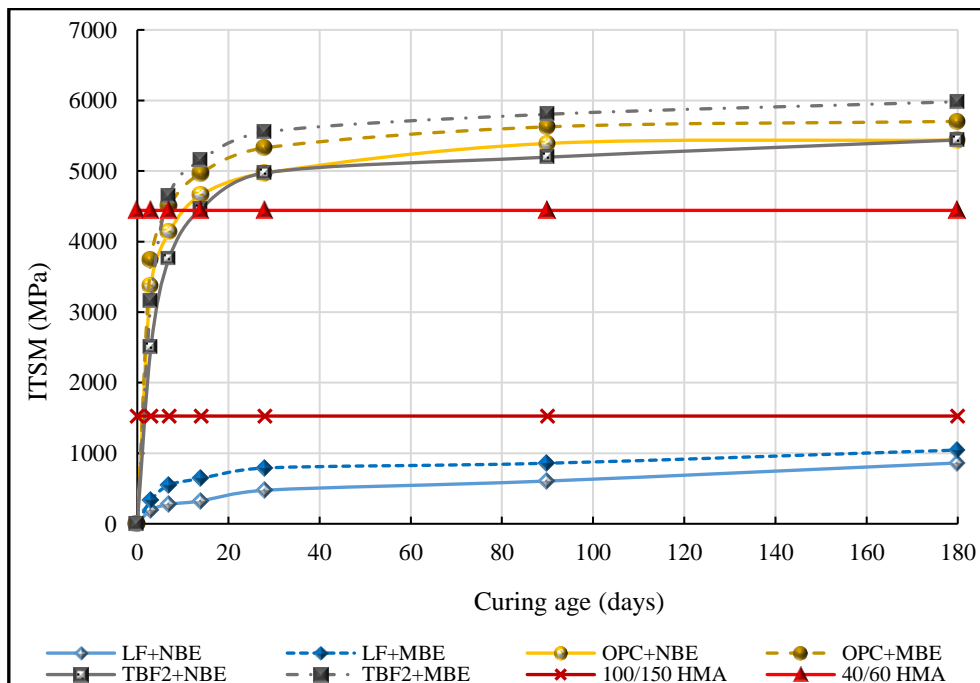


Figure 8.4: ITSMs of CBEM-TBF2 containing MBE at different curing times

8.4 CBEM incorporating ATBF2 and MBE

The last stage in the development process of the new/novel CBEM involves the addition of MBE to CBEM-ATBF2 (TBF2 + 3% waste calcium hydroxide solution instead of pre-wetting water): Chapter 6 (section 6.4), to facilitate further enhancement in ITSM values at early ages. The ITSM test was applied at different curing times, to identify the progress in performance of the newly developed mixture. A substantial increase in ITSM was observed at 3 days, approximately 11% compared to the same mixture made with NBE, as seen in Figure 8.5. The rate of improvement decreased with increasing curing times. The ITSM value of CBEM-ATBF2 with MBE at 3 days and at normal curing, was 2.5 times higher than traditional 100/150 HMA, this satisfying British and European requirements in terms of ITSM (European Committee for Standardization, 2016b). In addition, it was better than the CBEM-OPC mixtures containing NBE and MBE at 3 days, by approximately 16% and 5%, respectively. The CBEM-ATBF2 with MBE achieved a higher stiffness modulus than the control CBEM-LF and CBEM-OPC mixtures with both types of bitumen emulsion, and 100/150 HMA over all curing ages. Its performance also exceeded that of 40/60 HMA at 7 days, as illustrated in Figure 8.6.

The increase in stiffness modulus of the CBEM-ATBF2 mixture with MBE, is because the new emulsion has smaller bitumen droplets which provide an adequate and even coating to the aggregate particles, thus improving cohesion within the mixture. A coherent bitumen film coalesced on the aggregate particle surface after the cementitious filler consumed the trapped water through the hydration process. The bitumen coated aggregates and the hydration products worked together to improve the strength of the bitumen-aggregate bonding interface and thus upgraded the ITSM results of the developed mixture. The faster curing time is also enhanced due to the presence of the alkaline solution. This increases the alkalinity of the medium which

accelerates the breaking process of the glassy phases in the SSFA. This, in turn, helps to accelerate the hydration process, giving higher ITSM results.

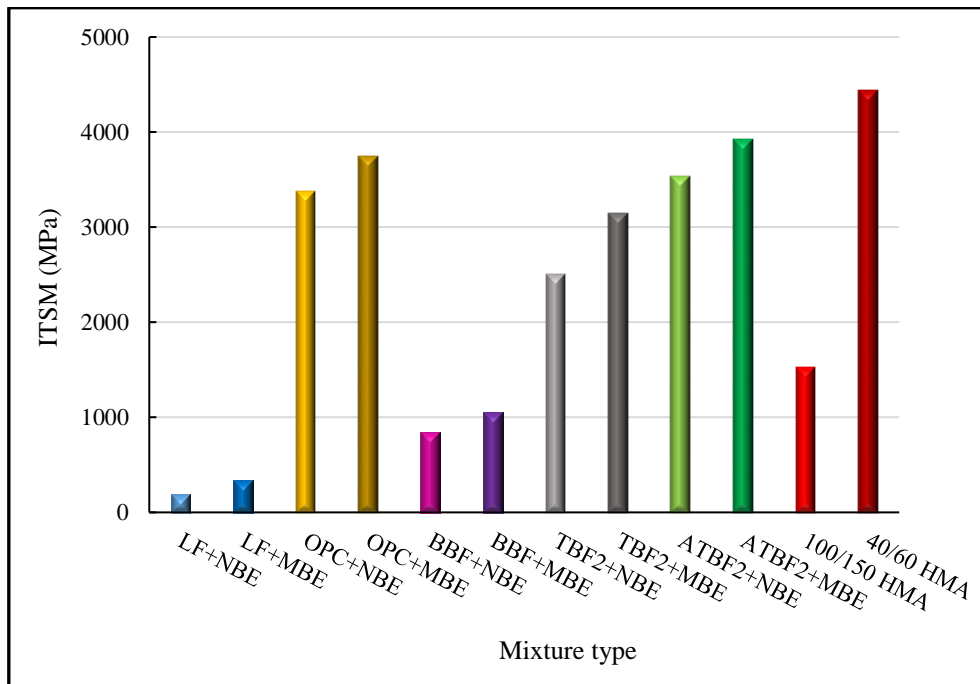


Figure 8.5: ITSM values of CBEM-ATBF2 with MBE at age 3 days

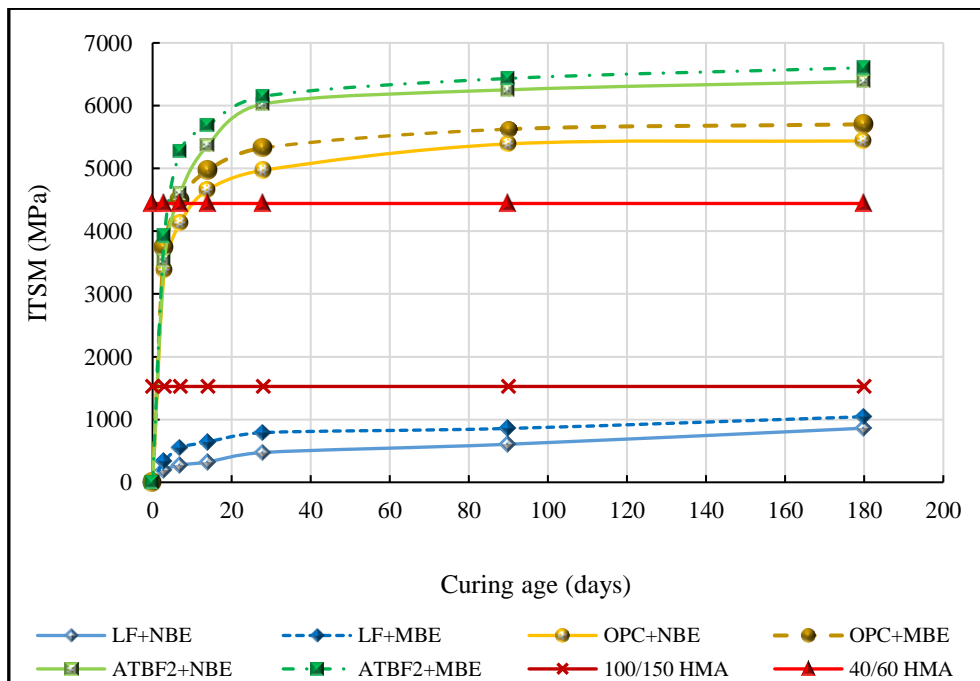


Figure 8.6: ITSM values of CBEM-ATBF2 containing MBE at different curing times

8.5 Water sensitivity

Water, or moisture damage, can be defined as the loss of strength in an asphalt pavement due to the influence of moisture which can be assessed by the loss of mechanical properties in asphalt mixtures (Little and Jones). Water is considered to be one of the most damaging factors to asphalt pavements because it has a negative impact on pavement performance. Moisture damage can cause different types of pavement distresses such as stripping, potholes, and ravelling. This usually occurs through the loss of adhesion between the asphalt and aggregate and a loss of cohesion within the asphalt binder (Souliman et al, 2015).

Conventional CBEMs containing LF are more sensitive to moisture than traditional asphalt mixtures due to the presence of trapped water in the coated aggregate (Ling et al, 2016). This is considered to be a major difficulty, limiting the application of conventional CBEM as an alternative to HMA in the field. There are two sources of water in conventional CBEMs: pre-wetting water and water already in the bitumen emulsion. In both cases, the water slowly evaporates with curing time; this affects the mixture's physical and mechanical response in two ways: 1) when the water within the binder film evaporates, the mixture starts to shrink and its density reduces, and 2) when water is trapped between aggregates, air voids are created (Swiertz et al, 2012). As a direct result of incomplete coating, bonding and residual moisture within the mixture, the sensitivity of conventional CBEM to moisture is a critical, premature distress.

In this section, water sensitivity for the CBEMs and the HMA used in this research, were evaluated in terms of stiffness modulus ratio (SMR) in accordance with BS EN 12697-12 (European Committee for Standardization, 2018c), which was described in detail in Chapter 3 (section 3.3.3.2). The effect caused by exposure of the CBEMs to subsurface water, is simulated by exposure to moisture using vacuum saturation (Asphalt Institute, 1989). This

method has been used successfully by previous researchers (Al Nageim et al, 2012; Al-Hdabi et al, 2014a; Dulaimi et al, 2016c; Nassar, 2016).

8.5.1 Results and Discussion

The results of water impact on the performance of CBEM-LF, CBEM-OPC, CBEM-TBF2 and CBEM-ATBF2, along with the two traditional hot mixes, are shown in Figure 8.7. All CBEMs were manufactured using NBE. It is clear that the CBEM-LF has the lowest SMR value, approximately 63%, compared to the other mixtures. This is due to the application of vacuum pressure and saturation of the CBEM-LF mixture with water at 40°C, creating a considerable reduction in the stiffness of this mixture. Therefore, conventional CBEM-LF has low resistance to water damage.

The same figure also shows that, the incorporation of OPC in CBEM enhances its performance against water damage, the mixture revealing a very small reduction in ITSM with 99% SMR. This SMR value is comparable to those of both hot mixes, 91% and 96% for 100/150 HMA and 40/60 HMA, respectively. The enhancement in performance of the conditioned samples in the CBEM-OPC mixture is attributed to the hydration process and the formation of a secondary cementitious binder, as shown and explained in Chapter 4 (section 4.5.2).

The ITSM values for the CBEM-TBF2 and CBEM-ATBF2, are also shown in Figure 8.7. CBEM-TBF2 and CBEM-ATBF2 developed substantial water resistance compared to conventional CBEM-LF, CBEM-OPC, 100/150 HMA and 40/60 HMA. Both mixtures have SMR values greater than 100%, CBEM-ATBF2 having the highest SMR (110%) overall.

In conclusion, CBEM-TBF2, CBEM-ATBF2 and CBEM-OPC are less sensitive to water damage and comply with the required ITSM performance recommended by Al-Busaltan et al (2012) and Dulaimi et al (2016b). Higher SMR values reflect the ability of these mixtures to

maintain their strength after exposure to moisture; this is attributed to the development of new hydration products as a result of pozzolanic and cementitious reactivity, as demonstrated in Chapter 7 (section 7.3). A high soaking water temperature (40°C) accelerated the hydration process for these mixtures (Dulaimi, 2017).

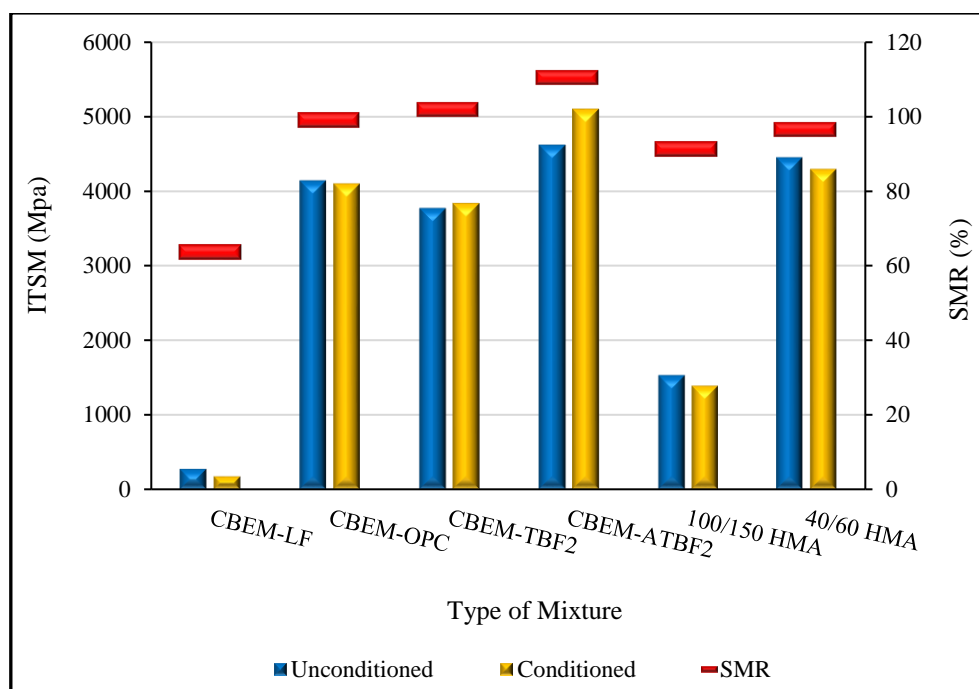


Figure 8.7: Water sensitivity results for the control and developed mixtures which included NBE

The resistance to water damage for the same mixtures but made with MBE, are given in Figure 8.8. There is a slight improvement of around 5% in the SMR for CBEM-LF with MBE, compared with the SMR for same mixture containing NBE. Nevertheless, the other mixtures i.e. CBEM-TBF2, CBEM-ATBF2 and CBEM-OPC, maintain their high resistance to water damage when replacing the NBE by MBE. This indicates that MBE made by ultrasound technology created no barriers to resistance to water damage for the CBEMs in terms of SMR values.

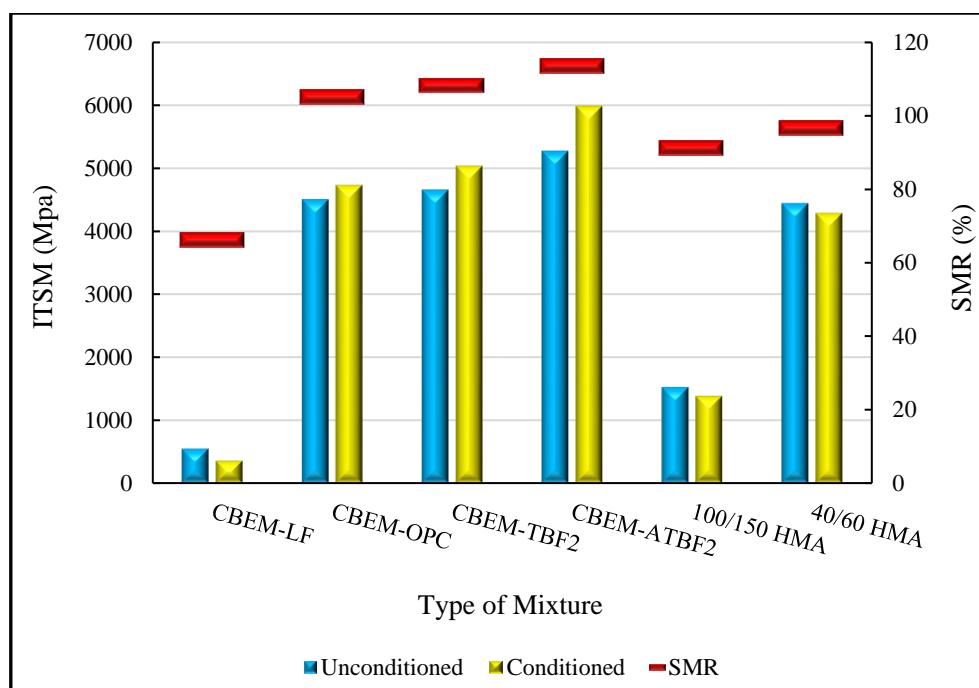


Figure 8.8: Water sensitivity results for the control and developed mixtures which included MBE

8.6 Long Term Age Hardening

The ageing of a bitumen binder occurs during the production of asphalt mixtures and while in service, when exposed to the surrounding environment. In general, bitumen ageing takes place in two stages; short term ageing which is associated with a loss of volatile components in asphalt at high temperature during mixing, storage and laying, and long term ageing which occurs as a result of progressive oxidation of in situ material in the field, this at a relatively low temperature, over a longer duration (Das, 2014). Both factors lead to an increase in the viscosity of the asphalt and consequent stiffening of the mixture (Bell, 1989). This in turn, causes the mixture to become excessively hard and brittle and susceptible to disintegration and cracking failures.

Ageing reduces the ductility and penetration of the bitumen while increasing the softening point and ignition temperature, as demonstrated by Siddiqui and Ali (1999). Sirin et al (2017) stated

that 5 years of field ageing in Middle East conditions causes a tenfold increase in the viscosity of bitumen binders.

Short term ageing is not investigated with CBEMs as no heating is applied during the preparation and construction phases. As such, only long term ageing was investigated using the method proposed by the Strategy Highway Research Program (SHRP) A-003A. This method was presented in detail in Chapter 3 (section 3.3.3.2).

8.6.1 Results and Discussion

To evaluate long term ageing, all mixtures in this chapter in addition to the two hot mix asphalts, were conditioned in an oven at 85°C for 5 days to simulate the age-hardening effect of 10 years prove this simulation. They were then subject to ITSM testing at 20°C, according to BS EN 12697-26 (European Committee for Standardization, 2018b).

Long term ageing was assessed in terms of SMR, the ratio between the average ITSM values for oven conditioned samples and the average ITSM values for samples cured at ambient temperature for 5 days. Figure 8.9 gives the ageing test results for CEBM-LF, CEBM-OPC, CEBM-TBF2 and CEBM-ATBF2, individually. All these mixtures were manufactured using NBE. This figure also shows the ageing results for 100/150 HMA and 40/60 HMA for comparison.

Several points can be drawn from the ageing test investigations:

1. All cold mixtures experienced a considerable improvement in ITSM values after ageing, compared to the corresponding HMA.
2. The conventional CEBM-LF achieved the highest SMR value, this reflecting a considerable improvement in the ITSM value after ageing (around 7 times), compared to the ITSM value before ageing. This improvement was a result of exposure to heating

at 85°C for 5 days. This assisted the evaporation of water and provided better cohesion properties thus providing better ageing ITSM results.

3. CBEM-ATBF2 showed the highest ITSM value after ageing (around 10642 MPa) compared to the other mixtures. This is attributed to the generation of hydration products covering more of the bitumen binder binding the aggregates, thereby preventing the loss of volatile components and oxidation (Dulaimi, 2017).

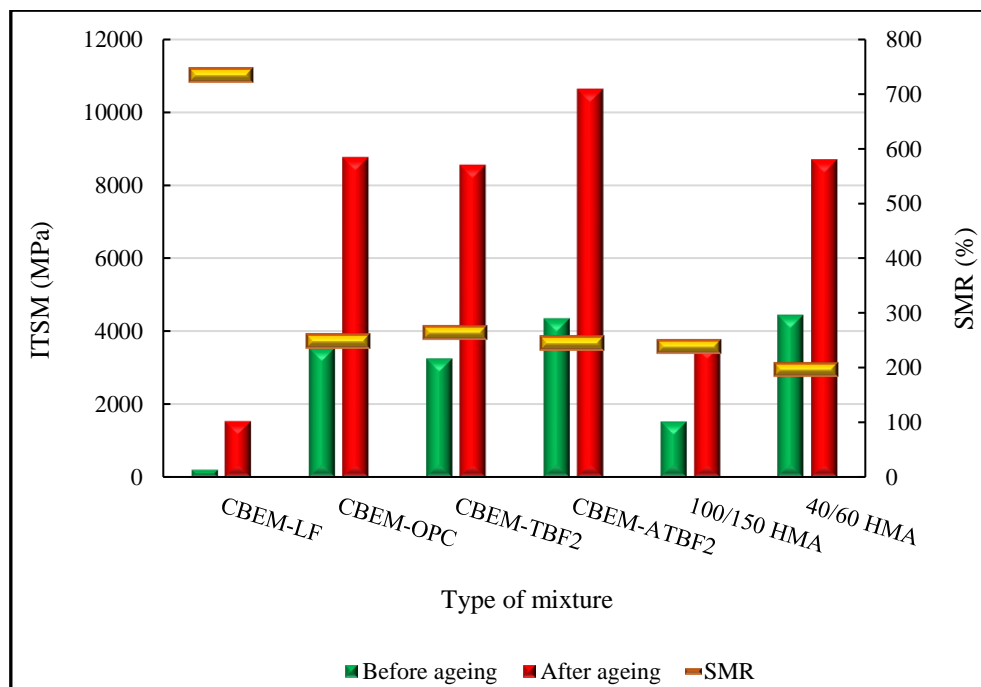


Figure 8.9: Effect of ageing on ITSM values for all CBEMs with NBE

The effect of ageing of the aforementioned mixtures made using the MBE is shown in Figure 8.10 which clearly shows outstanding enhancements in the ITSM values of all mixtures after ageing.

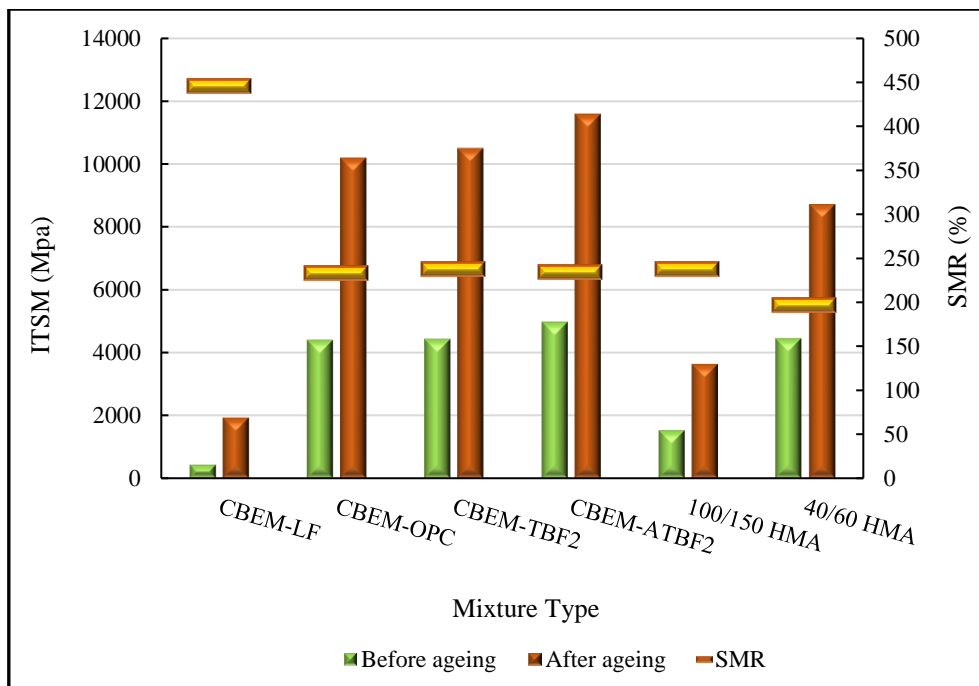


Figure 8.10: Effect of ageing on ITSM values for all CBEMs with MBE

In conclusion, and according to the above results, the new, fast curing, high ITSM CBEM-ATBF2 made from MBE using ultrasound technology, is considered by the author to be an appropriate material for use as a surface course layer, for major heavy trafficked roads and highways, due to its ability to reduce the loads transferred by traffic to the pavement foundation. This achievement also eliminates the limitations imposed by road engineers on conventional cold mixtures by reducing the curing time required to achieve full strength.

8.7 Summary

This chapter has resulted in several findings, namely:

- In general, all the developed mixtures, CBEM-BBF, CBEM-TBF2 and CBEM-ATBF2, in addition to the control CBEM-LF and CBEM-OPC mixtures, have shown a significant improvement in ITSM values when NBE is replaced by MBE.
- CBEM-ATBF2 containing MBE, achieved the highest ITSM value in both durability tests compared to all the other studied mixtures.
- All the developed CBEM mixtures containing normal and modified bitumen emulsions, had higher wet stiffness than dry stiffness. This was due to conditioning the samples in water at high temperatures, thereby creating a good environment to further activate hydration reactions.
- In terms of long term ageing, there was a reduction in SMR value (39%) for CBEM-LF made from MBE in comparison to the same mixture incorporating the NBE. There was also a considerable enhancement in the ITSM values for all the CBEM mixtures made from NBE and MBE, after ageing.
- According to the above, it can be stated that the new, fast curing, high performance CBEM, which contains a new cementitious filler and novel modified bitumen emulsion as a binder to the aggregate, gave outstanding results in terms of ITSM, water damage resistance and ageing susceptibility compared to the control CBEM-LF mixture and both HMAs. Accordingly, the newly developed mixture provides more economical, ecological and sustainable road surfacing materials.

The next chapter will investigate other mechanical properties of the newly developed mixture (CBEM-ATBF2) in terms of its resistance to permanent deformation and fatigue cracking.

Chapter 9: Deformation and Fatigue Resistance of the New CBEMs

9.1 Introduction

To further understand the behaviour of the new CBEM mixtures, permanent deformation and fatigue life have been investigated in this chapter. The resistance to permanent deformation was assessed using a wheel track test, while resistance to fatigue was evaluated using a four-point bending test. A full description of each test configuration, specimen preparation, results analyses and discussion are reported in detail below.

9.2 Resistance to Permanent Deformation (Wheel Track Test)

Asphalt pavement layers are subject to continuous flexing under traffic loads, this generating repeated stresses and strains (Nassar, 2016). Permanent deformation occurs in the pavement layer as a result of accumulated strain due to the increased tyre pressure, axle loads and time of loading, which subject the asphalt surfacing layers nearest the tyre-pavement contact area to increased stress. There are two major mechanisms of permanent deformation reported in the literature, namely: 1) densification due to the repeated loading, and 2) plastic shear deformation due to the repeated action of shear and tensile stresses (Taherkhani, 2006). The magnitude of pavement deformation is affected by the materials' properties, temperature, load level and loading time, as stated by Taherkhani (2006).

The permanent deformation of a mixture is influenced by the properties of bitumen and aggregate, the percentage of each in the mixture, compaction level and weather conditions. Bitumen grade, or hardness, is the main feature that protects the mixture from permanent deformation while aggregate gradation is considered one of the main factors affecting resistance to permanent deformation, as demonstrated by Oliver et al (1997). Aggregate

gradation is ranked in third place after binder content and temperature, according to a study conducted by Tarefder et al (2003). Brown and Cooper (1984) evaluated the rutting resistance for continuously graded and gap graded mixtures, finding that the former had a higher resistance than the latter at 30°C. Permanent deformation in asphalt layers on European roads, is the most common pavement degradation mode (ECFSTR, 1999) and as such, permanent deformation resistance has become one of the most important fundamental properties that should be assessed.

In this study, the resistance to permanent deformation for the control and new mixtures, was evaluated using a laboratory wheel tracking test as described in Chapter 3 (section 3.3.3.1). Tests of this nature have been used in many European countries to evaluate the rutting resistance of asphalt mixtures. They measure the rut created by the repeated passage of a wheel over an asphalt slab. The permanent deformation for CBEM-LF, CBEM-OPC and CBEM-ATBF2, was measured according to BS EN 12697-22 (European Committee for Standardization, 2003b). This test was carried out for all said mixtures made with normal bitumen emulsion (NBE) and modified bitumen emulsion (MBE). All the results were compared against the rutting resistance of the two control HMAs.

9.2.1 Test Configuration and Sample Preparation

Testing was conducted for each mixture at two different temperatures, 45°C and 60°C, for 10,000 load cycles, over a duration of 460 minutes. These two temperatures were selected according to PD 6691 (European Committee for Standardization, 2016b), in which 45°C represents moderate to heavily stressed sites requiring high rut resistance, 60°C representing very heavily stressed sites requiring very high rut resistance. The test was performed on a solid slab measuring 400 mm (length) × 305 mm (width) × 50 mm (thickness), made by compacting a loose bitumen mixture by means of a roller compactor at ambient temperature, as seen in

Figure 9.1. The samples were left in their moulds for 24 hours at room temperature, then cured for 14 days at 40°C in a ventilated oven to achieve completely cured conditions (Thanaya, 2003). The curing temperature needs to be lower than the bitumen softening point (50°C) to prevent the bitumen from ageing (Shanbara et al, 2018).

Prior to testing, each of the bituminous slab samples was conditioned at test temperature for at least 4 hours, after which a single wheel with a standard vehicle tyre pressure of 0.7 MPa, was applied on the top of the sample with a forward and backward motion at a frequency of 0.8 Hz. The vertical position of the wheel was mounted by means of an LVDT to record the progress of rutting in the sample over time.



Figure 9.1: Loose CBEM prior to compaction

9.2.2 Results and Discussion

9.2.2.1 Test Results at 45°C

The results of the wheel track test are shown in Figure 9.2 where the rutting depth has been plotted against the test time. The CBEM-LF with NBE has a higher rut depth than the other mixtures, this leading to deterioration of the slab sample. The rut depths for CBEM-LF, 100/150 HMA and 40/60 HMA, after 10,000 cycles were 5.1475 mm, 2.809 mm and 2.404 mm, respectively, as shown in Table 9.1. The inferior performance against rutting achieved by the CBEM-LF, makes use of this mixture as a pavement application inadvisable. However, the same mixture with ultrasound MBE, showed a better resistance to permanent deformation by about 10%.

Substituting LF with OPC in the conventional CBEM, gave a significant decrease in rut depth relative to conventional CBEM-LF and both HMA control mixtures. The accumulated rutting depth for CBEM-OPC decreased by approximately 82% compared to CBEM-LF, while the reduction was 66% and 61% compared to 100/150 HMA and 40/60 HMA, respectively. When replacing NBE with MBE in CBEM-OPC, the rutting depth reduced by about 7%. This improvement in rutting resistance demonstrates the positive effect of incorporating OPC in CBEM with regard to the hydration process as well as the effect of ultrasound technology on the performance of the bitumen emulsion.

A further reduction in rutting depth can be seen in the same figure when replacing OPC with the new cementitious filler. CBEM-ATBF2 has shown an increase in resistance to permanent deformation by about 89% compared with the rutting results of CBEM-LF, and 39% compared with CBEM-OPC. This mixture also has better resistance to permanent deformation in comparison to both 100/150 HMA and 40/60 HMA by approximately 80% and 76%, respectively. A substantial resistance to permanent deformation has been achieved by CBEM-

ATBF2. This can be attributed to the alkali media provided by the calcium carbide residue and waste alkali solution which increases the hydration process of the cementitious filler and generates a dense microstructure (Dulaimi, 2017). CBEM-ATBF2 has the lowest rutting depth compared to all other mixtures (0.472 mm) when MBE is incorporated. The rutting resistance was increased by approximately 16% compared to the same mixture with NBE.

Table 9.1 details the wheel track tests for all mixtures. The proportional rut depth (PRD_{AIR}) after 10,000 cycles at 45°C, has significantly decreased for the new mixtures. CBEM-ATBF2 with MBE as a replacement for NBE, showed high reductions of approximately 88%, 80% and 78% compared to CBEM-LF, 100/150 HMA and 40/60 HMA, respectively. The value of the wheel-tracking slope (WTS_{AIR}) for said mixture was also the lowest, relative to other studied mixtures.

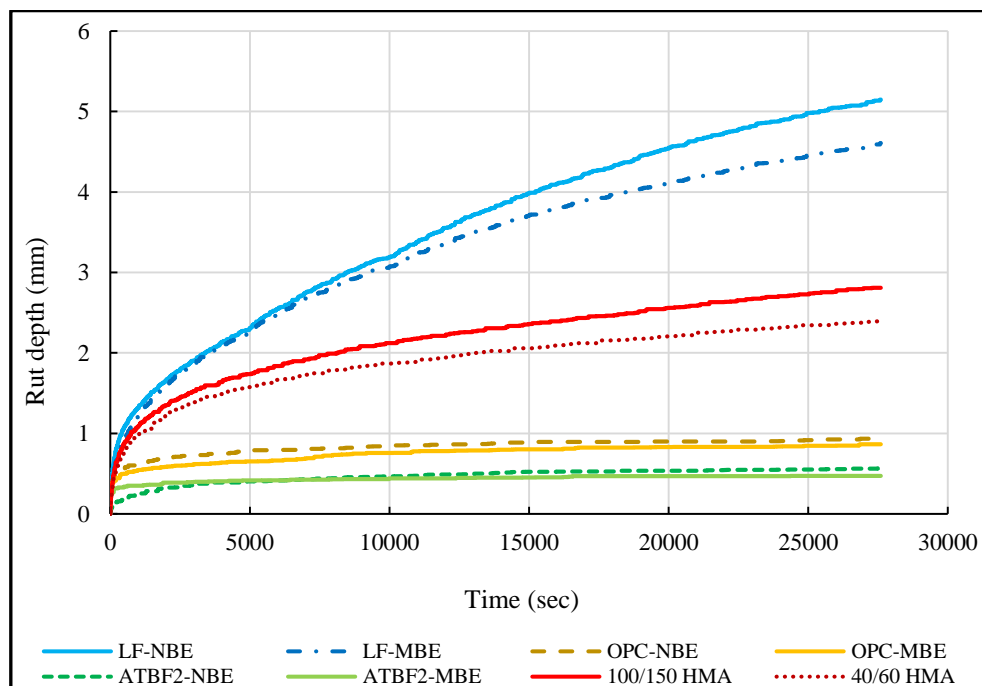


Figure 9.2: The rut depth of all CBEM and control HMA mixtures at 45°C

Table 9.1: Wheel track test results at 45°C

Mix type	Wheel track test results		
	WTS _{AIR} (mm/10 ³ cycle)	PRD _{AIR} (%)	Rut depth (mm)
<i>LF-NBE</i>	0.2659	10.295	5.1475
<i>LF-MBE</i>	0.2055	9.216	4.608
<i>OPC-NBE</i>	0.0118	1.868	0.934
<i>OPC-MBE</i>	0.0144	1.73	0.865
<i>ATBF2-NBE</i>	0.0112	1.13	0.565
<i>ATBF2-MBE</i>	0.0044	0.944	0.472
<i>100/150 HMA</i>	0.1004	5.618	2.809
<i>40/60 HMA</i>	0.076	4.808	2.404

9.2.2.2 Test Results at 60°C

Rutting is more pronounced in hot climate regions due to the significant impact of temperature on the viscosity of the bitumen, this being inversely related to rutting. Because of this, all mixtures investigated in this study were subjected to high temperatures (60°C) to investigate their suitability for use in very heavily stressed sites and hot climatic regions.

As can be seen from Figure 9.3, there was an increase in susceptibility to permanent deformation in CBEM-LF as the temperature increased. Most rutting occurred in the first 1,000 cycles under the wheel track load. This shows the poor performance of such mixtures in hot regions and its unsuitability for use in heavily trafficked roads. The same mixture had a reduced rut depth (9.925 mm) when manufactured with MBE in comparison to the conventional mix with NBE (10.811 mm), as shown in Table 9.2.

The same increase in rut depth at high temperature was noticed for all other mixtures. CBEM-OPC with NBE and MBE, achieved a rutting depth less than that of CBEM-LF with NBE by approximately 89% and 91%, respectively. Substantial reductions in rutting depths were recorded when CBEM-ATBF2 with NBE was tested, in that reductions were 93%, 91% and 84% compared to CBEM-LF with NBE, 100/150 HMA and 40/60 HMA, respectively. When MBE replaced NBE in the CBEM-ATBF2 mixture, a further reduction of approximately 12% was achieved compared to the same mix with NBE. The results of rut depth, PRD_{AIR} and WST_{AIR} , are shown in Table 9.2 confirming the better performance of CBEM-ATBF2 in comparison to all other mixtures in this study.

In summary, it can be concluded that CBEM treated with ATBF2 and MBE has considerably reduced susceptibility to permanent deformation at 45°C and 60°C, indicating the potential benefit of using this mixture as a surface road layer. It can also be stated that the enhancement in rutting resistance of said mixture can be due to the same reasons for ITSM improvements as discussed in Chapter 8 (section 8.4).

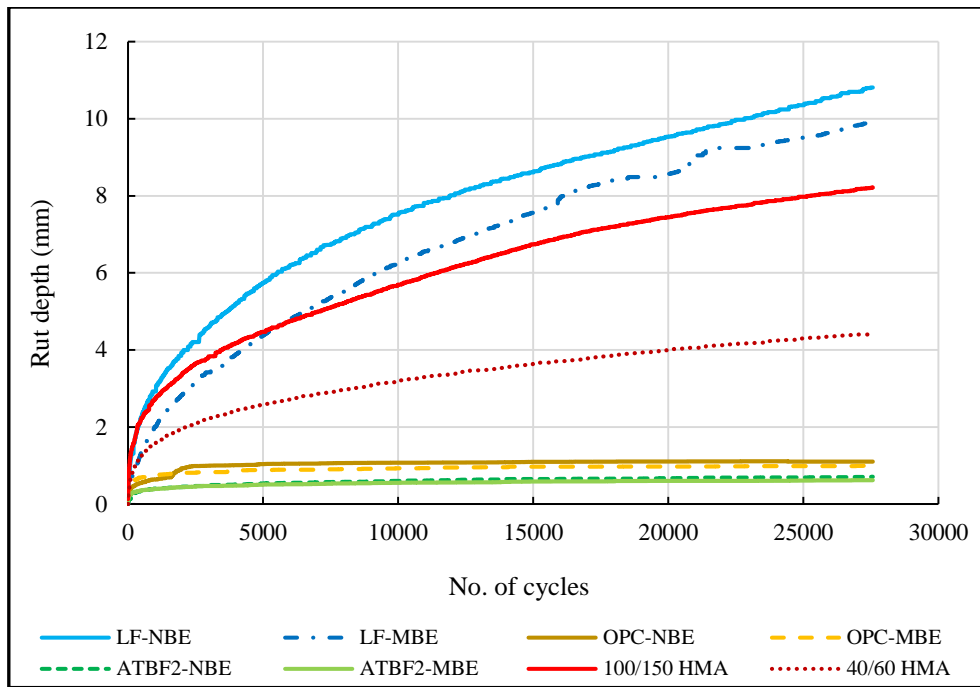


Figure 9.3: The rut depth of all developed and control mixtures at 60°C

Table 9.2: Wheel track test results at 60°C

Mix type	Wheel track test results		
	WTS _{AIR} (mm/10 ³ cycle)	PRD _{AIR} (%)	Rut depth (mm)
<i>LF-NBE</i>	0.4768	21.622	10.811
<i>LF-MBE</i>	0.5314	19.85	9.925
<i>OPC-NBE</i>	0.0034	2.200	1.1
<i>OPC-MBE</i>	0.0076	1.984	0.992
<i>ATBF2-NBE</i>	0.0144	1.414	0.707
<i>ATBF2-MBE</i>	0.0103	1.235	0.6175
<i>100/150 HMA</i>	0.3427	16.435	8.2175
<i>40/60 HMA</i>	0.179	8.854	4.427

9.3 Resistance to Fatigue (Four-point Bending Test)

Fatigue resistance of an asphalt mixture may be described as its ability to withstand repeated loading without fracturing. Fatigue cracking is traditionally considered to be one of the predominant distresses that occur in asphalt pavements, affecting its serviceability. There are many factors affecting the fatigue behaviour of asphalt mixtures such as the method of compaction, type and mode of loading, rest periods, material characteristics and environmental variables such as temperature, ageing and healing (Maggiore, 2014). Hu et al (2016) stated that temperature and initial air voids have a significant impact on fatigue performance, an increase in temperature negatively impacting fatigue performance. It appears that the stiffness of the mixture is strongly linked to its fatigue resistance, as mixtures with higher stiffness have a longer fatigue life when tested in stress control mode, as demonstrated by Pell (1973). Thanaya (2003), also reported that aggregate gradation has a substantial effect on fatigue life. Asphalt mixtures with finer gradations were found to perform better than those with coarser gradations.

In this study, the fatigue performance for all optimised and control mixtures was evaluated using a four-point bending test, as described in Chapter 3 (subsection 3.3.3.1), in accordance with standard BS EN 12697-24 (European Committee for Standardization, 2018d).

9.3.1 Test Configuration and Sample Preparation

Fatigue testing can be conducted using two different control modes: constant stress which is appropriate for a thick pavement layer (greater than 150 mm), and constant strain which is usually used to represent the response of thin layers (Huang, 1993). In the controlled stress mode, the applied stress remains unchanged while the strain increases with load repetitions. In the controlled strain mode, the applied strain is constant, the load decreasing with an increasing number of repetitions (Kuna, 2015).

Fatigue life can be investigated using different methods as noted in BS EN 12697-24 (European Committee for Standardization, 2018d) namely, bending tests and indirect tests. The former includes a two-point bending test on trapezoidal samples and prismatic samples, and three-point and four-point bending tests on prismatic samples, while the latter is represented by an indirect tensile test on cylindrical samples. The four-point bending test has been used by researchers to investigate the fatigue characteristics for bituminous mixtures because it simulates pavement failure realistically in terms of fatigue under traffic loading, as repeated loading leads to tension at the bottom of the sample (Maggiore, 2014).

Fatigue life is a key parameter used to describe the fatigue behaviour of an asphalt mixture; different approaches are used to define this. In the controlled strain mode, fatigue is considered to occur when the stiffness modulus reduces to 50% of its initial value, while for the controlled stress mode, a reduction of 10% in the initial stiffness modulus indicates its fatigue life.

Thanaya (2003) reported that fatigue cracking in asphalt mixtures usually occurs when the tensile strain falls between 30 and 200 microstrain. The strain levels in a pavement structure are likely to be below 200 microstrain, the actual value depending on several variables such as the type of mixture, subgrade and layer thickness and load, as stated by Brown and Needham (2000).

In the current study, a four-point bending (4PB) test was used to assess the fatigue characteristics of all the CBEMs and HMA mixtures in a controlled strain mode; fatigue life was specified as the number of cycles applied until the stiffness modulus reached 50% of its initial value. The 4PB test involves the application of a continuous sinusoidal waveform at the top of a prismatic sample by means of two load points (inner clamps). The prismatic samples were produced by cutting slabs of CBEM-LF, CBEM-OPC and CBEM-ATBF2 with NBE and MBE, and both bitumen grade asphalt concrete mixes. All slabs were produced, compacted

and cured following the approach used by Thanaya (2003). Each slab was cut into five specimens with dimensions 400 mm (length) × 50 mm (width) × 50 mm (thickness), trimmed and placed on a flat surface at lab temperature before testing.

9.3.2 Results and Discussion

Fatigue performance of all cold mixtures with NBE and MBE, i.e. CBEM-LF, CBEM-OPC and CBEM-ATBF2, along with the two hot asphalt mixtures, was evaluated using 4PB, as described earlier. The test was performed in a strain control mode under microstrains of 100, 125 and 150 at $20\pm 1^\circ\text{C}$ and a frequency of 10 Hz, as recommended by Read (1996) and Brown and Needham (2000). The fatigue life (N_f) for all mixtures is shown in Figure 9.4, based on 150 microstrain. From this figure, it can be seen that CBEM-LF with NBE has the lowest fatigue life (low fatigue resistance) compared to other mixtures, its poor resistance represented by low stiffness and high air voids. However, there was a 40% increment in fatigue resistance for this mixture when MBE was added, this indicating improvements in the cohesive characteristics of the mixture incorporating the sonicated emulsion.

Fatigue life increased substantially for CBEM treated with the developed SCF compared to the conventional cold and hot mixtures. Substitution of LF with ATBF2, extends fatigue life about 25, 2, 9 and 3 times greater than mixtures with LF, OPC, 100/150 HMA and 40/60 HMA, respectively. CBEM-ATBF2 with ultrasound MBE had an improvement in fatigue life of approximately 15% compared to the same mixture with NBE. This demonstrates that incorporating cementitious fillers significantly enhances fatigue resistance, the modified emulsion producing a cohesive mixture. The high performance of the developed mixture in terms of stiffness modulus described in Chapter 8 is resulted in high resistance to fatigue cracking of the said mixture.

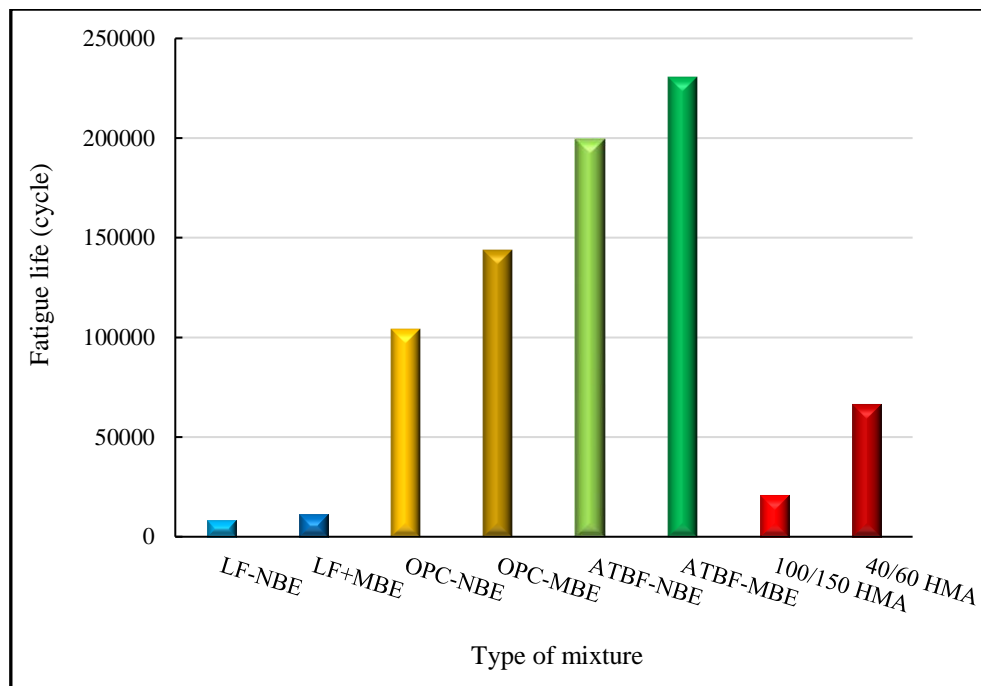


Figure 9.4: Fatigue performance for all cold and hot mixtures based on 150 micro-strain

The fatigue lines for CBEM-LF, CBEM-OPC and CBEM-ATBF2, with NBE or with MBE and both grades of HMA, are shown in Figure 9.5. The data for all mixtures were spread quite narrowly as R^2 was in the range of 0.9, as seen in Table 9.3. It can clearly be seen that CBEM-ATBF2 has the highest fatigue life of all the mixtures across all tensile strains.

Brown and Needham (2000) stated that the fatigue failure that might occur in a pavement structure is probably below 200 microstrain. Therefore, the results of this investigation show that CBEM-ATBF2 with ultrasound treated bitumen emulsion, considerably improves fatigue performance by extending fatigue life.

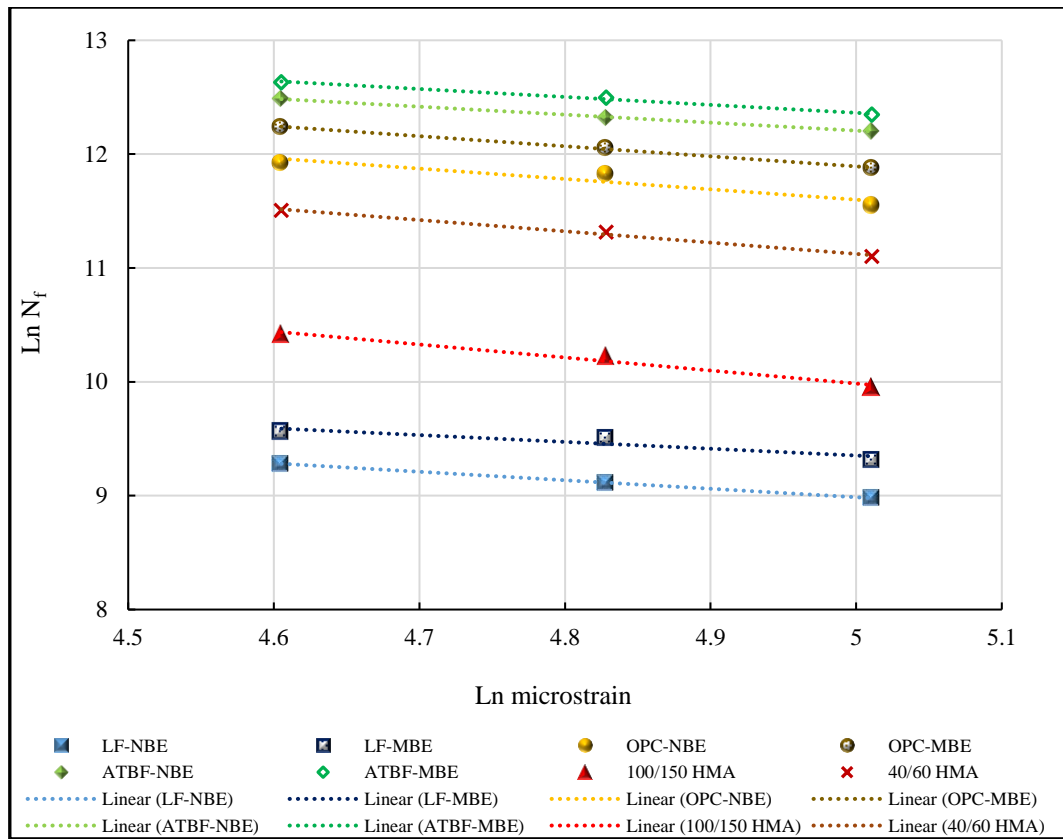


Figure 9.5: Fatigue line for all developed and control mixtures

Table 9.3: Fatigue equations for the developed and controlled mixtures

Type of Mixture	strain level (microstrain)	Fatigue life (N_f)	Fatigue life equation	Correlation Coefficient (R^2)
<i>LF-NBE</i>	100	10749	$y = -0.462x + 12.718$	0.9997
	125	9060		
	150	7945		
<i>LF-MBE</i>	100	14271	$y = -0.5987x + 12.346$	0.8802
	125	13458		
	150	11137		
<i>OPC-NBE</i>	100	151412	$y = -0.9106x + 16.153$	0.9014
	125	136864		
	150	103926		
<i>OPC-MBE</i>	100	206295	$y = -0.8852x + 16.318$	0.9973
	125	172005		
	150	143927		
<i>ATBF2-NBE</i>	100	265164	$y = -0.7023x + 15.718$	0.9967
	125	223616		
	150	199644		
<i>ATBF2-MBE</i>	100	306289	$y = -0.6976x + 15.851$	0.9927
	125	267516		
	150	230500		
<i>100/150 HMA</i>	100	33466	$y = -1.1431x + 15.701$	0.9776
	125	27500		
	150	20967		
<i>40/60 HMA</i>	100	99421	$y = -0.9932x + 16.09$	0.9929
	125	81954		
	150	66332		

9.4 Summary

In this chapter, the mechanical performance of the developed and the control mixtures was evaluated in terms of resistance to permanent deformation and resistance to fatigue cracking.

The following conclusions can be drawn:

- CBEM-LF performed poorly under wheel track testing after 10,000 cycles at 45°C and 60°C. A much better performance was given by CBEM containing ATBF2 and MBE against permanent deformation. This mixture is more resistant to rutting at both 45°C and 60°C as it develops a cohesive dense microstructure. As such, this mix is suitable for use in hot climates and heavily trafficked roads (this needs to be validated using site trials).
- The incorporation of ATBF2 and MBE in CBEM significantly enhances fatigue performance. It had a longer fatigue life under 4PB test at strains of 100, 125 and 150 microstrain, relative to conventional CBEM-LF and CBEM-OPC with both NBE and MBE and both grades of asphalt concrete. This improvement is attributed to the cohesive and better interlocking integral microstructure of the newly developed mixture, plus the generation of a rich binding paste in the hydration products.

Chapter 10: Environmental Investigation: Leaching of Heavy Metals into Water

10.1 Introduction

Potentially harmful metal contents are released into the environment through natural processes and anthropogenic activities like solid or liquid waste deposits, agricultural input and industrial wastes (Wilson and Pyatt, 2007). Such hazardous metals include nickel (Ni), copper (Cu), zinc (Zn), lead (Pb), cadmium (Cd), strontium (Sr) and chromium (Cr). The soil and sources of drinking water (e.g., surface water and underground water), are likely to be contaminated by heavy metals, this having consequences on food quality while also imposing a significant risk to humans. Although modest quantities of some heavy metals are necessary for human health, an excessive amount of these metals can cause chronic toxicity (U.S. Environmental Protection Agency (USEPA), 2015). Heavy metals from hazardous materials affect the main functions of the human body including kidneys, liver, heart, nervous system, immune system and joints. They also can hinder the absorption of other essential nutrients into the human body, something which is particularly problematic for children as this can seriously affect their development. Children exposed to heavy metals can suffer from memory impairments, learning disorders and behavioural problems (Askari, 2008). Heavy metals can also be toxic to plants and animals, if concentration levels increase.

Because pavement layers are continuously in direct contact with surface and underground water, the incorporation of waste and by-product materials in the manufacture of CBEMs can increase the risk of leaching hazardous metals into the surrounding soil and groundwater resources (Halim et al, 2003). As such, it is essential to inspect the concentrations of such heavy

metals in the waste materials used in this study. Accordingly, the Toxicity Characteristics Leaching Procedure (TCLP) test was used in this study to establish if the SSFA, FGD, CCR and waste alkaline solution are hazardous, individually and collectively, by virtue of their toxicity.

10.2 Toxicity Characteristics Leaching Procedure (TCLP) test

The Toxicity Characteristic Leaching Procedure (TCLP) test was established by USEPA to determine the mobility of both organic and inorganic analytes present in liquids (U.S. Environmental Protection Agency (USEPA), 1986). It is considered to be one of the most effective techniques used to investigate potential leaching of harmful metals into the environment (Xue et al, 2009; Modarres et al, 2015; Dulaimi et al, 2016a). Leaching is the mechanical or chemical percolation of waste constituents from stabilised layers in pavements to the surrounding environment by the passage of water or other solvents (Ling and Poon, 2014).

In this chapter, the TCLP test was carried out following the method recommended by the US Environmental Protection Agency (SW846-1311), to examine the potential for heavy metal leachate from the CBEMs treated by waste materials. The TCLP was first performed on the waste materials in a powder state, i.e. SSFA, FGD, CCR, BBF and TBF2 along with LF and OPC for comparison purposes. The test was also conducted on crushed samples of CBEM-TBF2 and CBEM-ATBF2. TCLP leachates were prepared by diluting 5.7 ml acetic acid with deionised water to a volume of 1 l. The pH of this fluid is 2.88 ± 0.05 when prepared. 10 grams of each sample were placed in an extractor vessel that already contained 200 ml of the TCLP leachant (Figure 10.1). A rotary extractor machine, seen in Figure 10.2, was used to agitate all the prepared samples at 30 ± 2 rpm for 18 ± 2 hours, at lab temperature. Following the extraction process, the solutions were filtered through a glass fibre filter, the filtrates then acidified to a

pH below 2, using acetic acid. Finally, the concentration of heavy metals was measured using an atomic adsorption spectrometer (type: Thermo, Model: ICE 3300), as seen in Figure 10.3.



Figure 10.1: Preparation of the TCLP samples



Figure 10.2: Rotary extractor machine



Figure 10.3: Atomic adsorption spectrometer

10.3 TCLP Results and Discussion

Table 10.1 presents the concentrations of heavy metals, Ni, Cu, Pb, Cd, Sr and Cr in the leachates. As can be seen, the concentration of zinc (Zn) in SSFA is higher than in other materials. However, this concentration is significantly reduced when SSFA is included in BBF and TBF2, dropping by approximately 77% in both fillers. It should be noted that all the heavy metals in SSFA are reduced when it is incorporated in BBF, TBF2, CBEM-TBF2 and CBEM-ATBF2 while concentrations of Ni, Cu and Cr are slightly higher than those in OPC and LF. According to EHSO (2016), the concentrations of the tested heavy metals in all materials and mixtures under study, met the standard limits required by set regulations.

In conclusion, the incorporation of the three waste materials used in this study, improved the performance properties of these mixtures, while decreasing the potentially harmful impact of these materials on the environment.

Table 10.1: Results of the TCLP test

Materials	Elements (mg/l)						
	Nickel (Ni)	Copper (Cu)	Lead (Pb)	Cadmium (Cd)	Zinc (Zn)	Strontium (Sr)	Chromium (Cr)
SSFA dust	0.0643	0.7580	0	0	1.2615	0	0.0393
FGD dust	0	0.0338	0	0	0.1971	0	0.0956
CCR dust	0	0.0049	0	0	0.0299	0	0.0907
BBF dust	0.0643	0.2160	0	0	0.2806	0	0.1988
TBF2 dust	0	0.1878	0	0	0.2937	0	0.0623
TBF2 mixture	0.0086	0.1704	0	0	0.2701	0	0
ATBF2 mixture	0.0056	0.1277	0	0	0.2777	0	0.0885
OPC	0	0	0.004	0.009	0.024	0.309	0.009
LF	0	0	0.006	0.012	0.307	0.253	0.003
TCLP regulatory level (EHSO, 2016)	25	25	5	1	25	-	5

10.4 Summary

The TCLP test was carried out to investigate the environmental impact of the waste materials used in production of the new CBEM. The environmental analysis of the three waste materials SSFA, FGD and CCR in the CBEMs revealed that these materials do not pose any threat to the environment. The concentration of heavy metals in the CBEM-TBF2, CBEM-ATBF2 and their raw state materials, were found to be less than the regulatory levels specified for hazardous materials, thereby satisfying the minimum requirements.

Chapter 11: Conclusions and Recommendations

11.1 Introduction

This study investigated improvements in the performance of cold bitumen emulsion mixtures (CBEMs) containing:

- i. A new bitumen emulsion modified using ultrasound technology;
- ii. A new secondary cementitious filler comprising a high volume of SSFA, OPC and CCR as a substitute for conventional LF; and
- iii. A waste alkali solution activator used as a replacement for pre-wetting water.

Characterisation of the newly developed mixture incorporating modified bitumen emulsion and the new cementitious filler, in terms of mechanical and durability properties, was conducted, supported by SEM and XRD investigation, to explain improvements in both the mechanical and durability properties of the developed CBEM.

This chapter summarises the main conclusions based on the findings obtained in this research and some recommendations for future studies.

11.2 Conclusions

11.2.1 CBEMs containing Limestone Filler and Ordinary Portland Cement

Several points can be concluded regarding the mechanical and durability properties of the CBEM containing conventional limestone filler (LF) and ordinary Portland cement (OPC):

1. The ITSM for CBEM-LF under normal curing conditions, was low in its early life but increased progressively with time due to an increase in the rate of water evaporation.

The development in ITSM value for this mixture mainly occurred during the first 28 days of curing.

2. The ITSM values of the CBEM-LF at all curing ages (3, 7, 14, 28, 90 and 180 days) are lower than the targeted ITSM values for 100/150 and 40/60 HMA due to the high air void contents created after most of the trapped water evaporated.
3. The conventional CBEM-LF has the lowest stiffness modulus ratio (SMR) compared to other mixtures indicating that this mixture is less resistant to moisture than the traditional hot asphalt mixtures due to the presence of trapped water in the mix.
4. Regarding long term age hardening, the ITSM value for CBEM-LF after ageing is substantially improved compared to its ITSM before ageing. This improvement is due to the evaporation of water as a result of heating at 85°C for 5 days.
5. The results of the wheel track test and four-point bending test for CBEM-LF revealed that this mixture has poor resistance to permanent deformation and fatigue cracking.
6. The use of OPC as a filler in CBEM to replace LF, significantly increases the ITSM value by approximately 17 times in comparison to conventional CBEM-LF after only 3 days. This mixture is also better than 100/150 HMA by about 2 times at 3 days of age. This improvement is due to water consumption during the hydration process and formation of hydration products, working as a secondary binder beside the bitumen in the CBEM.
7. Rutting resistance, fatigue resistance, moisture damage resistance and long-term ageing all improved significantly in CBEM-OPC compared to CBEM-LF and HMA.

11.2.2 Modification of the Bitumen Emulsion

Ultrasound treatment of bitumen emulsion was investigated in Chapter 4 to determine the optimum treatment time required to achieve the best properties in terms of viscosity, particle size and particle size distribution. The indirect tensile stiffness modulus test was carried out to

evaluate the mechanical response of CBEM with sonicated bitumen emulsion, compared to the conventional mixture with normal bitumen emulsion. Based on the laboratory test results and analyses, the following conclusions can be drawn:

1. The ultrasonic technique is very effective in reducing bitumen droplet size and the viscosity of the bitumen emulsion. This is apparent between 5 and 15 minutes time of sonication. The reduction in the viscosity at 7 minutes treatment, was approximately 28% compared to the untreated sample. This indicates that within this duration, the samples experience a reduction in the solution shearing resistance.
2. As sonication time increases (more than 7 minutes), the viscosity of the bitumen emulsion also increases. This can be attributed to the recoalescence of bitumen droplets because of over-processing.
3. The optimum sonication time was found to be 7 minutes. This resulted in an approximate 85% reduction in D50, 86% reduction in D10 and 90% decrease in D90. The PSD curve also become closer to the mean value and more uniformly distributed.
4. CBEM-LF made from bitumen emulsion sonicated for 7 minutes, gave an outstanding improvement in ITSM over all curing times (3, 7, 14, 28, 90 and 180 days). There was an approximate 70% enhancement in ITSM at 3 days curing, compared with the mixture containing normal emulsion. This treatment time also upgraded the volumetric properties of the CBEM-LF by reducing air void contents by about 33% compared to conventional CBEM-LF.
5. A significant improvement in ITSM was also found in CBEM containing OPC and modified bitumen emulsion. After 3 days of curing, the ITSM was improved by around 11% compared with the same mixture containing conventional emulsion.

11.2.3 Development of the new CBEM containing the new Secondary Cementitious Filler

In this study, the use of different types of waste materials to develop a new secondary cementitious filler (SCF) as a replacement to traditional limestone filler and upgrade the characteristics of CBEM, has been accomplished. The new SCF consists of 6% BBF [4.2% SSFA ground with 5% FGD + 1.8% OPC] and 2% CCR by total weight of aggregate. The new CBEM, as described in Chapter 6, is made with 3% alkali solution instead of pre-wetting water. The conclusions relating to the main findings of the new filler and the new cold asphalt mixture are as follows:

1. Chemical analysis of the SSFA showed a significant silica content, indicating its expected performance as a pozzolanic material. Grinding activation with 5% FGD was found to increase the fineness and pozzolanic reactivity of SSFA. This improvement is due to the activation of the pozzolanic properties of SSFA particles by breaking the glassy phases of non-amorphous silica and increasing the surface area of the particles.
2. The chemical analysis of CCR revealed that this material is extremely rich in calcium oxide (CaO) in a hydrated state $\text{Ca}(\text{OH})_2$, which was found to be vital for the development of new cementitious materials.
3. The development process of the new SCF indicated that the best performance of the CBEM in terms of ITSM, was achieved by blending 6% BBF with 2% CCR as an extra additive to generate TBF2. CBEM-TBF2 achieved a 13-fold increase in ITSM in comparison to CBEM-LF. This improvement was due to an increase in hydration products, achieved by adding CCR to CBEM-TBF2. As the curing time increased, additional cementitious binding materials were generated, leading to an increase in the absorption of trapped water as a result of the hydration process. This reduced the voids within CBEM-TBF2, producing a high performance CBEM mixture.

4. The creation of a high alkali environment to activate TBF2, was achieved by using waste calcium hydroxide solution as an alkali activator to increase the hydraulic reactivity of the cementitious components and accelerate the hydration process.
5. The ITSM for CBEM-ATBF2 increased more than 18 times at just 3 days of normal curing, compared to CBEM-LF. This enhancement is due to the continuous hydration of the SCF within the mixture, therefore more water is absorbed. The increase in the coalescence rate of the bitumen emulsion was due to an increase in the pH value of the liquid within the CBEM-ATBF2.
6. CBEM-ATBF2, in terms of ITSM, has considerably lower temperature susceptibility compared to CBEM-LF and the two grades of hot asphalt mixtures. As such, this mixture experienced less rutting in hot climatic conditions compared to the 100/150 and 40/60 hot asphalt mixtures. It also experienced the lowest rate of water loss as most of the trapped water was absorbed by the SCF and consumed during the hydration process.
7. The water sensitivity of CBEM was substantially improved when replacing LF with the new ATBF2. Its water sensitivity, measured by means of SMR, was approximately 2 times that of the CBEM-LF. In addition, the ITSM for the conditioned samples was higher than the unconditioned samples with an SMR of over 100%.
8. The environmental investigations for SSFA, FGD, CCR and their blends in the CBEMs by means of TCLP testing, revealed that there is no detrimental effect on the surrounding environment as heavy metal leaching is less than the specified limits determined for hazardous materials by Environmental Health & Safety Online (EHSO). Therefore, the aforementioned waste materials can be considered non-hazardous materials. This will help promote their use in pavements and construction.

9. The reasons for the improvements in the mechanical and durability performance of CBEM-ATBF2 have been explained by carrying out SEM and XRD analyses. SEM observations at different curing ages, revealed the formation of hydration products such as ettringite, portlandite (CH) and calcium silicate hydrate (CSH) gel. These products are responsible for building up a dense microstructure and help, along with the bitumen binder, to improve the mechanical strength and durability of the mixture.
10. XRD analysis proves the abovementioned formation of hydration products during curing of CBEM-ATBF2 paste. This was found to be in agreement with SEM analysis.

11.2.4 Development of Novel High Performance CBEM including the New Secondary Cementitious Filler and the Modified Bitumen Emulsion using Ultrasound Technology

A novel, fast curing, high quality and environmentally friendly cold bitumen emulsion mixture, for use as a surface course in road pavements, was developed at Liverpool Centre for Material Technology (LCMT). This new mixture provides sustainable benefits by being an eco friendly, energy and cost effective mixture. The following key conclusions can be drawn:

1. A significant enhancement was achieved in ITSM at both early and mature ages because of the addition of MBE and ATBF2 as replacements of conventional bitumen emulsion and limestone filler. After 3 days, the ITSM of the tested mixtures increased approximately 19 times compared to conventional CBEM-LF, and 2.5 times the ITSM for traditional 100/150 HMA. This improvement was because of the use of the new modified emulsion with smaller bitumen droplets which provide a greater surface area and more even coating on aggregate particles. This helped form a cohesive mixture in parallel with the hydration products which resulted from the hydration process of the SCF in the presence of water, within the bitumen-water solution. This outstanding

performance reduces the long curing time required to achieve ultimate strength in the case of conventional CBEMs, to less than 3 days.

2. In terms of the durability of CBEM-ATBF2, when mixed with MBE, this mix showed less sensitivity to water damage. The ITSM values for conditioned samples of the mixture improved giving an SMR value above 100%. Its resistance to water damage is almost 78% better than the values for conventional CBEM-LF. This is also better than those for both grades of hot asphalt mixtures.
3. Regarding long term ageing testing, the results revealed a promising performance for CBEM containing ATBF2 and modified emulsion. The performance of CBEM-ATBF2 with MBE is outstanding and comparable to that of the traditional hot mixtures. This mixture had the highest ITSM value after ageing (around 11595 MPa) compared to the other mixtures. This is due to hydration products covering more of the bitumen binder, resulting in the prevention of the loss of volatile components and oxidations.
4. The resistance of CBEM-ATBF2 containing MBE to permanent deformation is excellent. This mixture offered reduced rutting under wheel track testing at both 45°C and 60°C in comparison to conventional CBEM-LF. Its permanent deformation resistance was more than that of both the hot asphalt surface course mixtures. Therefore, this mixture can be used in heavily trafficked roads and in hot climatic regions. This improvement in rutting resistance for the CBEM-ATBF2 mixture can be explained in the same way as that detailed in this thesis for improvements in ITSM.
5. The fatigue resistance of the CBEM-ATBF2 containing MBE, has substantially improved. This mixture prolonged fatigue life to about 29 times that of conventional CBEM-LF at 150 microstrain. Its fatigue life is almost 11 and 3 times greater than 100/150 HMA and 40/60 HMA, respectively.

Overall, it can be stated that by developing the CBEM-ATBF2 with MBE, the aim of this research work has been achieved, this new mixture offering significant sustainable benefits in comparison to HMA including i) a reduction in the problems associated with carbon emissions during production and application processes, ii) an upgrade, for the first time worldwide, in the physical characteristics of the bitumen emulsion through the use of ultrasound technology. This will open a new gateway for future research which aims to further develop bitumen emulsions and the products associated with the new asphalt binder, iii) the use of a new secondary cementitious filler made from waste materials, will reduce the need for cement and will contribute to reductions in the cost and carbon footprint related to cement production, iv) the use of waste materials in high volumes i.e. SSFA, will reduce the impact on landfills, and v) the use of this CBEM-ATBF2 novel high performance mixture will help eliminate the restrictions imposed by road engineers on the use of conventional CBEM in surface course layers for heavy trafficked roads.

11.3 Recommendations for Future Works

Based on the findings reported in this thesis, the following work can be suggested:

1. For the first time, this research has improved cationic bitumen emulsion through the use of ultrasound technology, and has specified its characteristics such as viscosity, PS and PSD. Further research work is required on i) short and long term storage stability, and ii) its shear properties in terms of cohesion and angle of internal friction.
2. In the current study, ultrasonic modification has been applied on a pre-prepared cationic bitumen emulsion. It is recommended to use the new ultrasound technology in the production of bitumen emulsion. The type and amount of emulsifier, and bitumen type and content can be included in suggested studies.

3. A new study can consider the influence of the new cementitious filler on the optimum bitumen emulsion content and pre-wetting water content on CBEM mechanical and durability properties.
4. Since the outcomes of this research are from laboratory investigations, it is highly recommended to carry out road/field site trials to investigate and monitor the performance of the new CBEM and compare this with the laboratory results.
5. It is recommended to extend the evaluation of the other properties of the newly developed CBEM by conducting other laboratory tests such as resistance to ravelling, crack propagation, stripping test and skid resistance.
6. To increase the sustainability and the cost effectiveness of the new CBEM, further studies can be undertaken to investigate the incorporation of reclaimed asphalt pavement (RAP) in the CBEM containing the new cementitious filler and sonicated bitumen emulsion, in terms of mechanical and durability properties.
7. Although the effect of different curing temperatures on moisture loss has been studied in this research, an investigation on the microstructure of the new CBEM at various curing temperatures is recommended.
8. The traditional curing method with different curing temperatures, was used in this study. Trials with different heating techniques such as microwave, infrared heating and vacuuming treatment would be useful to investigate their effect on the performance of the modified bitumen emulsion and the newly developed CBEM.
9. To determine the cost effectiveness of the new cementitious filler as a replacement for conventional limestone filler and/or ordinary Portland cement, an economic study is recommended.

References

- Abtahi, S.M., Sheikhzadeh, M. and Hejazi, S.M. (2010) Fiber-reinforced asphalt-concrete—a review. *Construction and Building Materials*, 24 (6), 871-877.
- Aïtcin, P.C. (2016) 3 - Portland cement. In: Aïtcin, P.-C. and Flatt, R. J. (ed.) *Science and Technology of Concrete Admixtures*. Woodhead Publishing. pp. 27-51.
- Akzo Nobel. (2008) *Bitumen emulsion* [online]. Available at: <https://surfacechemistry.nouryon.com/siteassets/pdfs/brochure-Asphalt-Emulsion-English.pdf> [Accessed: 23/09/2018]
- Al-Busaltan, S. (2012) Development of New Cold Bituminous Mixtures for Road and Highway Pavements. *School of Built Environment*.
- Al-Busaltan, S., Al Nageim, H., Atherton, W. and Sharples, G. (2012) Mechanical properties of an upgrading cold-mix asphalt using waste materials. *Journal of materials in civil engineering*, 24 (12), 1484-1491.
- Al-Hdabi, A. (2014) *High strength cold rolled asphalt surface course mixture*thesis, Liverpool John Moores University.
- Al-Hdabi, A., Al Nageim, H., Ruddock, F. and Seton, L. (2013) Development of sustainable cold rolled surface course asphalt mixtures using waste fly ash and silica fume. *Journal of materials in civil engineering*, 26 (3), 536-543.
- Al-Hdabi, A., Al Nageim, H. and Seton, L. (2014a) Performance of gap graded cold asphalt containing cement treated filler. *Construction and Building Materials*, 69, 362-369.
- Al-Hdabi, A., Al Nageim, H. and Seton, L. (2014b) Superior cold rolled asphalt mixtures using supplementary cementations materials. *Construction and Building Materials*, 64, 95-102.
- Al Nageim, H., Al-Busaltan, S.F., Atherton, W. and Sharples, G. (2012) A comparative study for improving the mechanical properties of cold bituminous emulsion mixtures with cement and waste materials. *Construction and Building Materials*, 36, 743-748.
- Alizadeh, R.A. (2009) *Nanostructure and engineering properties of basic and modified calcium-silicate-hydrate systems*thesis, University of Ottawa (Canada).
- Amani, A., York, P., Chrystyn, H. and Clark, B.J. (2010) Factors affecting the stability of nanoemulsions—use of artificial neural networks. *Pharmaceutical research*, 27 (1), 37.
- Askari, H.M. (2008) *Studies of leaching, recovery and recycling of heavy metal*thesis, Brunel University Institute for the Environment PhD Theses.
- Asphalt Institute (1989) Asphalt Cold Mix Manual, Manual Series No. 14 (MS-14). *3rd Edition*, Lexington, Kentucky 4, USA.
- Asphalt Institute (2008) A Basic Asphalt Emulsion, Manual Series No. 19 (MS-19). *Inc., Lexington, Kentucky, USA*.

- Aydın, S., Karatay, Ç. and Baradan, B. (2010) The effect of grinding process on mechanical properties and alkali–silica reaction resistance of fly ash incorporated cement mortars. *Powder technology*, 197 (1-2), 68-72.
- Bakharev, T., Sanjayan, J.G. and Cheng, Y.-B. (1999) Alkali activation of Australian slag cements. *Cement and Concrete Research*, 29 (1), 113-120.
- Ban, C.C. and Ramli, M. (2010) Optimization of mix proportion of high performance mortar for structural applications. *Am. J. Engg. & Applied Sci*, 3 (4), 643-649.
- Baumgardner, G.L. (2006) Asphalt emulsion manufacturing today and tomorrow. *Asphalt Emulsion Technology*, 16-25.
- Beckman, C. (2016) *LS TM 13 320 MW laser diffraction particle size analyzer* [online] Available . [Accessed: 11/03/2018]
- Bell, C.A. (1989) *Summary report on aging of asphalt-aggregate systems*.
- Bermúdez-Aguirre, D., Mobbs, T. and Barbosa-Cánovas, G.V. (2011) Ultrasound Applications in Food Processing. In: (ed.) *Ultrasound Technologies for Food and Bioprocessing*. pp. 65-105.
- Bocci, M., Grilli, A., Cardone, F. and Graziani, A. (2011) A study on the mechanical behaviour of cement–bitumen treated materials. *Construction and Building Materials*, 25 (2), 773-778.
- Bocci, M., Virgili, A. and Colagrande, S. (2002) A study of the Mechanical Characteristics of Cold Recycled Bituminous Concretes. *PROCEEDINGS OF THE 4TH EUROPEAN SYMPOSIUM ON PERFORMANCE OF BITUMINOUS AND HYDRAULIC MATERIALS IN PAVEMENTS, BITMAT 4, 11-12 APRIL 2002, NOTTINGHAM, UK* of Conference.
- Bodin, D., Grenfell, J.R. and Collop, A.C. (2009) Comparison of small and large scale wheel tracking devices. *Road Materials and Pavement Design*, 10 (sup1), 295-325.
- Boussad, N. and Martin, T. (1996) Emulsifier content in water phase and particle size distribution: Two key-parameters for the management of bituminous emulsion performance. *EURASPHALT & EUROBITUME CONGRESS, STRASBOURG, 7-10 MAY 1996. VOLUME 3. PAPER E&E. 6.159* of Conference.
- Brouwers, H. (2006) Erratum: Particle-size distribution and packing fraction of geometric random packings [Phys. Rev. E 74, 031309 (2006)]. *Physical Review E*, 74 (6), 069901.
- Brown, S. and Cooper, K. (1984) The mechanical properties of bituminous materials for road bases and basecourses (with discussion). *Association of Asphalt Paving Technologists Proceedings* of Conference.
- Brown, S. and Needham, D. (2000) A study of cement modified bitumen emulsion mixtures. *Asphalt Paving Technology*, 69, 92-121.
- Canselier, J., Delmas, H., Wilhelm, A. and Abismail, B. (2002) Ultrasound emulsification—an overview. *Journal of Dispersion Science and Technology*, 23 (1-3), 333-349.
- Capitão, S., Picado-Santos, L. and Martinho, F. (2012) Pavement engineering materials: Review on the use of warm-mix asphalt. *Construction and Building Materials*, 36, 1016-1024.
- Cardone, F., Grilli, A., Bocci, M. and Graziani, A. (2015) Curing and temperature sensitivity of cement–bitumen treated materials. *International Journal of Pavement Engineering*, 16 (10), 868-880.

- Chalothorn, K. and Warisnoicharoen, W. (2012) Ultrasonic emulsification of whey protein isolate-stabilized nanoemulsions containing omega-3 oil from plant seed. *Am J Food Technol*, 7, 532-541.
- Chatterjee, A. (2001) 8-X-ray diffraction. *Handbook of analytical techniques in concrete science and technology*. Norwich (NY): William Andrew Publishing, 275-332.
- Chauhan, S.K., Sharma, S., Shukla, A. and Gangopadhyay, S. (2010) Recent trends of the emission characteristics from the road construction industry. *Environmental Science and Pollution Research*, 17 (9), 1493-1501.
- Chavez-Valencia, L., Alonso, E., Manzano, A., Pérez, J., Contreras, M. and Signoret, C. (2007) Improving the compressive strengths of cold-mix asphalt using asphalt emulsion modified by polyvinyl acetate. *Construction and Building Materials*, 21 (3), 583-589.
- Chen, M., Blanc, D., Gautier, M., Mehu, J. and Gourdon, R. (2013) Environmental and technical assessments of the potential utilization of sewage sludge ashes (SSAs) as secondary raw materials in construction. *Waste management*, 33 (5), 1268-1275.
- Comrie, D.C. and Kriven, W.M. (2006) Composite cold ceramic geopolymer in a refractory application. *Advances in Ceramic Matrix Composites IX*, 153, 211-225.
- Corroler, A.L. (2010) *The use of bitumen emulsion in Europe* [online]. Available at: <http://eapa.org/publications.php?c=73>. [Accessed: 14/01/2018]
- Cyr, M., Coutand, M. and Clastres, P. (2007) Technological and environmental behavior of sewage sludge ash (SSA) in cement-based materials. *Cement and Concrete Research*, 37 (8), 1278-1289.
- Das, A. (2008) Principles of bituminous pavement design and the recent trends. *Department of Civil Engineering, Indian Institute of Technology, Kanpur*.
- Das, P.K. (2014) *Ageing of asphalt mixtures: micro-scale and mixture morphology investigation* thesis, KTH Royal Institute of Technology.
- de S. Bueno, B., Da Silva, W.R., de Lima, D.C. and Minete, E. (2003) Engineering properties of fiber reinforced cold asphalt mixes. *Journal of Environmental Engineering*, 129 (10), 952-955.
- Dehghan, M. (2009) *Suspending process*. B.Sc. Thesis thesis, Islamic azad University.
- Deneuvillers, C. and Samanos, J. (2000) Relations between characteristics and properties of cationic bitumen emulsions. *Revue Generale des Routes* (780).
- Desrumaux, A. and Marcand, J. (2002) Formation of sunflower oil emulsions stabilized by whey proteins with high-pressure homogenization (up to 350 MPa): effect of pressure on emulsion characteristics. *International journal of food science & technology*, 37 (3), 263-269.
- Donatello, S., Tyrer, M. and Cheeseman, C. (2010) Comparison of test methods to assess pozzolanic activity. *Cement and Concrete Composites*, 32 (2), 121-127.
- Doyle, T.A., McNally, C., Gibney, A. and Tabaković, A. (2013) Developing maturity methods for the assessment of cold-mix bituminous materials. *Construction and Building Materials*, 38, 524-529.
- Du, S. (2015) Performance characteristic of cold recycled mixture with asphalt emulsion and chemical additives. *Advances in Materials Science and Engineering*, 2015.

- Dulaimi, A. (2017) *Development of a new cold binder course emulsion asphalt*thesis, Liverpool John Moores University.
- Dulaimi, A., Al Nageim, H., Hashim, K., Ruddock, F. and Seton, L. (2016a) Investigation into the stiffness improvement, microstructure and environmental impact of a novel fast-curing cold bituminous emulsion mixture. *Eurasphalt and Eurobitume Congress, European Asphalt Pavement Association (EAPA) and Eurobitume, Brussels, Belgium*of Conference.
- Dulaimi, A., Al Nageim, H., Ruddock, F. and Seton, L. (2016b) New cementitious material to use as a filler in a cold dense graded binder course mixture. *15th Annual International Conference Asphalt, Pavement Engineering and Infrastructure*,
- Dulaimi, A., Al Nageim, H., Ruddock, F. and Seton, L. (2016c) New developments with cold asphalt concrete binder course mixtures containing binary blended cementitious filler (BBCF). *Construction and Building Materials*, 124, 414-423.
- Dulaimi, A., Al Nageim, H., Ruddock, F. and Seton, L. (2017) High performance cold asphalt concrete mixture for binder course using alkali-activated binary blended cementitious filler. *Construction and Building Materials*, 141, 160-170.
- Ebels, L.-J. (2008) *Characterisation of material properties and behaviour of cold bituminous mixtures for road pavements*thesis, Stellenbosch: Stellenbosch University.
- ECFSTR, E.C.i.t.F.o.S.R. (1999) *COST 333: Development of New Bituminous Pavement Design Method: Final Report of the Action*. European Communities.
- EHSO. (2016) *The EPA TCLP: Toxicity characteristic leaching procedure and characteristic wastes (D-codes)* [online]. Available at: <http://www.ehso.com/cssepa/TCLP.htm>. [Accessed: 09/11/2018]
- El-Desawy, M. (2007) Characterization and application of aromatic self-assembled monolayers.
- Ensminger, D.E. (1986) Acoustic dewatering. *Advances in Solid-Liquid Separation, Batelle Press, Columbus, OH*.
- Esteves, L.P. (2011) On the hydration of water-entrained cement-silica systems: combined SEM, XRD and thermal analysis in cement pastes. *Thermochimica Acta*, 518 (1-2), 27-35.
- European Asphalt Pavement Association (2010) The use of warm mix asphalt. *European Asphalt Pavement Association, Brussels, Belgium*.
- European Committee for Standardization (2003a) *Bituminous mixtures —Test methods for hot mix asphalt — Specimen prepared by roller compactor*.BS EN 12697-33. London, UK: British Standards Institution.
- European Committee for Standardization (2003b) *Bituminous mixtures: Test methods for hot mix asphalt - Wheel tracking test methods for hot mix asphalt*.BS EN 12697-22. London, UK: British Standards Institution.
- European Committee for Standardization (2009) *Testing hardened concrete - Compressive strength of test specimens*.BS EN 12390-3. London, UK: British Standards Institution.
- European Committee for Standardization (2011) *Cement: Composition, specifications and conformity criteria for common cements*.BS EN 197-1. London, UK: British Standards Institution.

European Committee for Standardization (2012a) *Fly ash for concrete: Definition, specifications and conformity criteria*. BS EN 450-1. London, UK: British Standards Institution.

European Committee for Standardization (2012b) *Tests for Geometrical Properties of Aggregates: Determination of Particle Size Distribution-Sieving Method*. BS EN 933-1. London, UK: British Standards Institution.

European Committee for Standardization (2016a) *Bituminous mixtures materials specification - Asphalt Concrete*. BS EN 13108-1. London, UK: British Standards Institution.

European Committee for Standardization (2016b) *Guidance on the use of BS EN 13108, Bituminous mixtures – Material PD 6691:2015+A1:2016 specifications*. London, UK: British Standards Institution.

European Committee for Standardization (2016c) *Methods of testing cement - Determination of setting times and soundness*. BS EN 196-3. London, UK: British Standards Institution.

European Committee for Standardization (2018a) *Bitumen and bituminous binders - Determination of dynamic viscosity of bituminous binder using a rotating spindle apparatus*. BS EN 13302. London, UK: British Standards Institution.

European Committee for Standardization (2018b) *Bituminous mixtures: Test methods for hot mix asphalt- stiffness*. BS EN 12697-26. London, UK: British Standards Institution.

European Committee for Standardization (2018c) *Bituminous mixtures: Test methods for hot mix asphalt - Determination of the water sensitivity of bituminous specimens*. BS EN 12697-12. London, UK: British Standards Institution.

European Committee for Standardization (2018d) *Bituminous mixtures: Test methods for hot mix asphalt - Resistance to fatigue*. BS EN 12697-24. London, UK: British Standards Institution.

Fang, X., Garcia, A., Winnefeld, F., Partl, M.N. and Lura, P. (2016a) Impact of rapid-hardening cements on mechanical properties of cement bitumen emulsion asphalt. *Materials and Structures*, 49 (1-2), 487-498.

Fang, X., Winnefeld, F. and Lura, P. (2016b) Precipitation of anionic emulsifier with ordinary Portland cement. *Journal of colloid and interface science*, 479, 98-105.

Fatemi, A., Fuchs, H.O., Stephens, R.I. and Stephens, R.R. (2001) *Metal fatigue in engineering. A wiley-interscience Publication*.

Feldman, R.F. and Sereda, P.J. (1968) A model for hydrated Portland cement paste as deduced from sorption-length change and mechanical properties. *Matériaux et Construction*, 1 (6), 509-520.

Feng, H. and Yang, W. (2011) Ultrasonic processing. In: (ed.) *Nonthermal processing technologies for food*. Wiley-Blackwell and IFT Press, UK. pp. 135-154.

Ferrotti, G., Pasquini, E. and Canestrari, F. (2014) Experimental characterization of high-performance fiber-reinforced cold mix asphalt mixtures. *Construction and Building Materials*, 57, 117-125.

Fontes, C., Barbosa, M., Toledo Filho, R. and Goncalves, J. (2004) Potentiality of sewage sludge ash as mineral additive in cement mortar and high performance concrete. *Intern. RILEM Confe. on the Use of Recycled Materials in Buildings and Structures*, 797-806.

- García, A., Lura, P., Partl, M.N. and Jerjen, I. (2013) Influence of cement content and environmental humidity on asphalt emulsion and cement composites performance. *Materials and Structures*, 46 (8), 1275-1289.
- Ghosh, V., Mukherjee, A. and Chandrasekaran, N. (2013) Ultrasonic emulsification of food-grade nanoemulsion formulation and evaluation of its bactericidal activity. *Ultrasonics sonochemistry*, 20 (1), 338-344.
- Gingras, J.-P., Tanguy, P.A., Mariotti, S. and Chaverot, P. (2005) Effect of process parameters on bitumen emulsions. *Chemical Engineering and Processing: Process Intensification*, 44 (9), 979-986.
- Gómez-Meijide, B. and Pérez, I. (2014) Effects of the use of construction and demolition waste aggregates in cold asphalt mixtures. *Construction and Building Materials*, 51, 267-277.
- Habert, G. (2014) Assessing the environmental impact of conventional and 'green' cement production. In: (ed.) *Eco-efficient Construction and Building Materials*. Elsevier. pp. 199-238.
- Halim, C.E., Amal, R., Beydoun, D., Scott, J.A. and Low, G. (2003) Evaluating the applicability of a modified toxicity characteristic leaching procedure (TCLP) for the classification of cementitious wastes containing lead and cadmium. *Journal of hazardous materials*, 103 (1-2), 125-140.
- Head, R. (1974) An informal report of cold mix research using emulsified asphalt as a binder. *Association of Asphalt Paving Technologists Proconf Conference*.
- Hesami, S., Ahmadi, S. and Nematzadeh, M. (2014) Effects of rice husk ash and fiber on mechanical properties of pervious concrete pavement. *Construction and Building Materials*, 53, 680-691.
- Hielscher, T. (2005) Ultrasonic production of nano-size dispersions and emulsions, paper presented at 1st Workshop on Nano Technology Transfer. *ENS Paris.-14-16 December.-Paris France*.
- Hu, J., Liu, P., Wang, D., Oeser, M. and Tan, Y. (2016) Investigation on fatigue damage of asphalt mixture with different air-voids using microstructural analysis. *Construction and Building Materials*, 125, 936-945.
- Hu, S., Wang, T., Wang, F., Liu, Z. and Gao, T. (2009) Adsorption behaviour between cement and asphalt emulsion in CA mortar. *Adv Cem Res*, 21 (1), 11-14.
- Huang, Y.H. (1993) Pavement analysis and design.
- Jafari, S.M., Assadpoor, E., He, Y. and Bhandari, B. (2008) Re-coalescence of emulsion droplets during high-energy emulsification. *Food hydrocolloids*, 22 (7), 1191-1202.
- Jafer, H.M., Atherton, W., Sadique, M., Ruddock, F. and Loffill, E. (2018) Development of a new ternary blended cementitious binder produced from waste materials for use in soft soil stabilisation. *Journal of Cleaner Production*, 172, 516-528.
- Jakarn, F.M. (2012) *Adhesion of asphalt mixtures*. Ph.D. Thesis thesis, University of Nottingham.
- James, A. (2006) Overview of asphalt emulsion. *Transportation Research Circular E-C102: Asphalt Emulsion Technology*, 1-15.
- Jaturapitakkul, C. and Roongreung, B. (2003) Cementing material from calcium carbide residue-rice husk ash. *Journal of materials in civil engineering*, 15 (5), 470-475.

- Jayasooriya, S., Bhandari, B., Torley, P. and D'arcy, B. (2004) Effect of high power ultrasound waves on properties of meat: a review. *International Journal of Food Properties*, 7 (2), 301-319.
- Jenkins, K. and Twagira, M. (2008) *Updating Bituminous Stabilized Materials Guidelines: Mix Design Report, Phase II*. Technical Memorandum.
- Jenkins, K.J. (2000) *Mix design considerations for cold and half-warm bituminous mixes with emphasis of foamed bitumenthesis*, Stellenbosch: Stellenbosch University.
- Jha, A.K. and Sivapullaiah, P. (2016) Volume change behavior of lime treated gypseous soil—influence of mineralogy and microstructure. *Applied Clay Science*, 119, 202-212.
- Juhasz, Z.A. (1998) Colloid-chemical aspects of mechanical activation. *Particulate science and technology*, 16 (2), 145-161.
- Kaltsa, O., Gatsi, I., Yanniotis, S. and Mandala, I. (2014) Influence of ultrasonication parameters on physical characteristics of olive oil model emulsions containing xanthan. *Food and Bioprocess Technology*, 7 (7), 2038-2049.
- Kaltsa, O., Michon, C., Yanniotis, S. and Mandala, I. (2013) Ultrasonic energy input influence on the production of sub-micron o/w emulsions containing whey protein and common stabilizers. *Ultrasonics sonochemistry*, 20 (3), 881-891.
- Karpenko, F. and Gureev, A.A. (1998) Asphalt Emulsions. Principles of Physicochemical Technology for Production and Use.
- Katsioti, M., Tsakiridis, P., Giannatos, P., Tsibouki, Z. and Marinos, J. (2009) Characterization of various cement grinding aids and their impact on grindability and cement performance. *Construction and Building Materials*, 23 (5), 1954-1959.
- Kennedy, J. (1997) *Energy minimisation in road construction and maintenance*. Energy Efficiency Best Practice Programme.
- Khalid, H. and Eta, K. (1996) Laboratory and field performance of dense emulsified bitumen macadams used for highway reinstatement. *EURASPHALT & EUROBITUME CONGRESS, STRASBOURG, 7-10 MAY 1996. VOLUME 1. PAPER E&E. 1.093* of Conference.
- Khalid, H.A. and Monney, O.K. (2009) Moisture damage potential of cold asphalt. *International Journal of Pavement Engineering*, 10 (5), 311-318.
- Kim, Y., Im, S. and Lee, H.D. (2010) Impacts of curing time and moisture content on engineering properties of cold in-place recycling mixtures using foamed or emulsified asphalt. *Journal of materials in civil engineering*, 23 (5), 542-553.
- Kliwer, J.E., Bell, C.A. and Sosnovske, D.A. (1995) Investigation of the relationship between field performance and laboratory aging properties of asphalt mixtures. In: (ed.) *Engineering Properties of Asphalt Mixtures and the Relationship to Their Performance*. ASTM International.
- Kourounis, S., Tsivilis, S., Tsakiridis, P., Papadimitriou, G. and Tsibouki, Z. (2007) Properties and hydration of blended cements with steelmaking slag. *Cement and Concrete Research*, 37 (6), 815-822.
- Kuldiloke, J. (2002) Effect of ultrasound, temperature and pressure treatments on enzyme activity and quality indicators of fruit and vegetable juices.

- Kumar, S., Kumar, R., Bandopadhyay, A., Alex, T., Kumar, B.R., Das, S.K. and Mehrotra, S. (2008) Mechanical activation of granulated blast furnace slag and its effect on the properties and structure of portland slag cement. *Cement and Concrete Composites*, 30 (8), 679-685.
- Kuna, K. (2015) *Mix design considerations and performance characteristics of foamed bitumen mixtures (FBMs)*thesis, University of Nottingham.
- le Bouteiller, É. (2010) Asphalt Emulsions for Sustainable Pavements. *First International Conference on Pavement Preservation California Department of Transportation Federal Highway Administration Foundation for Pavement Preservation* of Conference.
- Lee, T.-C., Terrel, R.L. and Mahoney, J.P. (1983) *Test for efficiency of mixing of recycled asphalt paving mixtures*.
- Leech, D. (1994) Cold-mix bituminous materials for use in the structural layers of roads. *TRL Project Report* (PR 75).
- Leong, T., Wooster, T., Kentish, S. and Ashokkumar, M. (2009) Minimising oil droplet size using ultrasonic emulsification. *Ultrasonics sonochemistry*, 16 (6), 721-727.
- Li, Q., Chen, J., Shi, Q. and Zhao, S. (2014) Macroscopic and microscopic mechanisms of cement-stabilized soft clay mixed with seawater by adding ultrafine silica fume. *Advances in Materials Science and Engineering*, 2014.
- Ling, C., Hanz, A. and Bahia, H. (2016) Measuring moisture susceptibility of Cold Mix Asphalt with a modified boiling test based on digital imaging. *Construction and Building Materials*, 105, 391-399.
- Ling, T.-C. and Poon, C.-S. (2014) Use of recycled CRT funnel glass as fine aggregate in dry-mixed concrete paving blocks. *Journal of Cleaner Production*, 68, 209-215.
- Little, D. and Jones, I. DR 2003. Chemical and Mechanical Processes of Moisture Damage in Hot-Mix Asphalt Pavements. *Transportation Research Board National Seminar. San Diego, California* of Conference.
- Lu, D. and Wei, S. (1992) Effect of grinding aids on producing ultrafine particles. *Advanced Powder Technology*, 3 (1), 47-53.
- Ma, T., Wang, H., Huang, X., Wang, Z. and Xiao, F. (2015) Laboratory performance characteristics of high modulus asphalt mixture with high-content RAP. *Construction and Building Materials*, 101, 975-982.
- Maali, A. and Mosavian, M.H. (2013) Preparation and application of nanoemulsions in the last decade (2000–2010). *Journal of Dispersion Science and Technology*, 34 (1), 92-105.
- Maggiore, C. (2014) *A comparison of different test and analysis methods for asphalt fatigue*thesis, University of Nottingham.
- Mao, L., Xu, D., Yang, J., Yuan, F., Gao, Y. and Zhao, J. (2009) Effects of small and large molecule emulsifiers on the characteristics of β -carotene nanoemulsions prepared by high pressure homogenization. *Food Technology and Biotechnology*, 47 (3), 336-342.

- Marchal, J., Julien, P. and Boussad, N. (1993) Bitumen emulsion testing-towards a better understanding of emulsion behaviour. *Eurobitume Congress, 5th, 1993, Stockholm, Sweden* of Conference.
- Marchon, D. and Flatt, R.J. (2016) Mechanisms of cement hydration. In: (ed.) *Science and technology of concrete admixtures*. Elsevier. pp. 129-145.
- Marcotte, M., Taherian, A.R., Trigui, M. and Ramaswamy, H.S. (2001) Evaluation of rheological properties of selected salt enriched food hydrocolloids. *Journal of Food Engineering*, 48 (2), 157-167.
- Market Research Store (2015) Acetylene gas market for chemical production, welding & cutting and other applications: Global industry perspective, comprehensive analysis and forecast, 2014–2020. *Market Research Store Rep. Deerfield Beach, FL*, 110.
- Mathew, T.V. and Krishna Rao, K. (2007) Introduction to Transportation Engineering. Chapter 39. *Traffic Intersections, NPTEL*.
- Miljković, M. (2014) Influence of Bitumen Emulsion and Reclaimed Asphalt on Mechanical and Pavement Design-related Performance of Asphalt Mixtures.
- Miljković, M. and Radenberg, M. (2016) Effect of compaction energy on physical and mechanical performance of bitumen emulsion mortar. *Materials and Structures*, 49 (1-2), 193-205.
- Milton, L. and Earland, M. (1999) *Design guide and specification for structural maintenance of highway pavements by cold in-situ recycling*. Transport Research Laboratory Wokingham.
- Modarres, A., Rahmzadeh, M. and Ayar, P. (2015) Effect of coal waste powder in hot mix asphalt compared to conventional fillers: mix mechanical properties and environmental impacts. *Journal of Cleaner Production*, 91, 262-268.
- Mohammed, M.K., Dawson, A.R. and Thom, N.H. (2013) Production, microstructure and hydration of sustainable self-compacting concrete with different types of filler. *Construction and Building Materials*, 49, 84-92.
- Muthen, K. (1998) Foamed asphalt mixes-mix design procedure. *Transportation Research Record*, 898, 290-296.
- Napper, D.H. (1983) *Polymeric stabilization of colloidal dispersions*. Academic Pr.
- Nassar, A.I., Thom, N. and Parry, T. (2016) Optimizing the mix design of cold bitumen emulsion mixtures using response surface methodology. *Construction and Building Materials*, 104, 216-229.
- Nassar, A.I.M. (2016) *Enhancing the performance of cold bitumen emulsion mixture using supplementary cementitious material* thesis, University of Nottingham.
- Needham, D. (1996) *Developments in bitumen emulsion mixtures for road* thesis, University of Nottingham Nottingham.
- Niazi, Y. and Jalili, M. (2009) Effect of Portland cement and lime additives on properties of cold in-place recycled mixtures with asphalt emulsion. *Construction and Building Materials*, 23 (3), 1338-1343.

- Nikolaides, A. (1994) Construction and performance of dense cold bitumen mixtures as strengthening over layer and surface layer. *The 1st European Symposium on Performance and Durability of Bituminous Materials, London. University of Leeds.*
- O'Flaherty, C. (2007) *Highways the Location, Design, Construction and Maintenance of Road Pavements.* Butterworth Heinemann.
- O'Rourke, B., McNally, C. and Richardson, M.G. (2009) Development of calcium sulfate–ggbfs–Portland cement binders. *Construction and Building Materials*, 23 (1), 340-346.
- Ojum, C., Kuna, K., Thom, N. and Airey, G. (2014) An investigation into the effects of accelerated curing on Cold Recycled Bituminous Mixes. *International Conference on Asphalt Pavements, ISAPof Conference.*
- Ojum, C.K. (2015) *The design and optimisation of cold asphalt emulsion mixture*thesis, University of Nottingham.
- Oke, O.O. (2011) *A study on the development of guidelines for the production of bitumen emulsion stabilised RAPs for roads in the tropics*thesis, University of Nottingham.
- Oliver, J., Jameson, G., Sharp, K., Vertessy, N., Johnson-Clarke, J. and Alderson, A. (1997) Evaluation of rut-resistant properties of asphalt mixes under field and laboratory conditions. *Transportation Research Record: Journal of the Transportation Research Board* (1590), 53-61.
- Oruc, S., Bostancioglu, M. and Yilmaz, B. (2013) Effect of Residual Asphalt Content on Creep Strain of Cement Modified Emulsified Asphalt Mixtures. *J. Civ. Eng. Urbanism*, 3 (3), 122-127.
- Oruc, S., Celik, F. and Akpinar, M.V. (2007) Effect of cement on emulsified asphalt mixtures. *Journal of Materials Engineering and Performance*, 16 (5), 578-583.
- Oruc, S., Celik, F. and Aksoy, A. (2006) Performance of cement modified dense graded cold-mix asphalt and establishing mathematical model.
- Palaniandy, S. and Azizli, K.A.M. (2009) Mechanochemical effects on talc during fine grinding process in a jet mill. *International Journal of Mineral Processing*, 92 (1-2), 22-33.
- Pan, S.-C., Tseng, D.-H., Lee, C.-C. and Lee, C. (2003) Influence of the fineness of sewage sludge ash on the mortar properties. *Cement and Concrete Research*, 33 (11), 1749-1754.
- Patist, A. and Bates, D. (2011) Industrial applications of high power ultrasonics. In: (ed.) *Ultrasound technologies for food and bioprocessing.* Springer. pp. 599-616.
- Pell, P.S. (1973) Characterization of fatigue behavior. *Highway Research Board Special Report* (140).
- Puppala, A.J., Pedarla, A. and Bheemasetti, T. (2015) Soil Modification by Admixtures: Concepts and Field Applications. In: (ed.) *Ground Improvement Case Histories.* Elsevier. pp. 291-309.
- Querol Solà, N. (2013) *Highly concentrated bitumen emulsions. A state of the art, review of experimental results*thesis.
- Ravikumar, D., Peethamparan, S. and Neithalath, N. (2010) Structure and strength of NaOH activated concretes containing fly ash or GGBFS as the sole binder. *Cement and Concrete Composites*, 32 (6), 399-410.

- Rayner, C.S. and Marchal, J.L. (1991) *Bitumen emulsions*. Patent Application 2 225 291A, E. UK
- Read, J. and Whiteoak, D. (2003) *The Shell bitumen handbook 5th Edition, Shell UK Oil Products Limited*. Thomas Telford Publishing. London.
- Read, J.M. (1996) *Fatigue cracking of bituminous paving mixtures*thesis, University of Nottingham England.
- Rêgo, J., Nepomuceno, A., Figueiredo, E. and Hasparyk, N. (2015) Microstructure of cement pastes with residual rice husk ash of low amorphous silica content. *Construction and Building Materials*, 80, 56-68.
- Roberts, F.L., Kandhal, P.S., Brown, E.R., Lee, D.-Y. and Kennedy, T.W. (1991) Hot mix asphalt materials, mixture design and construction.
- Robinson, H. (1997) Thin asphalt surfacings using cold mix technology. *Performance and durability of bituminous materials. Proceedings of the second european symposium on performance and durability of bituminous materials, Leeds*of Conference.
- Rossen, J. and Scrivener, K. (2017) Optimization of SEM-EDS to determine the C–A–S–H composition in matured cement paste samples. *Materials Characterization*, 123, 294-306.
- Rovnaník, P. (2010) Effect of curing temperature on the development of hard structure of metakaolin-based geopolymer. *Construction and Building Materials*, 24 (7), 1176-1183.
- Rubio, M.C., Martínez, G., Baena, L. and Moreno, F. (2012) Warm mix asphalt: an overview. *Journal of Cleaner Production*, 24, 76-84.
- Sadique, M. and Al-Nageim, H. (2012) Hydration kinetics of a low carbon cementitious material produced by physico-chemical activation of high calcium fly ash. *Journal of Advanced Concrete Technology*, 10 (8), 254-263.
- Sadique, M., Al-Nageim, H., Atherton, W., Seton, L. and Dempster, N. (2012a) A laboratory study for full cement replacement by fly ash and silica fume. *Magazine of Concrete Research*, 64 (12), 1135-1142.
- Sadique, M., Al-Nageim, H., Atherton, W., Seton, L. and Dempster, N. (2013) Mechano-chemical activation of high-Ca fly ash by cement free blending and gypsum aided grinding. *Construction and Building Materials*, 43, 480-489.
- Sadique, M., Al Nageim, H., Atherton, W., Seton, L. and Dempster, N. (2012b) A new composite cementitious material for construction. *Construction and Building Materials*, 35, 846-855.
- Sadique, M. and Coakley, E. (2016) The influence of physico-chemical properties of fly ash and CKD on strength generation of high-volume fly ash concrete. *Advances in Cement Research*, 28 (9), 595-605.
- Sajedi, F. and Razak, H.A. (2011) Comparison of different methods for activation of ordinary Portland cement-slag mortars. *Construction and Building Materials*, 25 (1), 30-38.
- Saldanha, R.B., Scheuermann Filho, H.C., Mallmann, J.E.C., Consoli, N.C. and Reddy, K.R. (2018) Physical–mineralogical–chemical characterization of carbide lime: An environment-friendly chemical additive for soil stabilization. *J. Mater. Civ. Eng*, 30 (6), 06018004.

- Salomon, D.R. (2006) *Asphalt emulsion technology*. Transportation Research Board.
- Salvia-Trujillo, L., Rojas-Graü, A., Soliva-Fortuny, R. and Martín-Belloso, O. (2013) Physicochemical characterization of lemongrass essential oil–alginate nanoemulsions: effect of ultrasound processing parameters. *Food and Bioprocess Technology*, 6 (9), 2439-2446.
- Santos, H.M., Lodeiro, C. and Capelo-Martínez, J.L. (2008) Power ultrasound meets protomics. *Ultrasound Chem Anal Appl*, 107-127.
- Sarkar, S.L., Aimin, X. and Jana, D. (2001) Scanning electron microscopy, x-ray microanalysis of concretes. In: (ed.) *Handbook of Analytical Techniques in Concrete Science and Technology*. Elsevier. pp. 231-274.
- Schmidt, R., Santucci, L. and Coyne, L. (1973) Performance characteristics of cement-modified asphalt emulsion mixes. *Association of Asphalt Paving Technologists Proconf Conference*.
- Schneider, M., Romer, M., Tschudin, M. and Bolio, H. (2011) Sustainable cement production—present and future. *Cement and Concrete Research*, 41 (7), 642-650.
- Sekulić, Ž., Popov, S., Đuričić, M. and Rosić, A. (1999) Mechanical activation of cement with addition of fly ash. *Materials Letters*, 39 (2), 115-121.
- Serfass, J.-P., Poirier, J.-E., Henrat, J.-P. and Carbonneau, X. (2004) Influence of curing on cold mix mechanical performance. *Materials and Structures*, 37 (5), 365-368.
- Shanbara, H.K., Ruddock, F. and Atherton, W. (2018) A laboratory study of high-performance cold mix asphalt mixtures reinforced with natural and synthetic fibres. *Construction and Building Materials*, 172, 166-175.
- Shi, C. and Day, R.L. (2000) Pozzolanic reaction in the presence of chemical activators: Part II—Reaction products and mechanism. *Cement and Concrete Research*, 30 (4), 607-613.
- Siddiqui, M.N. and Ali, M.F. (1999) Investigation of chemical transformations by NMR and GPC during the laboratory aging of Arabian asphalt. *Fuel*, 78 (12), 1407-1416.
- Sirin, O., Paul, D.K. and Kassem, E. (2018) State of the Art Study on Aging of Asphalt Mixtures and Use of Antioxidant Additives. *Advances in Civil Engineering*, 2018.
- Sirin, O., Paul, D.K., Kassem, E. and Ohiduzzaman, M. (2017) Effect of ageing on asphalt binders in the State of Qatar: a case study. *Road Materials and Pavement Design*, 18 (sup4), 165-184.
- Sjoblom, J. (2001) *Encyclopedic handbook of emulsion technology*. CRC Press.
- Sjoblom, J. (2005) *Emulsions and emulsion stability: Surfactant science series/61*. CRC Press.
- Snellings, R., Mertens, G. and Elsen, J. (2012) Supplementary cementitious materials. *Reviews in Mineralogy and Geochemistry*, 74 (1), 211-278.
- Souliman, M.I., Piratheepan, M., Hajj, E.Y., Sebaaly, P.E. and Sequeira, W. (2015) Impact of lime on the mechanical and mechanistic performance of hot mixed asphalt mixtures. *Road Materials and Pavement Design*, 16 (2), 421-444.

- Speweik, J. (2011) *The Lime Cycle* [online]. Available at: <https://johnspeweik.com/2011/10/27/the-lime-cycle/>
- Striegel, A.M. (2003) Influence of chain architecture on the mechanochemical degradation of macromolecules. *Journal of biochemical and biophysical methods*, 56 (1-3), 117-139.
- Su, K., Maekawa, R. and Hachiya, Y. (2009) Laboratory evaluation of WMA mixture for use in airport pavement rehabilitation. *Construction and Building Materials*, 23 (7), 2709-2714.
- Sunarjono, S. (2008) The influence of foamed bitumen characteristics on cold-mix asphalt properties. *Doctor of Philosophy, Nottingham Transportation Engineering Centre, the University of Nottingham, School of Civil Engineering*.
- Swiertz, D., Johannes, P., Tashman, L. and Bahia, H. (2012) Evaluation of laboratory coating and compaction procedures for cold mix asphalt. *Asphalt Paving Technology-Proceedings Association of Asphalt Technologists*, 81, 81.
- Swiss Patent (1944). 394.
- Tadros, T., Izquierdo, P., Esquena, J. and Solans, C. (2004) Formation and stability of nano-emulsions. *Advances in colloid and interface science*, 108, 303-318.
- Taherkhani, H. (2006) *Experimental characterisation of the compressive permanent deformation behaviour in asphaltic mixtures*thesis, University of Nottingham UK.
- Tang, S.Y., Shridharan, P. and Sivakumar, M. (2013) Impact of process parameters in the generation of novel aspirin nanoemulsions—comparative studies between ultrasound cavitation and microfluidizer. *Ultrasonics sonochemistry*, 20 (1), 485-497.
- Tarefder, R., Zaman, M. and Hobson, K. (2003) A laboratory and statistical evaluation of factors affecting rutting. *International Journal of Pavement Engineering*, 4 (1), 59-68.
- Teklu, W. (2015) *Effect of Gradation of aggregates on the rutting performance of hot mix asphalt*thesis, ADDIS ABABA UNIVERSITY ADDIS ABABA.
- Terrell, R. and Wang, C. (1971) Early curing behavior of cement modified asphalt emulsion mixtures. *Association of Asphalt Paving Technologists Procof Conference*.
- Thanaya, I. (2003) *Improving the performance of cold bituminous emulsion mixtures (CBEMs) incorporating waste material*thesis.
- Thanaya, I., Forth, P. and Zoorob, S. (2006) Utilisation of coal ashes in hot and on cold bituminous mixtures. *Int. Coal Ash Technology Conf of Conference*.
- Thanaya, I.N.A. (2007) Review and Recommendation of Cold Asphalt Emulsion Mixtures Caems Design. *Civil Engineering Dimension*, 9 (1), 49-56.
- Thom, N.H. (2009) Cold-Mix Asphalt. *Lecture Notes] Pavement Engineering. School of Civil Engineering, University of Nottingham*.
- Transport Road Research Laboratory (1969) Bituminous Materials in Road Construction. *Crowthorne, Berkshire, England*.

- U.S. Environmental Protection Agency (USEPA) (1986) *Toxicity Characteristic Leaching Procedure (TCLP)*. 40 CFR. 50: 406–943.
- U.S. Environmental Protection Agency (USEPA) (2000) *Hot Mix Asphalt Plants Emissions Assessment Report*. North Carolina, USA: U.S. ENVIRONMENTAL PROTECTION AGENCY.
- U.S. Environmental Protection Agency (USEPA) (2011) *Inventory of U.S. greenhousegas emissions and sinks: 1990–2011*. Washington, USA: U.S. Environmental Protection Agency.
- U.S. Environmental Protection Agency (USEPA). (2015) *Regulated drinking water contaminants* [online]. Available at: <http://www.epa.gov/dwstandardsregulations#Disinfectants>. [Accessed: 08/08/2018]
- Vaitkus, A., Čygas, D., Laurinavičius, A. and Perveneckas, Z. (2009) ANALYSIS AND EVALUATION OF POSSIBILITIES FOR THE USE OF WARM MIX ASPHALT IN LITHUANIA. *Baltic Journal of Road & Bridge Engineering*, 4 (2).
- Vichan, S. and Rachan, R. (2013) Chemical stabilization of soft Bangkok clay using the blend of calcium carbide residue and biomass ash. *Soils and Foundations*, 53 (2), 272-281.
- Wang, F., Liu, Y. and Hu, S. (2013) Effect of early cement hydration on the chemical stability of asphalt emulsion. *Construction and Building Materials*, 42, 146-151.
- Wang, Z. and Sha, A. (2010) Micro hardness of interface between cement asphalt emulsion mastics and aggregates. *Materials and Structures*, 43 (4), 453-461.
- Wang, Z., Wang, H. and Guo, Q. (2006) Effect of ultrasonic treatment on the properties of petroleum coke oil slurry. *Energy & fuels*, 20 (5), 1959-1964.
- Wilson, B. and Pyatt, F. (2007) Heavy metal dispersion, persistence, and bioaccumulation around an ancient copper mine situated in Anglesey, UK. *Ecotoxicology and Environmental Safety*, 66 (2), 224-231.
- Winnefeld, F., Leemann, A., Lucuk, M., Svoboda, P. and Neuroth, M. (2010) Assessment of phase formation in alkali activated low and high calcium fly ashes in building materials. *Construction and Building Materials*, 24 (6), 1086-1093.
- Wirtgen, F. (2004) Cold recycling manual. *Windhagen, Alemania*.
- Xu, S.F., Zhao, Z.C., Xu, Y. and Wang, X.X. (2015) Mixture Design and Performance Evaluation of Cold Asphalt Mixture Using Polymer Modified Emulsion. *Advanced Materials Research of Conference*.
- Xue, Y., Hou, H., Zhu, S. and Zha, J. (2009) Utilization of municipal solid waste incineration ash in stone mastic asphalt mixture: pavement performance and environmental impact. *Construction and Building Materials*, 23 (2), 989-996.
- Ye, Q., Wu, S. and Li, N. (2009) Investigation of the dynamic and fatigue properties of fiber-modified asphalt mixtures. *International Journal of Fatigue*, 31 (10), 1598-1602.
- Zaumanis, M. (2010) Warm mix asphalt investigation. *Master of science thesis. Kgs. Lyngby: Technical University of Denmark in cooperation with the Danish Road Institute, Department of Civil Engineering*.

Zhang, T., Yu, Q., Wei, J., Zhang, P. and Chen, P. (2011) A gap-graded particle size distribution for blended cements: analytical approach and experimental validation. *Powder technology*, 214 (2), 259-268.

Zhao, J., Wang, D., Wang, X., Liao, S. and Lin, H. (2015) Ultrafine grinding of fly ash with grinding aids: Impact on particle characteristics of ultrafine fly ash and properties of blended cement containing ultrafine fly ash. *Construction and Building Materials*, 78, 250-259.

Zhao, J., Wang, D., Yan, P., Zhao, S. and Zhang, D. (2016) Particle characteristics and hydration activity of ground granulated blast furnace slag powder containing industrial crude glycerol-based grinding aids. *Construction and Building Materials*, 104, 134-141.

Research Contributions

List of peer-reviewed published conference papers

- Manar Herez, Hassan Al Nageim and Anmar Dulaimi. Evaluation of Rutting Resistance of Micro-asphalt Incorporating Recycled Asphalt Pavement (RAP) Using Cementitious Filler. **The 16th Annual International Conference Asphalt, Pavement Engineering and Infrastructure**. 22nd- 23rd February 2017. Liverpool, UK.
- Manar Herez, Hassan Al Nageim, Clare Harris and Linda Seton. Development of a High Quality Cold Mix Asphalt. **The 17th Annual International Conference Asphalt, Pavement Engineering and Infrastructure**. 21st -22nd February 2018. Liverpool, UK.
- Anmar Dulaimi, Manar Herez, Hassnen M. Jafer and Hassan Al Nageim. Performance of a cold close graded surface course mixture using a new cementations material from GGBS and waste lime. **The 17th Annual International Conference Asphalt, Pavement Engineering and Infrastructure**. 21st -22nd February 2018. Liverpool, UK.
- Manar Herez, Hassan Al Nageim, Clare Harris and Linda Seton. Developing a Premium Cementitious Filler Incorporating High Content of Sewage Sludge Fly Ash. Proceeding of 2nd International Conference Trends and Recent Advances in Civil Engineering, Noida, India.

List of under preparation journal papers

- Manar Herez, Hassan Al Nageim, Clare Harris and Linda Seton. Upgraded the Performance of Cold Bituminous Emulsion Mixture using a Sustainable Ternary Blended Cementitious Filler. **Construction and Building materials journals**.
- Manar Herez, Hassan Al Nageim, Clare Harris and Linda Seton. A Laboratory Study of a Novel Cold Asphalt Surface Course Mixture incorporating Alkali Activated Ternary Blended Cementitious Filler. **Construction and Building materials journals**.